

AOP ID and Title:

AOP 482: Deposition of energy leading to occurrence of bone loss
Short Title: Deposition of energy leading to bone loss

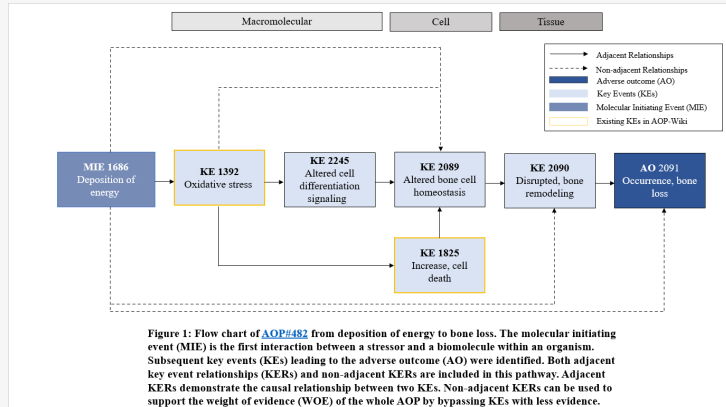
Graphical Representation

Figure 1: Flow chart of AOP#482 from deposition of energy to bone loss. The molecular initiating event (MIE) is the first interaction between a stressor and a biomolecule within an organism. Subsequent key events (KEs) leading to the adverse outcome (AO) were identified. Both adjacent key event relationships (KERs) and non-adjacent KERs are included in this pathway. Adjacent KERs demonstrate the causal relationship between two KEs. Non adjacent KERs can be used to support the weight of evidence (WOE) of the whole AOP by bypassing KEs with less evidence.

Authors

Snehal Sandhu¹, Mitchell Keyworth¹, Syna Karimi-Jashni¹, Dalya Alomar¹, Benjamin Smith¹, Tatiana Kozbenko¹, Robyn Hocking², Carole Yauk³, Ruth C. Wilkins¹, Vinita Chauhan¹

(1) Consumer and Clinical Radiation Protection Bureau, Health Canada, Ottawa, Ontario, Canada

(2) Learning and Knowledge and Library Services, Health Canada, Ottawa, Ontario, Canada

(3) Department of Biology, University of Ottawa, Ottawa, Ontario, Canada

Consultants

Stephen Doty¹, Nobuyuki Hamada², Robert Reynolds³, Ryan T. Scott⁴, Sylvain V. Costes⁵, Afshin Behesht^{6,7}

(1) Hospital for Special Surgery Research Institute, New York City, New York, USA

(2) Biology and Environmental Chemistry Division, Sustainable System Research Laboratory, Central Research Institute of Electric Power Industry (CRIEPI), Chiba, Japan

(3) KBR, NASA Johnson Space Center, Houston, TX 77058 USA;

(4) KBR, NASA Ames Research Center, Moffett Field, CA 94035 USA;

(5) NASA Ames Research Center, Space Biosciences Research Branch, Mountain View, CA, USA;

(6) KBR, NASA Ames Research Center, Space Biosciences Division, Moffett Field, CA 94035, USA;

(7) Stanley Center for Psychiatric Research, Broad Institute of MIT and Harvard, Cambridge, MA 02142, USA;

Status

Author status	OECD status	OECD project	SAAOP status
Open for citation & comment	Under Review	1.89	

Abstract

The present AOP describes Key Events (KEs) from deposition of energy, the molecular initiating event (MIE), to bone loss, the adverse outcome (AO) and is part of a broader network to three other AOs relevant to radiation exposures: impaired learning and memory, cataracts, and vascular remodeling. The AOP begins with the deposition of energy (KE#1686) that can lead directly to oxidative stress (KE#1392), defined as an imbalance of oxidants and antioxidants. Oxidation of key functional amino acids can alter signaling proteins, resulting in downstream effects in bone-regulating signaling pathways (KE#2245), specifically the Wnt/β-catenin pathway and the receptor activator of nuclear factor kappa B ligand (RANK-L) pathway. Concurrently, oxidative damage to vital cellular components, such as the nucleus, mitochondria or cell membrane, can induce oxidative stress-driven cell death (KE#1825), such as apoptosis, autophagy, and necrosis. Cell death can reduce osteocyte and osteoblast cell numbers or initiate the secretion of osteoclast-stimulatory molecules that can alter bone cell homeostasis (KE#2089). Impaired activity and differentiation of osteoblasts decreases bone formation, while increased activity and differentiation of osteoclasts increases bone destruction.

Subsequent bone remodeling (KE#2090) is then altered, defined by bone resorption being increased above bone formation. Bone density and quality can then be changed, leading to bone loss (KE#2091), the AO. The overall evidence for this AOP is moderate based on the literature to support the pathway. Although biological plausibility is well established and the evidence supporting the essentiality of most KEs is high or moderate, the quantitative understanding of the AOP is weak. Modulating factors for this relationship include age and genotype. Overall, the AOP identifies data gaps that can inform new experiments to improve quantitative understanding and could serve as a basis for developing strategies mitigating the risks of long duration spaceflight and radiotherapy treatments.

Background

Bone loss, as observed in a variety of conditions such as osteopenia and osteoporosis, is a skeletal disorder characterized by decreased bone density and quality resulting in porous, fracture-prone bones (Rachner, Khosla, and Hofbauer, 2011). In the United States, it has been estimated that 2 million fractures per year are due to osteoporosis, costing \$57 billion per year from direct medical costs combined with productivity losses and informal caregiving (Lewiecki et al., 2019). Bone loss is more common in white women, and older people (Sozen, Ozisik, and Basaran, 2017). Risk factors for fractures include low body mass index, previous fractures, glucocorticoid treatment, and other conditions like rheumatoid arthritis and type 1 diabetes mellitus (Sozen, Ozisik, and Basaran, 2017).

Growing evidence suggests that acute and chronic radiation exposure can contribute to the loss of bone mass, bone strength and changed bone quality (Donaubauer et al., 2020; Willey et al., 2011; Willey et al., 2013; Wissing, 2015; Wright, 2018). Clinical studies have shown that skeletal sites receiving high doses of ionizing radiation (25 Gy or higher) have increased fracture risk (Baxter et al., 2005; Oeffinger et al., 2006; Willey et al., 2011). For example, radiotherapy for pelvic malignancies causes an increased risk of hip fractures (Baxter et al., 2005; Williams and Davies, 2006). Similarly, radiotherapy for breast cancer or rectal carcinoma has been shown to increase the risk of fracture to the ribs or pelvis/femoral neck, respectively (Holm et al., 1996; Overgaard, 1988). Low to moderate doses of radiation as received during long-term spaceflight contribute to bone loss (Stavichuk et al., 2020; Willey et al., 2011), but is the focus of fewer studies. Radiation-induced bone loss has also been investigated through modeling-based approaches utilizing *in vivo* data to comprehend the underlying mechanisms of bone turnover (Ayati et al., 2010; Boaretti et al., 2023; Gerhard et al., 2009). Therefore, identifying essential early endpoints relevant to radiation-induced bone loss through the development of AOPs can inform mitigation strategies to reduce the risks from radiation exposures.

Summary of the AOP

Events

Molecular Initiating Events (MIE), Key Events (KE), Adverse Outcomes (AO)

Sequence	Type	Event ID	Title	Short name
	MIE	1686	Deposition of Energy	Energy Deposition
	KE	1392	Oxidative Stress	Oxidative Stress
	KE	2245	Altered Cell Differentiation Signaling	Altered cell differentiation signaling
	KE	1825	Increase, Cell death	Increase, Cell death
	KE	2089	Altered Bone Cell Homeostasis	Altered Bone Cell Homeostasis
	KE	2090	Increase, Bone Remodeling	Bone Remodeling
	AO	2091	Occurrence, Bone Loss	Bone Loss

Key Event Relationships

Upstream Event	Relationship Type	Downstream Event	Evidence	Quantitative Understanding
Deposition of Energy	adjacent	Oxidative Stress	High	Moderate
Oxidative Stress	adjacent	Increase, Cell death	Moderate	Low
Oxidative Stress	adjacent	Altered Cell Differentiation Signaling	High	Low
Increase, Cell death	adjacent	Altered Bone Cell Homeostasis	High	Low
Altered Cell Differentiation Signaling	adjacent	Altered Bone Cell Homeostasis	High	Moderate
Altered Bone Cell Homeostasis	adjacent	Increase, Bone Remodeling	Moderate	Low
Increase, Bone Remodeling	adjacent	Occurrence, Bone Loss	Moderate	Low
Oxidative Stress	non-adjacent	Altered Bone Cell Homeostasis	Moderate	Low
Deposition of Energy	non-adjacent	Altered Bone Cell Homeostasis	High	Low
Deposition of Energy	non-adjacent	Increase, Bone Remodeling	High	Low
Deposition of Energy	non-adjacent	Occurrence, Bone Loss	High	Moderate

Stressors

Name	Evidence
Ionizing Radiation	

Overall Assessment of the AOP

This AOP collates peer-reviewed published data in the space field and studies from other radiation exposure scenarios that are not encountered during space travel to strengthen the weight of evidence. The search prioritized chronic low- to moderate-dose radiation emitted from high linear energy transfer (LET) particles, which is most applicable to long-term spaceflight. High doses from low-LET acute radiation studies were included as well; thus, AOP is also relevant to bone loss from radiotherapy. Other stressors that are space-relevant but not radiation-related like microgravity are also used to strengthen the AOP. However, not all KERs are equally supported by the multitude of stressors encountered during space travel, as some KERs have different responses dependent on the stressor. A few studies show additive effects when combining radiation and microgravity stressors in animal models, demonstrating that these stressors may encourage bone loss through separate pathways (Willey et al., 2021). However, particularly in studies using chronic or fractionated exposures, radiation did not exacerbate the effects of microgravity (Kondo et al., 2010; Willey et al., 2021). This could be because the identical components of each mechanism are saturated by the individual stressor (Kondo et al., 2010).

Biological Plausibility

Overall, each KER in the AOP is well understood mechanistically and biological plausibility is high. Mechanisms such as altered bone cell homeostasis and bone remodeling are well accepted biological events contributing to bone loss (details provided in tables). The deposition of energy (MIE) causes the ionization of water molecules within cells, producing free radicals that combine to more stable reactive oxygen species (ROS) (Eaton, 1994; Padgaonkar et al., 2015; Rehman et al., 2016; Varma et al., 2011). Additionally, deposited energy can directly upregulate enzymes involved in reactive oxygen and nitrogen species (RONS) production (de Jager, Cockrell and Du Plessis, 2017). This, along with positive feedback loops that further generate RONS, contributes to oxidative stress as RONS overwhelm the cells' antioxidant defence systems and subsequently damage macromolecules and organelles (Balasubramanian, 2000; Ganea and Harding, 2006; Karimi et al., 2017; Zigmant et al., 2000).

It is well established that oxidative damage can cause both cell death and altered signaling. Oxidation of key amino acids in proteins from major signaling pathways will cause conformational and functional changes to these signaling molecules, inducing changes in the activity of the entire pathway (Ping et al., 2020; Schmidt-Ullrich et al., 2000; Valerie et al., 2007). Oxidative stress can indirectly affect signaling through oxidative DNA damage, which influences the expression and activity of signaling molecules, such as the molecules involved in the MAPK pathway (Nagane et al., 2021; Ping et al., 2020; Schmidt-Ullrich et al., 2000; Valerie et al., 2007). Additionally, extensive damage to DNA, mitochondria, or the cell membrane can induce cell death (Jilka, Noble and Weinstein, 2013).

In bones, the combined influence of altered cell differentiation signaling and increased cell death will alter bone cell homeostasis, characterized by an increase in osteoclasts (bone resorbing cells) and a decrease in osteoblasts (bone forming cells). Mature bone tissue is relatively radioresistant compared to the highly radiosensitive bone marrow, which is a critical source of stem and progenitor cells essential for skeletal health (ICRP, 2007). Large bolus doses of radiation can cause acute cell death or marrow depletion, while smaller doses allow for recovery through stem cell proliferation, though late effects may still occur (Turner et al., 2013; Cao et al., 2011; Green et al., 2012; Kim et al., 2014; Tataria and Monzen, 2023; Suva et al., 1993; Otsuka et al., 2008; Greenberger and Epperly, 2009; Chatterjee et al., 2012; Rastogi et al., 2012). Trabecular bone shows more immediate and pronounced effects post-irradiation, as evidenced in rodent studies (Kondo et al., 2010), whereas cortical bone effects are subtler and dose-dependent (Lloyd et al., 2008; Wernle et al., 2010; Oest et al., 2015; Sugimoto et al., 1991). Additionally, radiation exposure leads to the rapid infiltration of adipocytes into the bone marrow, significantly decreasing trabecular and total bone volume (Costa and Reagan, 2019).

Upregulated signaling from the RANK-L pathway will increase osteoclastogenesis, while impaired Wnt/β-catenin signaling will decrease osteoblastogenesis (Arfat et al., 2014; Bellido, 2014; Boyce and Xing, 2007; Chatziravdeli, Katsaras and Lambrou, 2019; Chen, Deng and Li, 2012; Donaubauer et al., 2020; Maeda et al., 2019; Manolagas and Almeida, 2007; Smith, 2020a; Smith, 2020b; Willey et al., 2011). Osteoblast death will reduce osteoblast numbers, while osteocyte death will free osteoclast-stimulating molecules (Jilka, Noble, and Weinstein, 2013; Komori, 2013; Li et al., 2015; O'Brien, Nakashima, and Takayanagi, 2013; Plotkin, 2014; Wang et al., 2020; Xiong and O'Brien, 2012). As bone cells are dysregulated, subsequent bone remodeling results in a greater rate of resorption than formation of bone (Bikle

and Halloran, 1999; Donaubauer et al., 2020; Morey-Holton et al., 1991; Smith, 2020b; Tian et al., 2017). Consequently, bones exhibit reduced volume, density, mineralization, and strength as bone loss occurs (Bikle and Halloran, 1999; Donaubauer et al., 2020; Morey-Holton and Arnaud, 1991; Tian et al., 2017). A complete understanding of the relationship across taxonomy and sex is lacking at the time of AOP development; this is an area that requires further research.

Temporal, Dose, and Incidence Concordance

Evidence for time, dose, and incidence concordance in this AOP is moderate, as evidence to support the modified Bradford Hill criteria is often limited due to space travel conditions, where there are restrictions on the number of animals, doses and timepoints represented. For this reason, data from other exposure scenarios are used to help strengthen the adjacent relationships, in keeping with the principles of AOP development. In contrast, there was a larger evidence base for the non-adjacent relationships that were directly linked to the MIE, as there is much radiobiological research to support MIE's causal association to each of the KEs in the AOP.

In general, many studies demonstrated that the upstream KEs occurred earlier than the downstream KEs in time course experiments. The temporal responses of energy deposition to bone loss have not been comprehensively examined across all KEs in a single study, with most data focusing on the interval from radiation exposure to bone loss. It is well accepted that deposition of energy occurs immediately following irradiation, and downstream changes will always occur later in a time course. The subsequent radical formation occurs within microseconds (Azzam, Jay-Gerin, and Pain, 2012), and studies have observed the resulting oxidative stress as early as 2 minutes post-irradiation (Wortel et al., 2019). Altered cell differentiation signaling is a molecular-level KE like oxidative stress, and both KEs occur with a similar time course, making the assessment of time concordance difficult between these KEs. However, oxidative stress can still be observed slightly earlier than altered cell differentiation signaling (Wortel et al., 2019). The ensuing cell death due to oxidative stress often occurs within days post-irradiation, while altered bone cell homeostasis owing to both altered cell differentiation signaling and cell death is subsequently observed about a week after irradiation (Liu et al., 2018). Then, from multiple weeks to a month post-irradiation, bone remodeling is observed to favor resorption over formation (Alwood et al., 2010; Chandra et al., 2017; Chandra et al., 2014; Zhai et al., 2019). The resulting bone loss presents after this, with the greatest bone loss and risk of fractures observed months to years following irradiation (Holm et al., 1996; Nishiyama et al., 1992; Oest et al., 2018; Zou et al., 2016). However, in animal models studies consistently show that irradiation leads to an early increase in osteoclast number and activity, marked by elevated serum TRAP5b levels within 24 hours and significant bone loss within a week, although this response can vary based on the type and administration of radiotherapy (Zhai et al. 2019; Willey et al. 2011; Oest et al. 2015).

Radiation at any dose and dose rate will deposit energy. Extensive evidence shows that upstream KEs can be observed at the same doses or lower doses as downstream KEs. For example, Kondo et al. (2009) and Kondo et al. (2010) showed that ROS levels and osteoclastogenesis were increased by both 1 and 2 Gy of gamma radiation, while bone loss and remodeling endpoints occurred at 2 Gy but not 1 Gy. In another study, X-ray irradiation at both 2 and 24 Gy led to increased osteoclast activity, while only 24 Gy led to consistent decreases in areal bone mineral density (ABMD) and mineral apposition rate (MAR) (Zhai et al., 2019). Dose concordance is not consistently observed across studies, but this may be due to different models, timepoints, and radiation types used.

A few studies support incidence concordance. Although many studies demonstrate equal changes between the two KEs, less than half of the studies across KERs show that the upstream KE produces a greater change than the downstream KE following a stressor. One KER showing strong incidence concordance is altered signaling leading to altered bone cell homeostasis. For example, Sambandam et al. (2016) showed that tumor necrosis factor receptor-associated factor 6 (TRAF6) and tumor necrosis factor-related apoptosis inducing ligand (TRAIL) signaling molecules were increased 6 and 14.5-fold, respectively, while tartrate-resistant acid phosphatase (TRAP) staining (indicative of bone cell homeostasis) was just increased 1.7-fold by microgravity.

Uncertainties and Inconsistencies

There are some notable knowledge gaps in the understanding of the biological mechanism involved in the deposition of energy leading to bone loss. In the space environment, both microgravity and radiation stressors are present. However, the differences in the underlying molecular changes following each stressor are currently uncertain (Willey et al., 2021). More research should be focused on understanding differential effects of microgravity and radiation on bone loss. Furthermore, studies using multi-ion radiation and chronic radiation exposure in addition to microgravity could better represent the space environment (Willey et al., 2021).

Some studies also show conflicting results. For example, a few studies demonstrate bone cell differentiation and activity at doses of ionizing radiation at 2 Gy or below (Li et al., 2020b), while others show no effects (Kook et al., 2015; He et al., 2019). Differences may be due to experimental designs related to timepoints, histology measurements, models, radiation quality, doses, and dose rates. This often complicates the ability to evaluate the strength of the evidence due to inconsistent results. Studies were also limited in the range of doses or timepoints used, which challenged the identification of dose and time concordance data. Often studies measured KEs at a single dose or timepoint. Furthermore, no single study evaluated all KEs in the AOP, which would have provided ideal evidence to determine the weight of evidence supporting this AOP.

Other aspects for consideration are interspecies differences. During the first few months of spaceflight, bone resorption increases greatly in humans (Stavnichuk et al., 2020). In rats, however, resorption does not change during spaceflight (Fu et al., 2021). Mouse models are more representative of the altered bone cell homeostasis KE than rat models, as they show consistent increases in resorption during spaceflight (Vico and Hargens, 2018). In addition, there are differences in measurements used to assess the resorption of bone in humans and experimental animals (Fu et al., 2021).

Human spaceflight studies indicate either no change in bone formation or an increase in bone formation (Stavnichuk et al., 2020; Smith et al. 2015, Smith, 2014).

Most animal literature demonstrates decreased formation occurred in growing animals; mature animals models suggest no change in bone formation. (Smith et al. 2002. Findings related to bone formation may differ based on life stage.

Lastly, the bone remodeling KE includes endpoints to measure changes in the bone formation rate but has fewer endpoints to measure bone resorption. Resorption endpoints are often cell-level and are included in the altered bone cell homeostasis KE. Changes to resorption in the bone remodeling KE are determined indirectly through changes to bone formation and bone volume. Consequently, it is difficult to quantify bone resorption in the bone remodeling KE, even though it is an important contributor to bone loss. Further studies could be undertaken to examine bone resorption rate in the context of downstream KEs in the AOP by using time-lapsed micro computed-tomography (CT) imaging or advanced CT imaging in measurements.

Domain of Applicability

Life Stage Applicability

Life Stage Evidence

All life stages	High
-----------------	------

Taxonomic Applicability

Term	Scientific Term	Evidence	Links
human	Homo sapiens	High	NCBI
mouse	Mus musculus	High	NCBI
rat	Rattus norvegicus	High	NCBI
rhesus monkeys	Macaca mulatta	Low	NCBI

Sex Applicability

Sex Evidence

Male	High
Female	High

This AOP is relevant to vertebrates, such as humans, mice, and rats. The taxonomic evidence supporting the AOP is derived from studies in human (*Homo sapiens*) and human-derived cell lines, mouse (*Mus musculus*), rat (*Rattus norvegicus*), and rhesus monkey (*Macaca mulatta*) (Chandra et al., 2014; Nishiyama et al., 1992; Willey et al., 2011; Zerath et al., 2002). Across all species, most available data was from adult and adolescent models with less available data from preadolescent models.

The AOP is applicable to both sexes, with most studies using either male or female animal models but not both. In humans, spaceflight-induced bone loss has also been observed in both sexes (Smith et al., 2014).

The AOP is applicable to all life stages, with extensive studies in adult humans and animals and fewer studies in adolescent and preadolescent animals. However,

bone loss can be more prevalent in the aging population (>~50 years) (Riggs, Khosla, and Melton, 1998; Pacheco and Stock, 2013).

Essentiality of the Key Events

Modulation of upstream KEs often influences the occurrence or extent of downstream KEs, making the evidence of essentiality moderate for the KEs in the AOP. Below are a few examples showing how downstream KEs are affected by upstream modulation.

Essentiality of the Deposition of Energy (MIE#1686)

- The effect of radiation shielding on altered bone cell homeostasis (KE#2089)
- Increased osteoclast numbers were not observed in shielded contralateral bones following irradiation (Wright et al., 2015). However, a few studies show equal changes to osteoblast and osteoclast number *in vivo* in irradiated and contralateral limbs, possibly due to the abscopal effects of radiation (Zhang et al., 2019; Zou et al., 2016).
- The effect of radiation shielding on disrupted bone remodeling (KE#2090)
- Shielded limbs show a higher bone formation rate than directly irradiated limbs (Wright et al., 2015; Zhai et al., 2019).
- The effect of radiation shielding on occurrence of bone loss (AO#2091)
- Multiple studies measuring bone loss in shielded limbs contralateral to the irradiation show a greater loss of bone in the irradiated limb (Baxter et al., 2005; Oest et al., 2018; Wright et al., 2015). Although a few studies find equal changes in irradiated and contralateral limbs, this may be due to the abscopal effects of radiation (Zhang et al., 2019; Zou et al., 2016).

Essentiality of Oxidative Stress (KE#1392)

- The effect of antioxidants on altered cell differentiation signaling (KE#2245)
- Antioxidants including N-acetyl cysteine, curcumin, melatonin, polyphenol S3, and hydrogen water restore signaling in the Wnt/β-catenin pathway and inhibit signaling in the RANK/RANK-L pathway (Diao et al., 2018; Kook et al., 2015; Sun et al., 2013; Xin et al., 2015; Yoo, Han & Kim, 2016).
- The effect of antioxidants on increased cell death (KE#1825).
- Antioxidants including α-2-macroglobulin (α2M), semaphorin 3A (sema3a), amifostine (AMI), and melatonin reduce apoptosis levels induced by radiation or microgravity (Huang et al., 2019; Huang et al., 2018; Liu et al., 2018; Li et al., 2018a; Yoo, Han and Kim, 2016).
- The effect of antioxidants on altered bone cell homeostasis (KE#2089)
- Antioxidants including N-acetyl cysteine, α2M, AMI, curcumin, cerium (IV) oxide, and hydrogen water restore osteoblastogenesis and reduce osteoclastogenesis following radiation or microgravity (Diao et al., 2018; Huang et al., 2019; Huang et al., 2018; Kook et al., 2015; Liu et al., 2018; Sun et al., 2013; Wang et al., 2016; Xin et al., 2015; Zhang et al., 2020).

Essentiality of Altered Cell Differentiation Signaling (KE#2245)

- The effect of modulated signaling on altered bone cell homeostasis (KE#2089)
- Modulation of osteoclastogenesis-related signaling – Inhibitors of the RANK/RANK-L pathway or other osteoclast-stimulating molecules reduce osteoclast activity after it is increased by exposure to gamma rays, X-rays, and microgravity (He et al., 2019; Li et al., 2018b; Rucci et al., 2007; Sambandam et al., 2016; Zhang et al., 2019; Zhou et al., 2008).
- Modulation of osteoblastogenesis-related signaling – Activation of pathways leading to runt-related transcription factor 2 (Runx2) activation or the Wnt/β-catenin pathway restored osteoblast activity after it is decreased by exposure to X-rays and microgravity (Chandra et al., 2017; Chen et al., 2020; Li et al., 2020b; Li et al., 2018b; Liu et al., 2018). In contrast, direct inhibition of the Wnt/β-catenin pathway impairs osteoblast activity (Chen et al., 2020).

Essentiality of Increase, Cell Death (KE#1825)

- The effect of modulating cell death on altered bone cell homeostasis (KE#2089)
- Osteoblast cell death decreases the number of osteoblasts, while osteocyte cell death can stimulate osteoclastogenesis. Inhibition of cell death by using drugs that promote cell survival or by inhibiting autophagy restores osteoblast numbers and activity as well as reducing osteoclast numbers and activity (Chandra et al., 2014; Huang et al., 2019; Li et al., 2020b; Liu et al., 2018; Wang et al., 2020; Wu et al., 2020; Yang et al., 2020).

Essentiality of Altered Bone Cell Homeostasis (KE#2089)

- No study directly modulating the changes to osteoblasts and osteoclasts and observing the results on downstream KEs was identified in the literature search.

Essentiality of Disrupted, Bone Remodeling (KE#2090)

- The effect of modulated bone remodeling on bone loss (AO#2091)
- Bone remodeling blocked by knockout of osteopontin, a mediator of bone remodeling, restores the bone volume after microgravity (Ishijima et al., 2001). Similarly, inhibition of Calponin h1, an inhibitor of bone formation, increases BMD following microgravity (Yotsumoto, Takeoka, and Yokoyama, 2010).

Weight of Evidence Summary

	Defining Question	High (Strong)	Moderate	Low (Weak)
1. Support for Biological Plausibility of KERs	Is there a mechanistic relationship between KEupstream and KEdownstream consistent with established biological knowledge?	Extensive understanding of the KER based on extensive previous documentation and broad acceptance; Established mechanistic basis	KER is plausible based on analogy to accepted biological relationships, but scientific understanding is not completely established	There is empirical support for statistical association between KEs, but the structural or functional relationship between them is not understood
MIE#1686 → KE#1392: Deposition of Energy leads to Oxidative Stress	High There is strong evidence of the biological plausibility of deposition of energy leading to oxidative stress. It is well understood that when deposited energy reaches a cell it reacts with water and organic materials to produce free radicals such as ROS. If the ROS cannot be eliminated quickly and efficiently enough by the cell's defence system, oxidative stress may ensue.			
KE#1392 → KE#1825: Oxidative stress leads to Increase, cell death	High It is well known that oxidative stress can lead to cell death. ROS lead to the release of pro-apoptotic factors, and enough ROS accumulation can lead to necrosis. Lipid and protein oxidation of key structures within the cell will also lead to cell death.			

KE#1392 → KE#2245: Oxidative stress leads to Altered Cell Differentiation Signaling	High There is much evidence demonstrating the biological plausibility of the link between oxidative stress and altered cell differentiation signaling. The direct and indirect mechanisms of oxidative stress leading to altered signaling are well known. Directly, oxidative stress conditions can lead to oxidation of amino acid residues. This can cause conformational changes, protein modifications, protein degradation, and impaired activity, leading to changes in the activity and level of signaling proteins. Indirectly, oxidative stress can damage DNA causing changes in the expression of signaling proteins as well as the activation of DNA damage response signaling.								
Non-adjacent KE#1392 → KE#2089: Oxidative stress leads to → Altered Bone Cell Homeostasis	High It is well understood that an increase in cellular oxidative stress indirectly leads to altered bone cell homeostasis. An increase in oxidative stress and the resulting decrease in osteoblast activity and increase in osteoclast activity have been discussed and well documented, in several reviews.								
KE#1825 → KE#2089: Increase, Cell Death leads to Altered Bone Cell Homeostasis	High It is well understood that the induction of different forms of cell death of osteoblasts, osteoclasts, and osteocytes leads to an increase in bone resorption and decrease in bone deposition. Osteocyte apoptosis results in rupture of the plasma membrane as phagocytes are unable to engulf these cells, allowing for the release of osteoclast-stimulatory molecules. Apoptotic osteocytes also signal to viable osteocytes in the vicinity to express osteoclast-stimulatory signals. Osteoblast death reduces the overall pool of active osteoblasts. Autophagy can also lead to cell death, and a few studies associate it with cell death in bone cells.								
KE#2245 → KE#2089: Altered Cell Differentiation Signaling leads to Altered Bone Cell Homeostasis	High It is very well understood that changes in osteoblast and osteoclast signaling pathways lead to decreased bone deposition and increased bone resorption. A few highly characterized pathways that are important for osteoblast and osteoclast differentiation are the Wnt/β-catenin pathway and the RANK/RANK-L pathway, respectively. Alterations in signaling from these pathways will alter bone cell numbers and activity.								
KE#2089 → KE#2090: Altered Bone Cell Homeostasis leads to Disrupted, Bone Remodeling	High Review papers strongly support the structural and functional relationship between altered bone cell homeostasis and bone remodeling. Decreased activity and differentiation of osteoblasts and increased activity and differentiation of osteoclasts lead to increased overall destruction of bone. Bone remodeling is therefore imbalanced to favor bone resorption over formation.								
KE#2090 → AO#2091: Disrupted, Bone Remodeling leads to Occurrence, Bone Loss	High The structural and functional relationship between bone remodeling and bone loss is well supported by review articles. Current literature on the subject establishes bone loss due to a decrease in bone formation and an increase in bone resorption by bone remodeling cells.								
Non-adjacent MIE#1686 → KE#2089: Deposition of Energy leads to Altered Bone Cell Homeostasis	High The structural and functional relationships connecting energy deposition to the loss of homeostasis among bone cells is well supported by several reviews on the subject related to space travel and clinical treatment. More specifically, reviews on ionizing radiation exposure have defined the biological mechanisms by which these stressors can indirectly induce the loss of homeostasis among bone cells.								
Non-adjacent MIE#1686 → KE#2090: Deposition of Energy leads to Disrupted, Bone Remodeling	High The biological plausibility for the indirect relationship between deposition of energy and imbalanced remodeling is strong. Reviews describe the impact of radiation on bone formation and resorption as well as the mechanisms involved.								
Non-adjacent MIE#1686 → AO#2091: Deposition of Energy leads to Bone Loss	High There is a high level of structural and functional evidence for the indirect relationship between deposition of energy and bone loss.								
2. Support for Essentiality of KEs	<table border="1"> <thead> <tr> <th>Defining Question</th> <th>High (Strong)</th> <th>Moderate</th> <th>Low (Weak)</th> </tr> </thead> <tbody> <tr> <td>Are downstream KEs and/or the AO prevented if an upstream KE is blocked?</td> <td>Direct evidence from specifically designed experimental studies illustrating essentiality for at least one of the important KEs</td> <td>Indirect evidence that sufficient modification of an expected modulating factor attenuates or augments a KE</td> <td>No or contradictory experimental evidence of the essentiality of any of the KEs</td> </tr> </tbody> </table>	Defining Question	High (Strong)	Moderate	Low (Weak)	Are downstream KEs and/or the AO prevented if an upstream KE is blocked?	Direct evidence from specifically designed experimental studies illustrating essentiality for at least one of the important KEs	Indirect evidence that sufficient modification of an expected modulating factor attenuates or augments a KE	No or contradictory experimental evidence of the essentiality of any of the KEs
Defining Question	High (Strong)	Moderate	Low (Weak)						
Are downstream KEs and/or the AO prevented if an upstream KE is blocked?	Direct evidence from specifically designed experimental studies illustrating essentiality for at least one of the important KEs	Indirect evidence that sufficient modification of an expected modulating factor attenuates or augments a KE	No or contradictory experimental evidence of the essentiality of any of the KEs						
MIE#1686: Deposition of energy	Moderate Numerous studies show that physical shielding or attenuating the amount of deposited energy can modulate the downstream KEs. However, some studies still show significant bone loss in shielded limbs, possibly due to the abscopal effects of radiation.								
KE#1392: Oxidative Stress	High Essentiality of oxidative stress is well-supported within literature. Many studies have shown that adding or withholding antioxidants such as catalase and glutathione peroxidase will decrease and increase the level of oxidative stress, respectively. Studies using antioxidants to attenuate oxidative stress show restored signaling and bone cell homeostasis, as well as reduced apoptosis.								

KE#2245: Altered Cell Differentiation Signaling	High	Studies strongly support the essentiality of altered cell differentiation signaling on downstream effects. Studies have used inhibitors or activators of various signaling pathways and observed attenuation of downstream KEs, particularly altered bone cell homeostasis.		
KE#1825: Increase, Cell Death	High	Essentiality of increased cell death is well supported within literature through evidence that inhibiting cell death attenuates downstream KEs. Multiple studies inhibit osteoblast and osteocyte cell death by preventing apoptosis or autophagy and find restored osteocyte numbers as well as restored osteoblast numbers and activity.		
KE#2089: Altered Bone Cell Homeostasis	Low	There were no studies found on the essentiality of this event; i.e., there were no studies that inhibited the alteration of bone cell homeostasis and measured the downstream KE.		
KE#2090: Disrupted, Bone Remodeling	Moderate	Essentiality of bone remodeling is moderately supported within literature. A small number of studies that inhibit bone resorption or induce bone formation show a reduction in bone loss.		
3. Empirical support for KERs	Defining Question	High (Strong)	Moderate	Low (Weak)
	Does KEupstream occur at lower doses and earlier timepoints than KEdownstream; is the incidence or frequency of KEupstream greater than that for KEdownstream for the same dose of tested stressor?	There is a dependent change in both events following exposure to a wide range of specific stressors (extensive evidence for temporal, dose-response and incidence concordance) and no or few data gaps or conflicting data.	There is demonstrated dependent change in both events following exposure to a small number of specific stressors and some evidence inconsistent with the expected pattern that can be explained by factors such as experimental design, technical considerations, differences among laboratories, etc.	There are limited or no studies reporting dependent change in both events following exposure to a specific stressor (i.e., endpoints never measured in the same study or not at all), and/or lacking evidence of temporal or dose-response concordance, or identification of significant inconsistencies in empirical support across taxa and species that don't align with the expected pattern for the hypothesized AOP.
MIE#1686 → KE#1392: Deposition of Energy leads to Oxidative Stress	High	There is a large body of evidence that supports an understanding of the time and dose relationship from deposition of energy leading to oxidative stress. The evidence collected to support this relationship was gathered from various studies using <i>in vitro</i> and <i>in vivo</i> rat, mice, rabbit, squirrel, bovine and human models. Various stressors were applied, including ultraviolet (UV) light (UV-B and UV-A) and ionizing radiation (gamma rays, X-rays, protons, photons, neutrons, and heavy ions). Studies that examined the effects of range of ionizing radiation doses (0-10 Gy) discovered that oxidative stress increases in a dose-dependent manner.		
KE#1392 → KE#1825: Oxidative Stress leads to Increase, Cell Death	Moderate	There is moderate empirical evidence to support the relationship between oxidative stress and increased cell death. Many studies demonstrate incidence concordance, dose concordance, and time concordance. However, there are limited data pertaining to low doses of the radiation stressors (X-rays, gamma rays, ¹² C ions) used to investigate the relationship.		
KE#1392 → KE#2245: Oxidative Stress leads to Altered Cell Differentiation Signaling	High	There is strong empirical evidence for this relationship. A number of studies demonstrated incidence concordance. Most studies that examined the effects of a range of stressor doses showed dose concordance, and most studies that analyzed oxidative stress and signaling pathways over multiple timepoints supported temporal concordance. This evidence was collected from studies using a variety of stressors, including ionizing radiation in doses as low as 0.125 Gy, in <i>in vitro</i> cell and <i>in vivo</i> mouse, rat, and pig models.		
Non-adjacent KE#1392 → KE#2089: Oxidative Stress leads to Altered Bone Cell Homeostasis	Moderate	There is a moderate body of evidence showing concordance between oxidative stress and altered bone cell homeostasis. A few studies demonstrated incidence concordance, most studies that examined the effects of a range of doses demonstrated dose concordance, and most studies that examined oxidative stress and bone cell dysfunction over multiple timepoints provided evidence in support of temporal concordance. However, the evidence for dose concordance is weak as only a single study measured the KEs at multiple doses. Ionizing radiation (X-rays and gamma rays) in doses as low as 1 Gy and microgravity were the stressors used in studies. The models used included <i>in vitro</i> cells and <i>in vivo</i> rats and mice.		
KE#1825 → KE#2089: Increase, Cell Death leads to Altered Bone Cell Homeostasis	High	There is a large body of evidence indicating concordance between increased cell death to altered bone cell homeostasis. Most studies demonstrated time, dose, and incidence concordance. Ionizing radiation (X-rays and gamma rays) in doses as low as 0.5 Gy and microgravity were the stressors used in studies. The models used included <i>in vitro</i> cells and <i>in vivo</i> rats and mice.		
KE#2245 → KE#2089: Altered Cell Differentiation Signaling leads to Altered Bone Cell Homeostasis	High	There is strong evidence showing concordance to support the KER. Evidence in most of the studies collected supported time, dose, and incidence concordance. Ionizing radiation (X-rays and gamma rays) at doses as low as 0.5 Gy and microgravity were the stressors used in studies. The models used included <i>in vitro</i> cells and <i>in vivo</i> rats and mice.		
KE#2089 → KE#2090: Altered Bone Cell Homeostasis leads to Disrupted, Bone Remodeling	Moderate	Dose and time concordance between altered bone cell homeostasis and bone remodeling are currently supported by moderate evidence. A number of studies demonstrate incidence concordance and most studies that analyzed altered bone cell homeostasis and bone remodeling over multiple timepoints demonstrated time concordance. However, some studies showed changes to one or more endpoints that were inconsistent with the change expected following the stressors. Also, there were no studies that could be used to evaluate the dose concordance of the KEs at multiple doses. The relationship was demonstrated using X-rays at doses as low as 2 Gy and microgravity in <i>in vitro</i> cell and <i>in vivo</i> rat and mouse models.		
KE#2090 → AO#2091: Disrupted, Bone Remodeling leads to Occurrence, Bone Loss	Moderate	There is moderate evidence for concordance between bone remodeling and bone loss. Most studies demonstrate time and incidence concordance. However, no studies measured both KEs at multiple doses of the stressor. The relationship was demonstrated using X-rays at doses as low as 2 Gy and microgravity in <i>in vitro</i> cell and <i>in vivo</i> rat, mouse, and monkey models.		

Non-adjacent MIE#1686 → KE#2089: Deposition of Energy leads to Altered Bone Cell Homeostasis	High A strong body of evidence shows dose- and time-response effects of ionizing radiation. Data from studies show that radiation exposure indirectly increases osteoclast activity and decreases osteoblast activity in a dose-dependent manner. X-rays and gamma rays in doses ranging from 0-30 Gy were used to study the effects of radiation on bone cells in <i>in vitro</i> and <i>ex vivo</i> cell models, <i>in vivo</i> mouse and rat models, and human models. About a week after radiation exposure, with increasing radiation doses, numbers and activity of osteoblasts decrease, while numbers of osteoclasts increase.
Non-adjacent MIE#1686 → KE#2090: Deposition of Energy leads to Disrupted, Bone Remodeling	High The empirical evidence for deposition of energy leading to bone remodeling is high. Imbalanced bone remodeling caused by ionizing radiation is directly related to the absorbed dose. Bone remodeling is affected after exposure of mice and rats to 0.5-24 Gy of X-ray, gamma ray, proton, and ⁵⁶ Fe ion radiation. Few studies examine the time course of this KER, but changes to bone remodeling occur from 7 to 60 days post-irradiation.
Non-adjacent MIE#1686 → AO#2091: Deposition of Energy leads to Occurrence, Bone Loss	High There is strong evidence for the deposition of energy leading to bone loss. X-rays, gamma rays, protons, and heavy ions from 0.05 to 64 Gy delivered to rat, mouse, and human models were used to assess this relationship. By comparing the results of studies using either high or low dose radiation, there is a consensus that bone loss from low dose exposure is less than that from high dose exposure. Studies also show that bone loss can be observed from 1 week to years after irradiation but is mostly found in the first few months after exposure.

Quantitative Consideration

There is a low quantitative understanding for the KERs in this AOP. Many studies have quantified the changes in consecutive KEs after a specific stressor dose. However, due to varying experimental parameters, including experimental model, radiation type, doses, dose rate, and timepoints, a quantitative relationship is difficult to determine between most adjacent KEs in the pathway. KERs between the MIE and downstream KEs are readily quantified, as changes to the upstream KE, in this case the dose, dose rate, and radiation type applied to the model, are determined in the experimental method and can be more easily standardized across studies. KERs that do not include the MIE are more difficult to quantify, as the perturbation to the upstream KE cannot be standardized to determine its effects on a downstream KE, as it is the product of the applied stressor and the resulting changes to KEs that came before it in the pathway.

	Defining Question	High (Strong)	Moderate	Low (Weak)
Review of the Quantitative Understanding for each KER	To what extent can a change in KE _{downstream} be predicted from KE _{upstream} ? With what precision can the uncertainty in the prediction of KE _{downstream} be quantified? To what extent are the known modulating factors of feedback mechanisms accounted for? To what extent can the relationships described be reliably generalized across the applicability domain of the KER?	Change in KE _{downstream} can be precisely predicted based on a relevant measure of KE _{upstream} ; uncertainty in the quantitative prediction can be precisely estimated from the variability in the relevant KE _{upstream} measure. Known modulating factors and feedback/feedforward mechanisms are accounted for in the quantitative description. Evidence that the quantitative relationship between the KEs generalizes across the relevant applicability domain of the KER.	Change in KE _{downstream} can be precisely predicted based on a relevant measure of KE _{upstream} ; uncertainty in the quantitative prediction is influenced by factors other than the variability in the relevant KE _{upstream} measure. Quantitative description does not account for all known modulating factors and/or known feedback/feedforward mechanisms. The quantitative relationship has only been demonstrated for a subset of the overall applicability domain of the KER.	Only a qualitative or semi-quantitative prediction of the change in KE _{down} can be determined from a measure of KE _{up} . Known modulating factors and feedback/feedforward mechanisms are not accounted for. Quantitative relationship has only been demonstrated for a narrow subset of the overall applicability domain of the KER.
MIE#1686 → KE#1392: Deposition of Energy leads to Oxidative Stress	Moderate The quantitative understanding of the MIE leading to oxidative stress is moderate. The most common dose of radiation applied to models when examining the effects of energy deposition on oxidative stress is 2 Gy. In general, exposure to 2 Gy of low LET radiation, such as X-rays, gamma rays, or protons, resulted in increased ROS production compared to high LET radiation, such as heavy ions. 2 Gy of low LET radiation results in increases of ~15-200% to ROS production and ~136-433% to levels of other oxidative stress markers, as well as decreases of ~9-70% to levels of antioxidants, with some studies not demonstrating significant changes to any oxidative stress endpoints. 2 Gy of high LET radiation results in increases of ~120-125% to ROS production.			
KE#1392 → KE#1825: Oxidative Stress leads to Increase, Cell Death	Low The quantitative understanding of oxidative stress leading to cell death is low. Increases of ~20-400% in ROS levels and ~100% in other oxidative stress markers as well as decreases of ~34-75% in antioxidants cause a ~60-440% increase in apoptosis and a ~125% increase in autophagy. Some studies show significant changes to one or more endpoints that are inconsistent with the expected effect of the stressor.			
KE#1392 → KE#2245: Oxidative Stress leads to Altered Cell Differentiation Signaling	Low The quantitative understanding of oxidative stress leading to altered cell differentiation signaling is low. A ~35-260% increase in RONS, a ~20-110% increase in oxidative stress markers (such as malondialdehyde (MDA), protein carbonylation, p67 levels), and/or a ~10-76% decrease in antioxidants results in a ~20-500% increase in expression and activity of osteoclast differentiation signaling molecules and/or a ~10-96% decrease in expression and activity of osteoblast differentiation signaling molecules. Some studies show significant changes to one or more endpoints that are inconsistent with the expected effect of the stressor.			
Non-adjacent KE#1392 → KE#2089: Oxidative Stress leads to Altered Bone Cell Homeostasis	Low The quantitative understanding of oxidative stress leading to altered bone cell homeostasis is low. Many studies quantify oxidative stress and altered bone cell homeostasis following a stressor; however, studies often measure different endpoints in different experimental models and the change to bone cell homeostasis cannot be precisely predicted from the level of oxidative stress. Furthermore, the effect of modulating factors is not well quantified in studies.			
KE#1825 → KE#2089: Increase, Cell Death leads to Altered Bone Cell Homeostasis	Low The quantitative understanding of increased cell death leading to altered bone cell homeostasis is low. Increases of ~100-600% in osteoblast apoptosis and/or ~50-1500% osteocyte apoptosis result in decreases of ~30-63% in osteoblastogenesis markers and ~47-73% in osteoblast/osteocyte number, as well as increases of ~200-250% in osteoclastogenesis markers and ~50-1100% in osteoclast number.			

KE#2245 → KE#2089: Altered Cell Differentiation Signaling leads to Altered Bone Cell Homeostasis	Moderate The quantitative understanding of altered cell differentiation signaling leading to altered bone cell homeostasis is moderate. Altered bone cell homeostasis can be roughly predicted from measures of the protein expression and activity of key signaling molecules for osteoblasts and osteoclasts. Decreases of ~40-90% to expression and activity of osteoblast differentiation signaling molecules result in decreases of ~48.2-93.9% in osteoblastogenesis markers. Increases of ~30-300% to expression and activity of osteoclast differentiation signaling molecules result in increases of ~30-460% in osteoclastogenesis markers.
KE#2089 → KE#2090: Altered Bone Cell Homeostasis leads to Disrupted, Bone Remodeling	Low The quantitative understanding of altered bone cell homeostasis to bone remodeling is low. Decreases of ~17-75% in osteoblastogenesis markers and/or increases of ~22-300% in osteoclastogenesis markers resulted in decreases of ~16-100% in bone formation and increases of ~6-26% in the structural modeling index (SMI). Both microgravity and ionizing radiation exposure have the same effect on altered bone cell homeostasis and bone remodeling markers. However, these effects are more significant for ionizing radiation exposure.
KE#2090 → AO#2091: Disrupted, Bone Remodeling leads to Occurrence, Bone Loss	Low The quantitative understanding of bone remodeling leading to bone loss is low. There is an abundance of quantitative data pertaining to the effects of stressor-induced bone remodeling on bone loss. However, the decreases in bone formation do not precisely predict the resulting bone loss. Decreases of ~20-100% in bone formation and increases of ~6-26% in SMI, cause decreases of ~9-82% in bone structure. Some studies showed changes to one or more endpoints that are inconsistent with the expected effect of the stressor.
Non-adjacent MIE#1686 → KE#2089: Deposition of Energy leads to Altered Bone Cell Homeostasis	Low The quantitative understanding of the deposition of energy leading to altered bone cell homeostasis is low. Many studies quantify altered bone cell homeostasis following radiation exposure; however, it is difficult to compare results and quantify relationships as each study uses different models, stressors, doses and time points. In addition, the influence of modulating factors has not been completely assessed. Thus, no model has been established to predict the changes in bone cell homeostasis after the deposition of energy.
Non-adjacent MIE#1686 → KE#2090: Deposition of Energy leads to Disrupted, Bone Remodeling	Low The quantitative understanding of the deposition of energy leading to bone remodeling is low. Many studies quantify bone remodeling; however, it is difficult to compare results and quantify relationships as each study uses different stressors, doses and time points. In addition, the influence of modulating factors such as sex have not been completely assessed. Thus, no model has been established to predict the changes in bone remodeling after the deposition of energy.
Non-adjacent MIE#1686 → AO#2091: Deposition of Energy leads to Occurrence, Bone Loss	Moderate The quantitative understanding of the deposition of energy leading to bone loss is moderate. Bone loss can be partially predicted by the dose of deposited energy. For example, a 2 Gy dose of ⁵⁶ Fe ions will consistently reduce BV/TV by about 20-30%. However, these changes depend on the bone studied, the dose, the radiation type, and the time point. No model has been established to precisely predict the changes in bone loss after the deposition of energy.

Considerations for Potential Applications of the AOP (optional)

This AOP is one of four built to describe the causal connectivity of KEs leading to adverse health outcomes relevant to space travel and radiotherapy. In constructing the AOP, critical and well-understood biological events and data gaps in empirical evidence were identified. The weight of evidence summary for this AOP can thus be used to justify areas for future work. For example, studies using multi-ion radiation at sustained deliveries and at chronic low doses under microgravity conditions would better represent the space environment and could clarify uncertainties observed in current studies. In addition, a standard range of stressor doses and measurement timepoints would allow for more dose and time response/concordance data and would facilitate more accurate comparisons of evidence between KEs. This should include low doses, as existing low-dose evidence is often inconsistent. Quantitative understanding of each KER could be improved through experiments designed to measure multiple endpoints across dose- and time-ranges. Future studies should also strive to use models that are more applicable for assessing the risks of human space flight, as the proportion of human studies for each KER ranged from 0-33.3%, with only a few KERs containing human studies. In addition, further investigations are needed to consider sex differences in the study design. Gathering sex-specific data would strengthen the understanding of the sex differences within the AOP. The modulating factors and domain of applicability of this AOP can be used to develop risk mitigation strategies.

References

Alwood, J. S. et al. (2010), "Heavy ion irradiation and unloading effects on mouse lumbar vertebral microarchitecture, mechanical properties and tissue stresses", *Bone*, Vol. 47/2, Elsevier, Amsterdam, <https://doi.org/10.1016/j.bone.2010.05.004>

Arfat, Y. et al. (2014), "Physiological Effects of Microgravity on Bone Cells", *Calcified Tissue International*, Vol. 94/6, *Nature*<https://doi.org/10.1007/s00223-014-9851-x>

Ayati, B. P. et al. (2010), "A mathematical model of bone remodeling dynamics for normal bone cell populations and myeloma bone disease", *Biology direct*, Vol. 5/28, <https://doi.org/10.1186/1745-6150-5-28>

Azzam, E. I., J. P. Jay-Gerin, and D. Pain. (2012), "Ionizing radiation-induced oxidative stress and prolonged cell injury", *Cancer letters*, Vol. 327/1-2, Elsevier, Amsterdam, <https://doi.org/10.1016/j.canlet.2011.12.012>

Balasubramanian, D (2000), "Ultraviolet radiation and cataract", *Journal of ocular pharmacology and therapeutics*, Vol. 16/3, Mary Ann Liebert Inc., Larchmont, <https://doi.org/10.1089/jop.2000.16.285>.

Bandstra, E. R. et al. (2009), "Musculoskeletal changes in mice from 2050 cGy of simulated galactic cosmic rays", *Radiation Research*, Vol. 172/1, <https://doi.org/10.1667/RR1509.1>

Bandstra, E. R. et al. (2008), "Long-term dose response of trabecular bone in mice to proton radiation", *Radiation Research*, Vol. 169/6, <https://doi.org/10.1667/RR1310.1>

Baxter, N. N. et al. (2005), "Risk of Pelvic Fractures in Older Women Following Pelvic Irradiation", *JAMA*, Vol. 294/20<https://doi.org/10.1001/jama.294.20.2587>.

Bellido, T. (2014), "Osteocyte-Driven Bone Remodeling", *Calcified Tissue International*, Vol. 94/1, *Nature*<https://doi.org/10.1007/s00223-013-9774-y>.

Bikle, D. D. and B. P. Halloran. (1999), "The response of bone to unloading", *Journal of Bone and Mineral Metabolism*, Vol. 17/4, *Nature*, <https://doi.org/10.1007/s007740050090>.

Boaretti, D. et al. (2023), "Trabecular bone remodeling in the aging mouse: A micro-multiphysics agent-based in silico model using single-cell mechanomics", *Frontiers in bioengineering and biotechnology*, Vol. [11/1091294](https://doi.org/10.3389/fbioe.2023.1091294), <https://doi.org/10.3389/fbioe.2023.1091294>

Boyce, B. F. and L. Xing. (2007), "The RANKL/RANK/OPG pathway", *Current Osteoporosis Reports*, Vol. 5/3, *Nature*<https://doi.org/10.1007/s11914-007-0024-y>

Cao et al (2011). Irradiation induces bone injury by damaging bone marrow microenvironment for stem cells. *Proceedings of the National Academy of Sciences of the United States of America*, 108(4), 1609-1614. <https://doi.org/10.1073/pnas.1015350108>

Chandra, A. et al. (2017), "Suppression of Sclerostin Alleviates Radiation-Induced Bone Loss by Protecting Bone-Forming Cells and Their Progenitors Through Distinct Mechanisms", *Journal of Bone and Mineral Research*, Vol. 32/2, Wiley, <https://doi.org/10.1002/jbmr.2996>.

Chandra, A. et al. (2014), "PTH1-34 alleviates radiotherapy-induced local bone loss by improving osteoblast and osteocyte survival", *Bone*, Vol. 67, Elsevier, Amsterdam, <https://doi.org/10.1016/j.bone.2014.06.030>.

Chatterjee, A., Diordieva, I., Yumoto, K., Globus, R. K., & Bhattacharya, S. (2012). Protein array profiling of mouse serum, six months post whole body radiation with (56)Fe. *The Journal of toxicological sciences*, 37(1), 215-217. <https://doi.org/10.2131/jts.37.215>

Chatziravdeli, V., G. N. Katsaras and G. I. Lambrou. (2019), "Gene Expression in Osteoblasts and Osteoclasts Under Microgravity Conditions: A Systematic Review", *Current Genomics*, Vol. 20/3, Bentham Science Publishers, <https://doi.org/10.2174/1389202920666190422142053>.

Chen, Z. et al. (2020), "Recombinant irisin prevents the reduction of osteoblast differentiation induced by stimulated microgravity through increasing β -catenin expression", *International Journal of Molecular Sciences*, Vol. 21/4, MDPI, Basel, <https://doi.org/10.3390/ijms21041259>

Chen, G., C. Deng and Y.-P. Li. (2012), "TGF- β and BMP Signaling in Osteoblast Differentiation and Bone Formation", *International Journal of Biological Sciences*, Vol. 8/2, Ivspring International Publisher, <https://doi.org/10.7150/ijbs.2929>

Costa S, Reagan MR. (2019). Therapeutic Irradiation: Consequences for Bone and Bone Marrow Adipose Tissue. *Frontiers in endocrinology*, 10, 587.

de Jager, T. L., A. E. Cockrell, S. S. Du Plessis (2017), "Ultraviolet Light Induced Generation of Reactive Oxygen Species", in: *Ultraviolet Light in Human Health, Diseases and Environment*, vol 996. Springer Cham, https://doi.org/10.1007/978-3-319-56017-5_2.

Diao, Y. et al. (2018), "Polyphenols (S3) Isolated from Cone Scales of *Pinus koraiensis* Alleviate Decreased Bone Formation in Rat under Simulated Microgravity", *Scientific Reports*, Vol. 8/1, Nature <https://doi.org/10.1038/s41598-018-30992-8>

Donaubauer, A.-J. et al. (2020), "The Influence of Radiation on Bone and Bone Cells—Differential Effects on Osteoclasts and Osteoblasts", *International Journal of Molecular Sciences*, Vol. 21/17, MDPI, Basel, <https://doi.org/10.3390/ijms21176377>.

Eaton, J. W. (1994), "UV-mediated cataractogenesis: A radical perspective", *Documenta ophthalmologica*, Vol. 88, Springer, London, <https://doi.org/10.1007/BF01203677>.

Fu, J. et al. (2021), "Bone health in spacefaring rodents and primates: systematic review and meta-analysis", *npj Microgravity*, Vol. 7/1, Nature, <https://doi.org/10.1038/s41526-021-00147-7>.

Ganea, E. and J. J. Harding (2006), "Glutathione-related enzymes and the eye", *Current eye research*, Vol. 31/1, Informa, London, <https://doi.org/10.1080/02713680500477347>.

Gerhard, F. A. et al. (2009), "In silico biology of bone modelling and remodelling: adaptation. Philosophical transactions", Series A, Mathematical, physical, and engineering sciences, Vol. 367/1895, 2011-2030. <https://doi.org/10.1098/rsta.2008.0297>

Green, D. E., Adler, B. J., Chan, M. E., & Rubin, C. T. (2012). Devastation of adult stem cell pools by irradiation precedes collapse of trabecular bone quality and quantity. *Journal of bone and mineral research : the official journal of the American Society for Bone and Mineral Research*, 27(4), 749-759. <https://doi.org/10.1002/jbmr.1505>

Greenberger, J. S., & Epperly, M. (2009). Bone marrow-derived stem cells and radiation response. *Seminars in radiation oncology*, 19(2), 133-139. <https://doi.org/10.1016/j.semradonc.2008.11.006>

He, F. et al. (2019), "Irradiation-Induced Osteocyte Damage Promotes HMGB1-Mediated Osteoclastogenesis In Vitro", *Journal of Cellular Physiology*, Vol. 234/10, Wiley, New York City, <https://doi.org/10.1002/jcp.28351>

Holm, T. et al. (1996), "Adjuvant preoperative radiotherapy in patients with rectal carcinoma: Adverse effects during long term follow-up of two randomized trials", *Cancer*, Vol. 78/5, Wiley, [https://doi.org/10.1002/\(SICI\)1097-0142\(19960901\)78:5<968::AID-CNCR5>3.0.CO;2-8](https://doi.org/10.1002/(SICI)1097-0142(19960901)78:5<968::AID-CNCR5>3.0.CO;2-8)

Huang, B. et al. (2019), "Amifostine Suppresses the Side Effects of Radiation on BMSCs by Promoting Cell Proliferation and Reducing ROS Production", *Stem Cells International*, Vol. 2019, Hindawi, <https://doi.org/10.1155/2019/8749090>.

Huang, B. et al. (2018), "Sema3a inhibits the differentiation of Raw264.7 cells to osteoclasts under 2Gy radiation by reducing inflammation", *PLOS ONE*, Vol. 13/7, PLOS, San Francisco, <https://doi.org/10.1371/journal.pone.0200000>.

International Commission on Radiological Protection (ICRP). (2007) Recommendations of the International Commission on Radiological Protection. ICRP Publication 103. *Annals of the ICRP*, 37, 2-4

Ishijima, M. et al. (2001), "Enhancement of Osteoclastic Bone Resorption and Suppression of Osteoblastic Bone Formation in Response to Reduced Mechanical Stress Do Not Occur in the Absence of Osteopontin", *The Journal of Experimental Medicine*, Vol. 193/3, <https://doi.org/10.1084/jem.193.3.399>

Jilka, R. L., B. Noble and R. S. Weinstein. (2013), "Osteocyte Apoptosis", *Bone*, Elsevier, Amsterdam <https://doi.org/10.1016/j.BONE.2012.11.038>.

Karimi, N. et al. (2017), "Radioprotective effect of hesperidin on reducing oxidative stress in the lens tissue of rats", *International Journal of Pharmaceutical Investigation*, Vol. 7/3, https://doi.org/10.4103/ijphi.IPHI_60_17.

Kim S, Kim D, Cho SW, Kim J, Kim JS. (2014). Highly efficient RNA-guided genome editing in human cells via delivery of purified Cas9 ribonucleoproteins. *Genome research*, 24(6), 1012-1019. <https://doi.org/10.1101/gr.171322.113>

Komori, T. (2013), "Functions of the osteocyte network in the regulation of bone mass", *Cell and Tissue Research*, Vol. 352, Nature <https://doi.org/10.1007/s00441-012-1546-x>

Kondo, H. et al. (2010), "Oxidative stress and gamma radiation-induced cancellous bone loss with musculoskeletal disuse", *Journal of Applied Physiology*, Vol. 108/1, American Physiological Society, <https://doi.org/10.1152/japplphysiol.00294.2009>.

Kondo, H. et al. (2009), "Total-body irradiation of postpubertal mice with 137Cs acutely compromises the microarchitecture of cancellous bone and increases osteoclasts", *Radiation Research*, Vol. 171/3, BioOne, <https://doi.org/10.1667/RR1463.1>.

Kook, S.-H. et al. (2015), "Irradiation inhibits the maturation and mineralization of osteoblasts via the activation of Nrf2/HO-1 pathway", *Molecular and Cellular Biochemistry*, Vol. 410/1-2, Nature, <https://doi.org/10.1007/s11010-015-2559-z>.

Kozbenko, T. et al. (2022), "Deploying elements of scoping review methods for adverse outcome pathway development: a space travel case example", *International Journal of Radiation Biology*, Informa, London, <https://doi.org/10.1080/09553002.2022.2110306>

Lang, T. et al. (2017), "Towards human exploration of space: the THESEUS review series on muscle and bone research priorities", *npj Microgravity*, Vol. 3/1, Nature, <https://doi.org/10.1038/s41526-017-0013-0>.

Lewiecki, E. M. et al. (2019), "Healthcare Policy Changes in Osteoporosis Can Improve Outcomes and Reduce Costs in the United States", *JBMR Plus*, Vol. 3/9, Wiley, <https://doi.org/10.1002/jbm4.10192>.

Li, J. et al. (2020a), "Effect of α 2-macroglobulin in the early stage of jaw osteoradionecrosis", *International Journal of Oncology*, Vol. 57/1, Spandidos Publications, <https://doi.org/10.3892/ijio.2020.5051>

Li, R. et al. (2020b), "Effect of autophagy on irradiation-induced damage in osteoblast-like MC3T3-E1 cells", *Molecular Medicine Reports*, Spandidos Publications, <https://doi.org/10.3892/mmr.2020.11425>

Li, J. et al. (2018a), "Protective role of α 2-macroglobulin against jaw osteoradionecrosis in a preclinical rat model", *Journal of Oral Pathology and Medicine*, 48/2, Wiley, <https://doi.org/10.1111/jop.12809>

Li, W. Y. et al. (2018b), "Pulsed electromagnetic fields prevented the decrease of bone formation in hindlimb-suspended rats by activating sAC/cAMP/PKA/CREB signaling pathway", *Bioelectromagnetics*, Vol. 39/8, Wiley, <https://doi.org/10.1002/bem.22150>

Li, X. F. et al. (2015), "Inhibitory effects of autologous γ -irradiated cell conditioned medium on osteoblasts in vitro", *Molecular Medicine Reports*, Vol. 12/1, Spandidos Publications, <https://doi.org/10.3892/mmr.2015.3354>

Liu, Y. et al. (2018), "Protective effects of α -2-macroglobulin on human bone marrow mesenchymal stem cells in radiation injury", *Molecular Medicine Reports*, Spandidos Publications, <https://doi.org/10.3892/mmr.2018.9449>.

Lloyd SA, Bandstra ER, Travis ND, et al. (2008). Spaceflight-relevant types of ionizing radiation and cortical bone: Potential LET effect?. *Advances in space research* : the official journal of the Committee on Space Research (COSPAR), 42(12), 1889-1897. <https://doi.org/10.1016/j.asr.2008.08.006>

Lloyd, S. A. et al. (2015), "Osteoprotegerin is an effective countermeasure for spaceflight-induced bone loss in mice", *Bone*, Vol. 81, Elsevier, Amsterdam, <https://doi.org/10.1016/j.bone.2015.08.021>.

Maeda, K. et al. (2019), "The Regulation of Bone Metabolism and Disorders by Wnt Signaling", *International Journal of Molecular Sciences*, Vol. 20/22, MDPI, Basel, <https://doi.org/10.3390/ijms2022525>.

Manolagas, S. C. and M. Almeida. (2007), "Gone with the Wnts: β -Catenin, T-Cell Factor, Forkhead Box O, and Oxidative Stress in Age-Dependent Diseases of Bone, Lipid, and Glucose Metabolism", *Molecular Endocrinology*, Vol. 21/11, Oxford University Press, Oxford, <https://doi.org/10.1210/me.2007-0259>.

Morey-Holton, E. and S. B. Arnaud. (1991), "NASA Technical Memorandum 103890".

Moussa, M. S., M. Goldsmith and S. V. Komarova. (2022), "Craniofacial Bones and Teeth in Spacefarers: Systematic Review and Meta-analysis", *JDR Clinical & Translational Research*, SAGE, <https://doi.org/10.1177/23800844221084985>.

Nagane, M. et al. (2021), "DNA damage response in vascular endothelial senescence: Implication for radiation-induced cardiovascular diseases", *Journal of radiation research*, Vol. 62/4, Oxford University Press, Oxford, <https://doi.org/10.1093/jrr/rab032>

Nishiyama, K. et al. (1992), "Radiation osteoporosis? An assessment using single energy quantitative computed tomography", *European Radiology*, Vol. 2/4, *Nature*, <https://doi.org/10.1007/BF00175435>.

O'Brien, C. A., T. Nakashima and H. Takayanagi (2013), "Osteocyte control of osteoclastogenesis", *Bone*, Vol. 54/2, Elsevier, Amsterdam, <https://doi.org/10.1016/j.bone.2012.08.121>

Oeffinger, K. C. et al. (2006), "Chronic Health Conditions in Adult Survivors of Childhood Cancer", *New England Journal of Medicine*, Vol. 355/15, <https://doi.org/10.1056/NEJMsa060185>

Oest, M. E., Franken, V., Kuchera, T., Strauss, J., & Damron, T. A. (2015). Long-term loss of osteoclasts and unopposed cortical mineral apposition following limited field irradiation. *Journal of orthopaedic research : official publication of the Orthopaedic Research Society*, 33(3), 334-342. <https://doi.org/10.1002/jor.22761>

Oest, M. E., et al. (2018), "Longitudinal Effects of Single Hindlimb Radiation Therapy on Bone Strength and Morphology at Local and Contralateral Sites" *Journal of bone and mineral research*, Vol. 33/1, <https://doi.org/10.1002/jbm.3289>

Otsuka, K., Koana, T., Tomita, M., Ogata, H., & Tauchi, H. (2008). Rapid myeloid recovery as a possible mechanism of whole-body radioadaptive response. *Radiation research*, 170(3), 307-315. <https://doi.org/10.1667/RR1146.1>

Overgaard, M. (1988), "Spontaneous Radiation-Induced Rib Fractures in Breast Cancer Patients Treated with Postmastectomy Irradiation—A Clinical Radiobiological Analysis of the Influence of Fraction Size and Dose-Response Relationships on Late Bone Damage", *Acta Oncologica*, Vol. 27/2, Informa, London, <https://doi.org/10.3109/02841868809090331>

Pacheco, R. and H. Stock. (2013), "Effects of Radiation on Bone", *Current Osteoporosis Reports*, Vol. 11/4, *Nature* <https://doi.org/10.1007/s11914-013-0174-z>.

Padgaonkar, V. A. et al. (2015) "Thioredoxin reductase activity may be more important than GSH level in protecting human lens epithelial cells against UVA light", *Photochemistry and photobiology*, Vol. 91/2, Wiley-Blackwell, Hoboken, <https://doi.org/10.1111/php.12404>

Ping, Z. et al. (2020), "Oxidative Stress in Radiation-Induced Cardiotoxicity", *Oxidative Medicine and Cellular Longevity*, Vol. 2020, Hindawi, London, <https://doi.org/10.1155/2020/3579143>

Plotkin, L. I. (2014), "Apoptotic osteocytes and the control of Targeted Bone Resorption", *Current Osteoporosis Reports*, Vol. 12/1, *Nature*, <https://doi.org/10.1007/s11914-014-0194-3>

Rachner, T. D., S. Khosla and L. C. Hofbauer. (2011), "Osteoporosis: now and the future", *The Lancet*, Vol. 377/9773, Elsevier, Amsterdam, [https://doi.org/10.1016/S0140-6736\(10\)62349-5](https://doi.org/10.1016/S0140-6736(10)62349-5)

Rastogi, S., Coates, P. J., Lorimore, S. A., & Wright, E. G. (2012). Bystander-type effects mediated by long-lived inflammatory signaling in irradiated bone marrow. *Radiation research*, 177(3), 244-250. <https://doi.org/10.1667/rr2805.1>

Rehman, M. U. et al. (2016), "Comparison of free radicals formation induced by cold atmospheric plasma, ultrasound, and ionizing radiation", *Archives of biochemistry and biophysics*, Vol. 605, Elsevier, Amsterdam, <https://doi.org/10.1016/j.abb.2016.04.005>.

Riggs, B. L., S. Khosla and L. J. Melton. (1998), "A Unitary Model for Involutorial Osteoporosis: Estrogen Deficiency Causes Both Type I and Type II Osteoporosis in Postmenopausal Women and Contributes to Bone Loss in Aging Men", *Journal of Bone and Mineral Research*, Vol. 13, Wiley <https://doi.org/10.1359/jbmr.1998.13.5.763>

Rucci, N. et al. (2007), "Modeled microgravity stimulates osteoclastogenesis and bone resorption by increasing osteoblast RANKL/OPG ratio", *Journal of Cellular Biochemistry*, Vol. 100/2, Wiley, <https://doi.org/10.1002/jcb.21059>

Sambandam, Y. et al. (2016), "Microgravity Induction of TRAIL Expression in Preosteoclast Cells Enhances Osteoclast Differentiation", *Scientific Reports*, Vol. 6, *Nature*, <https://doi.org/10.1038/srep25143>

Schmidt-Ullrich, R. K. et al. (2000), "Signal transduction and cellular radiation responses.", *Radiation research*, Vol. 153/3, BioOne [https://doi.org/10.1667/0033-7587\(2000\)153\[0245:stacr\]2.0.co;2](https://doi.org/10.1667/0033-7587(2000)153[0245:stacr]2.0.co;2)

Smith, B. J. et al. (2002), "Skeletal unloading and dietary copper depletion are detrimental to bone quality of mature rats", *The Journal of nutrition*, Vol. 132/2, 190-196. <https://doi.org/10.1093/jn/132.2.190>

Smith, J. K. (2020a), "Microgravity, Bone Homeostasis, and Insulin-Like Growth Factor-1", *Applied Sciences*, Vol. 10/13, MDPI, Basel, <https://doi.org/10.3390/app10134433>.

Smith, J. K. (2020b), "Osteoclasts and microgravity", *Life*, Vol. 10/9, MDPI, Basel, <https://doi.org/10.3390/life10090207>

Smith, S. M. et al. (2014), "Men and Women in Space: Bone Loss and Kidney Stone Risk After Long-Duration Spaceflight", *Journal of Bone and Mineral Research*, Vol. 29/7, The American Society for Bone and Mineral Research, <https://doi.org/10.1002/jbm.2185>

Smith, S. M. et al. (2015), "Bone metabolism and renal stone risk during International Space Station missions", *Bone*, Vol. 81, 712-720. <https://doi.org/10.1016/j.bone.2015.10.002>

Sozen, T., L. Ozisik and N. Calik Basaran. (2017), "An overview and management of osteoporosis", *European Journal of Rheumatology*, Vol. 4/1, <https://doi.org/10.5152/eurirheum.2016.048>.

Stavnichuk, M. et al. (2020), "A systematic review and meta-analysis of bone loss in space travelers", *npj Microgravity*, Vol. 6/1, *Nature*, <https://doi.org/10.1038/s41526-020-0103-2>.

Sugimoto, M., Takahashi, S., Toguchida, J., Kotoura, Y., Shibamoto, Y., & Yamamoto, T. (1991). Changes in bone after high-dose irradiation. *Biomechanics and histomorphology*, The Journal of bone and joint surgery. British volume, 73(3), 492-497. <https://doi.org/10.1302/0301-620X.73B3.1670456>

Sun, Y. et al. (2013), "Treatment of hydrogen molecule abates oxidative stress and alleviates bone loss induced by modeled microgravity in rats", *Osteoporosis International*, Vol. 24/3, *Nature*, <https://doi.org/10.1007/s00198-012-2028-4>.

Suva LJ, Seedor JG, Endo N, et al. (1993). Pattern of gene expression following rat tibial marrow ablation. *Journal of bone and mineral research : the official journal of the American Society for Bone and Mineral Research*, 8(3), 379-388. <https://doi.org/10.1002/jbmr.5650080315>

Tatara, Y., & Monzen, S. (2023). Proteomics and secreted lipidomics of mouse-derived bone marrow cells exposed to a lethal level of ionizing radiation. *Scientific reports*, 13(1), 8802. <https://doi.org/10.1038/s41598-023-35924-9>

Tian, Y. et al. (2017), "The impact of oxidative stress on the bone system in response to the space special environment", *International Journal of Molecular Sciences*, Vol. 18/10, MDPI, Basel, <https://doi.org/10.3390/ijms18102132>.

Turner, M. R., Bowser, R., Bruijn, L., Dupuis, L., Ludolph, A., McGrath, M., Manfredi, G., Maragakis, N., Miller, R. G., Pullman, S. L., Rutkove, S. B., Shaw, P. J., Shefner, J., & Fischbeck, K. H. (2013). Mechanisms, models and biomarkers in amyotrophic lateral sclerosis. *Amyotrophic lateral sclerosis & frontotemporal degeneration*, 14 Suppl 1(0 1), 19-32. <https://doi.org/10.3109/21678421.2013.778554>

Valerie, K. et al. (2007), "Radiation-induced cell signaling: inside-out and outside-in", *Molecular Cancer Therapeutics*, Vol. 6/3, American Association for Cancer Research, <https://doi.org/10.1158/1535-7163.MCT-06-0596>

Varma, S. D. et al. (2011), "Role of ultraviolet irradiation and oxidative stress in cataract formation-medical prevention by nutritional antioxidants and metabolic agonists", *Eye & contact lens*, Vol. 37/4, Lippincot Williams & Wilkins, Philadelphia, <https://doi.org/10.1097/ICL.0b013e31821ec4f2>.

Vico, L. and A. Hargens. (2018), "Skeletal changes during and after spaceflight", *Nature Reviews Rheumatology*, Vol. 14, Nature, <https://doi.org/10.1038/nrrheum.2018.37>

Wang, Y. et al. (2020), "Targeted Overexpression of the Long Noncoding RNA ODSM can Regulate Osteoblast Function In Vitro and In Vivo", *Cell Death and Disease*, Vol. 11, Springer Nature, Berlin, <https://doi.org/10.1038/s41419-020-2325-3>

Wang, C. et al. (2016), "Protective effects of cerium oxide nanoparticles on MC3T3-E1 osteoblastic cells exposed to X-ray irradiation", *Cellular Physiology and Biochemistry*, Vol. 38/4, Karger, Basel, <https://doi.org/10.1159/000443092>

Wernle, J. D., Damron, T. A., Allen, M. J., & Mann, K. A. (2010). Local irradiation alters bone morphology and increases bone fragility in a mouse model. *Journal of biomechanics*, 43(14), [2738-2746](https://doi.org/10.1016/j.jbiomech.2010.06.017). <https://doi.org/10.1016/j.jbiomech.2010.06.017>

Willey, J. S. et al. (2021), "The individual and combined effects of spaceflight radiation and microgravity on biologic systems and functional outcomes", *Journal of environmental science and health. Part C*, Vol. 39/2, Informa, London, <https://doi.org/10.1080/26896583.2021.1885283>

Willey, J. S. et al. (2011), "Ionizing Radiation and Bone Loss: Space Exploration and Clinical Therapy Applications", *Clinical Reviews in Bone and Mineral Metabolism*, Vol. 9, Nature, <https://doi.org/10.1007/s12018-011-9092-8>.

Willey, J. S. et al. (2010), "Risedronate prevents early radiation-induced osteoporosis in mice at multiple skeletal locations", *Bone*, Vol. 46/1, Elsevier, <https://doi.org/10.1016/j.bone.2009.09.002>.

Willey, J. S., Lloyd, S.A.J. and Bateman, T.A (2013). 'Radiation Therapy-Induced Osteoporosis.' in C.J. Rosen (ed.), *Primer on the Metabolic Bone Diseases and Disorders of Mineral Metabolism*, Eighth Edition (John Wiley & Sons, Inc: ASBMR).

Williams, H. J. and A. M. Davies. (2006), "The effect of X-rays on bone: a pictorial review", *European Radiology*, Vol. 16/3, Nature <https://doi.org/10.1007/s00330-005-0010-7>.

Wissing, M. D. (2015), "Chemotherapy- and Irradiation-Induced Bone Loss in Adults with Solid Tumors", *Current Osteoporosis Reports*, Vol. 13/3, Nature, <https://doi.org/10.1007/s11914-015-0266-z>.

Wortel, R. C. et al. (2019), "Sildenafil Protects Endothelial Cells From Radiation-Induced Oxidative Stress", *The Journal of Sexual Medicine*, Vol. 16/11, Elsevier, Amsterdam, <https://doi.org/10.1016/j.jsxm.2019.08.015>

Wright, L. E. (2018) *Radiotherapy-Induced Osteoporosis.* in J.P. Bilezikian (ed.), *Primer on the Metabolic Bone Diseases and Disorders of Mineral Metabolism*, Ninth edition (John Wiley & Sons, Inc: ASBMR).

Wright, L. E. et al. (2015), "Single-Limb Irradiation Induces Local and Systemic Bone Loss in a Murine Model", *Journal of Bone and Mineral Research*, Vol. 108/2, Wiley, <https://doi.org/10.1002/jbmr.2458>.

Xin, M. et al. (2015), "Attenuation of hind-limb suspension-induced bone loss by curcumin is associated with reduced oxidative stress and increased vitamin D receptor expression", *Osteoporosis International*, Vol. 26/11, Nature, <https://doi.org/10.1007/s00198-015-3153-7>

Xiong, J. and C. A. O'Brien. (2012), "Osteocyte RANKL: New Insights into the Control of Bone Remodeling", *Journal of Bone Mineral Research*, Vol. 27/3, Wiley, <https://doi.org/10.1002/jbmr.1547>

Yang, J. et al. (2020), "Blocking Glucocorticoid Signaling in Osteoblasts and Osteocytes Prevents Mechanical Unloading-Induced Cortical Bone Loss", *Bone*, Vol. 130, Elsevier, Amsterdam, <https://doi.org/10.1016/j.bone.2019.115108>

Yang, M. et al. (2019), "Treatment with hydrogen sulfide donor attenuates bone loss induced by modeled microgravity", *Canadian Journal of Physiology and Pharmacology*, Vol. 97/7, Canadian Science Publishing, <https://doi.org/10.1139/cjpp-2018-0521>.

Yoo, Y. M., T. Y. Han and H. S. Kim. (2016), "Melatonin suppresses autophagy induced by clinostat in preosteoblast MC3T3-E1 cells", *International Journal of Molecular Sciences*, Vol. 17/4, MDPI, Basel, <https://doi.org/10.3390/ijms17040526>

Yotsumoto, N., M. Takeoka and M. Yokoyama. (2010), "Tail-suspended mice lacking calponin H1 experience decreased bone loss.", *The Tohoku journal of experimental medicine*, Vol. 221/3, Tohoku University Medical Press, Tohoku, <https://doi.org/10.1620/tjem.221.221>

Zerath, E. et al. (2002), "Spaceflight affects bone formation in rhesus monkeys: a histological and cell culture study", *Journal of Applied Physiology*, Vol. 93/3, American Physiological Society, <https://doi.org/10.1152/japplphysiol.00610.2001>

Zhai, et al. (2019), "Influence of radiation exposure pattern on the bone injury and osteoclastogenesis in a rat model", *International journal of molecular medicine*, Vol. 44/6, Spandidos Publications, <https://doi.org/10.3892/ijmm.2019.4369>

Zhang, L. et al. (2020), "Amifostine inhibited the differentiation of RAW264.7 cells into osteoclasts by reducing the production of ROS under 2 Gy radiation", *Journal of Cellular Biochemistry*, Vol. 121/1, Wiley, <https://doi.org/10.1002/jcb.29247>.

Zhang, J. et al. (2019), "Lowering iron level protects against bone loss in focally irradiated and contralateral femurs through distinct mechanisms", *Bone*, Vol. 120, Elsevier, <https://doi.org/10.1016/j.bone.2018.10.005>.

Zhou, Z. et al. (2008), "HMGB1 Regulates RANKL-Induced Osteoclastogenesis in a Manner Dependent on RAGE", *Journal of Bone and Mineral Research*, Vol. 23/7, Wiley, <https://doi.org/10.1359/jbmr.080234>

Zigman, S. et al. (2000), "Effects of intermittent UVA exposure on cultured lens epithelial cells", *Current Eye Research*, Vol. 20/2, Informa UK Limited, London, [https://doi.org/10.1076/0271-3683\(200002\)2021-DFT095](https://doi.org/10.1076/0271-3683(200002)2021-DFT095).

Zou, Q., et al. (2016), "Bone marrow stem cell dysfunction in radiation-induced abscopal bone loss", *Journal of orthopaedic surgery and research*, Vol. 11, Nature, <https://doi.org/10.1186/s13018-015-0339-9>

Appendix 1

List of MIEs in this AOP

Event: 1686: Deposition of Energy

Short Name: Energy Deposition

Key Event Component

Process	Object	Action
energy deposition event		increased

AOPs Including This Key Event

AOP ID and Name	Event Type
Aop:272 - Deposition of energy leading to lung cancer	MolecularInitiatingEvent
Aop:432 - Deposition of Energy by Ionizing Radiation leading to Acute Myeloid Leukemia	MolecularInitiatingEvent
Aop:386 - Deposition of ionizing energy leading to population decline via inhibition of photosynthesis	MolecularInitiatingEvent
Aop:387 - Deposition of ionising energy leading to population decline via mitochondrial dysfunction	MolecularInitiatingEvent
Aop:388 - Deposition of ionising energy leading to population decline via programmed cell death	MolecularInitiatingEvent
Aop:435 - Deposition of ionising energy leads to population decline via pollen abnormal	MolecularInitiatingEvent
Aop:216 - Deposition of energy leading to population decline via DNA strand breaks and follicular atresia	MolecularInitiatingEvent
Aop:238 - Deposition of energy leading to population decline via DNA strand breaks and oocyte apoptosis	MolecularInitiatingEvent
Aop:311 - Deposition of energy leading to population decline via DNA oxidation and oocyte apoptosis	MolecularInitiatingEvent
Aop:299 - Deposition of energy leading to population decline via DNA oxidation and follicular atresia	MolecularInitiatingEvent
Aop:441 - Ionizing radiation-induced DNA damage leads to microcephaly via apoptosis and premature cell differentiation	MolecularInitiatingEvent
Aop:444 - Ionizing radiation leads to reduced reproduction in <i>Eisenia fetida</i> via reduced spermatogenesis and cocoon hatchability	MolecularInitiatingEvent
Aop:470 - Deposition of energy leads to abnormal vascular remodeling	MolecularInitiatingEvent
Aop:473 - Energy deposition from internalized Ra-226 decay lower oxygen binding capacity of hemocyanin	MolecularInitiatingEvent
Aop:478 - Deposition of energy leading to occurrence of cataracts	MolecularInitiatingEvent
Aop:482 - Deposition of energy leading to occurrence of bone loss	MolecularInitiatingEvent
Aop:483 - Deposition of Energy Leading to Learning and Memory Impairment	MolecularInitiatingEvent

Stressors

Name
Ionizing Radiation

Biological Context**Level of Biological Organization**

Molecular

Domain of Applicability**Taxonomic Applicability**

Term	Scientific Term	Evidence	Links
human	<i>Homo sapiens</i>	Moderate	NCBI
rat	<i>Rattus norvegicus</i>	Moderate	NCBI
mouse	<i>Mus musculus</i>	Moderate	NCBI
nematode	<i>Caenorhabditis elegans</i>	High	NCBI
zebrafish	<i>Danio rerio</i>	High	NCBI
thale-cress	<i>Arabidopsis thaliana</i>	High	NCBI
Scotch pine	<i>Pinus sylvestris</i>	Moderate	NCBI
Daphnia magna	<i>Daphnia magna</i>	High	NCBI
Chlamydomonas reinhardtii	<i>Chlamydomonas reinhardtii</i>	Moderate	NCBI
common bradling worm	<i>eisenia fetida</i>	Moderate	NCBI
Lemna minor	<i>Lemna minor</i>	High	NCBI
Salmo salar	<i>Salmo salar</i>	Low	NCBI

Life Stage Applicability**Life Stage Evidence**

All life stages	High
-----------------	------

Sex Applicability**Sex Evidence**

Unspecific	Low
------------	-----

Energy can be deposited into any substrate, both living and non-living; it is independent of age, taxa, sex, or life-stage.

Taxonomic applicability: This MIE is not taxonomically specific.**Life stage applicability:** This MIE is not life stage specific.**Sex applicability:** This MIE is not sex specific.

Key Event Description

Deposition of energy refers to events where energetic subatomic particles, nuclei, or electromagnetic radiation deposit energy in the media through which they transverse. The energy may either be sufficient (e.g. ionizing radiation) or insufficient (e.g. non-ionizing radiation) to ionize atoms or molecules (Beir et al., 1999).

Ionizing radiation can cause the ejection of electrons from atoms and molecules, thereby resulting in their ionization and the breakage of chemical bonds. The excitation of molecules can also occur without ionization. These events are stochastic and unpredictable. The energy of these subatomic particles or electromagnetic waves ranges from 124 keV to 5.4 MeV and is dependent on the source and type of radiation (Zyla et al., 2020). Not all electromagnetic radiation is ionizing; as the incident radiation must have sufficient energy to free electrons from the electron orbitals of the atom or molecule. The energy deposited can induce direct and indirect ionization events and can result from internal (injections, inhalation, ingestion) or external exposure.

Direct ionization is the principal path where charged particles interact with biological structures such as DNA, proteins or membranes to cause biological damage. Photons, which are electromagnetic waves can also deposit energy to cause direct which themselves can indirectly damage critical targets such as DNA (Beir et al., 1999; Balagamwala et al., 2013) or alter cellular processes. Given the fundamental nature of energy deposition by radioactive/unstable nuclei, nucleons or elementary particles in material, this process is universal to all biological contexts.

The spatial structure of ionizing energy deposition along the resulting particle track is represented as linear energy transfer (LET) (Hall and Giaccia, 2018 UNSCEAR, 2020). High LET refers to energy mostly above 10 keV μm^{-1} which produces more complex, dense structural damage than low LET radiation (below 10 keV μm^{-1}). Low-LET particles produce sparse ionization events such as photons (X- and gamma rays), as well as high-energy protons. Low LET radiation travels farther into tissue but deposits smaller amounts of energy, whereas high LET radiation, which includes heavy ions, alpha particles and high-energy neutrons, does not travel as far but deposits larger amounts of energy into tissue at the same absorbed dose. The biological effect of the deposition of energy can be modulated by varying dose and dose rate of exposure, such as acute, chronic, or fractionated exposures (Hall and Giaccia, 2018).

Non-ionizing radiation is electromagnetic waves that does not have enough energy to break bonds and induce ion formation but it can cause molecules to excite and vibrate faster resulting in biological effects. Examples of non-ionizing radiation include radio waves (wavelength: 100 km-1m), microwaves (wavelength: 1m-1mm), infrared radiation (wavelength: 1mm- 1 um), visible light (wavelengths: 400-700 nm), and ultraviolet radiation of longer wavelengths such as UVB (wavelengths: 315-400nm) and UVA (wavelengths: 280-315 nm).

How it is Measured or Detected

Radiation type	Assay Name	References	Description	OECD Approved Assay
Ionizing radiation	Monte Carlo Simulations (eg. Geant4)	Douglass et al., 2013; Douglass et al., 2012; Zyla et al., 2020	Monte Carlo simulations are based on a computational algorithm that mathematically models the deposition of energy into materials.	No
Ionizing radiation	Fluorescent Nuclear Track Detector (FNTD)	Sawakuchi, 2016; Niklas, 2013; Kodaira & Konishi, 2015	FNTDs are biocompatible chips with crystals of aluminum oxide doped with carbon and magnesium; used in conjunction with fluorescent microscopy, these FNTDs allow for the visualization and the linear energy transfer (LET) quantification of tracks produced by the deposition of energy into a material.	No
Ionizing radiation	Tissue equivalent proportional counter (TEPC)	Straume et al, 2015	Measure the LET spectrum and calculate the equivalent dose	No
Ionizing radiation	alanine dosimeters/NanoDots	Lind et al. 2019 Xie et al., 2022	Alanine dosimeters use the amino acid alanine to detect radiation-induced changes, and nanodots leverage nano-scale technology to provide high precision and sensitivity in radiation dose measurements	No
Non-ionizing radiation	UV meters or radiometers	Xie et al., 2020	UVA/UVB (irradiance intensity), UV dosimeters (accumulated irradiance over time), Spectrophotometer (absorption of UV by a substance or material)	No

References

Balagamwala, E. H. et al. (2013), "Introduction to radiotherapy and standard teletherapy techniques", *Dev Ophthalmol*, Vol. 52, Karger, Basel, <https://doi.org/10.1159/000351045>

Beir, V. et al. (1999), "The Mechanistic Basis of Radon-Induced Lung Cancer", in *Health Risks of Exposure to Radon: BEIR VI*, National Academy Press, Washington, D.C., <https://doi.org/10.17226/5499>

Douglass, M. et al. (2013), "Monte Carlo investigation of the increased radiation deposition due to gold nanoparticles using kilovoltage and megavoltage photons in a 3D randomized cell model", *Medical Physics*, Vol. 40/7, American Institute of Physics, College Park, <https://doi.org/10.1118/1.4808150>

Douglass, M. et al. (2012), "Development of a randomized 3D cell model for Monte Carlo microdosimetry simulations.", *Medical Physics*, Vol. 39/6, American Institute of Physics, College Park, <https://doi.org/10.1118/1.4719963>

Hall, E. J. and Giaccia, A.J. (2018), *Radiobiology for the Radiologist*, 8th edition, Wolters Kluwer, Philadelphia.

Kodaira, S. and Konishi, T. (2015), "Co-visualization of DNA damage and ion traversals in live mammalian cells using a fluorescent nuclear track detector.", *Journal of Radiation Research*, Vol. 56/2, Oxford University Press, Oxford, <https://doi.org/10.1093/jrr/rru091>

Lind, O.C., D.H. Oughton and Salbu B. (2019), "The NMBU FIGARO low dose irradiation facility", *International Journal of Radiation Biology*, Vol. 95/1, Taylor & Francis, London, <https://doi.org/10.1080/09553002.2018.1516906>.

Sawakuchi, G.O. and Akselrod, M.S. (2016), "Nanoscale measurements of proton tracks using fluorescent nuclear track detectors.", *Medical Physics*, Vol. 43/5, American Institute of Physics, College Park, <https://doi.org/10.1118/1.4947128>

Straume, T. et al. (2015), "Compact Tissue-equivalent Proportional Counter for Deep Space Human Missions.", *Health Physics*, Vol. 109/4, Lippincott Williams & Wilkins, Philadelphia, <https://doi.org/10.1097/HP.0000000000000334>

Niklas, M. et al. (2013), "Engineering cell-fluorescent ion track hybrid detectors.", *Radiation Oncology*, Vol. 8/104, BioMed Central, London, <https://doi.org/10.1186/1748-717X-8-141>

UNSCEAR (2020), *Sources, effects and risks of ionizing radiation*, United Nations.

Xie, Li. et al. (2022), "Ultraviolet B Modulates Gamma Radiation-Induced Stress Responses in *Lemna Minor* at Multiple Levels of Biological Organisation", *SSRN*, Elsevier, Amsterdam, <http://dx.doi.org/10.2139/ssrn.4081705>

Zyla, P.A. et al. (2020), *Review of particle physics: Progress of Theoretical and Experimental Physics*, 2020 Edition, Oxford University Press, Oxford.

List of Key Events in the AOP**Event: 1392: Oxidative Stress**

Short Name: Oxidative Stress**Key Event Component**

Process	Object	Action
oxidative stress		increased

AOPs Including This Key Event

AOP ID and Name	Event Type
Aop:220 - Cyp2E1 Activation Leading to Liver Cancer	KeyEvent
Aop:17 - Binding of electrophilic chemicals to SH(thiol)-group of proteins and /or to seleno-proteins involved in protection against oxidative stress during brain development leads to impairment of learning and memory	KeyEvent
Aop:284 - Binding of electrophilic chemicals to SH(thiol)-group of proteins and /or to seleno-proteins involved in protection against oxidative stress leads to chronic kidney disease	KeyEvent
Aop:377 - Dysregulated prolonged Toll Like Receptor 9 (TLR9) activation leading to Multi Organ Failure involving Acute Respiratory Distress Syndrome (ARDS)	KeyEvent
Aop:411 - Oxidative stress Leading to Decreased Lung Function	MolecularInitiatingEvent
Aop:424 - Oxidative stress Leading to Decreased Lung Function via CFTR dysfunction	MolecularInitiatingEvent
Aop:425 - Oxidative Stress Leading to Decreased Lung Function via Decreased FOXJ1	MolecularInitiatingEvent
Aop:429 - A cholesterol/glucose dysmetabolism initiated Tau-driven AOP toward memory loss (AO) in sporadic Alzheimer's Disease with plausible MIE's plug-ins for environmental neurotoxicants	KeyEvent
Aop:452 - Adverse outcome pathway of PM-induced respiratory toxicity	KeyEvent
Aop:464 - Calcium overload in dopaminergic neurons of the substantia nigra leading to parkinsonian motor deficits	KeyEvent
Aop:470 - Deposition of energy leads to abnormal vascular remodeling	KeyEvent
Aop:478 - Deposition of energy leading to occurrence of cataracts	KeyEvent
Aop:479 - Mitochondrial complexes inhibition leading to left ventricular function decrease via increased myocardial oxidative stress	KeyEvent
Aop:481 - AOPs of amorphous silica nanoparticles: ROS-mediated oxidative stress increased respiratory dysfunction and diseases.	KeyEvent
Aop:482 - Deposition of energy leading to occurrence of bone loss	KeyEvent
Aop:483 - Deposition of Energy Leading to Learning and Memory Impairment	KeyEvent
Aop:505 - Reactive Oxygen Species (ROS) formation leads to cancer via inflammation pathway	KeyEvent
Aop:521 - Essential element imbalance leads to reproductive failure via oxidative stress	KeyEvent
Aop:26 - Calcium-mediated neuronal ROS production and energy imbalance	AdverseOutcome
Aop:488 - Increased reactive oxygen species production leading to decreased cognitive function	KeyEvent
Aop:396 - Deposition of ionizing energy leads to population decline via impaired meiosis	KeyEvent
Aop:437 - Inhibition of mitochondrial electron transport chain (ETC) complexes leading to kidney toxicity	KeyEvent
Aop:535 - Binding and activation of GPER leading to learning and memory impairments	KeyEvent
Aop:171 - Chronic cytotoxicity of the serous membrane leading to pleural/peritoneal mesotheliomas in the rat.	KeyEvent
Aop:138 - Organic anion transporter (OAT1) inhibition leading to renal failure and mortality	KeyEvent
Aop:177 - Cyclooxygenase 1 (COX1) inhibition leading to renal failure and mortality	KeyEvent
Aop:186 - unknown MIE leading to renal failure and mortality	KeyEvent
Aop:200 - Estrogen receptor activation leading to breast cancer	KeyEvent
Aop:444 - Ionizing radiation leads to reduced reproduction in Eisenia fetida via reduced spermatogenesis and cocoon hatchability	KeyEvent
Aop:447 - Kidney failure induced by inhibition of mitochondrial electron transfer chain through apoptosis, inflammation and oxidative stress pathways	KeyEvent
Aop:476 - Adverse Outcome Pathways diagram related to PBDEs associated male reproductive toxicity	KeyEvent
Aop:497 - ERα inactivation alters mitochondrial functions and insulin signalling in skeletal muscle and leads to insulin resistance and metabolic syndrome	KeyEvent
Aop:457 - Succinate dehydrogenase inhibition leading to increased insulin resistance through reduction in circulating thyroxine	KeyEvent
Aop:459 - AhR activation in the thyroid leading to Subsequent Adverse Neurodevelopmental Outcomes in Mammals	KeyEvent
Aop:507 - Nrf2 inhibition leading to vascular disrupting effects via inflammation pathway	KeyEvent
Aop:509 - Nrf2 inhibition leading to vascular disrupting effects through activating apoptosis signal pathway and mitochondrial dysfunction	KeyEvent
Aop:510 - Demethylation of PPAR promotor leading to vascular disrupting effects	KeyEvent
Aop:511 - The AOP framework on ROS-mediated oxidative stress induced vascular disrupting effects	KeyEvent
Aop:538 - Adverse outcome pathway of PFAS-induced vascular disrupting effects via activating oxidative stress related pathways	KeyEvent
Aop:260 - CYP2E1 activation and formation of protein adducts leading to neurodegeneration	KeyEvent
Aop:450 - Inhibition of AChE and activation of CYP2E1 leading to sensory axonal peripheral neuropathy and mortality	KeyEvent
Aop:501 - Excessive iron accumulation leading to neurological disorders	KeyEvent
Aop:540 - Oxidative Stress in the Fish Ovary Leads to Reproductive Impairment via Reduced Vitellogenin Production	KeyEvent
Aop:471 - Various neuronal effects induced by elavl3, sox10, and mbp	KeyEvent
Aop:31 - Oxidation of iron in hemoglobin leading to hematotoxicity	KeyEvent

Stressors**Name**

Name

Acetaminophen
 Chloroform
 furan
 Platinum
 Aluminum
 Cadmium
 Mercury
 Uranium
 Arsenic
 Silver
 Manganese
 Nickel
 Zinc
 nanoparticles

Biological Context**Level of Biological Organization**

Molecular

Domain of Applicability**Taxonomic Applicability**

Term	Scientific Term	Evidence	Links
rodents	rodents	High	NCBI
Homo sapiens	Homo sapiens	High	NCBI

Life Stage Applicability**Life Stage Evidence**

All life stages	High
-----------------	------

Sex Applicability

Sex	Evidence
Mixed	High

Taxonomic applicability: Occurrence of oxidative stress is not species specific.

Life stage applicability: Occurrence of oxidative stress is not life stage specific.

Sex applicability: Occurrence of oxidative stress is not sex specific.

Evidence for perturbation by prototypic stressor: There is evidence of the increase of oxidative stress following perturbation from a variety of stressors including exposure to ionizing radiation and altered gravity (Bai et al., 2020; Ungvari et al., 2013; Zhang et al., 2009).

Key Event Description

Oxidative stress is defined as an imbalance in the production of reactive oxygen species (ROS) and antioxidant defenses. High levels of oxidizing free radicals can be very damaging to cells and molecules within the cell. As a result, the cell has important defense mechanisms to protect itself from ROS. For example, Nrf2 is a transcription factor and master regulator of the oxidative stress response. During periods of oxidative stress, Nrf2-dependent changes in gene expression are important in regaining cellular homeostasis (Nguyen, et al., 2009) and can be used as indicators of the presence of oxidative stress in the cell.

In addition to the directly damaging actions of ROS, cellular oxidative stress also changes cellular activities on a molecular level. Redox sensitive proteins have altered physiology in the presence and absence of ROS, which is caused by the oxidation of sulphydryls to disulfides on neighboring amino acids (Antelmann & Helmann 2011). Importantly Keap1, the negative regulator of Nrf2, is regulated in this manner (Itoh, et al. 2010).

ROS also undermine the mitochondrial defense system from oxidative damage. The antioxidant systems consist of superoxide dismutase, catalase, glutathione peroxidase and glutathione reductase, as well as antioxidants such as α -tocopherol and ubiquinol, or antioxidant vitamins and minerals including vitamin E, C, carotene, lutein, zeaxanthin, selenium, and zinc (Fletcher, 2010). The enzymes, vitamins and minerals catalyze the conversion of ROS to non-toxic molecules such as water and O₂. However, these antioxidant systems are not perfect and endogenous metabolic processes and/or exogenous oxidative influences can trigger cumulative oxidative injuries to the mitochondria, causing a decline in their functionality and efficiency, which further promotes cellular oxidative stress (Balasubramanian, 2000; Ganea & Harding, 2006; Guo et al., 2013; Karimi et al., 2017).

However, an emerging viewpoint suggests that ROS-induced modifications may not be as detrimental as previously thought, but rather contribute to signaling processes (Foyer et al., 2017).

Sources of ROS Production

Direct Sources: Direct sources involve the deposition of energy onto water molecules, breaking them into active radical species. When ionizing radiation hits water, it breaks it into hydrogen (H⁺) and hydroxyl (OH[·]) radicals by destroying its bonds. The hydrogen will create hydroxylperoxyl free radicals (HO₂[·]) if oxygen is available, which can then react with another of itself to form hydrogen peroxide (H₂O₂) and more O₂ (Elgazzar and Kazem, 2015). Antioxidant mechanisms are also affected by radiation, with catalase (CAT) and peroxidase (POD) levels rising as a result of exposure (Seen et al. 2018; Ahmad et al. 2021).

Indirect Sources: An indirect source of ROS is the mitochondria, which is one of the primary producers in eukaryotic cells (Powers et al., 2008). As much as 2% of the electrons that should be going through the electron transport chain in the mitochondria escape, allowing them an opportunity to interact with surrounding structures. Electron-oxygen reactions result in free radical production, including the formation of hydrogen peroxide (H₂O₂) (Zhao et al., 2019). The electron transport chain, which also creates ROS, is activated by free adenosine diphosphate (ADP), O₂, and inorganic phosphate (Pi) (Hargreaves et al. 2020; Raimondi et al. 2020; Vargas-Mendoza et al. 2021). The first and third complexes of the transport chain are the most relevant to mammalian ROS production (Raimondi et al., 2020). The mitochondria has its own set of DNA and it is a prime target of oxidative damage (Guo et al., 2013). ROS is also produced through nicotinamide adenine dinucleotide phosphate oxidase (Nox) stimulation, an event commenced by angiotensin II, a product/effect of the renin-angiotensin system (Nguyen Dinh Cat et al. 2013; Forrester et al. 2018). Other ROS producers include xanthine oxidase, immune cells (macrophage, neutrophils, monocytes, and eosinophils), phospholipase A2 (PLA2), monoamine oxidase (MAO), and carbon-based nanomaterials (Powers et al. 2008; Jacobsen et al. 2008; Vargas-Mendoza et al. 2021).

How it is Measured or Detected

Oxidative Stress: Direct measurement of ROS is difficult because ROS are unstable. The presence of ROS can be assayed indirectly by measurement of cellular antioxidants, or by ROS-dependent cellular damage. Listed below are common methods for detecting the KE, however there may be other comparable methods that are not listed

- Detection of ROS by chemiluminescence (<https://www.sciencedirect.com/science/article/abs/pii/S0165993606001683>)
- Detection of ROS by chemiluminescence is also described in OECD TG 495 to assess phototoxic potential.
- Glutathione (GSH) depletion. GSH can be measured by assaying the ratio of reduced to oxidized glutathione (GSH:GSSG) using a commercially available kit (e.g., <http://www.abcam.com/gshgssg-ratio-detection-assay-kit-fluorometric-green-ab138881.html>).
- TBARS. Oxidative damage to lipids can be measured by assaying for lipid peroxidation using TBARS (thiobarbituric acid reactive substances) using a commercially available kit.
- 8-oxo-dG. Oxidative damage to nucleic acids can be assayed by measuring 8-oxo-dG adducts (for which there are a number of ELISA based commercially available kits), or HPLC, described in Chepelev et al. (Chepelev, et al. 2015).

Molecular Biology: Nrf2. Nrf2's transcriptional activity is controlled post-translationally by oxidation of Keap1. Assay for Nrf2 activity include:

- Immunohistochemistry for increases in Nrf2 protein levels and translocation into the nucleus Western blot for increased Nrf2 protein levels
- Western blot of cytoplasmic and nuclear fractions to observe translocation of Nrf2 protein from the cytoplasm to the nucleus qPCR of Nrf2 target genes (e.g., Nqo1, Hmox-1, Gcl, Gst, Prx, Trxr, Srxn), or by commercially available pathway-based qPCR array (e.g., oxidative stress array from SABiosciences)
- Whole transcriptome profiling by microarray or RNA-seq followed by pathway analysis (in IPA, DAVID, metacore, etc.) for enrichment of the Nrf2 oxidative stress response pathway (e.g., Jackson et al. 2014)
- OECD TG422D describes an ARE-Nrf2 Luciferase test method

In general, there are a variety of commercially available colorimetric or fluorescent kits for detecting Nrf2 activation/Oxidative Stress. Direct measurement of ROS is difficult because ROS are unstable. The presence of ROS can be assayed indirectly by measurement of cellular antioxidants, or by ROS-dependent cellular damage. Listed below are common methods for detecting the KE, however there may be other comparable methods that are not listed

- Detection of ROS by chemiluminescence (<https://www.sciencedirect.com/science/article/abs/pii/S0165993606001683>)
- Detection of ROS by chemiluminescence is also described in OECD TG 495 to assess phototoxic potential.
- Glutathione (GSH) depletion. GSH can be measured by assaying the ratio of reduced to oxidized glutathione (GSH:GSSG) using a commercially available kit (e.g., <http://www.abcam.com/gshgssg-ratio-detection-assay-kit-fluorometric-green-ab138881.html>).
- TBARS. Oxidative damage to lipids can be measured by assaying for lipid peroxidation using TBARS (thiobarbituric acid reactive substances) using a commercially available kit.
- 8-oxo-dG. Oxidative damage to nucleic acids can be assayed by measuring 8-oxo-dG adducts (for which there are a number of ELISA based commercially available kits), or HPLC, described in Chepelev et al. (Chepelev, et al. 2015).

Molecular Biology: Nrf2. Nrf2's transcriptional activity is controlled post-translationally by oxidation of Keap1. Assay for Nrf2 activity include:

- Immunohistochemistry for increases in Nrf2 protein levels and translocation into the nucleus Western blot for increased Nrf2 protein levels
- Western blot of cytoplasmic and nuclear fractions to observe translocation of Nrf2 protein from the cytoplasm to the nucleus qPCR of Nrf2 target genes (e.g., Nqo1, Hmox-1, Gcl, Gst, Prx, Trxr, Srxn), or by commercially available pathway-based qPCR array (e.g., oxidative stress array from SABiosciences)
- Whole transcriptome profiling by microarray or RNA-seq followed by pathway analysis (in IPA, DAVID, metacore, etc.) for enrichment of the Nrf2 oxidative stress response pathway (e.g., Jackson et al. 2014)
- OECD TG422D describes an ARE-Nrf2 Luciferase test method

In general, there are a variety of commercially available colorimetric or fluorescent kits for detecting Nrf2 activation

Assay Type & Measured Content	Description	Dose Range Studied	Assay Characteristics (Length/Ease of use/Accuracy)
ROS Formation in the Mitochondria assay (Shaki et al., 2012)	"The mitochondrial ROS measurement was performed flow cytometry using DCFH-DA. Briefly, isolated kidney mitochondria were incubated with UA (0, 50, 100 and 200 μ M) in respiration buffer containing (0.32 mM sucrose, 10mM Tris, 20 mM Mops, 50 μ M EGTA, 0.5 mM MgCl ₂ , 0.1 mM KH ₂ PO ₄ and 5 mM sodium succinate) [32]. In the interval times of 5, 30 and 60 min following the UA addition, a sample was taken and DCFH-DA was added (final concentration, 10 μ M) to mitochondria and was then incubated for 10 min. Uranyl acetate-induced ROS generation in isolated kidney mitochondria were determined through the flow cytometry (Partec, Deutschland) equipped with a 488-nm argon ion laser and supplied with the Flomax software and the signals were obtained using a 530-nm bandpass filter (FL-1 channel). Each determination is based on the mean fluorescence intensity of 15,000 counts."	0, 50, 100 and 200 μ M of Uranyl Acetate	Long/ Easy High accuracy
Mitochondrial Antioxidant Content Assay Measuring GSH content (Shaki et al., 2012)	"GSH content was determined using DTNB as the indicator and spectrophotometer method for the isolated mitochondria. The mitochondrial fractions (0.5 mg protein/ml) were incubated with various concentrations of uranyl acetate for 1 h at 30 °C and then 0.1 ml of mitochondrial fractions was added into 0.1 mol/l of phosphate buffers and 0.04% DTNB in a total volume of 3.0 ml (pH 7.4). The developed yellow color was read at 412 nm on a spectrophotometer (UV-1601 PC, Shimadzu, Japan). GSH content was expressed as μ g/mg protein."	0, 50, 100, or 200 μ M Uranyl Acetate	
H ₂ O ₂ Production Assay Measuring H ₂ O ₂ Production in isolated mitochondria (Heyno et al., 2008)	"Effect of CdCl ₂ and antimycin A (AA) on H ₂ O ₂ production in isolated mitochondria from potato. H ₂ O ₂ production was measured as scopoletin oxidation. Mitochondria were incubated for 30 min in the measuring buffer (see the Materials and Methods) containing 0.5 mM succinate as an electron donor and 0.2 μ M mesoxalonitrile 3-chlorophenylhydrazone (CCCP) as an uncoupler, 10 U horseradish peroxidase and 5 μ M scopoletin."	0, 10, 30 μ M Cd ²⁺ and 2 μ M antimycin A	

Flow Cytometry ROS & Cell Viability (Kruiderig et al., 1997)	"For determination of ROS, samples taken at the indicated time points were directly transferred to FACScan tubes. Dih123 (10 mM, final concentration) was added and cells were incubated at 37°C in a humidified atmosphere (95% air/5% CO2) for 10 min. At t 5 9, propidium iodide (10 mM, final concentration) was added, and cells were analyzed by flow cytometry at 60 ml/min. Nonfluorescent Dih123 is cleaved by ROS to fluorescent R123 and detected by the FL1 detector as described above for Dc (Van de Water 1995)" "For determination of ROS, samples taken at the indicated time points were directly transferred to FACScan tubes. Dih123 (10 mM, final concentration) was added and cells were incubated at 37°C in a humidified atmosphere (95% air/5% CO2) for 10 min. At t 5 9, propidium iodide (10 mM, final concentration) was added, and cells were analyzed by flow cytometry at 60 ml/min. Nonfluorescent Dih123 is cleaved by ROS to fluorescent R123 and detected by the FL1 detector as described above for Dc (Van de Water 1995)"		Strong/easy medium
DCFH-DA Assay Detection of hydrogen peroxide production (Yuan et al., 2016)	Intracellular ROS production was measured using DCFH-DA as a probe. Hydrogen peroxide oxidizes DCFH to DCF. The probe is hydrolyzed intracellularly to DCFH carboxylate anion. No direct reaction with H2O2 to form fluorescent production.	0-400 μ M	Long/ Easy High accuracy
H2-DCF-DA Assay Detection of superoxide production (Thiebault et al., 2007)	This dye is a stable nonpolar compound which diffuses readily into the cells and yields H2-DCF. Intracellular OH or ONOO- react with H2-DCF when cells contain peroxides, to form the highly fluorescent compound DCF, which effluxes the cell. Fluorescence intensity of DCF is measured using a fluorescence spectrophotometer.	0-600 μ M	Long/ Easy High accuracy
CM-H2DCFDA Assay (Eruslanov & Kusmartsev, 2009)	The dye (CM-H2DCFDA) diffuses into the cell and is cleaved by esterases, the thiol reactive chloromethyl group reacts with intracellular glutathione which can be detected using flow cytometry.		Long/Easy/ High Accuracy

Method of Measurement	References	Description	OECD-Approved Assay
Chemiluminescence	(Lu, C. et al., 2006; Griendling, K. K., et al., 2016)	ROS can induce electron transitions in molecules, leading to electronically excited products. When the electrons transition back to ground state, chemiluminescence is emitted and can be measured. Reagents such as luminol and lucigenin are commonly used to amplify the signal.	No
Spectrophotometry	(Griendling, K. K., et al., 2016)	NO has a short half-life. However, if it has been reduced to nitrite (NO2-), stable azocompounds can be formed via the Griess Reaction, and further measured by spectrophotometry.	No
Direct or Spin Trapping-Based electron paramagnetic resonance (EPR) Spectroscopy	(Griendling, K. K., et al., 2016)	The unpaired electrons (free radicals) found in ROS can be detected with EPR and is known as electron paramagnetic resonance. A variety of spin traps can be used.	No
Nitroblue Tetrazolium Assay	(Griendling, K. K., et al., 2016)	The Nitroblue Tetrazolium assay is used to measure O2- levels. O2- reduces nitroblue tetrazolium (a yellow dye) to formazan (a blue dye), and can be measured at 620 nm.	No
Fluorescence analysis of dihydroethidium (DHE) or Hydrocyans	(Griendling, K. K., et al., 2016)	Fluorescence analysis of DHE is used to measure O2- levels. O2- is reduced to O2 as DHE is oxidized to 2-hydroxyethidium, and this reaction can be measured by fluorescence. Similarly, hydrocyans can be oxidized by any ROS, and measured via fluorescence.	No
Amplex Red Assay	(Griendling, K. K., et al., 2016)	Fluorescence analysis to measure extramitochondrial or extracellular H2O2 levels. In the presence of horseradish peroxidase and H2O2, Amplex Red is oxidized to resorufin, a fluorescent molecule measurable by plate reader.	No
Dichlorodihydrofluorescein Diacetate (DCFH-DA)	(Griendling, K. K., et al., 2016)	An indirect fluorescence analysis to measure intracellular H2O2 levels. H2O2 interacts with peroxidase or heme proteins, which further react with DCFH, oxidizing it to dichlorofluorescein (DCF), a fluorescent product.	No
HyPer Probe	(Griendling, K. K., et al., 2016)	Fluorescent measurement of intracellular H2O2 levels. HyPer is a genetically encoded fluorescent sensor that can be used for in vivo and in situ imaging.	No
Cytochrome c Reduction Assay	(Griendling, K. K., et al., 2016)	The cytochrome c reduction assay is used to measure O2- levels. O2- is reduced to O2 as ferricytochrome c is oxidized to ferrocyanochrome c, and this reaction can be measured by an absorbance increase at 550 nm.	No
Proton-electron double-resonance imaging (PEDRI)	(Griendling, K. K., et al., 2016)	The redox state of tissue is detected through nuclear magnetic resonance/magnetic resonance imaging, with the use of a nitroxide spin probe or biradical molecule.	No
Glutathione (GSH) depletion	(Biesemann, N. et al., 2018)	A downstream target of the Nrf2 pathway is involved in GSH synthesis. As an indication of oxidation status, GSH can be measured by assaying the ratio of reduced to oxidized glutathione (GSH:GSSG) using a commercially available kit (e.g., http://www.abcam.com/gshgssg-ratio-detection-assay-kit-fluorometric-green-ab138881.html).	No
Thiobarbituric acid reactive substances (TBARS)	(Griendling, K. K., et al., 2016)	Oxidative damage to lipids can be measured by assaying for lipid peroxidation with TBARS using a commercially available kit.	No
Protein oxidation (carbonylation)	(Azimzadeh et al., 2017; Azimzadeh et al., 2015; Ping et al., 2020)	Can be determined with ELISA or a commercial assay kit. Protein oxidation can indicate the level of oxidative stress.	No
Seahorse XFp Analyzer	Leung et al. 2018	The Seahorse XFp Analyzer provides information on mitochondrial function, oxidative stress, and metabolic dysfunction of viable cells by measuring respiration (oxygen consumption rate; OCR) and extracellular pH (extracellular acidification rate; ECAR).	No

Molecular Biology: Nrf2. Nrf2's transcriptional activity is controlled post-translationally by oxidation of Keap1. Assays for Nrf2 activity include:

Method of Measurement	References	Description	OECD-Approved Assay
Immunohistochemistry	(Amsen, D., de Visser, K. E., and Town, T., 2009)	Immunohistochemistry for increases in Nrf2 protein levels and translocation into the nucleus	No
qPCR	(Forlenza et al., 2012)	qPCR of Nrf2 target genes (e.g., Nqo1, Hmox-1, Gcl, Gst, Prx, TrxR, Srxn), or by commercially available pathway-based qPCR array (e.g., oxidative stress array from SABiosciences)	No
Whole transcriptome profiling via microarray or via RNA-seq followed by a pathway analysis	(Jackson, A. F. et al., 2014)	Whole transcriptome profiling by microarray or RNA-seq followed by pathway analysis (in IPA, DAVID, metacore, etc.) for enrichment of the Nrf2 oxidative stress response pathway	No

References

Ahmad, S. et al. (2021), "60Co-γ Radiation Alters Developmental Stages of *Zeugodacus cucurbitae* (Diptera: Tephritidae) Through Apoptosis Pathways Gene Expression", *Journal Insect Science*, Vol. 21/5, Oxford University Press, Oxford, <https://doi.org/10.1093/jisesa/leab080>

Antelmann, H. and J. D. Helmann (2011), "Thiol-based redox switches and gene regulation.", *Antioxidants & Redox Signaling*, Vol. 14/6, Mary Ann Leibert Inc., Larchmont, <https://doi.org/10.1089/ars.2010.3400>

Amsen, D., de Visser, K. E., and Town, T. (2009). "Approaches to determine expression of inflammatory cytokines", in *Inflammation and Cancer*, Humana Press, Totowa, https://doi.org/10.1007/978-1-59745-447-6_5

Azimzadeh, O. et al. (2015), "Integrative Proteomics and Targeted Transcriptomics Analyses in Cardiac Endothelial Cells Unravel Mechanisms of Long-Term Radiation-Induced Vascular Dysfunction", *Journal of Proteome Research*, Vol. 14/2, American Chemical Society, Washington, <https://doi.org/10.1021/pr501141b>

Azimzadeh, O. et al. (2017), "Proteome analysis of irradiated endothelial cells reveals persistent alteration in protein degradation and the RhoGDI and NO signalling pathways", *International Journal of Radiation Biology*, Vol. 93/9, Informa, London, <https://doi.org/10.1080/09553002.2017.1339332>

Azzam, E. I. et al. (2012), "Ionizing radiation-induced metabolic oxidative stress and prolonged cell injury", *Cancer Letters*, Vol. 327/1-2, Elsevier, Ireland, <https://doi.org/10.1016/j.canlet.2011.12.012>

Bai, J. et al. (2020), "Irradiation-induced senescence of bone marrow mesenchymal stem cells aggravates osteogenic differentiation dysfunction via paracrine signaling", *American Journal of Physiology - Cell Physiology*, Vol. 318/5, American Physiological Society, Rockville, <https://doi.org/10.1152/ajpcell.00520.2019>

Balasubramanian, D (2000), "Ultraviolet radiation and cataract", *Journal of ocular pharmacology and therapeutics*, Vol. 16/3, Mary Ann Leibert Inc., Larchmont, <https://doi.org/10.1089/jop.2000.16.285>.

Biesemann, N. et al., (2018), "High Throughput Screening of Mitochondrial Bioenergetics in Human Differentiated Myotubes Identifies Novel Enhancers of Muscle Performance in Aged Mice", *Scientific Reports*, Vol. 8/1, Nature Portfolio, London, <https://doi.org/10.1038/s41598-018-27614-8>.

Elgazzar, A. and N. Kazem. (2015), "Chapter 23: Biological effects of ionizing radiation" in *The Pathophysiologic Basis of Nuclear Medicine*, Springer, New York, pp. 540-548

Eruslanov, E., & Kusmartsev, S. (2010). Identification of ROS using oxidized DCFDA and flow-cytometry. *Methods in molecular biology* ,N.J., Vol. 594, https://doi.org/10.1007/978-1-60761-411-1_4

Fletcher, A. E (2010), "Free radicals, antioxidants and eye diseases: evidence from epidemiological studies on cataract and age-related macular degeneration", *Ophthalmic Research*, Vol. 44, Karger International, Basel, <https://doi.org/10.1159/000316476>.

Forlenza, M. et al. (2012), "The use of real-time quantitative PCR for the analysis of cytokine mRNA levels" in *Cytokine Protocols*, Springer, New York, https://doi.org/10.1007/978-1-61779-439-1_2

Forrester, S.J. et al. (2018), "Angiotensin II Signal Transduction: An Update on Mechanisms of Physiology and Pathophysiology", *Physiological Reviews*, Vol. 98/3, American Physiological Society, Rockville, <https://doi.org/10.1152/physrev.00038.201>

Foyer, C. H., A. V. Ruban, and G. Noctor (2017), "Viewing oxidative stress through the lens of oxidative signalling rather than damage", *Biochemical Journal*, Vol. 474/6, Portland Press, England, <https://doi.org/10.1042/BCJ20160814>

Ganea, E. and J. J. Harding (2006), "Glutathione-related enzymes and the eye", *Current eye research*, Vol. 31/1, Informa, London, <https://doi.org/10.1080/02713680500477347>.

Griendling, K. K. et al. (2016), "Measurement of reactive oxygen species, reactive nitrogen species, and redox-dependent signaling in the cardiovascular system: a scientific statement from the American Heart Association", *Circulation research*, Vol. 119/5, Lippincott Williams & Wilkins, Philadelphia, <https://doi.org/10.1161/RES.000000000000110>

Guo, C. et al. (2013), "Oxidative stress, mitochondrial damage and neurodegenerative diseases", *Neural regeneration research*, Vol. 8/21, Publishing House of Neural Regeneration Research, China, <https://doi.org/10.3969/j.issn.1673-5374.2013.21.009>

Hargreaves, M., and L. L. Spriet (2020), "Skeletal muscle energy metabolism during exercise.", *Nature Metabolism*, Vol. 2, Nature Portfolio, London, <https://doi.org/10.1038/s42255-020-0251-4>

Hladik, D. and S. Tapio (2016), "Effects of ionizing radiation on the mammalian brain", *Mutation Research/Reviews in Mutation Research*, Vol. 770, Elsevier, Amsterdam, <https://doi.org/10.1016/j.mrrev.2016.08.003>

Itoh, K., J. Mimura and M. Yamamoto (2010), "Discovery of the negative regulator of Nrf2, Keap1: a historical overview", *Antioxidants & Redox Signaling*, Vol. 13/11, Mary Ann Leibert Inc., Larchmont, <https://doi.org/10.1089/ars.2010.3222>

Jackson, A.F. et al. (2014), "Case study on the utility of hepatic global gene expression profiling in the risk assessment of the carcinogen furan.", *Toxicology and Applied Pharmacology*, Vol. 274/11, Elsevier, Amsterdam, <https://doi.org/10.1016/j.taap.2013.10.019>

Jacobsen, N.R. et al. (2008), "Genotoxicity, cytotoxicity, and reactive oxygen species induced by single-walled carbon nanotubes and C60 fullerenes in the FE1-MutaTM Mouse lung epithelial cells", *Environmental and Molecular Mutagenesis*, Vol. 49/6, John Wiley & Sons, Inc., Hoboken, <https://doi.org/10.1002/em.20406>

Karimi, N. et al. (2017), "Radioprotective effect of hesperidin on reducing oxidative stress in the lens tissue of rats", *International Journal of Pharmaceutical Investigation*, Vol. 7/3, Phcog Net, Bengaluru, https://doi.org/10.4103/jphi.JPHI_60_17.

Leung, D.T.H., and Chu, S. (2018), "Measurement of Oxidative Stress: Mitochondrial Function Using the Seahorse System" In: Murthi, P., Vaillancourt, C. (eds) *Preeclampsia. Methods in Molecular Biology*, vol 1710. Humana Press, New York, NY. https://doi.org/10.1007/978-1-4939-7498-6_22

Lu, C., G. Song, and J. Lin (2006), "Reactive oxygen species and their chemiluminescence-detection methods", *TrAC Trends in Analytical Chemistry*, Vol. 25/10, Elsevier, Amsterdam, <https://doi.org/10.1016/j.trac.2006.07.007>

Nguyen Dinh Cat, A. et al. (2013), "Angiotensin II, NADPH oxidase, and redox signaling in the vasculature", *Antioxidants & redox signaling*, Vol. 19/10, Mary Ann Leibert, Larchmont, <https://doi.org/10.1089/ars.2012.4641>

Ping, Z. et al. (2020), "Oxidative Stress in Radiation-Induced Cardiotoxicity", *Oxidative Medicine and Cellular Longevity*, Vol. 2020, Hindawi, <https://doi.org/10.1155/2020/3579143>

AOP482

Powers, S.K. and M.J. Jackson. (2008), "Exercise-Induced Oxidative Stress: Cellular Mechanisms and Impact on Muscle Force Production", *Physiological Reviews*, Vol. 88/4, American Physiological Society, Rockville, <https://doi.org/10.1152/physrev.00031.2007>

Raimondi, V., F. Ciccarese and V. Ciminale. (2020), "Oncogenic pathways and the electron transport chain: a dangeROS liaison", *British Journal of Cancer*, Vol. 122/2, Nature Portfolio, London, <https://doi.org/10.1038/s41416-019-0651-y>

Seen, S. and L. Tong. (2018), "Dry eye disease and oxidative stress", *Acta Ophthalmologica*, Vol. 96/4, John Wiley & Sons, Inc., Hoboken, <https://doi.org/10.1111/aos.13526>

Ungvari, Z. et al. (2013), "Ionizing Radiation Promotes the Acquisition of a Senescence-Associated Secretory Phenotype and Impairs Angiogenic Capacity in Cerebromicrovascular Endothelial Cells: Role of Increased DNA Damage and Decreased DNA Repair Capacity in Microvascular Radiosensitivity", *The Journals of Gerontology Series A: Biological Sciences and Medical Sciences*, Vol. 68/12, Oxford University Press, Oxford, <https://doi.org/10.1093/gerona/glt057>.

Vargas-Mendoza, N. et al. (2021), "Oxidative Stress, Mitochondrial Function and Adaptation to Exercise: New Perspectives in Nutrition", *Life*, Vol. 11/11, Multidisciplinary Digital Publishing Institute, Basel, <https://doi.org/10.3390/life1111269>

Wang, H. et al. (2019), "Radiation-induced heart disease: a review of classification, mechanism and prevention", *International Journal of Biological Sciences*, Vol. 15/10, Iivyspring International Publisher, Sydney, <https://doi.org/10.7150/ijbs.35460>

Zhang, R. et al. (2009), "Blockade of AT1 receptor partially restores vasoreactivity, NOS expression, and superoxide levels in cerebral and carotid arteries of hindlimb unweighting rats", *Journal of applied physiology*, Vol. 106/1, American Physiological Society, Rockville, <https://doi.org/10.1152/japplphysiol.01278.2007>.

Zhao, R. Z. et al. (2019), "Mitochondrial electron transport chain, ROS generation and uncoupling", *International journal of molecular medicine*, Vol. 44/1, Spandidos Publishing Ltd., Athens, <https://doi.org/10.3892/ijmm.2019.4188>

[Event: 2245: Altered Cell Differentiation Signaling](#)

Short Name: Altered cell differentiation signaling

Key Event Component

Process	Object	Action
cell differentiation		abnormal
cell surface receptor signaling pathway		increased

AOPs Including This Key Event

AOP ID and Name	Event Type
Aop:482 - Deposition of energy leading to occurrence of bone loss	KeyEvent

Biological Context

Level of Biological Organization

Molecular

Domain of Applicability

Taxonomic Applicability

Term	Scientific Term	Evidence	Links
human	Homo sapiens	Moderate	NCBI
rat	Rattus norvegicus	Moderate	NCBI
mouse	Mus musculus	Moderate	NCBI

Life Stage Applicability

Life Stage Evidence

All life stages Moderate

Sex Applicability

Sex Evidence

Unspecific Low

Taxonomic applicability: Altered signaling is applicable to all animals as cell signaling occurs in animal cells. This includes vertebrates such as humans, mice and rats (Nair et al., 2019).

Life stage applicability: Life stage applicability is pathway dependent.

Sex applicability: This key event is not sex specific.

Evidence for perturbation by a stressor: Multiple studies show that signaling pathways can be disrupted by many types of stressors including ionizing radiation and altered gravity (Su et al., 2020; Yentrapalli et al., 2013).

Key Event Description

Cell differentiation pathways are the processes through which unspecialized cells, such as stem cells, develop into specialized cells with distinct functions (Soumelis and Liu, 2006). These pathways are tightly regulated by a complex interplay of signaling molecules and their receptors, the binding dynamics of transcription factors, and epigenetic modifications. Signaling molecules like growth factors and cytokines bind to cell surface receptors, triggering intracellular cascades that activate specific transcription factors. Transcription factors regulate dynamically during cell differentiation, they can be classified as static, dynamic, enhanced and suppressed states. These transcription factors then bind to DNA, regulating the expression of genes necessary for the specialized function of the cell. Epigenetic modifications, such as DNA methylation and histone modification, further ensure that the gene expression patterns are stably maintained over cell divisions (Tanabe, 2015).

Disruptions in cell differentiation pathways can occur due to various mechanisms, including genetic mutations, epigenetic alterations, and environmental factors. Mutations in genes encoding signaling molecules, receptors, or transcription factors can lead to aberrant activation or suppression of these pathways, preventing proper cell differentiation. Epigenetic alterations, such as aberrant DNA methylation or histone modification patterns, can also result in inappropriate gene expression, further hindering the differentiation process (Miller and Grant, 2013). Environmental factors, including exposure to toxins, radiation, or pathogens, can

induce oxidative stress or DNA damage, leading to the activation of stress response pathways that interfere with normal differentiation. Persistent activation or inhibition of these pathways can lead to aberrant cell fate decisions (Kharrazian, 2021). These disruptions can have significant consequences, contributing to developmental disorders, cancer, and other diseases (Wu et al., 2023).

Key Differentiation Pathways: Description and Components for Measurement

WNT/β-Catenin Pathway:

The WNT/β-Catenin pathway plays a role in regulating the differentiation of various cell types by controlling gene expression. It is crucial for embryonic development, tissue homeostasis, and stem cell maintenance (Clevers et al., 2014). In particular, WNT signalling regulates bone cell homeostasis, and activation of this pathway results in increased bone mass and strength (Baron and Kneissel, 2013). The pathway is activated by WNT proteins binding to Frizzled receptors and LRP5/6 co-receptors, leading to the stabilization and nuclear translocation of β-catenin (Qin et al. 2024). One key component of this pathway is WNT Ligands, secreted proteins which initiate the signaling cascade. WNT ligands are lipid modified and have a variety of roles in embryonic development (Basson, 2012). Frizzled receptors are cell surface receptors that bind to WNT ligands. β-Catenin acts as the central mediator that enters the nucleus to activate target gene transcription, and TCF/LEF transcription factors bind to β-catenin to regulate gene expression (Nusse and Clevers, 2017; Steinhart and Angers, 2018).

Notch Pathway:

The Notch pathway plays a role in cell differentiation by influencing cell fate decisions, particularly in the nervous system, blood cells, and epithelial cells (Brandstädter and Maillard. 2019). The pathway also is a key contributor in maintaining cell polarity, proliferation, apoptosis and epithelial-mesenchymal transition (Parambath et al., 2024) This pathway operates through direct cell-cell interactions and is activated when Notch receptors on one cell bind to Delta or Jagged ligands on an adjacent cell. This binding triggers the cleavage of the Notch receptor and releases the Notch Intracellular Domain (Basson, 2012). The NICD then translocates to the nucleus, where it associates with the transcriptional regulator RBP-Jκ to activate target genes. Key components of this pathway include the transmembrane Notch receptors (Notch1-4) and their ligands, Delta and Jagged, which are essential for the pathway's activation and function (Miyamoto and Weinmaster. 2009)

Hedgehog Pathway:

The Hedgehog pathway is essential for the differentiation and development of various tissues, including the neural tube, limbs, and skin, as well as helping to maintain stem cells in adults. Activation of this pathway begins when Hedgehog ligands bind to the Patched (PTCH) receptor. This binding alleviates PTCH's inhibition of the Smoothened (SMO) receptor, thereby activating downstream signaling (Carballo et al. 2018). A key component of the Hedgehog pathway includes the Hedgehog ligands (Sonic, Indian and Desert), which are secreted proteins that initiate the pathway (Basson, 2012). The PTCH receptor inhibits the pathway in the absence of these ligands, while the SMO receptor activates the pathway once Hedgehog binds to PTCH. GLI transcription factors then regulate target gene expression in response to the activation of the pathway (Briscoe and Therond, 2013).

TGF-β/SMAD pathway:

The TGF-β/SMAD pathway is important for the differentiation of various cell types, including mesenchymal, epithelial, and immune cells. It also plays significant roles in cell proliferation, apoptosis, and extracellular matrix production (Flanders et al., 2009). Activation of this pathway occurs when TGF-β ligands bind to type II and type I serine/threonine kinase receptors, leading to the phosphorylation and activation of SMAD proteins. The key components of this pathway include TGF-β ligands, which are transforming growth factor-beta (TGF-β) proteins that initiate signaling, and the type I and II receptors that propagate the signal. Upon activation, receptor-regulated SMADs (SMAD2/3) are phosphorylated and form complexes with the common-mediator SMAD (SMAD4). These complexes then regulate gene expression to mediate the pathway's effects (Deryck and Zhang, 2003).

JAK-STAT Pathway:

The JAK-STAT pathway mediates responses to cytokines and growth factors, thereby influencing the differentiation of immune cells, hematopoietic cells, and other cell types. Activation of this pathway begins when cytokines bind to their receptors, leading to the activation of Janus Kinases (JAKs) (Hu et al. 2023). JAKs phosphorylate signal transducers and activators of transcription (STATs), allowing them to dimerize and translocate to the nucleus to regulate gene expression (Garrido-Trigo and Salas. 2019). Cytokine receptors are key components of the JAK-STAT pathway, which bind cytokines and activate JAKs. Other key components include JAKs, which are tyrosine kinases responsible for phosphorylating and activating STATs, and STATs which are transcription factors that mediate gene expression in response to cytokine signaling (Bezbradica and Medzhitov, 2009).

Hippo Pathway:

The Hippo pathway plays a role in controlling organ size by regulating cell proliferation, apoptosis, and stem cell self-renewal. It also influences the differentiation of various cell types. Activation of this pathway involves a kinase cascade that ultimately phosphorylates and inactivates the transcriptional co-activators YAP and TAZ. Key components of the Hippo pathway include MST1/2 (Mammalian Ste20-like Kinase), which initiates the kinase cascade, and LATS1/2 (Large Tumor Suppressor Kinase), which phosphorylate and inhibit YAP/TAZ (Zhou et al. 2024). When not phosphorylated, yes-associated protein/transcriptional co-activator with PDZ-binding motif (YAP/TAZ) act as transcriptional co-activators that regulate gene expression. They partner with TEAD (TEA Domain Transcription Factors) to regulate target gene expression, thereby influencing cell behaviour and fate.

ERK/MAPK pathway:

The ERK/MAPK pathway is essential for regulating cell proliferation, differentiation, and survival, playing a pivotal role in the differentiation of various cell types in response to growth factors and other extracellular signals. Activation of this pathway involves a kinase cascade where MAPK/ERK is activated by MEK, which is in turn activated by RAF (Bahar et al. 2023). Key components of the ERK/MAPK pathway include RAF (Rapidly Accelerated Fibrosarcoma Kinase), which initiates the kinase cascade, and MEK (MAPK/ERK Kinase), which activates ERK through phosphorylation. ERK (Extracellular Signal-Regulated Kinase) then phosphorylates various target proteins, including transcription factors such as ELK1 and c-FOS, to regulate gene expression and influence cell behaviour (Arthur and Ley, 2013; Yue and López, 2020).

How it is Measured or Detected

Pathway	Method of Measurement	Description	Reference	OECD Approved Assay
WNT/β-Catenin	Western Blot	Detects β-catenin protein levels by using specific primary antibodies.	Zhang et al., 2019	No
	Immunofluorescence	Evaluated β-catenin expression in the nucleus and cytoplasm	Rong et al., 2022	No
	qPCR	Measures expression of WNT/β-catenin signaling pathway-related genes and mRNA levels.	Wang et al., 2023	No
Notch	Luciferase reporter assay	Evaluates WNT/β-catenin pathway activity by performing reporter gene assays with luciferase expression vectors containing wild-type and mutant TCF/LEF binding sites, comparing luciferase activities	Fröhlich et al., 2023	No
	qPCR	Quantifies mRNA levels of Notch1,3 and 4 as well as notch signalling downstream targets.	Ibrahim et al., 2017	No
	Immunofluorescence	Evaluated notch fluorescence levels using anti-Notch1 primary antibody	Rong et al., 2022	No
Hedgehog	Western Blot	Measures protein expression of Notch1 using bicinchoninic acid protein assay kit.	Rong et al., 2022	No
	Immunohistochemistry	Measures expression of levels of SHH pathway members.	Ke et al., 2020	No
	Western Blot	Detects GLI protein levels and their activation state.	Ke et al., 2020	No
TGF-β/SMAD	ELISA	Quantifies TGF-β ligand concentration in samples.	Rouce et al., 2016	No
	Immunofluorescence	Visualizes nuclear vs. cytoplasmic localization of SMAD2/3.	Liu et al., 2016	No
	Western Blot	Detects phosphorylation status of SMAD2/3 proteins.	Liu et al., 2016	No
JAK-STAT	qRT-PCR	Quantifies mRNA levels of AKT1 and PI3K.	Xia and Tang 2023	No
	Western Blot	Measures levels of JAK2 and STAT3.	Broughton and Burfoot, 2001; Mao et al., 2023	No
	Electrophoretic Mobility Shift Assay (EMSA)	Measures DNA-binding activity of STAT proteins to specific response elements.	Broughton and Burfoot; Jiao et al., 2003	No

Hippo	Western Blot	Detects expression levels of Hippo pathway proteins.	Wang et al., 2024; Chen et al., 2020	No
	Immunofluorescence	Visualizes nuclear vs. cytoplasmic localization of Hippo pathway expression.	Chen et al., 2020;	No
	Chromatin immunoprecipitation (ChIP)	Measures expression of genes regulated by the Hippo pathway.	Wang et al., 2024;	No
ERK/MAPK	Western Blot	Detects the phosphorylation state of MAPK family members (ERK, JNK, p38), indicating activation.	Tan et al. 2022; Xia and Tang 2023	No
	qRT-PCR	Quantifies mRNA levels of JNK, MAPK1(ERK), and MAPK14(p38)	Xia and Tang 2023	No

References

Arthur, J. S. and S. C. Ley (2013), "Mitogen-activated protein kinases in innate immunity", *Nature Reviews Immunology*, Vol. 13/9, Springer, New York, <https://doi.org/10.1038/nri3495>

Bahar, M. E., Kim, H. J., and Kim, D. R. (2023), "Targeting the RAS/RAF/MAPK pathway for cancer therapy: from mechanism to clinical studies", *Signal transduction and targeted therapy*, Vol. 8/1, <https://doi.org/10.1038/s41392-023-01705-z>

Baron, R. and M. Kneissel (2013), "WNT signaling in bone homeostasis and disease: from human mutations to treatments", *Nature medicine*, Vol. 19/2, doi:10.1038/nm.3074

Basson, M. A. (2012), "Signaling in cell differentiation and morphogenesis", *Cold Spring Harbor perspectives in biology*, Vol. 4/6, doi:10.1101/cshperspect.a008151

Bezbradica, J. S. and R. Medzhitov (2009), "Integration of cytokine and heterologous receptor signaling pathways", *Nature immunology*, Vol. 10, <https://doi.org/10.1038/ni.1713>

Briscoe, J. and P. P. Therond (2013), "The mechanisms of Hedgehog signalling and its roles in development and disease", *Nature Reviews Molecular Cell Biology*, Vol. 14/7, Springer, London, <https://doi.org/10.1038/nrm3598>

Carballo, G. B. et al. (2018), "A highlight on Sonic hedgehog pathway", *Cell communication and signaling : CCS* Vol 16/1. <https://doi.org/10.1186/s12964-018-0220-7>

Chen, Y. et al. (2020), "Systematic analysis of the Hippo pathway organization and oncogenic alteration in evolution", *Scientific reports*, Vol. 10/1, Springer, London, <https://doi.org/10.1038/s41598-020-60120-4>

Cheng, Y. P. et al. (2017), "Acid sphingomyelinase/ceramide regulates carotid intima-media thickness in simulated weightless rats", *Pflugers Archiv European Journal of Physiology*, Vol. 469, Springer, New York, <https://doi.org/10.1007/s00424-017-1969-z>

Clevers, H. et al. (2014), "Stem cell signaling. An integral program for tissue renewal and regeneration: Wnt signaling and stem cell control", *Science (New York, N.Y.)*, Vol. 346/6205, American Association for the Advancement of Science, New York <https://doi.org/10.1126/science.1248012>

Derynck, R. and Y. E. Zhang (2003), "Smad-dependent and Smad-independent pathways in TGF-beta family signalling", *Nature*, Vol. 425/6958, Springer, London, <https://doi.org/10.1038/nature02006>

Flanders, K. C. and L. M. Wakefield (2009), "Transforming growth factor-(beta)s and mammary gland involution: functional roles and implications for cancer progression", *Journal of mammary gland biology and neoplasia* Vol. 14/2, Springer, London, <https://doi.org/10.1007/s10911-009-9122-z>

Fröhlich, J., Rose, K., and Hecht, A. (2023), "Transcriptional activity mediated by β-CATENIN and TCF/LEF family members is completely dispensable for survival and propagation of multiple human colorectal cancer cell lines", *Scientific reports*, Vol.13, <https://doi.org/10.1038/s41598-022-27261-0>

Garrido-Trigo, A., and Salas, A. (2020), "Molecular Structure and Function of Janus Kinases: Implications for the Development of Inhibitors", *Journal of Crohn's & colitis*, Vol. 14. <https://doi.org/10.1093/ecco-jcc/jjz206>

Hu, Q., et al. (2023), "JAK/STAT pathway: Extracellular signals, diseases, immunity, and therapeutic regimens", *Frontiers in bioengineering and biotechnology*, Vol.11, Frontiers, Lausanne, 1110765. <https://doi.org/10.3389/fbioe.2023.1110765>

Ibrahim, S. A., et al. (2017), "Syndecan-1 is a novel molecular marker for triple negative inflammatory breast cancer and modulates the cancer stem cell phenotype via the IL-6/STAT3, Notch and EGFR signaling pathways", *Molecular cancer*, Vol.16 <https://doi.org/10.1186/s12943-017-0621-z>

Ke, B. et al. (2020), "Sonic Hedgehog/Gli1 Signaling Pathway Regulates Cell Migration and Invasion via Induction of Epithelial-to-mesenchymal Transition in Gastric Cancer", *Journal of Cancer*, Vol. 11/13, <https://doi.org/10.7150/jca.42900>

Kharazian D. (2021), "Exposure to Environmental Toxins and Autoimmune Conditions", *Integrative medicine (Encinitas, Calif.)*, Vol. 20/2.

Liu, L. et al. (2016), "Smad2 and Smad3 have differential sensitivity in relaying TGFβ signaling and inversely regulate early lineage specification", *Scientific reports*, Vol. 6, Springer, London, <https://doi.org/10.1038/srep21602>

Miller, J. L. and P. A. Grant (2013), "The role of DNA methylation and histone modifications in transcriptional regulation in humans", *Sub-cellular biochemistry*, Vol. 61, https://doi.org/10.1007/978-94-007-4525-4_13

Miyamoto, A. and G. Weinmaster (2009), "Notch Signal Transduction: Molecular and Cellular Mechanisms", *Encyclopedia of Neuroscience*, <https://doi.org/10.1016/B978-008045046-9.01026-3>

Nair, A. et al. (2019), "Conceptual Evolution of Cell Signaling", *International journal of molecular sciences* Vol. 20/13, Multidisciplinary Digital Publishing Institute, Basel, <https://doi.org/10.3390/ijms2013292>

Nusse, R. and H. Clevers (2017), "Wnt/β-Catenin Signaling, Disease, and Emerging Therapeutic Modalities", *Cell*, Vol. 169/6, Elsevier, Amsterdam, <https://doi.org/10.1016/j.cell.2017.05.016>

Parambath, S. et al. (2024), "Notch Signaling: An Emerging Paradigm in the Pathogenesis of Reproductive Disorders and Diverse Pathological Conditions", *International journal of molecular sciences*, Vol. 25, Multidisciplinary Digital Publishing Institute, Basel, <https://doi.org/10.3390/ijms25105423>

Qin, et al. (2024), "Canonical and noncanonical Wnt signaling: Multilayered mediators, signaling mechanisms and major signaling crosstalk", *Genes & Disease*, Vol. 11, <https://doi.org/10.1016/j.gendis.2023.01.030>.

Rong, X. et al. (2022), "ED-71 Prevents Glucocorticoid-Induced Osteoporosis by Regulating Osteoblast Differentiation via Notch and Wnt/β-Catenin Pathways", *Drug design, development and therapy*, Vol. 16, <https://doi.org/10.2147/DDDT.S377001>

Rouce, R. et al. (2016), "The TGF-β/SMAD pathway is an important mechanism for NK cell immune evasion in childhood B-acute lymphoblastic leukemia", *Leukemia*, Vol. 30/4, Springer, London, <https://doi.org/10.1038/leu.2015.327>

Sita, G. et al. (2023), "The Unfolded Protein Response in a Murine Model of Alzheimer's Disease: Looking for Predictors", *International journal of molecular sciences* Vol. 24/22, Multidisciplinary Digital Publishing Institute, Basel, <https://doi.org/10.3390/ijms242216200>

Soumelis, V. and Y. J. Liu (2006), "From plasmacytoid to dendritic cell: morphological and functional switches during plasmacytoid pre-dendritic cell differentiation", *European journal of immunology*, Vol. 36/9, Wiley, Hoboken, <https://doi.org/10.1002/eji.200636026>

Steinhart, Z. and S. Angers (2018), "Wnt signaling in development and tissue homeostasis", *Development (Cambridge, England)*, Vol. 145/11, The Company of Biologists, Cambridge, <https://doi.org/10.1242/dev.146589>

Su, Y. T. et al. (2020), "Acid sphingomyelinase/ceramide mediates structural remodeling of cerebral artery and small mesenteric artery in simulated weightless rats", *Life Sciences*, Vol. 243, Elsevier, Amsterdam, <https://doi.org/10.1016/j.lfs.2019.117253>

Tan, B. et al. (2022), "Changes in the histopathology and in the proteins related to the MAPK pathway in the brains of rats exposed to pre and postnatal

AOP482

radiofrequency radiation over four generations", *Journal of chemical neuroanatomy*, Vol.126, Elsevier, Amsterdam, <https://doi.org/10.1016/j.jchemneu.2022.102187>

Tanabe S. (2015), "Signaling involved in stem cell reprogramming and differentiation", *World journal of stem cells* Vol. 7/7, Baishideng publishing group, Pleasonton, <https://doi.org/10.4252/wjsc.v7.i7.992>

Wang, D. et al. (2024), "Circular RNA HSDL2 promotes breast cancer progression via miR-7978 ZNF704 axis and regulating hippo signaling pathway" *Breast cancer research : BCR*, Vol. 26/1, Springer, London <https://doi.org/10.1186/s13058-024-01864-z>

Wu, H. et al., (2023), "Molecular mechanisms of environmental exposures and human disease. Nature reviews" *Genetics*, Vol. 24/5, Springer, London, <https://doi.org/10.1038/s41576-022-00569-3>

Xia, Z., Li, Q. and Z. Tang (2023), "Network pharmacology, molecular docking, and experimental pharmacology explored Ermiao wan protected against periodontitis via the PI3K/AKT and NF- κ B/MAPK signal pathways." *Journal of ethnopharmacology*, Vol. 303, Elsevier, Amsterdam, <https://doi.org/10.1016/j.jep.2022.115900>

Yentrapalli, R. et al. (2013), "The PI3K/Akt/mTOR pathway is implicated in the premature senescence of primary human endothelial cells exposed to chronic radiation", *PLoS one*, Vol. 8/8, PLOS, San Francisco, <https://doi.org/10.1371/journal.pone.0070024>

Yue, J. and J. M. López (2020), "Understanding MAPK Signaling Pathways in Apoptosis", *International journal of molecular sciences* Vol. 21/7, Multidisciplinary Digital Publishing Institute, Basel, <https://doi.org/10.3390/ijms21072346>

Zhang, Y. et al. (2019), "Captopril attenuates TAC-induced heart failure via inhibiting Wnt3a/ β -catenin and Jak2/Stat3 pathways" *Biomedicine & pharmacotherapy = Biomedecine & pharmacotherapie*, Vol. 113, <https://doi.org/10.1016/j.biopha.2019.108780>

Zhou, X., Li, W. Y., and Wang, H. Y. (2017), "The roles and mechanisms of MST1/2 in the innate immune response." *Yi chuan = Hereditas*, Vol. 39, <https://doi.org/10.16288/j.yczz.17-066>

Event: 1825: Increase, Cell death

Short Name: Increase, Cell death

Key Event Component

Process	Object	Action
cell death	bone cell	increased

AOPs Including This Key Event

AOP ID and Name	Event Type
Aop:291 - Mitochondrial ATP synthase antagonism leading to growth inhibition (2)	KeyEvent
Aop:287 - Mitochondrial complex III antagonism leading to growth inhibition (2)	KeyEvent
Aop:368 - Cytochrome oxidase inhibition leading to olfactory nasal lesions	KeyEvent
Aop:377 - Dysregulated prolonged Toll Like Receptor 9 (TLR9) activation leading to Multi Organ Failure involving Acute Respiratory Distress Syndrome (ARDS)	KeyEvent
Aop:410 - GSK3beta inactivation leading to increased mortality via defects in developing inner ear	KeyEvent
Aop:418 - Aryl hydrocarbon receptor activation leading to impaired lung function through AHR-ARNT toxicity pathway	KeyEvent
Aop:464 - Calcium overload in dopaminergic neurons of the substantia nigra leading to parkinsonian motor deficits	KeyEvent
Aop:468 - Binding of SARS-CoV-2 to ACE2 leads to hyperinflammation (via cell death)	KeyEvent
Aop:482 - Deposition of energy leading to occurrence of bone loss	KeyEvent

Stressors

Name
Food deprivation
Gentamicin

Biological Context

Level of Biological Organization
Cellular

Cell term

Cell term
cell

Organ term

Organ term
organ

Domain of Applicability

Taxonomic Applicability			
Term	Scientific Term	Evidence	Links
zebrafish	Danio rerio	High	NCBI
human	Homo sapiens	High	NCBI
rat	Rattus norvegicus	High	NCBI

Term	Scientific Term	Evidence	Links
mouse	Mus musculus	High	NCBI

Life Stage Applicability**Life Stage Evidence**

All life stages	High
-----------------	------

Sex Applicability**Sex Evidence**

Unspecific	High
------------	------

The process of cell death is highly conserved within multi-cellular organisms. (Lockshin & Zakeri, 2004).

Taxonomic applicability: Increased cell death is applicable to all animals. This includes vertebrates such as humans, mice and rats (Alberts et al., 2002).

Life stage applicability: There is insufficient data on life stage applicability of this KE.

Sex applicability: This key event is not sex specific (Forger and de Vries, 2010; Ortona Matarrese, and Malorni, 2014).

Evidence for perturbation by a stressor: Multiple studies show that cell death can be increased or disrupted by many types of stressors including ionizing radiation and altered gravity (Zhu et al., 2016).

Key Event Description

Cell death is part of normal development and maturation cycle, and is the component of many response patterns of living tissues to xenobiotic agents (i.e.. microorganisms and chemicals) and to endogenous modulations, such as inflammation and disturbed blood supply (Kanduc et al., 2002). Many physiological processes require cell death for their function (e.g., embryonal development and immune selection of B and T cells) (Bertheloot et al., 2021). Defects in cells that result in their inappropriate survival or untimely death can negatively impact development or contribute to a variety of human pathologies, including cancer, AIDS, autoimmune disorders, and chronic infection. Cell death may also occur following exposure to environmental toxins or cytotoxic chemicals. Although this is often harmful, it can be beneficial in some cases, such as in the treatment of cancer (Crowley et al., 2016).

Cell death can be divided into: programmed cell death (cell death as a normal component of development) and non-programmed cell death (uncontrolled death of the cell). Although this simplistic view has blurred the intricate mechanisms separating these forms of cell death, studies have and will uncover new effectors, cell death pathways and reveal a more complex and intertwined landscape of processes involving cell death (Bertheloot et al., 2021).

Programmed cell death: is a form of cell death in which the dying cell plays an active part in its own demise (Cotter & Al-Rubeai, 1995).

Apoptosis At a morphological level, it is characterized by cell shrinkage rather than the swelling seen in necrotic cell death. It is characterized by a number of characteristic morphological changes in the structure of the cell, together with a number of enzyme-dependent biochemical processes. The result of it being the clearance of cells from the body, with minimal damage to surrounding tissues. An essential feature of apoptosis is the release of cytochrome c from mitochondria, regulated by a balance between proapoptotic and antiapoptotic proteins of the BCL-2 family, initiator caspases (caspase-8, -9 and -10) and effector caspases (caspase-3, -6 and -7). Apoptosis culminates in the breakdown of the nuclear membrane by caspase-6, the cleavage of many intracellular proteins (e.g., PARP and lamin), membrane blebbing, and the breakdown of genomic DNA into nucleosomal structures (Bertheloot et al., 2021). Mechanistically, two main pathways contribute to the caspase activation cascade downstream of mitochondrial cytochrome c release:

- Intrinsic pathway is triggered by dysregulation of or imbalance in intracellular homeostasis by toxic agents or DNA damage. It is characterized by mitochondrial outer membrane permeabilization (MOMP), which results in the release of cytochrome c into the cytosol.
- Extrinsic pathway is initiated by activation of cell surface death receptors. Proapoptotic death receptors include TNFR1/2, Fas and the TNF-related apoptosis-inducing ligand (TRAIL) receptors DR4 and DR5.

Other pathways of programmed cell death are called »non-apoptotic programmed cell-death« or »caspase-independent programmed cell-death« (Blank & Shiloh, 2007).

Necroptosis: This type of regulated cell death, occurs following the activation of the tumour necrosis receptor (TNFR1) by TNF α . Activation of other cellular receptors triggers necroptosis. These receptors include death receptors (i.e., Fas/FasL), Toll-like receptors (TLR4 and TLR3) and cytosolic nucleic acid sensors such as RIG-I and STING, which induce type I interferon (IFN-I) and TNF α production and thus promote necroptosis in an autocrine feedback loop. Most of these pathways trigger NFKB-dependent proinflammatory and prosurvival signals.

Pyroptosis is a type of cell death culminating in the loss of plasma membrane integrity and induced by activation of so-called inflammasome sensors. These include the Nod-like receptor (NLR) family, the DNA receptor Absent in Melanoma 2 (AIM2) and the Pyrin receptor.

Autophagy: is a process where cellular components such as macro proteins or even whole organelles are sequestered into lysosomes for degradation (Mizushima et al., 2008; Shintani & Klionsky, 2004). The lysosomes are then able to digest these substrates, the components of which can either be recycled to create new cellular structures and/or organelles or alternatively can be further processed and used as a source of energy (D'Arcy, 2019).

Anoikis is apoptosis induced by loss of attachment to substrate or to other cells (anoikis). Anoikis overlaps with apoptosis in molecular terms, but is classified as a separate entity because of its specific form of induction (Blank & Shiloh, 2007). Induction of anoikis occurs when cells lose attachment to ECM, or adhere to an inappropriate type of ECM, the latter being the more relevant *in vivo* (Gilmore, 2005).

Cornification: is programmed cell death of keratinocytes. Cell death in the context of cornification involves distinct enzyme classes such as transglutaminases, proteases, DNases and others (Eckhart et al., 2013).

Non-programmed cell death: occurs accidentally in an unplanned manner.

Necrosis is generally characterized to be the uncontrolled death of the cell, usually following a severe insult, resulting in the spillage of the contents of the cell into surrounding tissues and subsequent damage thereof (D'Arcy, 2019).

How it is Measured or Detected**Assays for Quantitating Cell Death:**

- Cell death can be measured by staining a sample of cells with trypan blue, assay is described in protocol: Measuring Cell Death by Trypan Blue Uptake and Light Microscopy (Crowley, Marfell, Christensen, et al., 2015d). Or with propidium iodide, assay is described in protocol: Measuring Cell Death by Propidium Iodide (PI) Uptake and Flow Cytometry (Crowley & Waterhouse, 2015a)
- TUNEL technique: *in situ* terminal deoxynucleotidyl transferase (TdT)-mediated dUTP nick-end labelling can be used to detect apoptotic cells (Bever & Fekete, 1999; Uribe et al., 2013).

Assays for Quantitating Cell Survival

Colony-forming assay can be used to define the number of cells in a population that are capable of proliferating and forming large groups of cells. Described in Protocol: Measuring Survival of Adherent Cells with the Colony-Forming Assay (Crowley, Christensen, & Waterhouse, 2015c); Measuring Survival of Hematopoietic

Cancer Cells with the Colony-Forming Assay in Soft Agar (Crowley & Waterhouse, 2015b).

ASSAYS TO DISTINGUISH APOPTOSIS FROM NECROSIS AND OTHER DEATH MODALITIES

Detecting Nuclear Condensation: The nucleus is generally round in healthy cells but fragmented in apoptotic cells. Dyes such as Giemsa or hematoxylin, which are purple in colour and therefore easily viewed using light microscopy, are commonly used to stain the nucleus. Other features of apoptosis and necrosis, such as plasma membrane blebbing or rupture, can be identified by staining the cytoplasm with eosin. Eosin is pinkish in colour and can also be viewed using light microscopy. Hematoxylin and eosin are, therefore, commonly used together to stain cells. Assay is described in Protocol: Morphological Analysis of Cell Death by Cytopinning Followed by Rapid Staining (Crowley, Marfell, & Waterhouse, 2015c); Analyzing Cell Death by Nuclear Staining with Hoechst 33342 (Crowley, Marfell, & Waterhouse, 2015a).

Detection of DNA Fragmentation: Apoptotic cells with fragmented DNA can be identified and distinguished from live cells by staining with Propidium Iodide (PI) and measuring DNA content by flow cytometry. This assay is described in Protocol: Measuring the DNA Content of Cells in Apoptosis and at Different Cell-Cycle Stages by Propidium Iodide Staining and Flow Cytometry (Crowley, Chojnowski, & Waterhouse, 2015a). TUNEL technique can also be used: *in situ* terminal deoxynucleotidyl transferase (TdT)-mediated dUTP nick-end labelling can be used to detect apoptotic cells (Bever & Fekete, 1999; Crowley, Marfell, & Waterhouse, 2015b; Uribe et al., 2013).

Detecting Phosphatidylserine Exposure: Apoptosis is also characterized by exposure of phosphatidylserine (PS) on the outside of apoptotic cells, which acts as a signal that triggers removal of the dying cell by phagocytosis. Annexin V, can selectively bind to PS to label apoptotic cells in which PS is exposed. Purified annexin V can be conjugated to various fluorochromes, which can then be visualized by fluorescence microscopy or detected by flow cytometry. This assay is described in protocol: Quantitation of Apoptosis and Necrosis by Annexin V Binding, Propidium Iodide Uptake, and Flow Cytometry (Crowley, Marfell, Scott, et al., 2015e).

Detecting Caspase Activity: antibodies that specifically recognize the cleaved fragments of caspases and their substrates can be used to specifically detect caspase activity in apoptotic cells by immunocytochemistry. Flow cytometry (using primary antibodies conjugated to fluorescent molecules, or by counter staining with fluorescently labelled antibodies against the primary antibody) can then be used to quantitate the number of apoptotic cells. This assay is described in protocol: Detecting Cleaved Caspase-3 in Apoptotic Cells by Flow Cytometry (Crowley & Waterhouse, 2015a).

Detecting Mitochondrial Damage: flow cytometry can be used to quantitate the number of cells that have reduced mitochondrial transmembrane potential, which is commonly associated with cytochrome c release during apoptosis. For this assay see protocol: Measuring Mitochondrial Transmembrane Potential by TMRE Staining (Crowley, Christensen, & Waterhouse, 2015b).

Listed below are common methods for detecting the KE, however there may be other comparable methods that are not listed.

Measures of apoptotic cytomorphological alterations:

Apoptotic cells exhibit electron dense nuclei, nuclear fragmentation, intact cell membrane up to the disintegration phase, disorganized cytoplasmic organelles, large clear vacuoles, blebs at cell surface, and apoptotic bodies, which can be visualized with various methods. (Elmore, 2007; Watanabe et al., 2002)

Method of Measurement	Reference	Description	OECD Approved Assay
Transmission electron microscopy (TEM) / Scanning electron microscopy (SEM) / Fluorescence microscopy	Martinez, Reif, and Pappas, 2010; Watanabe et al., 2002	TEM and SEM can image the cytomorphological alterations caused by apoptosis.	No
Stains:			
Hematoxylin with eosin	Elmore, 2007	Hematoxylin stains nuclei blue and eosin stains the cytoplasm/extracellular matrix pink, allowing for the visualization of the cytomorphological alterations of cells.	No
Toluidine blue or methylene blue	Watanabe et al., 2002	Toluidine blue stains cellular nuclei, and identifies malignant tissue, which has an increased DNA content and a higher nuclear-to-cytoplasmic ratio. Methylene blue stain applied to a healthy cell sample results in a colourless stain. This is due to the cell's enzymes, which reduce the methylene blue, thereby, reducing its colour. Methylene blue stain applied to a dead cell sample turns blue.	No
DAPI	Crowley, Marfell, and Waterhouse, 2016	Binds strongly to adenine-thymine-rich regions in the DNA. DAPI can stain live and fixed cells. It passes less efficiently through the membrane in live cells.	Yes
Hoescht 33342	Crowley, Marfell, and Waterhouse, 2016	Binds to DNA in live and fixed cells, used to measure DNA condensation.	Yes
Acridine Orange (AO)	Watanabe et al., 2002	Interacts with DNA/RNA through intercalation/electrostatic interaction, is able to penetrate cell membranes. Stains live cells green and dead cells red.	No
Nile blue sulphate	Watanabe et al., 2002	Stains cell nuclei and lysosomes, indicating apoptotic bodies.	No
Neutral red	Watanabe et al., 2002	Measures lysosomal membrane integrity	No
LysoTracker Red	Watanabe et al., 2002	Measures phagolysosomal activity that occurs due to the engulfment of apoptotic bodies.	No

DNA damage/fragmentation assays:

Assay	Reference	Description	OECD Approved Assay
Terminal deoxynucleotidyl transferase-mediated dUTP nick end-labelling (TUNEL) assay	Kressel and Groscurth, 1994	Apoptosis is detected with the TUNEL method to assay the endonuclease cleavage products by enzymatically end-labelling the DNA strand breaks.	Yes
Nicoletti Assay (SubG1 cell fragment measurement)	Nicoletti et al., 1991	Measures DNA content in nuclei at the pre-G1 phase of the cell cycle (apoptotic nuclei have less DNA than nuclei in healthy cells).	No
Cell Death Detection ELISA kit	Parajuli, 2014	Apoptotic nucleosomes are detected using the Cell Death Detection ELISA kit, which were calculated as absorbance subtraction at 405 nm and 490 nm.	No

Measurement of apoptotic markers through immunochemistry:

Method of Measurement	Reference	Description	OECD Approved Assay
Western blot / immunofluorescence microscopy / immunohistochemistry	Elmore 2007; Martinez, Reif, and Pappas, 2010; Parajuli et al., 2014	Apoptosis can be detected with the expression of various apoptotic markers by western blotting using antibodies. Markers can include: cytosolic cytochrome-c; caspases 2, 3, 6, 7, 8, 9, 10; Bax; Bcl-2 (apoptosis inhibitor); BIRC2; BIRC3; GAPDH; PARP; CDK2; cyclin D1; p53; p63; p73; cytokeratin-18	No

Measures of altered caspase activity:

Method of Measurement	Reference	Description	OECD Approved Assay
Caspase-3 and caspase-9 activity is measured with the enzyme-catalyzed release of p-nitroanilide (pNA) and quantified at 405 nm	Wu, 2016	Visualizes caspase-3 and caspase-9 activity	No
PhiPhiLux Assay	Watanabe et al., 2002	The PhiPhiLux molecule becomes fluorescent once it is cleaved by caspase-3, indicating caspase activity.	No
Ferrocene reporter	Martinez, Reif, and Pappas, 2010	An electrochemical method to detect apoptosis. Ferrocene is attached to a peptide. The peptide sequence is caspase 3 cleavage site and the ferrocene acts as the electrochemical reporter. The more caspase cleavage that occurs, the more ferrocene molecules are cleaved, the stronger the signal.	No
Self-assembled monolayers for matrix assisted laser desorption ionization time-of-flight mass spectrometry (SAMDI-MS) assay	Martinez, Reif, and Pappas, 2010	This assay detects caspase activity.	No

Measures of altered mitochondrial physiology:

Method of Measurement	Reference	Description	OECD Approved Assay
Laser scanning confocal microscopy (LSCM)	Watanabe et al., 2002	LCSM can monitor many mitochondrial events following staining of cells, such as: mitochondrial permeability transition, depolarization of the inner mitochondrial membrane, which may be indicative of apoptosis.	No
Fluorescent, cationic, lipophilic mitochondrial dyes, such as: JC-1 dye, Rhodamine, DiOC ₆ , Mitotracker red	Martinez, Reif, and Pappas, 2010; Sivandzade, Bhalerao, and Cucullo, 2019	These mitochondrial dyes can indicate disintegration of the mitochondrial outer membrane's electrochemical gradient, as different fluorescence is observed between healthy and apoptotic cells. In healthy cells the dye accumulates in aggregates, but in apoptotic cells missing the electrochemical membrane, the dye will spread out into the cytoplasm providing different fluorescent signals.	No

Other measures:

Method of measurement	Reference	Description	OECD Approved Assay
Apoptosis PCR microarray	Elmore, 2007	A method to profile the gene expression of many apoptotic-related genes, for example: ligands, receptors, intracellular modulators, and transcription factors.	No
Fluorescence correlation spectroscopy (FCS) or dual-colour fluorescence cross-correlation spectroscopy (dcFCCS)	Martinez, Reif, and Pappas, 2010	Used to measure protease activity.	No
Apoptosis is measured with Annexin V-FITC probes	Elmore, 2007; Wu et al., 2016	A measure of apoptotic membrane alterations. Annexin-V detects externalized phosphatidylserine residues, a result of apoptosis. Can be conducted in conjunction with propidium iodide (PI) staining. The relative percentage of Annexin V-FITC-positive/PI-negative cells is analyzed by flow cytometry.	Yes

References

Alberts, B. et al. (2002), "Programmed Cell Death (Apoptosis)", in Molecular Biology of the Cell. 4th edition, Garland Science, New York, <https://www.ncbi.nlm.nih.gov/books/NBK26873/>

Bertheloot, D., Latz, E., and B. S. Franklin (2021), "Necroptosis, pyroptosis and apoptosis: an intricate game of cell death", Cellular & Molecular Immunology, 18, 1106-1121. <https://doi.org/10.1038/s41423-020-00630-3>

Bever, M. M., and D. M. Fekete (1999), "Ventromedial focus of cell death is absent during development of Xenopus and zebrafish inner ears", Journal of Neurocytology, 28(10- 11), 781-793. <https://doi.org/10.1023/a:1007005702187>

Blank, M., and Y. Shiloh (2007), "Cell Cycle Programs for Cell Death: Apoptosis is Only One Way to Go", Cell Cycle, 6(6), 686-695. <https://doi.org/10.4161/cc.6.6.3990>

Cotter, T. G., and M. Al-Rubeai (1995), "Cell death (apoptosis) in cell culture systems", Trends in Biotechnology, 13(4), 150-155. [https://doi.org/10.1016/S0167-7799\(00\)88926-X](https://doi.org/10.1016/S0167-7799(00)88926-X)

Crowley, L. C., Chojnowski, G., and N. J Waterhouse (2015a), "Measuring the DNA content of cells in apoptosis and at different cell-cycle stages by propidium iodide staining and flow cytometry", Cold Spring Harbor Protocols, 10, 905-910. <https://doi.org/10.1101/pdb.prot087247>

Crowley, L. C., Christensen, M. E., and N. J Waterhouse (2015b), "Measuring mitochondrial transmembrane potential by TMRE staining", Cold Spring Harbor Protocols, 12, 1092-1096. <https://doi.org/10.1101/pdb.prot087361>

Crowley, L. C., Christensen, M. E., and N. J Waterhouse (2015c), "Measuring survival of adherent cells with the Colony-forming assay", Cold Spring Harbor Protocols, 8, 721- 724. <https://doi.org/10.1101/pdb.prot087171>

Crowley, L. C. et al. (2015d), "Measuring cell death by trypan blue uptake and light microscopy", Cold Spring Harbor Protocols, 7, 643-646. <https://doi.org/10.1101/pdb.prot087155>

Crowley, L. C. et al. (2016), "Dead cert: Measuring cell death", Cold Spring Harbor Protocols, 2016(12), 1064-1072. <https://doi.org/10.1101/pdb.top070318>

Crowley, L. C. et al. (2015e), "Quantitation of apoptosis and necrosis by annexin V binding, propidium iodide uptake, and flow cytometry", Cold Spring Harbor Protocols, 11, 953-957. <https://doi.org/10.1101/pdb.prot087288>

Crowley, L. C., Marfell, B. J., and N. J Waterhouse (2015a), "Analyzing cell death by nuclear staining with Hoechst 33342", Cold Spring Harbor Protocols, 9, 778-781. <https://doi.org/10.1101/pdb.prot087205>

Crowley, L. C., Marfell, B. J., and N. J Waterhouse (2015b), "Detection of DNA fragmentation in apoptotic cells by TUNEL", Cold Spring Harbor Protocols, 10, 900-905. <https://doi.org/10.1101/pdb.prot087221>

Crowley, L. C., Marfell, B. J., and N. J Waterhouse (2015c), "Morphological analysis of cell death by cytopinning followed by rapid staining", Cold Spring Harbor Protocols, 9, 773-777. <https://doi.org/10.1101/pdb.prot087197>

Crowley, L. C. and N. J Waterhouse (2015a), "Detecting cleaved caspase-3 in apoptotic cells by flow cytometry", Cold Spring Harbor Protocols, 11, 958-962. <https://doi.org/10.1101/pdb.prot087312>

Crowley, L. C. and N. J Waterhouse (2015b), "Measuring survival of hematopoietic cancer cells with the Colony-forming assay in soft agar", Cold Spring Harbor

AOP482

Protocols, 8, 725. <https://doi.org/10.1101/pdb.prot087189>

D'Arcy, M. S. (2019), "Cell death: a review of the major forms of apoptosis, necrosis and autophagy", Cell Biology International, 43(6), 582-592. <https://doi.org/10.1002/cbin.11137>

Eckhart, L. et al. (2013), "Cell death by cornification", Biochimica et Biophysica Acta - Molecular Cell Research, 1833(12), 3471-3480. <https://doi.org/10.1016/j.bbamcr.2013.06.010>

Elmore, S. (2007), "Apoptosis: A Review of Programmed Cell Death", Toxical Pathology, Vol. 35/4, SAGE, <https://doi.org/10.1080/01926230701320337>.

Forger, N. G. and G. J. de Vries (2010), "Cell death and sexual differentiation of behavior: worms, flies, and mammals", Current opinion in neurobiology, Vol. 20/6, Elsevier, Amsterdam, <https://doi.org/10.1016/j.conb.2010.09.006>

Gilmore, A. P. (2005), "Anoikis", Cell Death and Differentiation, 12, 1473-1477. <https://doi.org/10.1038/sj.cdd.4401723>

Kanduc, D. et al. (2002), "Cell death: apoptosis versus necrosis (review)", International Journal of Oncology, 21(1), 165-170. <https://doi.org/10.3892/ijo.21.1.165>

Kressel, M. and P. Groscurth (1994), "Distinction of apoptotic and necrotic cell death by in situ labelling of fragmented DNA", Cell and tissue research, Vol. 278/3, Nature, <https://doi.org/10.1007/BF00331373>.

Lockshin, R. A., and Z. Zakeri (2004), "Apoptosis, autophagy, and more", International Journal of Biochemistry and Cell Biology, 36(12), 2405-2419. <https://doi.org/10.1016/j.biocel.2004.04.011>

Martinez, M. M., R. D. Reif, and D. Pappas (2010), "Detection of apoptosis: A review of conventional and novel techniques", Analytical Methods, Vol. 2/8, Royal Society of Chemistry, <https://doi.org/10.1039/COAY00247>

Mizushima, N. et al. (2008), "Autophagy fights disease through cellular self-digestion", Nature, 451(7182), 1069-1075. <https://doi.org/10.1038/nature06639>

Nicoletti I. et al. (1991), "A rapid and simple method for measuring thymocyte apoptosis by propidium iodide staining and flow cytometry", Journal of Immunological Methods, Vol. 139/2, Elsevier, Amsterdam, [https://doi.org/10.1016/0022-1759\(91\)90198-O](https://doi.org/10.1016/0022-1759(91)90198-O)

Ortona, E., P. Matarrese, and W. Malorni (2014), "Taking into account the gender issue in cell death studies", Cell Death & Disease, Vol. 5, Nature, <https://doi.org/10.1038/cddis.2014.73>.

Parajuli, K. R. et al. (2014), "Methoxyacetic acid suppresses prostate cancer cell growth by inducing growth arrest and apoptosis", American journal of clinical and experimental urology, Vol. 2/4, pp. 300-312.

Shintani, T., and D. J. Kionsky (2004), "Autophagy in health and disease: A double-edged sword", Science, 306(5698), 990-995. <https://doi.org/10.1126/science.1099993>

Sivandzade, F., A. Bhalerao and L. Cucullo (2019), "Analysis of the Mitochondrial Membrane Potential Using Cationic JC-1 Dye as a Sensitive Fluorescent Probe", Bio Protocol, Vol. 9/1, <https://doi.org/10.21769/BioProtoc.3128>.

Uribe, P. M. et al. (2013), "Aminoglycoside-Induced Hair Cell Death of Inner Ear Organs Causes Functional Deficits in Adult Zebrafish (Danio rerio)", PLoS ONE, 8(3), 58755. <https://doi.org/10.1371/journal.pone.0058755>

Wade, M. G. et al. (2008), "Methoxyacetic acid-induced spermatocyte death is associated with histone hyperacetylation in rats", Biology of Reproduction, Vol. 78/5, Oxford University Press, Oxford, <https://doi.org/10.1093/biolreprod.107.065151>

Watanabe, M., et al. (2002), "The pros and cons of apoptosis assays for use in the study of cells, tissues, and organs", Microscopy and microanalysis, Vol. 8/5, Cambridge University Press, Cambridge, <https://doi.org/10.1017/S1431927602010346>.

Wu, R. et al. (2016), "microRNA-497 induces apoptosis and suppressed proliferation via the Bcl-2/Bax-caspase9-caspase 3 pathway and cyclin D2 protein in HUVECs", PLoS One, Vol. 11/12, PLOS, San Francisco, <https://doi.org/10.1371/journal.pone.0167052>.

Zhu, M., et al. (2021), "Immunogenic Cell Death Induction by Ionizing Radiation", Frontiers in Immunology, Vol. 12, <https://doi.org/10.3389/FIMMU.2021.705361>

Event: 2089: Altered Bone Cell Homeostasis

Short Name: Altered Bone Cell Homeostasis

Key Event Component

Process	Object	Action
osteoblast differentiation		decreased
osteoclast differentiation		increased

AOPs Including This Key Event

AOP ID and Name	Event Type
Aop:482 - Deposition of energy leading to occurrence of bone loss	KeyEvent

Biological Context

Level of Biological Organization

Cellular

Cell term

Cell term

eukaryotic cell

Domain of Applicability

Taxonomic Applicability

Term	Scientific Term	Evidence	Links
human	Homo sapiens	Low	NCBI
rat	Rattus norvegicus	Moderate	NCBI
mouse	Mus musculus	Moderate	NCBI

Life Stage Applicability**Life Stage Evidence**

All life stages	Moderate
-----------------	----------

Sex Applicability**Sex Evidence**

Unspecific	Moderate
------------	----------

Taxonomic applicability: Altered bone cell homeostasis is applicable to all vertebrates such as humans, mice, and rats (Donaubauer et al., 2020; Smith, 2020).

Life stage applicability: There is insufficient data on life stage applicability of this KE.

Sex applicability: Osteoblast/osteoclastogenesis is sexually dimorphic and influenced by genetic factors (Lorenzo J. 2020; Zanotti et al., 2014; Steppe et al., 2022; Mun et al., 2021).

Evidence for perturbation by a stressor: Multiple studies show that bone cell homeostasis can be disrupted by many types of stressors including ionizing radiation and altered gravity (Donaubauer et al., 2020; Smith, 2020).

Key Event Description

Osteogenesis is the process by which new bone is formed through the balanced action of bone depositing osteoblasts and bone resorbing osteoclasts. Osteogenesis is regulated by the differentiation and activity of osteoblasts/clasts. Dysregulation of bone cell differentiation and functional activity leads to imbalanced osteogenesis and altered bone matrix (Smith, 2020).

Osteoclast precursors are of hematopoietic origin and differentiated into mature, multi-nucleated osteoclasts based on external signals in the microenvironment, of which the cytokine macrophage colony stimulating factor (M-CSF, also known as CSF-1) and receptor activator of NF- κ B ligand (RANKL, aka TNFSF11) are key components (Donaubauer et al., 2020; Smith, 2020). Osteoclasts bone resorbing activity is a result of enzymes expressed in cellular lysosomes that are involved in the degradation extracellular components, including tartrate-resistant acid phosphatase (TRAP), cathepsin K (CTSK), and matrix metalloproteinases (MMPs), among others. Cellular lysosomes are shuttled to the resorption lacunae, located under the ruffled osteoclast membrane, from which they begin degrading the bone matrix (Lacombe, Karsenty, and Ferron, 2013; Smith, 2020).

Osteoblasts differentiate from precursors of mesenchymal origin through various differentiation pathways activated by growth factors and signaling proteins such as bone morphogenic protein 2 (BMP-2) and transforming growth factor B (TGF- β), among others. Pre-osteoblasts migrate to the site of bone resorption, where they become fully functioning osteoblasts capable of depositing new bone matrix (Donaubauer et al., 2020). Osteoblasts will synthesize and secrete bone matrix, most importantly collagen, and participate in the mineralization of bone to regulate the balance of calcium and phosphate ions in bone. Key molecular components involved in bone formation are alkaline phosphatase (ALP), osteocalcin (OCN), and procollagen type I C- and N-terminal propeptides (PICP and PINP), among others (Chen, Deng, and Ling, 2012; Rowe et al., 2021).

How it is Measured or Detected

Listed below are common methods for detecting the KE; however, there may be other comparable methods that are not listed.

Markers of Osteoblast differentiation and activity:

Method(s) of Measurement	References	Description / Marker	OECD-Approved Assay
L-type Wako ALP J2 assay	Abe et al., 2019		
Iso-ALP assay			
Tandem-R Ostase assay	Calvo, Eyre, and Gundberg, 1996	These assays measure a mineralization protein produced by osteoblasts, Alkaline phosphatase (ALP).	No
Alkphase-B assay			
Tandem-MP Ostase immunoassay	Broyles et al., 1998	This assay measures a mineralization protein produced by osteoblasts, bone-specific alkaline phosphatase (BAP)	No
Bovine assays: Ostk-PR assay NovoCalcin assay			
Human assays: OSCAtest osteocalcin assay	Calvo, Eyre, and Gundberg, 1996	These assays measure a mineralization protein produced by osteoblasts, osteocalcin (OCN).	No
Intact osteocalcin assay			
ELISA-OST-NAT assay			
ELIS-OSTEO assay			
Mid-Tact osteocalcin assay			
Procollagen PICP assay	Calvo, Eyre, and Gundberg, 1996	Type I collagen (COL1A1 gene) is the most common form of collagen found in bone. During osteoblastic collagen production and processing, procollagen type I N-terminal peptide (PINP) and procollagen I C-terminal (PICP) are generated and released into the bloodstream.	No
Prolagen-C assay			
Proliferation assay: Bromodeoxyuridine (BrdU) labelling	Bodine and Komm, 2006	Measures cell proliferation.	No
Osteoblast numbers and surface	Willey et al., 2011	Osteoblast formation can be determined by comparing the number of osteoblasts before and after a stressor in cell culture and histological bone samples.	No
Alizarin red stain for calcium deposition	Huang et al., 2019	Alizarin red staining can be used to visualize calcified elements of the bone, the final step of osteoblastic bone formation and mineralization activity.	No

Markers of Osteoclast differentiation and activity:

Method(s) of Measurement	References	Description / Marker	OECD-Approved Assay
BoneTRAP assay	Calvo, Eyre, and Gundberg, 1996 Wu et al., 2009	Measures tartrate-resistant acid phosphatase (TRAP), an osteoclast specific bone-resorbing molecule.	No
Pirijiinorin ICTP via RIA2 antibody assay	Abe et al., 2019		
ICTP assay	Calvo, Eyre, and Gundberg, 1996	Measures C-terminal type I collagen telopeptide (ICTP or CTX), a product of bone collagen degradation.	No
Crosslap assay			
CTX assays	Seibel, 2005		
Osteomark Ntx urine or serum ELISA assay	Calvo, Eyre, and Gundberg, 1996		
NTX assays	Seibel, 2005	Measures N-terminal type I collagen telopeptide (NTX), a product of bone collagen degradation.	No
Colorimetric assays			
HPLC-UV	Calvo, Eyre, and Gundberg, 1996	Measures hydroxyproline, a product of bone collagen degradation.	No
Hypronosticon assay			
HPLC		Measures hydroxylysine glycosides, products of bone collagen degradation.	
ELISA	Seibel, 2005	Hydroxylysine glycosides include: <ul style="list-style-type: none">Galactosyl hydroxylysine (GHYL or GHL)Glycosyl-galactosyl-hydroxylysine (GGHL)	No
Pyrilinks assay			
Pyrilinks D assay	Seibel, 2005	Measures deoxypyridinoline (dpy), a product of bone collagen degradation.	No
Total Dpy assay			
Free Dpy assay			
Immunocytochemical assays for cathepsin K	Seibel, 2005	Measures cathepsin K, a collagen cleaving molecule.	No
Immunoassays for non-collagenous matrix proteins	Seibel, 2005	Non-collagenous matrix proteins, such as bone sialoprotein (BSP), osteonectin, osteopontin, and matrix gla protein (MGP) can be measured via immunoassays. Changes in the amount of non-collagenous matrix proteins before and after a stressor indicate alterations in bone formation.	No
Osteoclast numbers and surface	Willey et al., 2011	Osteoclast formation can be determined by comparing the number of osteoclasts before and after a stressor.	No

References

Abe, Y., et al. (2019), "Increase in Bone Metabolic Markers and Circulating Osteoblast-Lineage Cells after Orthognathic Surgery", *Scientific Reports*, Vol. 9, Nature, <https://doi.org/10.1038/s41598-019-56484-x>.

Bodine, P. V. N., and B. S. Komm (2006), "Wnt Signaling and Osteoblastogenesis", *Reviews in Endocrine and Metabolic Disorders*, Vol. 7, Nature, <https://doi.org/10.1007/s11154-006-9002-4>.

Broyles, D. L., et al. (1998), "Analytical and Clinical Performance Characteristics of Tandem-MP Ostase, a New Immunoassay for Serum Bone Alkaline Phosphatase", *Clinical Chemistry*, Vol. 44/10, Oxford University Press, Oxford, <https://doi.org/10.1093/clinchem/44.10.2139>.

Calvo, M. S., D. R. Eyre, and C. M. Gundberg (1996), "Molecular Basis and Clinical Application of Biological Markers of Bone Turnover", *Endocrine Reviews*, Vol. 17, Oxford University Press, Oxford, <https://doi.org/10.1210/edrv-17-4-333>

Chen, G., C. Deng, and Y.-P. Ling (2012), "TGF- β and BMP signaling in osteoblast differentiation and bone formation", *International Journal of Biological Sciences* Vol. 8/2, Iivyspring International Publisher, <https://doi.org/10.7150/ijbs.2929>

Donaubauer, A., et al. (2020), "The Influence of Radiation on Bone and Bone cells - Differential Effects on Osteoclasts and Osteoblasts", *International Journal of Molecular Sciences*, Vol. 21/17, MDPI, Basel, <https://doi.org/10.3390/ijms21176377>

Huang, B. et al. (2019), "Amifostine Suppresses the Side Effects of Radiation on BMSCs by Promoting Cell Proliferation and Reducing ROS Production", *Stem cells international*, Vol. 2019, Hindawi, <https://doi.org/10.1155/2019/8749090>

Lacombe, J., G. Karsenty, and M. Ferron (2013), "Regulation of Lysosome Biogenesis and Functions in Osteoclasts", *Cell Cycle*, Vol. 12/17, Informa, London, <https://doi.org/10.4161/cc.25825>

Lorenzo J. (2020), "Sexual Dimorphism in Osteoclasts", *Cells*, 9(9), 2086. <https://doi.org/10.3390/cells9092086>

Mun, S. H. et al., (2021) "Sexual Dimorphism in Differentiating Osteoclast Precursors Demonstrates Enhanced Inflammatory Pathway Activation in Female Cells", *Journal of bone and mineral research : the official journal of the American Society for Bone and Mineral Research* B6(6), 1104-1116. <https://doi.org/10.1002/jbm.4270>

Rowe, P., A. Koller, and S. Sharma (Updated January 2022), "Physiology, Bone Remodeling", StatPearls Publishing www.ncbi.nlm.nih.gov/books/NBK499863/

Seibel, M. J. (2005), "Biochemical Markers of Bone Turnover: Part I: Biochemistry and Variability", *The Clinical Biochemist Reviews*, Vol. 26/4, pp. 97-122.

Smith, J.K. (2020), "Osteoclasts and Microgravity", *Life*, Vol. 10/9, MDPI, Basel, <https://doi.org/10.3390/life10090207>

Steppe, L. et al., (2022) "Bone Mass and Osteoblast Activity Are Sex-Dependent in Mice Lacking the Estrogen Receptor α in Chondrocytes and Osteoblast Progenitor Cells", *International Journal of Molecular Sciences* 23, no. 5: 2902. <https://doi.org/10.3390/ijms23052902>

Willey, J. S. et al. (2011), "Space Radiation and Bone Loss", *Gravitational and space biology bulletin*, Vol. 25/1, pp. 14-21.

Wu, Y., et al. (2009), "Tartrate-Resistant Acid Phosphatase (TRAP 5b): A Biomarker of Bone Resorption Rate in Support of Drug Development: Modification, Validation and Application of the BoneTRAP® Kit Assay", *Journal of Pharmaceutical and Biomedical Analysis* Vol. 49/5, Elsevier, Amsterdam, <https://doi.org/10.1016/j.jpba.2009.03.002>.

Zanotti, S. et al., (2014) "Sex and genetic factors determine osteoblastic differentiation potential of murine bone marrow stromal cells", *PloS one*, 9(1), e86757.

<https://doi.org/10.1371/journal.pone.0086757>

Event: 2090: Increase, Bone Remodeling

Short Name: Bone Remodeling

Key Event Component

Process	Object	Action
bone mineralization		decreased
positive regulation of bone resorption		occurrence
abnormal bone remodeling		occurrence

AOPs Including This Key Event

AOP ID and Name	Event Type
Aop:482 - Deposition of energy leading to occurrence of bone loss	KeyEvent

Biological Context

Level of Biological Organization

Tissue

Domain of Applicability

Taxonomic Applicability

Term	Scientific Term	Evidence	Links
human	Homo sapiens	Moderate	NCBI
rat	Rattus norvegicus	Moderate	NCBI
mouse	Mus musculus	Moderate	NCBI

Life Stage Applicability

Life Stage Evidence

All life stages Moderate

Sex Applicability

Sex Evidence

Unspecific Moderate

Taxonomic applicability: Bone remodeling is applicable to all vertebrates such as humans, mice and rats (Bikle and Halloran, 1999; Donaubauer et al., 2020).

Life stage applicability: There is insufficient data on life stage applicability of this KE.

Sex applicability: There is insufficient data on sex applicability of this KE.

Evidence for perturbation by a stressor: Multiple studies show that bone remodeling can be disrupted by many types of stressors including ionizing radiation and altered gravity (Bikle and Halloran, 1999; Donaubauer et al., 2020).

Key Event Description

Bone remodeling is a lifelong process where mature bone tissue is removed by bone resorbing osteoclasts and new bone is formed by bone forming osteoblasts. Each local remodeling event involves a team called the basic multicellular unit (BMU) (Slyfield et al., 2012). Each BMU consists of several morphologically and functionally different cell types, mainly osteoblasts and osteoclasts, that act in coordination on the bone remodeling compartment to replace old bone by new bone.

Physiological bone remodeling, responsible for repairing damaged bone and for mineral homeostasis, is a highly coordinated process that requires balance between bone resorption and bone formation (Raggatt and Partridge, 2010). This tight regulation is necessary to maintain skeletal size, shape, and structural integrity (Raggatt and Partridge, 2010). Mechanical strain or stimulation of bone cells by hormones activates bone remodeling and causes the recruitment of osteoclast precursors, like hematopoietic stem cells (HSCs), to the remodeling site to initiate resorption (Raggatt and Partridge, 2010). Osteocytes, mechanosensory cells that regulate bone homeostasis, basally produce transforming growth factor beta (TGF- β) which inhibits osteoclastogenesis. TGF- β levels are lowered following damage to the bone matrix through osteocyte apoptosis, removing this inhibitory signal (Raggatt and Partridge, 2010). Osteoblasts recruit osteoclast precursors to the remodeling site through the production of monocyte chemoattractant protein-1 (MCP-1). Osteoblasts can then induce osteoclastogenesis through the increased expression of colony stimulating factor 1 (CSF-1) and the receptor activator of nuclear factor kappa B ligand (RANK-L), as well as the decreased expression of osteoprotegerin (OPG), the inhibitor of RANK-L (Donaubauer et al., 2020; Raggatt and Partridge, 2010). Mature osteoclasts produce resorption pits also called resorption bays or Howship's lacunae (Slyfield et al., 2012). Matrix metalloproteinases (MMPs) secreted by osteoblasts degrade the osteoid lining the bone surface, exposing the bone for osteoclast attachment. A resorption cavity is formed as mature osteoclasts degrade the matrix (Raggatt and Partridge, 2010; Slyfield et al., 2012). The acidic environment produced by osteoclasts dissolves the mineralized matrix, while enzymes like Cathepsin K (CTSK) degrade the organic matrix. Reversal cells then remove the undigested demineralized collagen matrix to prepare for bone formation by osteoblasts. TGF- β acts as the signal for the recruitment of osteoblast progenitor mesenchymal stem cells (MSCs). Osteocytes also basally secrete sclerostin, which inhibits the Wnt pathway for osteoblastogenesis. Mechanical strain and parathyroid hormone (PTH) signaling contribute to suppression of sclerostin and subsequent osteoblastogenesis (Raggatt and Partridge, 2010). Mature osteoblasts create the osteoid (unmineralized) matrix with collagen and subsequently mineralize new bone tissue with hydroxyapatite, involving various enzymes including alkaline phosphatase (ALP) (Donaubauer et al., 2020; Raggatt and Partridge, 2010).

Disruption to this process results in an imbalance in the equilibrium of bone resorption and formation. For example, increased resorption by stimulation of osteoclast activity can lead to excessive bone resorption and subsequent weakening of bone structure. The impairment of osteoblast function and survival osteoclasts and increased mineralization by osteoblasts will increase the rate of bone resorption and decrease can decrease the rate of bone formation. Stimulation of osteoclast activity can lead to excessive bone resorption and subsequent weakening of bone structure. The impairment of osteoblast function and survival can decrease the rate of bone formation. These are measurable events.

How it is Measured or Detected

Bone remodeling can be measured by the detection of biochemical markers of bone formation and bone resorption in blood serum, dynamic bone histomorphometry in bone biopsies, or via X-ray imaging techniques *in vivo*. Listed below are common methods for detecting the KE; however, there may be other comparable methods that are not listed.

Method of Measurement	References	Description	OECD Approved Assay
X-ray and imaging options: <ul style="list-style-type: none"> • Single-energy x-ray absorptiometry (S[EA]XA) • Dual-energy x-ray absorptiometry (D[EA]XA) • Single-photon absorptiometry (SPA) • Dual-photon absorptiometry (DPA) • Quantitative computed tomography (QCT) 	Carter, Bouxsein and, Marcus, 1992 Cummings et al., 2002	Recurrent imaging of the same bone region in a specific time interval and subsequent overlay of these images, allows for the identification of bone remodeling units and state of bone remodeling.	No
Measurements of bone minerals in bodily fluids: <ul style="list-style-type: none"> • Calcium stable isotope tracers • Spectrophotometry • Ion-sensitive electrode techniques for ionized calcium 	Smith et al., 2005	Measurement of inorganic skeletal matrix markers such as calcium, phosphorus which, above all, reflect calcium-phosphorus homeostasis and are indicators for the status of bone mineralization.	No
Dynamic bone histomorphometry (2D and 3D kinetic measurements) include: <ul style="list-style-type: none"> • Mineral apposition rate • MAR • Mineral formation rate • Mineralization lag time • Adjusted apposition rate • Osteoid apposition rate • Osteoid maturation time • Bone formation rate • Double-labeled formation events • Formation period • Bone resorption rate • Resorption period • Reversal period • Remodeling period • Quiescent period • Total period • Activation frequency • Structural modeling index (SMI) • Serial block imaging (also known as serial block-face scanning electron microscopy) 	Dempster et al., 2013	Dynamic histomorphometry comprised the evaluation of bone mineralization from fluorochrome labeled samples. Thus, it is a quantitative measure of bone remodeling in addition to evaluation of bone structure over time. Dynamic histomorphometry can be performed in trabecular and cortical bone.	No

Trabeculae measurements:				
<ul style="list-style-type: none"> • Rod volume density (Ro.BV/TV) • Plate volume density (Pi.BV/TV) % rod volume fraction (Ro.BV/BV) • % plate volume fraction (Pi.BV/BV) • Rod volume (Ro.V) • Rod surface (Ro.S) • Rod thickness (Ro.Th) • Rod orientation (Ro.θ) • Rod slenderness (Ro.SI) • Rod mean curvature (Ro. <H>) • Plate volume (Pi.V) • Plate surface (Pi.S) • Plate thickness (Pi.Th) • Plate mean curvature (Pi. <H>) 	Stauber et al., 2006	Rods and plates forming the trabecular can indicate bone remodeling by altering the bone turnover states (bone formation and resorption) and microarchitecture (Compston, 2016).	No	

References

Bikle, D. D., and B.P. Halloran (1999), "The response of bone to unloading", *Journal of Bone and Mineral Metabolism*, Vol. 17/4, Springer Nature, <https://doi.org/10.1007/s007740050090>.

Carter, D. R., M.L. Bouxsein and R. Marcus (1992), "New Approaches for Interpreting Projected Bone Densitometry Data", *Journal of Bone and Mineral Research*, Vol. 7/2, Wiley, <https://doi.org/10.1002/jbmr.5650070204>.

Compston, Juliet (2006), "Bone quality: what is it and how is it measured?", *Arquivos Brasileiros de Endocrinologia & Metabologia*, Vol. 50/4, <https://doi.org/10.1590/S0004-27302006000400003>

Cummings, S. R., D. Bates and D.M. Black (2002), "Clinical Use of Bone Densitometry: Scientific Review", *Journal of the American Medical Association*, Vol. 288/15, JAMA Network, <https://doi.org/10.1001/jama.288.15.1889>.

Dempster, D. W. et al. (2013), "Standardized Nomenclature, Symbols, and Units for Bone Histomorphometry: A 2012 Update of the Report of the ASBMR Histomorphometry Nomenclature Committee", *Journal of Bone and Mineral Research*, Vol. 28, Wiley, <https://doi.org/10.1002/jbmr.1805>.

Donaubauer, A. J., et al. (2020), "The Influence of Radiation on Bone and Bone Cells-Differential Effects on Osteoclasts and Osteoblasts", *International journal of molecular sciences*, Vol. 21/17, MDPI, Basel <https://doi.org/10.3390/ijms21176377>.

Raggatt, L. J., and N.C. Partridge (2010), "Cellular and Molecular Mechanisms of Bone Remodeling", *Journal of Biological Chemistry*, Vol. 285/33, Elsevier, Amsterdam, <https://doi.org/10.1074/jbc.R109.041087>.

Slyfield, C. R. et al. (2012), "Three-Dimensional Dynamic Bone Histomorphometry", *Journal of Bone and Mineral Research*, Vol. 27/2, Wiley, <https://doi.org/10.1002/jbmr.553>

Smith, S. M., et al. (2005), "Bone Markers, Calcium Metabolism, and Calcium Kinetics during Extended-Duration Space Flight on the Mir Space Station", *Journal of Bone and Mineral Research*, Vol. 20/2, Wiley, <https://doi.org/10.1359/JBMR.041105>.

Stauber et al. (2006), "Importance of Individual Rods and Plates in the Assessment of Bone Quality and Their Contribution to Bone Stiffness", *Journal of Bone and Mineral Research*, Vol. 21/4, Wiley, <https://doi.org/10.1359/jbmr.060102>.

Wang, Y. H. et al. (2006), "Examination of Mineralized Nodule Formation in Living Osteoblastic Cultures Using Fluorescent Dyes", *Biotechnology Progress*, Vol. 22/6, Wiley, <https://doi.org/10.1021/bp060274b>

List of Adverse Outcomes in this AOP

Event: 2091: Occurrence, Bone Loss

Short Name: Bone Loss

Key Event Component

Process	Object	Action
decreased trabecular bone volume		occurrence
decreased bone mineral density		occurrence

AOPs Including This Key Event

AOP ID and Name	Event Type
Aop:482 - Deposition of energy leading to occurrence of bone loss	AdverseOutcome

Biological Context

Level of Biological Organization

Organ

Domain of Applicability

Taxonomic Applicability

Term	Scientific Term	Evidence	Links
human	<i>Homo sapiens</i>	Moderate	NCBI
rat	<i>Rattus norvegicus</i>	Moderate	NCBI
mouse	<i>Mus musculus</i>	Moderate	NCBI

Life Stage Applicability**Life Stage Evidence**

All life stages	Moderate
-----------------	----------

Sex Applicability**Sex Evidence**

Unspecific	Moderate
------------	----------

Taxonomic applicability: Bone loss is applicable to all vertebrates such as humans, mice and rats.

Life stage applicability: There is insufficient data on life stage applicability of this KE.

Sex applicability: According to a study of astronauts who spent 170 days living in the international space station, women demonstrated greater preservation of their musculoskeletal tissues during the mission compared to males, (33 men, 9 women) (Lang et al., 2017). However, other studies have indicated that the rates of regional and whole-body bone loss were similar in male and female astronauts (Lang et al., 2017).

Evidence for perturbation by a stressor: Multiple studies showed that many types of stressors including ionizing radiation and altered gravity (Bikle and Halloran, 1999; Donaubauer et al., 2020) can interfere with bone remodeling.

Key Event Description

Bone loss describes the reduction in bone mass or density, which can be caused by various processes and is a characteristic of osteopenia, and osteoporosis, and can lead to bone fracture. An imbalance between bone resorption and formation towards higher bone abrasion contributes to bone loss (Bikle and Halloran, 1999). A decline of bone mineralization and bone density over time or a significant deviation from established reference ranges are direct indicators of bone loss (Cummings, Bates, and Black, 2002). In addition, bone loss can lead to increased risk of bone fractures as bone loss interferes with overall bone integrity and its capacity to withstand mechanical load (Cummings, Bates, and Black, 2002).

How it is Measured or Detected

Listed below are common methods for detecting the KE; however, there may be other comparable methods that are not listed

Measurement method	Reference	Description	OECD Approved Assay
X-ray and imaging options: <ul style="list-style-type: none"> Single energy x-ray absorptiometry (S[E]XA) Dual-energy x-ray absorptiometry (D[E]XA) Single-photon absorptiometry (SPA) Dual-photon absorptiometry (DPA) Quantitative computed tomography (QCT) Radiographic absorptiometry Ultrasound (quantitative bone ultrasonography) Magnetic resonance imaging (MRI) 	Carter, Bouxsein, and Marcus, 1992 Cummings, Bates, and Black, 2002 Russo, 2009 Rho, Ashman, and Turner, 1993	Bone mineral density (BMD) is a direct measurement of bone matrix composition. Less mineral dense bones indicate bone loss.	No
Measurement of bone minerals via staining methods: <ul style="list-style-type: none"> Xylenol orange (bone formation marker) Calcein green (bone formation marker) Tetracycline (bone formation marker) Von Kossa (calcium salt stain, non-specific) Alizarin red (calcium cation stain) All listed chemicals stain calcium.	Kulak and Dempster, 2010 Wang et al., 2006	<p>Less bone deposition and/or reduced mineral dense bones indicate bone loss.</p> <p>Comment: xylenol orange, calcein green, and tetracycline are calcium binding fluorescent dyes that are used to label new bone deposition.</p> <p>Von Kossa method is based on the binding of silver ions to anions (phosphates, sulphates, or carbonates) of calcium salts and the reduction of silver salts to form dark brown or black metallic silver staining. Unlike the non-specificity of von Kossa for calcium, alizarin red reacts with calcium cation to form a chelate.</p>	No

Static bone histomorphometry of an intact iliac crest bone biopsy (2D and 3D Structural measurements): <ul style="list-style-type: none">• Marrow diameter• Marrow area• Marrow volume• Trabecular number, spacing, width, diameter, thickness• Cortical thickness, area, and porosity (bone-specific surface)• Cancellous bone volume• Mineralized volume, thickness• Osteoid surface, volume, thickness• Interstitial thickness• Bone volume fraction (BV/TV)• Wall width, thickness• Percent eroded surface• Serial block imaging (aka serial block-face scanning electron microscopy)	Dempster et al., 2013	Static bone histomorphometry with structural measurements is the quantitative measure of bone structure at a fixed time point. Bone histomorphometry is most useful when interpreted in the context with other data such as structural analysis (CT, DEXA), serum markers of bone turnover etc.	No
Measurements of bone mechanical resistance: <ul style="list-style-type: none">• Energy-absorbing bone capacity. Bones that cannot absorb as much energy after trauma are more likely to fracture.• Stress-strain curve. Measures the strain exhibited on a bone according to increasing applied stress until fracture.• Three-point bending test. Is a structural mechanical test where the entire bone is held in a fixture attached to a material testing machine and the mid-diaphysis is loaded until broken. 3PB measures applied load and corresponding bone displacement indicating bone mechanical properties. Combination of 3PB and microCT data of the mid-diaphysis allows to calculate bone material properties.	Fonseca et al., 2013; Sharir, Barak, and Shahar, 2008; Walker et al., 2015; Turner, 2002	Measurements of bone mechanical resistance indicates changes in bone integrity possibly due to bone loss, as weaker bones are unable to withstand to as much mechanical force as healthy bones. Often measures Young's modulus (E) which indicates the property of an object to stretch and deform and is defined as the ratio of applied stress to measured strain on an object.	No
Measurements of bone connectivity: <ul style="list-style-type: none">• Euler's characteristic• Betti numbers• Connectivity density (Conn. D)	Odgaard and Gundersen, 1993	These mathematical models allow for the 3D reconstruction of connectivity in cancellous bone. Bone loss, as seen as a decrease in strength and bone stiffness, can result from a decrease in connective bone tissue.	No

References

Bikle, D. D., & B. P. Halloran (1999), "The response of bone to unloading", *Journal of Bone and Mineral Metabolism*, Vol. 17, Nature, <https://doi.org/10.1007/s007740050090>

Carter, D. R., M. L. Bouxsein, and R. Marcus. (1992), "New Approaches for Interpreting Projected Bone Densitometry Data", *Journal of Bone and Mineral Research*, Vol. 7/2, Wiley, <https://doi.org/10.1002/jbmr.5650070204>.

Cummings, S. R., D. Bates, and D. M. Black (2002), "Clinical Use of Bone Densitometry: Scientific Review", *Journal of the American Medical Association*, Vol. 288/15, <https://doi.org/10.1001/jama.288.15.1889>.

Dempster, D. W., et al. (2013), "Standardized Nomenclature, Symbols, and Units for Bone Histomorphometry: A 2012 Update of the Report of the ASBMR Histomorphometry Nomenclature Committee", *American Society for Bone and Mineral Research* Vol. 28/1, Wiley, <https://doi.org/10.1002/jbmr.1805>.

Fonseca, H., et al. (2013), "Bone Quality: The Determinants of Bone Strength and Fragility", *Sports Medicine*, Vol. 44/1, Nature, <https://doi.org/10.1007/s40279-013-0100-7>

Kulak, C. A. M and D. W. Dempster (2010), "Bone histomorphometry: a concise review for endocrinologists and clinicians", *Arquivos Brasileiros de Endocrinologia & Metabologia*, Vol. 54/2, Sociedade Brasileira de Endocrinologia e Metabologia, Sao Paulo, <https://doi.org/10.1590/S0004-27302010000200002>

Lang, T. et al. (2017), "Towards human exploration of space: The THESEUS review series on muscle and bone research priorities", *npj Microgravity*, Vol. 3/1, Nature, <https://doi.org/10.1038/s41526-017-0013-0>.

Odgaard, A. and H. J. G. Gundersen (1993), "Quantification of connectivity in cancellous bone, with special emphasis on 3-D reconstructions", *Bone*, Vol. 14, Elsevier, Amsterdam, [https://doi.org/10.1016/8756-3282\(93\)90245-6](https://doi.org/10.1016/8756-3282(93)90245-6)

Rho, J. Y., R. B. Ashman, and C. H. Turner (1993), "Young's modulus of trabecular and cortical bone material: Ultrasonic and microtensile measurements", *Journal of Biomechanics*, Vol. 26/2, Elsevier, Amsterdam, [https://doi.org/10.1016/0021-9290\(93\)90042-D](https://doi.org/10.1016/0021-9290(93)90042-D)

Russo, C. R. (2009), "The effects of exercise on bone. Basic concepts and implications for the prevention of fractures", *Clinical Cases Mineral and Bone Metabolism*, Vol. 6/3, pp. 223-228.

Sharir, A., M. M. Barak, and R. Shahar (2008), "Whole bone mechanics and mechanical testing", *The Veterinary Journal*, Vol. 177/1, Elsevier, Amsterdam, <https://doi.org/10.1016/j.tvjl.2007.09.012>

Turner, C. H. (2002), "Biomechanics of Bone: Determinants of Skeletal Fragility and Bone Quality", *Osteoporosis International*, Vol. 13, Nature, <https://doi.org/10.1007/s001980200000>

Walker, A. H. et al. (2015), "Changes in Mechanical Properties of Rat Bones under Simulated Effects of Microgravity and Radiation", *Physics Procedia*, Vol. 66, Elsevier, Amsterdam, <https://doi.org/10.1016/j.phpro.2015.05.081>

Wang, Y. H., et al. (2006), "Examination of Mineralized Nodule Formation in Living Osteoblastic Cultures Using Fluorescent Dyes", *Biotechnology Progress*, Vol. 22/6, Wiley, <https://doi.org/10.1021/bp060274b>

Appendix 2

List of Key Event Relationships in the AOP

List of Adjacent Key Event Relationships

Relationship: 2769: Energy Deposition leads to Oxidative Stress

AOPs Referencing Relationship

AOP Name	Adjacency	Weight of Evidence	Quantitative Understanding
Deposition of energy leads to abnormal vascular remodeling	adjacent	High	High
Deposition of Energy Leading to Learning and Memory Impairment	adjacent	High	Moderate
Deposition of energy leading to occurrence of bone loss	adjacent	High	Moderate
Deposition of energy leading to occurrence of cataracts	adjacent	High	High

Evidence Supporting Applicability of this Relationship

Taxonomic Applicability

Term	Scientific Term	Evidence	Links
human	<i>Homo sapiens</i>	Moderate	NCBI
mouse	<i>Mus musculus</i>	Moderate	NCBI
rat	<i>Rattus norvegicus</i>	High	NCBI
rabbit	<i>Oryctolagus cuniculus</i>	Low	NCBI

Life Stage Applicability

Life Stage Evidence

Juvenile	High
Adult	Moderate

Sex Applicability

Sex	Evidence
Male	High
Female	Moderate
Unspecific	High

Most evidence is derived from in vitro studies, predominately using rabbit models. Evidence in humans and mice is moderate, while there is considerable available data using rat models. The relationship is applicable in both sexes; however, males are used more often in animal studies. No studies demonstrate the relationship in preadolescent animals, while adolescent animals were used very often, and adults were used occasionally in vivo studies.

Key Event Relationship Description

Energy deposited onto biomolecules stochastically in the form on ionizing and non-ionizing radiation can cause direct and indirect molecular-level damage. As energy is deposited in an aqueous solution, water molecules can undergo radiolysis, breaking bonds to produce reactive oxygen species (ROS) (Ahmadi et al., 2021; Karimi et al., 2017) or directly increase function of enzymes involved in ROS generation (i.e. catalase). Various species of ROS can be generated with differing degrees of biological effects. For example, singlet oxygen, superoxide, and hydroxyl radical are highly unstable, with short half-lives and react close to where they are produced, while species like H₂O₂ are much more stable and membrane permeable, meaning they can travel from the site of production, reacting elsewhere as a much weaker oxidant (Spector, 1990). In addition, enzymes involved in reactive oxygen and nitrogen species (RONS) production can be directly upregulated following the deposition of energy (de Jager, Cockrell and Du Plessis, 2017). Although less common than ROS, reactive nitrogen species (RNS) can also be produced by energy deposition resulting in oxidative stress (Cadet et al., 2012; Tangvarasittichai & Tangvarasittichai, 2019), a state in which the amount of ROS and RNS, collectively known as RONS, overwhelms the cell's antioxidant defence system. This loss in redox homeostasis can lead to oxidative damage to macromolecules including proteins, lipids, and nucleic acids (Schoenfeld et al., 2012; Tangvarasittichai & Tangvarasittichai, 2019; Turner et al., 2002).

Evidence Supporting this KER

Overall weight of evidence: High

Biological Plausibility

A large body of literature supports the linkage between the deposition of energy and oxidative stress. Multiple reviews describe the relationship in the context of ROS production (Marshall, 1985; Balasubramanian, 2000; Jurja et al., 2014), antioxidant depletion (Cabrera et al., 2011; Fletcher, 2010; Ganea & Harding, 2006; Hamada et al., 2014; Spector, 1990; Schoenfeld et al., 2012; Wegener, 1994), and overall oxidative stress (Eaton, 1994; Tangvarasittichai & Tangvarasittichai, 2019). This includes investigations into the mechanism behind the relationship (Ahmadi et al., 2021; Balasubramanian, 2000; Cencer et al., 2018; Eaton, 1994; Fletcher, 2010; Jiang et al., 2006; Jurja et al., 2014; Padgaonkar et al., 2015; Quan et al., 2021; Rong et al., 2019; Slezak et al., 2015; Solovieva & Kizub, 2019; Tian et al., 2017; Tahimic & Globus, 2017; Varma et al., 2011; Venkatesulu et al., 2018; Wang et al., 2019a; Yao et al., 2008; Yao et al., 2009; Zigman et al., 2000).

Water radiolysis is a main source of free radicals. Energy ionizes water and free radicals are produced that combine to create more stable ROS, such as hydrogen peroxide, hydroxide, superoxide, and hydroxyl (Eaton, 1994; Rehman et al., 2016; Tahimic & Globus, 2017; Tian et al., 2017; Varma et al., 2011; Venkatesulu et al., 2018). ROS formation causes ensuing damage to the body, as ~80% of tissues are comprised of water (Wang et al., 2019a). Ionizing radiation (IR) is a source of energy deposition, it can also interact with molecules, such as nitric oxide (NO), to produce less common free radicals, including RNS (Slezak et al., 2015; Tahimic & Globus, 2017; Wang et al., 2019a). Free radicals can diffuse throughout the cell and damage vital cellular components, such as proteins, lipids, and DNA, as well as dysregulate cellular processes, such as cell signaling (Slezak et al., 2015; Tian et al., 2017).

ROS are also commonly produced by nicotinamide adenine dinucleotide phosphate (NADPH) oxidase (NOX). Deposition of energy can activate NOX and induce expression of its catalytic and cytosolic components, resulting in increased intracellular ROS (Solovieva & Kizub, 2019). Intracellular ROS production can also be initiated through the expression of protein kinase C, which in turn activates NOX through phosphorylation of its cytosolic components (Solovieva & Kizub, 2019). Alternatively, ROS are often formed at the electron transport chain (ETC) of the mitochondria, due to IR-induced electron leakage leading to ionization of the surrounding O₂ to become superoxide (Solovieva & Kizub, 2019). Additionally, energy reaching a cell can be absorbed by an unstable molecule, often NADPH, known as a chromophore, which leads to the production of ROS (Balasubramanian, 2000; Cencer et al., 2018; Jiang et al., 2006; Jurja et al., 2014; Padgaonkar et al., 2015; Yao et al., 2009; Zigman et al., 2000).

Energy deposition can also weaken a cell's antioxidant defence system through the depletion of certain antioxidant enzymes, such as superoxide dismutase (SOD) and catalase (CAT). Antioxidants are consumed during the process of neutralizing ROS, so as energy deposition stimulates the formation of ROS it begins to outpace the rate at which antioxidants are replenished; this results in an increased risk of oxidative stress when their concentrations are low (Belkacem et al., 2001; Giblin et al., 2002; Ji et al., 2014; Kang et al., 2020; Karimi et al., 2017; Padgaonkar et al., 2015; Rogers et al., 2004; Slezak et al., 2015; Tahimic & Globus, 2017; Wang et al., 2019a; Wegener, 1994; Weinreb & Dovrat, 1996; Zhang et al., 2012; Zigman et al., 1995; Zigman et al., 2000). When the amount of ROS overwhelms the antioxidant defence system, the cell will enter oxidative stress leading to macromolecular and cellular damage (Tangvarasittichai & Tangvarasittichai, 2019).

Empirical Evidence

The relationship between energy deposition and oxidative stress is strongly supported by primary research on the effects of IR on ROS and antioxidant levels (Bai et al., 2020; Cervelli et al., 2017; Hatoum et al., 2006; Huang et al., 2018; Huang et al., 2019; Karam & Radwan, 2019; Kook et al., 2015; Liu et al., 2018; Liu et al.,

2019; Mansour, 2013; Philipp et al., 2020; Ramadan et al., 2020; Sharma et al., 2018; Shen et al., 2018; Soltani et al., 2016; Soucy et al., 2010; Soucy et al., 2011; Ungvari et al., 2013; Wang et al., 2016; Wang et al., 2019b; Zhang et al., 2018; Zhang et al., 2020). Of note is that the relationship is demonstrated across studies conducted using various cell types, models and using broad dose ranges as summarized below. Much evidence is available and described to help discern the quantitative understanding of the relationship, since it is well established.

Dose Concordance

It is well-accepted that any dose of radiation will deposit energy onto matter. Doses as low as 1 cGy support this relationship (Tseung et al., 2014). Following the deposition of energy, markers of oxidative stress are observed in the form of RONS, a change in levels of antioxidants, and oxidative damage to macromolecules. These effects have been shown across various organs/tissues and cell types as described below.

RONS

Cardiovascular tissue:

There is a considerable amount of evidence to support this relationship in cell types and tissues of relevance to the cardiovascular system. Recent studies have shown a linear increase in ROS in human umbilical vein endothelial cells (HUVECs) following 0.5 Gy gamma irradiation (Wang et al., 2019b). HUVECs irradiated with 0.25 Gy X-rays (Cervelli et al., 2017) and 9 Gy 250kV photons (Sharma et al., 2018) show increased ROS. Gamma ray irradiated rats at 5 Gy display increased ROS levels in the aorta (Soucy et al., 2010). A study using cerebromicrovascular endothelial cell (CMVECs) showed a dose-dependent increase in ROS from 0.8 Gy gamma irradiation (Ungvari et al., 2013). Additionally, telomerase-immortalized coronary artery endothelial (TICAЕ) and telomerase-immortalized microvascular endothelial (TIME) cells irradiated with 0.1 and 5 Gy of X-rays displayed increased ROS production (Ramadan et al., 2020). Gut arterioles of rats showed increased ROS following multiple fractions of 2.5 Gy X-ray rat irradiation (Hatoum et al., 2006). Additionally, rats irradiated with 1 Gy of 56Fe expressed increased ROS levels in the aorta (Soucy et al., 2011).

Brain tissue:

Markers of oxidative stress have also been consistently observed in brain tissue. Human neural stem cells subjected to 1, 2 or 5 Gy gamma rays showed a dose-dependent increase in RONS production (Acharya et al., 2010). A dose-dependent increase in ROS was observed in rat brains following 1-10 Gy gamma rays (Collins-Underwood et al., 2008). Neural precursor cells exposed to 0-10 Gy of X-irradiation showed increased ROS levels (Giedzinski et al., 2005; Limoli et al., 2004). Mice brain tissue displayed increased ROS following proton irradiation (Baluchamy et al., 2012; Giedzinski et al., 2005). Neural processor cells expressed linearly increased ROS levels following doses of 56Fe (Limoli et al., 2007). A dose-dependent increase in RONS was also observed after exposure to 1-15 cGy 56Fe irradiation in mice neural stem/precursor cell (Tseng et al., 2014). Human neural stem cells exposed to 5-100 cGy of various ions demonstrated a dose-dependent increase in RONS (Baulch et al., 2015).

Eye tissue:

The eye is also sensitive to the accumulation of free radicals, in a state of antioxidant decline. It has been shown in human lens epithelial cells (HLECs) and HLE-B3 following gamma irradiation of 0.25 and 0.5 Gy that ROS levels are markedly increased (Ahmadi et al., 2021). Exposure to non-ionizing radiation, such as ultraviolet (UV)-B, has also led to increased ROS in HLECs and mice lenses (Ji et al., 2015; Kubo et al., 2010; Rong et al., 2019; Yang et al., 2020)

Bone tissue:

Rat bone marrow-derived mesenchymal stem cell (bmMSCs) irradiated with 2, 5 and 10 Gy gamma rays and murine MC3T3-E1 osteoblast cells irradiated with 2, 4, and 8 Gy of X-rays have shown a dose-dependent increase in ROS levels (Bai et al., 2020; Kook et al., 2015). Murine RAW264.7 cells and rat bmMSC irradiated with 2 Gy of gamma rays displayed increased ROS levels (Huang et al., 2019; Huang et al., 2018; hang et al., 2020). Human bone marrow-derived mesenchymal stem cell (hBMMSCs) irradiated with 2 or 8 Gy X-rays showed increased ROS (Liu et al., 2018; Zhang et al., 2018). Similarly, murine MC3T3-E1 osteoblast-like cells irradiated with 6 Gy of X-rays also displayed increased ROS (Wang et al., 2016). Finally, whole-body irradiation of mice with 2 Gy of 31.6 keV although LET 12C heavy ions showed increased ROS (Liu et al., 2019).

Antioxidants

Blood:

Workers exposed to X-rays at less than 1 mSv/year for an average of 15 years showed around 20% decreased antioxidant activity compared to unexposed controls (Klucinski et al., 2008). Similarly, adults exposed to high background irradiation of 260 mSv/year showed about 50% lower antioxidant activity power compared to controls (Attar, Kondolousy and Khansari, 2007).

Cardiovascular tissue:

Heart tissue of rats following gamma irradiation of rats at 5 and 6 Gy resulted in a decrease in antioxidant levels (Karam & Radwan, 2019; Mansour, 2013). Similarly, HUVECs (Soltani, 2016) and TICAЕ cells (Philipp et al., 2020) irradiated at 2 Gy and 0.25-10 Gy gamma rays, respectively, displayed decreased antioxidant levels. Mice exposed to 18 Gy of X-ray irradiation showed decreased antioxidants in the aorta (Shen et al., 2018).

Brain tissue:

Mice brain tissue following 2, 10 and 50 cGy whole-body gamma irradiation revealed a dose-dependent change in SOD2 activity (Veeraraghavan et al., 2011). Mice brain tissue showed decreased glutathione (GSH) and SOD levels following proton irradiation (Baluchamy et al., 2012)

Eye tissue:

Rats exposed to 15 Gy gamma rays demonstrated decreased antioxidants in the lens tissue (Karimi et al., 2017). Neutron irradiation of rats at 3.6 Sv resulted in a decrease in antioxidants in lens (Chen et al., 2021). A few studies found a dose concordance between UV irradiation and decreased antioxidant levels (Hua et al., 2019; Ji et al., 2015; Zigman et al., 2000; Zigman et al., 1995). HLECs following UV exposure from 300 J/m² to 14,400 J/m² in HLECs showed linear decreases in antioxidant activity (Ji et al., 2015). Similarly, HLEC exposed to 4050, 8100 and 12,150 J/m² found decreased antioxidant levels (Hua et al., 2019). Following UV irradiation of rabbit and squirrel lens epithelial cells (LECs) showed a linear decrease of antioxidant level, CAT (Zigman et al., 2000; Zigman et al., 1995). Mice exposed to UV irradiation found decreased antioxidant levels in lens (Zhang et al., 2012). Similarly, SOD levels decreased following 0.09 mW/cm² UVB exposure of HLECs (Kang et al., 2020).

Bone tissue:

Rat bmMSCs irradiated with 2, 5 and 10 Gy gamma rays and Murine MC3T3-E1 osteoblast cells irradiated with 2, 4, and 8 Gy of X-rays showed a dose-dependent decrease in antioxidant levels (Bai et al., 2020; Kook et al., 2015). hBMMSCs irradiated with 8 Gy X-rays also showed a decrease in antioxidant, SOD, levels (Liu et al., 2018).

Oxidative Damage

Cardiovascular tissue:

HUVECs and rat hearts irradiated by gamma rays at 2 and 6 Gy, respectively, resulted in increased levels of oxidative stress markers, such as malondialdehyde (MDA), and thiobarbituric reactive substances (TBARS) (Mansour, 2013; Soltani, 2016).

Brain tissue:

Mice brain tissue were shown to have increased lipid peroxidation (LPO) as determined by MDA measurements, following proton irradiation at 1 and 2 Gy (Baluchamy et al., 2012). Neural precursor cells from rat hippocampus exposed to 0, 1, 5 and 10 Gy of X-irradiation resulted in increased lipid peroxidation (Limoli et al., 2004).

Eye tissue:

Rats exposed to 15 Gy gamma rays demonstrated increased MDA in lens tissue (Karimi et al., 2017). Neutron irradiation of rats at 3.6 Sv resulted in an initial decrease, followed by an increase in MDA in lens (Chen et al., 2021). Following UV irradiation at 300, 4050, 8100 and 12,150 J/m², there was an increase in LPO in human lens (Chitchumroonchokchai et al., 2004; Hua et al., 2019). Similarly, LPO increased following 0.09 mW/cm² UVB exposure of HLECs (Kang et al., 2020).

Time Concordance

It is well-accepted that deposition of energy into matter results in immediate vibrational changes to molecules or ionization events. Deposition of energy is therefore

an upstream event to all follow-on latent events like oxidative stress.

RONS

Cardiovascular tissue:

In TICAE and TIME cells, ROS increased at 45 minutes after X-ray irradiation (Ramadan et al., 2020). Superoxide and peroxide production were increased 1 day after 2-8 Gy of gamma irradiation in CMVECs (Unvari et al., 2013).

Bone tissue:

hBMMSCs irradiated with X-rays at 2 Gy showed peak ROS production at 2-8h post-irradiation (Zhang et al., 2018). Murine RAW264.7 cells (can undergo osteoclastogenesis) irradiated with 2 Gy of gamma rays showed increased ROS at 2-8h post- irradiation (Huang et al., 2018).

Brain tissue:

In human lymphoblast cells exposed to 2 Gy of X-rays, ROS were increased at various times between 13 and 29 days post- irradiation (Rugo and Schiestl, 2004). RONS were increased in human neural stem cells at 12-48h post-irradiation with 2 and 5 Gy of gamma rays (Acharya et al., 2010). ROS levels were increased in rat neural precursor cells at 6-24h after irradiation with 1-10 Gy of protons (Giedzinski et al., 2005). Both 56Fe (1.3 Gy) and gamma ray (2 Gy) irradiation of mice increased ROS levels after 2 months post-irradiation in the cerebral cortex (Suman et al., 2013). ROS were also increased 12 months after 56Fe irradiation (Suman et al., 2013). RONS increased as early as 12h post-irradiation continuing to 8 weeks with 2-200 cGy doses of 56Fe irradiation of mouse neural stem/precursor cells (Tseng et al., 2014). The same cell type irradiated with 1 and 5 Gy of 56Fe irradiation showed increased ROS at 6h post-irradiation, with the last increase observed 25 days post-irradiation (Limoli et al., 2004).

Eye tissue:

Mice exposed to 11 Gy of X-rays showed increased ROS at 9 months post-irradiation in lenses (Pendergrass et al., 2010). In human lens cells, ROS were found increased at 1h after 0.25 Gy gamma ray irradiation (Ahmadi et al., 2021), 15 minutes after 30 mJ/cm² UV radiation (Jiang et al., 2006), 2.5-120 minutes after 0.014 and 0.14 J/cm² UV radiation (Cencer et al., 2018), and 24h after 30 mJ/cm² UVB-radiation (Yang et al., 2020).

Antioxidants

Cardiovascular tissue:

CAT antioxidant enzyme was decreased in mice aortas as early as 3 days post-irradiation, remaining decreased until 84 days after irradiation with 18 Gy of X-rays (Shen et al., 2018). The antioxidant enzymes peroxiredoxin 5 (PRDX5) and SOD were both shown to have the greatest decrease at 24h after 2 Gy gamma irradiation of TICAE cells (Philipp et al., 2020).

Eye tissue:

Bovine lenses irradiated with 44.8 J/cm² of UVA radiation showed decreased CAT levels at 48-168h post-irradiation (Weinreb and Dovrat, 1996). UV irradiation of mice at 20.6 kJ/m² led to decreased GSH at both 1 and 16 months post-irradiation in the lens (Zhang et al., 2012). Bovine lens cells exposed to 10 Gy of X-rays showed decreased levels of the antioxidant GSH at 24 and 120h after exposure (Belkacemi et al., 2001).

Oxidative damage markers

Cardiovascular tissue:

Oxidative damage markers 4-hydroxynonenal (4-HNE) and 3-Nitrotyrosine (3-NT) were both significantly increased in the aorta of mice at 3 days post-irradiation, remaining increased until 84 days after irradiation with 18 Gy of X-rays (Shen et al., 2018).

Essentiality

Radiation has been found to induce oxidative stress above background levels. Many studies have shown that lower doses of ionizing radiation resulted in decreased levels in markers of oxidative stress in multiple cell types (Acharya et al., 2010; Ahmadi et al., 2021; Bai et al., 2020; Baluchamy et al., 2012; Chen et al., 2021; Collins-Underwood et al., 2008; Giedzinski et al., 2005; Kook et al., 2015; Kubo et al., 2010; Philipp et al., 2020; Ramadan et al., 2020; Ungvari et al., 2013; Veeraraghavan et al., 2011; Wang et al., 2019b; Zigman et al., 2000; Zigman et al., 1995). The essentiality of deposition of energy can be assessed through the removal of deposited energy, a physical stressor that does not require to be metabolized in order to elicit downstream effects on a biological system. Studies that do not deposit energy are observed to have no downstream effects.

Uncertainties and Inconsistencies

There are several uncertainties and inconsistencies in this KER.

- Chen et al. (2021) found that radiation can have adaptive responses. The study used three neutron radiation doses, 0.4 and 1.2 Sv, and 3.6 Sv. After 0.4 and 1.2 Sv, the activity of antioxidant enzymes GSH and SOD increased, and the concentration of malondialdehyde, a product of oxidative stress, decreased. After 3.6 Sv, the opposite was true.
- While the concentration of most antioxidant enzymes decreases after energy deposition, there is some uncertainty with SOD. Certain papers have found that its concentration decreases with dose (Chen et al., 2021; Hua et al., 2019; Ji et al., 2015; Kang et al., 2020) while others found no difference after irradiation (Rogers et al., 2004; Zigman et al., 1995). Several studies have also found that higher levels of SOD do not increase resistance to UV radiation (Eaton, 1994; Hightower, 1995).
- At 1-week post-irradiation with 10 Gy of 60Co gamma rays, TICAE cells experienced a significant increase in levels of the antioxidant, PRDX5, contrary to the decrease generally seen in antioxidant levels following radiation exposure (Philipp et al., 2020).
- Various studies found an increase in antioxidant SOD levels within the brain after radiation exposure (Acharya et al., 2010; Baluchamy et al., 2012; Baulch et al., 2015; Veeraraghavan et al., 2011).
- Chien et al. (2015) found no changes to ROS levels in hippocampal neurons five days after 0.2 Gy of electron radiation.
- Antioxidants that increase in expression are indicative of the presence of RONS. When antioxidants decrease in expression/activity, this is most likely due to the overwhelming of the antioxidant defence mechanisms
- There is limited data to support an understanding of deposition of energy leading to oxidative stress at low doses.

Quantitative Understanding of the Linkage

The table below provides some representative examples of quantitative linkages between the two key events. It was difficult to identify a general trend across all the studies due to differences in experimental design and reporting of the data. All data is statistically significant unless otherwise stated.

Response-response relationship

Dose Concordance

Reference	Experiment Description	Result
Attar, Kondolousy and Khansari, 2007	In vivo. One hundred individuals between 20 and 50 years old in two villages in Iran exposed to background IR at 260 mSv/year had antioxidant levels measured. The control group was from two villages not exposed to the high background radiation. The total antioxidant levels in the blood were determined by the ferric reducing/antioxidant power assay.	The total antioxidant level was significantly reduced from 1187±199 µmol in the control to 686±170 µmol in the exposed group.

Klucinski et al., 2008	<p>In vivo. A group of 14 men and 31 women aged 25-54 years working X-ray equipment (receiving doses of less than 1 mSv/year) for an average of 15.3 years (range of 2-33 years) were compared to a control group for antioxidant activity. Antioxidant activity of SOD, glutathione peroxidase (GSH-Px), and CAT in erythrocytes were measured in U/g of hemoglobin.</p>	<p>Enzymes (SOD, GSH, CAT) showed significantly decreased antioxidant activity in the workers.</p> <p>In the controls (U/g of Hb):</p> <ul style="list-style-type: none"> • SOD: 1200 ± 300 • GSH-Px: 39 ± 7 • CAT: 300 ± 60 <p>In the workers (U/g of Hb):</p> <ul style="list-style-type: none"> • SOD: 1000 ± 200 • GSH-Px: 29 ± 4 • CAT: 270 ± 50
Limoli et al., 2007	<p>In vitro. Neural precursor cells isolated from rat hippocampi was exposed to 0.25-5 Gy of 56Fe irradiation at dose rates of 0.5-1.0 Gy/min. ROS were measured 6h post-irradiation.</p>	<p>At a low dose of 0.25 Gy and 0.5 Gy, relative ROS levels were significantly elevated and showed a linear dose response (from ~ 1 to ~ 2.25 relative ROS levels) until 1 Gy, where it reached its peak (~ 3 relative ROS levels). At higher doses, the relative ROS levels decreased.</p>
Tseng et al., 2014	<p>In vitro. Neural stem/precursor cells isolated from mouse subventricular and hippocampal dentate subgranular zones were exposed to 1-15 cGy of 56Fe irradiation at dose rates ranging from 5-50 cGy/min. RONS levels were measured.</p>	<p>A dose-dependent and significant rise in RONS levels was detected after 56Fe irradiation. 12 h post-irradiation, a steady rise was observed and reached a 6-fold peak after 15 cGy.</p>
Limoli et al., 2004	<p>In vitro. Neural precursor cells from rat hippocampus were exposed to 0, 1, 5 and 10 Gy of X-irradiation at a dose rate of 4.5 Gy/min. ROS levels were measured.</p> <p>In vivo. MDA was used to quantify oxidative stress.</p>	<p>A dose-dependent increase in ROS levels was seen in the first 12 h post-irradiation, with relative maximums at 12 h after 5 Gy (35% increase) and 24 h after 1 Gy (31% increase). ROS levels measured 1 week after 5 Gy were increased by 180% relative to sham-irradiated controls. MDA levels increased significantly (approximately 1.3-fold) after exposure to 10 Gy.</p>
Collins-Underwood et al., 2008	<p>In vitro. Immortalized rat brain microvascular endothelial cells were exposed to 1-10 Gy of 137Cs-irradiation at a dose rate of 3.91 Gy/min. Intracellular ROS and O₂- production were both measured.</p>	<p>Irradiation resulted in a significant dose-dependent increase in intracellular ROS generation from 1-10 Gy. At 5 Gy, there was an approximate 10-fold increase in ROS levels, and at 10 Gy there was an approximate 20-fold increase.</p>
Giedzinski et al., 2005	<p>In vitro. Neural precursor cells were irradiated with 1, 2, 5 and 10 Gy of 250 MeV protons (1.7-1.9 Gy/min) and X-irradiation (4.5 Gy/min). ROS levels were measured.</p>	<p>There was a rapid increase in ROS at 6, 12, 18 and 24h after proton irradiation, with an exception at the 1 Gy 18h point. Most notably, at 6h post-irradiation, a dose-dependent increase in relative ROS levels from 1 to 10 Gy was seen that ranged from 15% (at 1 Gy) to 65% (at 10 Gy). Linear regression analysis showed that at ≤ 2 Gy, ROS levels increased by 16% per Gy. The linear dose response obtained at 24h showed that proton irradiation increased the relative ROS levels by 3% per Gy.</p>
Veeraraghavan et al., 2011	<p>In vivo. Adult mice were exposed to 2, 10 or 50 cGy of whole-body gamma irradiation at 0.81 Gy/min. Brain tissues were harvested 24h post-irradiation. SOD2 levels and activity were measured.</p>	<p>Compared to the controls, the levels of SOD2 expression increased in the brain after 2, 10 and 50 cGy. Analysis revealed a significant and dose-dependent change in SOD2 activity. More specifically, SOD2 activity showed significant increases after 10 ($\sim 25\%$ increase above control) and 50 cGy ($\sim 60\%$ increase above control), but not 2 cGy.</p>
Baluchamy et al., 2012	<p>In vivo. Male mice were exposed to whole-body irradiation with 250 MeV protons at 0.01, 1 and 2 Gy and the whole brains were dissected out. ROS, LPO, GSH and total SOD were measured.</p>	<p>Dose-dependent increases in ROS levels was observed compared to controls, with a two-fold increase at 2 Gy. A 2.5 to 3-fold increase in LPO levels was also seen at 1 and 2 Gy, respectively, which was directly correlated with the increase in ROS levels. Additionally, results showed a significant reduction in GSH ($\sim 70\%$ decrease at 2 Gy) and SOD activities (~ 2-fold decrease) following irradiation that was dose-dependent.</p>
Acharya et al., 2010	<p>In vitro. Human neural stem cells were subjected to 1, 2 or 5 Gy of gamma irradiation at a dose rate of 2.2 Gy/min. RONS and superoxide levels were determined.</p>	<p>Intracellular RONS levels increased by approximately 1.2 to 1.3-fold compared to sham-irradiated controls and was found to be reasonable dose-responsive.</p> <p>At 12h, levels of superoxide increased 2 and 4-fold compared to control for 2 and 5 Gy, respectively. At 24h and 48h, there was a dose-dependent increase in RONS levels. At 7 days, levels of RONS increased approximately 3 to 7-fold for 2 and 5 Gy, respectively.</p>
Baulch et al., 2015	<p>In vitro. Human neural stem cells were exposed to 5-100 cGy of 16O, 28Si, 48Ti or 56Fe particles (600 MeV) at 10-50 cGy/min. RONS and superoxide levels were determined.</p>	<p>3 days post-irradiation, oxidative stress was found to increase after particle irradiation. Most notably, exposure to 56Fe resulted in a dose-dependent increase with 100% increase in RONS levels at 100 cGy. Dose-dependent increase was also seen in superoxide levels after 56Fe irradiation. At 7 days post-irradiation, 56Fe irradiation induced significantly lower nitric oxide levels by 47% (5 cGy), 55% (25 cGy) and 45% (100 cGy).</p>
Bai et al., 2020	<p>In vitro. bmMSCs were taken from 4-week-old, male Sprague-Dawley rats. After extraction, cells were then irradiated with 2, 5, and 10 Gy of 137Cs gamma rays. Intracellular ROS levels and relative mRNA expression of the antioxidants, SOD1, SOD2, and CAT2, were measured to assess the extent of oxidative stress induced by IR.</p>	<p>Cellular ROS levels increased significantly in a dose-dependent manner from 0-10 Gy. Compared to sham-irradiated controls, ROS levels increased by $\sim 15\%$, $\sim 55\%$, and $\sim 105\%$ after exposure to 2, 5, and 10 Gy, respectively. Antioxidant mRNA expression decreased in a dose-dependent manner from 0-10 Gy, with significant increases seen at doses 2 Gy for SOD1 and CAT2 and 5 Gy for SOD2. Compared to sham-irradiated controls, SOD1 expression decreased by $\sim 9\%$, $\sim 18\%$, and $\sim 27\%$ after exposure to 2, 5, and 10 Gy, respectively. SOD2 expression decreased by $\sim 31\%$ and $\sim 41\%$ after exposure to 5 and 10 Gy, respectively. CAT2 expression decreased by $\sim 15\%$, $\sim 33\%$, and $\sim 58\%$ after exposure to 2, 5, and 10 Gy, respectively.</p>
Liu et al., 2018	<p>In vitro. hBMSCs were irradiated with 8 Gy of X-rays at a rate of 1.24 Gy/min. Intracellular ROS levels and SOD activity were measured to analyze IR-induced oxidative stress.</p>	<p>Compared to sham-irradiated controls, hBMSCs irradiated with 8 Gy of X-rays experienced a significant increase to intracellular ROS levels. hBMSCs irradiated with 8 Gy of X-rays experienced a $\sim 46\%$ reduction in SOD activity.</p>
Kook et al., 2015	<p>In vitro. Murine MC3T3-E1 osteoblast cells were irradiated with 2, 4, and 8 Gy of X-rays at a rate of 1.5 Gy/min. Intracellular ROS levels and the activity of antioxidant enzymes, including GSH, SOD, CAT, were measured to assess the extent of oxidative stress induced by IR exposure.</p>	<p>Compared to sham-irradiated controls, irradiated MC3T3-E1 cells experienced a dose-dependent increase in ROS levels, with significant increases at 4 and 8 Gy ($\sim 26\%$ and $\sim 38\%$, respectively). Antioxidant enzyme activity initially increased by a statistically negligible amount from 0-2 Gy and then decreased in a dose-dependent manner from 2-8 Gy. SOD activity decreased significantly at 4 and 8 Gy by $\sim 29\%$ and $\sim 59\%$, respectively. GSH activity similarly decreased significantly at 4 and 8 Gy by $\sim 30\%$ and $\sim 48\%$, respectively. CAT activity did not change by a statistically significant amount.</p>

Liu et al., 2019	In vivo. 8–10-week-old, juvenile, female SPF BALB/c mice underwent whole-body irradiation with 2 Gy of 31.6 keV/μm 12C heavy ions at a rate of 1 Gy/min. ROS levels were measured from femoral bone marrow mononuclear cells of the irradiated mice to analyze IR-induced oxidative stress.	Compared to sham-irradiated controls, irradiated mice experienced a ~120% increase in ROS levels.
Zhang et al., 2020	In vitro. Murine RAW264.7 osteoclast precursor cells were irradiated with 2 Gy of 60Co gamma rays at a rate of 0.83 Gy/min. ROS levels were measured to determine the extent of oxidative stress induced by IR exposure.	Compared to sham-irradiated controls, ROS levels in irradiated RAW264.7 cells increased by ~100%.
Wang et al., 2016	In vitro. Murine MC3T3-E1 osteoblast-like cells were irradiated with 6 Gy of X-rays. Intracellular ROS production was measured to assess oxidative stress from IR exposure.	Compared to sham-irradiated controls, intracellular ROS production increased by ~81%.
Huang et al., 2018	In vitro. Murine RAW264.7 osteoblast-like cells were irradiated with 2 Gy of gamma rays at a rate of 0.83 Gy/min. ROS levels were measured to analyze IR-induced oxidative stress.	Compared to sham-irradiated controls, ROS levels in RAW264.7 cells increased by ~138% by 2 h post-irradiation.
Zhang et al., 2018	In vitro. hBMMSCs were irradiated with 2 Gy of X-rays at a rate of 0.6 Gy/min. Relative ROS concentration was measured to assess the extent of oxidative stress induced by IR.	Compared to sham-irradiated controls, irradiated hBMMSCs experienced a maximum increase of ~90% to ROS levels at 3 h post-irradiation.
Huang et al., 2019	In vitro. Rat bmMSC were irradiated with 2 Gy of 60Co gamma rays at a rate of 0.83 Gy/min. ROS levels were measured to assess IR-induced oxidative stress.	Compared to sham-irradiated controls, ROS levels in irradiated bone marrow stromal cells increased by approximately 2-fold.
Soucy et al., 2011	In vivo. 7- to 12-month-old, adult, male Wistar rats underwent whole-body irradiation with 1 Gy of 56Fe heavy ions. ROS production in the aorta was measured along with changes in activity of the ROS-producing enzyme xanthine oxidase (XO) to assess IR-induced oxidative stress.	Compared to sham-irradiated controls, irradiated mice experienced a 74.6% increase in ROS production (from 4.84 to 8.45) and XO activity increased by 36.1% (6.12 to 8.33).
Soucy et al., 2010	In vivo. 4-month-old, adult, male Sprague-Dawley rats underwent whole-body irradiation with 5 Gy of 137Cs gamma rays. Changes in XO activity and ROS production were measured in the aortas of the mice to assess IR-induced oxidative stress.	Compared to sham-irradiated controls, irradiated mice experienced a ~68% increase in ROS production and a ~46% increase in XO activity.
Karam & Radwan, 2019	In vivo. Adult male Albino rats underwent irradiation with 5 Gy of 137Cs gamma rays at a rate of 0.665 cGy/s. Activity levels of the antioxidants, SOD and CAT, present in the heart tissue were measured to assess IR-induced oxidative stress.	Compared to the sham-irradiated controls, SOD and CAT activity decreased by 57% and 43%, respectively, after irradiation.
Cervelli et al., 2017	In vitro. HUVECs were irradiated with 0.25 Gy of X-rays at a rate of 91 mGy/min. ROS production was measured to analyze IR-induced oxidative stress.	Compared to the sham-irradiated controls, irradiated mice experienced a ~171% increase in ROS production (not significant).
Mansour, 2013	In vivo. Male Wistar rats underwent whole-body irradiation with 6 Gy of 137Cs gamma rays at a rate of 0.012 Gy/s. MDA was measured from heart homogenate, along with the antioxidants: SOD, GSH, and GSH-Px.	Compared to sham-irradiated controls, MDA increased by 65.9%. SOD, GSH-Px, and GSH decreased by 33.8%, 42.4%, and 50.0%, respectively.
Soltani, 2016	In vitro. HUVECs were irradiated with 2 Gy of 60Co gamma rays at a dose rate of 0.6 Gy/min. Markers of oxidative stress, including reduced GSH and TBARS, were measured to assess GSH depletion and LPO, respectively.	Compared to non-irradiated controls, sham-irradiated cells experienced a ~28% decrease in GSH and a ~433% increase in TBARS.
Wang et al., 2019b	In vitro. HUVECs were irradiated with 0.2, 0.5, 1, 2, and 5 Gy of 137Cs gamma rays. ROS production was measured to assess IR-induced oxidative stress.	Compared to sham-irradiated controls, ROS production increase significantly ~32% at 5 Gy. While changes to ROS production were insignificant at doses <2 Gy, following a linear increase from 0-5 Gy.
Sharma et al., 2018	In vitro. HUVECs were irradiated with 9 Gy of photons. ROS production was measured to determine the effects of IR on oxidative stress.	Compared to sham-irradiated controls, irradiated HUVECs displayed ~133% increase in ROS production.
Hatoum et al., 2006	In vivo. Sprague-Dawley rats were irradiated with 9 fractions of 2.5 Gy of X-rays for a cumulative dose of 22.5 Gy at a rate of 2.43 Gy/min. Production of the ROS superoxide and peroxide in gut arterioles were measured to determine the level of oxidative stress caused by irradiation.	ROS production started increasing compared to the sham-irradiated control after the second dose and peaked at the fifth dose. By the ninth dose, superoxide production increased by 161.4% and peroxide production increased by 171.3%.
Phillip et al., 2020	In vitro. Human TICAE cells were irradiated with 0.25, 0.5, 2, and 10 Gy of 60Co gamma rays at a rate of 0.4 Gy/min. Levels of the antioxidants, SOD1 and PRDX5 were measured to assess oxidative stress from IR exposure.	While SOD1 levels did not follow a dose-dependent pattern. At 2 Gy, SOD1 decreased about 0.5-fold. At 1 week post-irradiation, PRDX5 remained at approximately control levels for doses <2 Gy but increased by ~60% from 2-10 Gy. PRDX5 only decreased at 2 Gy and 24h post-irradiation.
Ramadan et al., 2020	In vitro. Human TICAE/TIME cells were irradiated with 0.1 and 5 Gy of X-rays at a dose rate of 0.5 Gy/min. Intracellular ROS production was measured to determine the extent of IR-induced oxidative stress.	ROS production saw a dose-dependent increase in both TICAE and TIME cells. By 45 min post-irradiation, 0.1 Gy of IR had induced increases to ROS production of ~3.6-fold and ~8-fold in TICAE and TIME cells, respectively, compared to sham-irradiated controls. 5 Gy of IR caused more significant increases to ROS production of ~18-fold and ~17-fold in TICAE and TIME cells, respectively, compared to sham-irradiated controls.

Shen et al., 2018	In vivo. 8-week-old, female, C57BL/6 mice were irradiated with 18 Gy of X-rays. Levels of the oxidative markers, 4-HNE and 3-NT, and the antioxidants, CAT and heme oxygenase 1 (HO-1) were measured in the aortas of the mice.	Compared to sham-irradiated controls, irradiated mice saw maximum increases of ~1.75-fold on day 14 and ~2.25-fold on day 7 to 4-HNE and 3-NT levels, respectively. While CAT levels decreased up to 0.33-fold on day 7, HO-1 levels increased by ~1.9-fold on day 7.
Ungvari et al., 2013	In vitro. The CMVECs of adult male rats were irradiated with 2, 4, 6, and 8 Gy of 137Cs gamma rays. Production of the reactive oxygen species, peroxide and O2-., were measured to assess the extent of IR-induced oxidative stress.	Compared to sham-irradiated controls, production of peroxide in CMVECs of irradiated mice 1 day post exposure increased in a dose-dependent manner from 0-8 Gy, with significant changes observed at doses >4 Gy. At 8 Gy, peroxide production had increased ~3.25-fold. Production of O2- followed a similar dose-dependent increase with significant observed at doses >6 Gy. At 8 Gy, O2- production increased ~1.6-fold. 14 days post-exposure, IR-induced changes to ROS production were not significant for either peroxide or O2- and did not show a dose-dependent pattern. ROS production progressively decreased from 0-4 Gy and then recovered from 6-8 Gy back to control levels.
Ahmadi et al., 2021	In vitro. HLEC and HLE-B3 cells were exposed to 0.1, 0.25 and 0.5 Gy of gamma irradiation at 0.3 and 0.065 Gy/min. Intracellular ROS levels were measured.	In HLE-B3 cells, there were about 7 and 17% ROS-positive cells 1 h after exposure to 0.25 and 0.5 Gy respectively at 0.3 Gy/min. 24 h after exposure there were about 10% ROS-positive cells after 0.5 Gy at 0.3 Gy/min. 1 h after exposure there were about 13 and 17% ROS-positive cells at 0.25 and 0.5 Gy and 0.065 Gy/min. 24 h after exposure there were 8% ROS-positive cells after 0.5 Gy and 0.065 Gy/min. In human lens epithelial cells 1 h after exposure there were about 10 and 19% ROS-positive cells after 0.25 and 0.5 Gy at 0.3 Gy/min. After exposure to 0.5 Gy at 0.065 Gy/min there were about 16 and 9% ROS-positive cells one and 24 h after exposure.
Ji et al, 2015	In vitro. HLECs were exposed to UVB irradiation (297 nm; 2 W/m2) for 0 – 120 min. Total antioxidative capability (T-AOC), ROS levels, MDA, and SOD were measured at various time points at 5-120 min.	HLECs exposed to 1 W/m2 UVB for 0 - 120 min (representative of dose) showed a gradual increase in ROS levels that began to plateau 105 min post-irradiation at an ROS level 750 000x control.
Hua et al, 2019	In vitro. HLECs were exposed to 4050, 8100 and 12,150 J/m2 of UVB-irradiation at 1.5, 3.0 and 4.5 W/m2. MDA, SOD, GSH-Px, and GSH were measured.	MDA activity as a ratio of the control increased about 1.5 at 3.0 W/m2 and about 3 at 4.5 W/m2. SOD activity as a ratio of the control decreased about 0.1 at 1.5 W/m2, 0.2 at W/m2, and 0.3 at 4.5 W/m2. GSH-Px activity as a ratio of the control decreased about 0.02 at 3.0 W/m2 and 0.2 at 4.5 W/m2. GSH activity as a ratio of the control decreased about 0.2 at 3.0 W/m2 and 0.7 at 4.5 W/m2.
Chen et al, 2021	In vivo. Male rats were irradiated with 0, 0.4, 1.2 and 3.6 Sv of neutron-irradiation at 14, 45 and 131 mSv/h. In rat lenses, MDA, GSH, and SOD, were measured.	MDA concentration decreased by about 1.5 nmol/mg protein at 1.2 Sv and increased by about 7.5 nmol/mg protein relative to the control at 3.6 Sv. GSH concentration increased by about 3.5 µg/mg protein and decreased by about 1 µg/mg protein relative to the control at 3.6 Sv (neutron radiation). SOD activity decreased by about 0.08 U/mg protein relative to the control at 3.6 Sv. It should be noted that Sv is not the correct unit when investigating animals and cultured cells, radiation should have been measured in Gy (ICRU, 1998).
Zigman et al., 2000	In vitro. Rabbit LECs were exposed to 3-12 J/cm2 of UVA-irradiation (300-400 nm range, 350 nm peak). CAT activity was assayed to demonstrate oxidative stress.	Rabbit LECs exposed to 3 – 12 J/cm2 UVA showed an approximately linear decrease in catalase activity (indicative of increased oxidative stress) with the maximum dose displaying a 3.8x decrease.
Chitchumroonchokchai et al, 2004	In vitro. HLECs were exposed to 300 J/m2 of UVB-irradiation at 3 mW/cm2. MDA and HAE were used to measure oxidative stress.	The concentration of MDA and HAE increased by about 900 pmol/mg protein compared to the control after irradiation with 300 J/m2 UVB.
Zigman et al, 1995	In vitro. Rabbit and squirrel LECs were exposed to 6, 9, 12, 15 and 18 J/m2 of UV-irradiation at 3 J/cm2/h (300-400 nm range, 350 nm peak). CAT was used to measure oxidative stress levels.	The CAT activity was 10% of the control activity at 6 J/cm2, and then decreased to 0% of the control activity at 18 J/cm2 (99.9% UV-A and 0.1% UV-B).
Karimi et al, 2017	In vivo. Adult rats were exposed to 15 Gy of gamma 60Co-irradiation at a dose rate of 98.5 cGy/min. In lens tissue, MDA, thiobarbituric acid (TBA), and GSH levels were used to indicate oxidative stress.	MDA concentration increased from 0.37 +/- 0.03 to 1.60 +/- 0.16 nmol/g of lens after irradiation. GSH concentration decreased from 0.99 +/- 0.06 to 0.52 +/- 0.16 µmol/g of lens after exposure.
Rong et al., 2019	In vitro. HLECs were exposed to UVB-irradiation (297 nm; 2 W/m2 for 10 min). Intracellular H ₂ O ₂ and superoxide levels were measured.	The amount of ROS was measured as the dicholofluorescein (DCFH-DA) fluorescence density, which increased about 10-fold relative to the control. A similar test but with dihydroethidium (DHE) staining showed a fluorescence density increase of about 3-fold relative to the control.
Kubo et al., 2010	In vitro. Lenses isolated from mice were exposed to 400 or 800 J/m2 of UVB-irradiation. ROS levels were measured.	The ratio of ROS level/survived LECs increased from about 175 to 250% after exposure to 400 and 800 J/m2 UVB respectively.
Kang et al., 2020	In vitro. HLECs were exposed to 0.09 mW/cm2 UVB-irradiation (275-400 nm range, 310 nm peak) for 15 min. MDA and SOD activity were measured.	MDA activity increased about 30% compared to control after 15 min of 0.09 mW/cm2 UVB exposure. SOD activity decreased about 50% compared to control under the same conditions.
Yang et al., 2020	In vitro. HLEs were irradiated with 30 mJ/cm2 of UVB-irradiation. ROS levels were determined.	The level of ROS production in HLEs increased approximately 5-fold as determined by 2',7'-dichlorofluorescein diacetate after exposure to 30 mJ/cm2 UVB.

Zhang et al., 2012	In vivo. Adult mice were exposed to 20.6 kJ/m ² UV-irradiation (313 nm peak; 1.6 mW/cm ²). GSH levels were measured in lens homogenates.	Decrease in GSH of about 1 and 2 μ mol/g wet weight compared to control after 1 and 16 months respectively after 20.6 kJ/m ² UV (313 nm peak) at 1.6 mW/cm ² .
--------------------	---	--

Time-scale**Time Concordance**

Reference	Experiment Description	Result
Tseng et al., 2014	In vitro. Neural stem/precursor cells isolated from mouse subventricular and hippocampal dentate subgranular zones were exposed to 1-200 cGy of 56Fe irradiation at dose rates ranging from 5-50 cGy/min. RONS were measured from 1 to 8 weeks post-irradiation.	Compared to sham-irradiated controls, a trend toward increasing oxidative stress was seen, particularly at 1- and 4-weeks post-irradiation where RONS levels showed dose-responsive increases. The greatest rise was also seen at 10 cGy where relative RONS levels increased ~2-fold from 1 to 4 weeks, ~3-fold from 4 to 6 weeks and ~2 fold from 6 to 8 weeks. RONS were also found increased at doses as low as 2 cGy at 12 and 24h post-irradiation.
Suman et al., 2013	In vivo. Female mice were exposed to either 1.3 Gy of 56Fe irradiation (1 GeV/nucleon; dose rate of 1 Gy/min) or 2 Gy of gamma irradiation (dose rate of 1 Gy/min). ROS were measured in cerebral cortical cells at 2 and 12 months.	ROS levels showed statistically significant increases after 56Fe irradiation at both 2 and 12 months, while gamma irradiation led to an increase at only 2 months. The percent fluorescence intensity of ROS levels for control, gamma irradiated and 56Fe-irradiated were approximately 100, 115 and 140 at 2 months, and 100, 90 and 125 at 12 months, respectively.
Limoli et al., 2004	In vitro. Neural stem/precursor cells isolated from mouse subventricular and hippocampal dentate subgranular zones were exposed to 1 or 5 Gy of 56Fe irradiation at dose rates ranging from 4.5 Gy/min. RONS were measured at various time points until 33 days post-exposure.	ROS levels exhibited statistically significant fluctuations, increasing over the first 12h before dropping at 18h and rising again at 24h. At 5 Gy, ROS levels fluctuated with a peak at 7 days, a decrease at 13 days, an increase at 25 days, and a decrease below control levels at 33 days. At 1 Gy, ROS levels peaked at 25 days and also decreased below control at 33 days.
Gledzinski et al., 2005	In vitro. Neural precursor cells derived from rats were irradiated with 1, 2, 5 and 10 Gy of proton (1.7-1.9 Gy/min). ROS levels were determined at 5-25h post-irradiation.	Proton irradiation led to a rapid rise in ROS levels, with the increase most marked at 6h (approximately 10-70% for 1 and 10 Gy, respectively). The increase in ROS persisted for 24h, mainly for 10 Gy where the ROS levels were around 30% above control at the 12, 18 and 24h mark.
Acharya et al., 2010	In vitro. Human neural stem cells were subjected to 1, 2 or 5 Gy of gamma irradiation at a dose rate of 2.2 Gy/min. RONS and superoxide levels were measured at various time points until 7 days.	Intracellular RONS and superoxide levels showed significant increase from 2- to 4-fold at 12h. At 7 days, levels of RONS increased and were dose-responsive, elevated by ~3- to 7-fold and 3- to 5-fold, respectively, over sham-irradiated controls.
Rugo and Schiestl, 2004	In vitro. Human lymphoblast cell lines (TK6 and TK6 E6) were irradiated with 2 Gy of X-irradiation at a dose rate of 0.72 Gy/min. ROS levels were measured at various time points until 29 days.	In the TK6 E6 clones, there was only a significant ROS increase at day 29 (45.7 DCF fluorescence units). In the TK6 clones, there were significant ROS increases at days 13 (26.0 DCF fluorescence units), 15 (26.3 DCF fluorescence units) and 20 (38.1 DCF fluorescence units), with a strong trend of increased ROS in the treated group at day 25. On day 18, ROS levels decreased in the irradiated group, and there was no significant difference at day 29.
Huang et al., 2018	In vitro. Murine RAW264.7 cells were irradiated with 2 Gy of gamma rays at a rate of 0.83 Gy/min. ROS levels were measured at 2 and 8 h post-irradiation.	ROS levels in irradiated RAW264.7 cells decreased by ~10% from 2 h post-exposure to 8 h post-exposure (from ~138% above control at 2 h to ~98% above control at 8).
Zhang et al., 2018	In vitro. hBMSCs were irradiated with 2 Gy of X-rays at a rate of 0.6 Gy/min. Relative ROS concentration was measured at 0, 0.5, 2, 3, 6, 8, and 12 h post-irradiation.	ROS levels increased in time dependent manner until a peak of ~90% above control level at 3 h post-irradiation, and then steadily declined back to approximately control levels at 12 h post-irradiation.
Phillip et al., 2020	In vitro. Human TICAE cells were irradiated with 0.25, 0.5, 2, and 10 Gy of 60Co gamma rays at a rate of 400 mGy/min. Levels of the antioxidants, SOD1 and PRDX5 were measured at 4 h, 24 h, 48 h, and 1-week post-irradiation to assess oxidative stress from IR exposure.	SOD1 levels did not follow a time-dependent pattern. However, SOD1 decreased at 2 Gy for every timepoint post-irradiation. While PRDX5 levels stayed at approximately baseline levels for the first two days after exposure to 10 Gy of radiation, levels elevated by ~1.6-fold after 1 week.
Ramadan et al., 2020	In vitro. Human TICAE/TIME cells were irradiated with 0.1 and 5 Gy of X-rays at a rate of 0.5 Gy/min. Intracellular ROS production was measured at 45 min, 2 h, and 3 h post-irradiation.	After irradiation, ROS production saw time-dependent decreases in both TICAE and TIME cells from 45 min to 3 h post-exposure. ROS production was elevated at 45 min but returned to approximately baseline levels at 2 and 3 h.
Shen et al., 2018	In vivo. 8-week-old, female, C57BL/6 mice were irradiated with 18 Gy of X-rays. Levels of the oxidative markers, 4-HNE and 3-NT, and the antioxidants, CAT and heme HO-1 were measured in the aortas of the mice at 3, 7, 14, 28, and 84 days post-irradiation.	Significant changes were observed in 4-HNE, 3-NT, CAT, and HO-1 levels of irradiated mice after 3 days. 3-NT and HO-1 levels increased from days 3 to 7 and then progressively decreased, while 4-HNE levels followed the same pattern but with a peak at day 14. CAT levels were at their lowest at day 3 and followed a time dependent increase until day 84.
Ungvari et al., 2013	In vitro. The CMVECs of adult male rats were irradiated with 2, 4, 6, and 8 Gy of 137Cs gamma rays. Production of the reactive oxygen species, peroxide and superoxide, were measured at 1- and 14-days post-irradiation.	ROS production was generally higher at day 1 than day 14, with the difference becoming progressively more significant from 2-8 Gy. Peroxide production was reduced from a ~3.25-fold increase compared to controls at day 1 back to baseline levels at day 14. Superoxide production had a ~1.6-fold increase at day 1 recover to baseline levels at day 14.
Ahmadi et al., 2021	In vitro. HLEC and HLE-B3 cells were exposed to 0.1, 0.25 and 0.5 Gy of gamma irradiation at 0.3 and 0.065 Gy/min. ROS levels were measured.	In human LECs immediately exposed to 0.25 Gy gamma rays, the level of ROS positive cells increased by 5%, relative to control, 1 h post-irradiation.
Jiang et al., 2006	In vitro. HLECs were exposed to UV-irradiation at a wavelength over 290 nm (30 mJ/cm ²). ROS levels were measured.	Approximately 10-fold increase in ROS generation 15 min after exposure to 30 mJ/cm ² UV.
Pendergrass et al., 2010	In vivo. Female mice were irradiated with 11 Gy of X-irradiation at a dose rate of 2 Gy/min. ROS levels in the lenses were used to represent oxidative stress.	9 months after irradiation with 11 Gy X-rays at 2 Gy/min there's 2250% cortical ROS relative to the control. 3 months after there was no significant change.
Belkacem et al., 2001	In vitro. Bovine lens cells were exposed to 10 Gy of X-irradiation at 2 Gy/min. GSH levels were measured.	The intracellular GSH pool was measured by a decrease of about 15% monobromobimane fluorescence relative to the control 24 h after exposure to 10 Gy X-rays at 2 Gy/min and there was a decrease of about 40% relative to the control by 120 h.
Weinreb and Dovrat, 1996	In vitro. Bovine lenses were irradiated with 22.4 J/cm ² (10 min) and 44.8 J/cm ² (100 min) of UVA-irradiation at 8.5 mW/cm ² . CAT levels were determined.	CAT activity decreased from 1.75 (control) to 0.5 U/mg protein at 48-168 h after exposure to 44.8 J/cm ² UV-A.

Cencer et al., 2018	In vitro. HLECs were exposed to 0.014 and 0.14 J/cm ² of UVB-irradiation at 0.09, 0.9 mW/cm ² for 2 and 5 min. ROS levels (mainly H ₂ O ₂) were measured.	About 5 min after exposure to both 0.09 and 0.9 mW/cm ² UVB for 2.5 min there is an increase of about 4 average brightness minus control (densitometric fluorescence scanning for ROS, mostly indicating H ₂ O ₂). About 90 and 120 min after exposure to 0.9 mW/cm ² the average brightness minus control is about 35 and 20 respectively.
Yang et al., 2020	In vitro. HLECs were irradiated with 30 mJ/cm ² of UVB-irradiation. Intracellular ROS levels were measured.	The level of ROS production in HLECs increased approximately 5-fold as determined by 2',7'-dichlorofluorescein diacetate 24 h after exposure to 30 mJ/cm ² UVB.
Zhang et al., 2012	In vivo. Adult mice were exposed to 20.6 kJ/m ² UV-irradiation (313 nm peak; 1.6 mW/cm ²). GSH levels were measured in lens homogenates.	Decrease in GSH of about 1 and 2 μmol/g wet weight compared to control after 1 and 16 months respectively after 20.6 kJ/m ² UV (313 nm peak) at 1.6 mW/cm ² .

Known modulating factors

Modulating Factors	MF details	Effects on the KER	References
Antioxidants	CAT, GSH-Px, SOD, PRDX, vitamin E, C, carotene, lutein, zeaxanthin, selenium, zinc, alpha-lipoic acid, melatonin, ginkgo biloba leaf, fermented ginkobiloba leaf, Nigella sativa oil, thymoquinone, and ferulic acid	Adding or withholding antioxidants will decrease or increase the level of oxidative stress respectively	(Zigman et al., 1995; Belkacémi et al., 2001; Chitchumroonchokchai et al., 2004; Fatma et al., 2005; Jiang et al., 2006; Fletcher, 2010; Karimi et al., 2017; Hua et al., 2019; Kang et al., 2020; Yang et al., 2020; Manda et al., 2008; Limoli et al., 2007; Manda et al., 2007; Taysi et al., 2012; Ismail et al., 2016; Demir et al., 2020; Chen et al., 2021)
Age	Increased age	Antioxidant levels are lower and show a greater decrease after radiation in older organisms. This compromises their defence system, resulting in ROS increases and therefore, an increased likelihood of oxidative stress	(Marshall, 1985; Spector, 1990; Giblin et al., 2002; Kubo et al., 2010; Pendergrass et al., 2010; Zhang et al., 2012; Hamada et al., 2014; Tangvarasittichai & Tangvarasittichai, 2019)
Oxygen	Increased oxygen levels	Higher oxygen concentrations increase sensitivity to ROS	(Hightower et al., 1992; Eaton, 1994; Huang et al., 2006; Zhang et al., 2010; Schoenfeld et al., 2012)

Known Feedforward/Feedback loops influencing this KER

The relationship between deposition of energy and increased oxidative stress leads to several feedforward loops. Firstly, ROS activates the transforming growth factor beta (TGF-β), which increases the production of ROS. This process is modulated in normal cells containing PRDX-6, or cells with added MnTBAP, which will both prevent TGF-β from inducing ROS formation (Fatma et al., 2005). Secondly, ROS can damage human mitochondrial DNA (mtDNA), this can then cause changes to the cellular respiration mechanisms, leading to increased ROS production (Turner et al., 2002; Zhang et al., 2010; Tangvarasittichai & Tangvarasittichai, 2019, Ahmad et al., 2021; Yves, 2000). Some other feedback loops through which deposition of energy causes oxidative stress are discussed by Soloviev & Kizub (2019).

References

Acharya, M. M. et al. (2010), "Consequences of ionizing radiation-induced damage in human neural stem cells", Free radical biology & medicine, Vol. 49/12, Elsevier, Amsterdam, <https://doi.org/10.1016/j.freeradbiomed.2010.08.021>.

Ahmadi, M. et al. (2021), "Early responses to low-dose ionizing radiation in cellular lens epithelial models", Radiation research, Vol. 197/1, Radiation Research Society, Bozeman, <https://doi.org/10.1667/RADE-20-00284.1>.

Attar, M., Y. M. Kondolousy, N. Khansari, (2007), "Effect of High Dose Natural Ionizing Radiation on the Immune System of the Exposed Residents of Ramsar Town, Iran", Iranian Journal of Allergy, Asthma and Immunology, Vol. 6/2, pp. 73-78.

Bai, J. et al. (2020), "Irradiation-induced senescence of bone marrow mesenchymal stem cells aggravates osteogenic differentiation dysfunction via paracrine signaling", American Journal of Physiology - Cell Physiology, Vol. 318/5, American Physiological Society, Rockville, <https://doi.org/10.1152/ajpcell.00520.2019>.

Balasubramanian, D (2000), "Ultraviolet radiation and cataract", Journal of ocular pharmacology and therapeutics, Vol. 16/3, Mary Ann Liebert Inc., Larchmont, <https://doi.org/10.1089/jop.2000.16.285>.

Baluchamy, S. et al. (2012), "Reactive oxygen species mediated tissue damage in high energy proton irradiated mouse brain", Molecular and cellular biochemistry, Vol. 360/1-2, Springer, London, <https://doi.org/10.1007/s11010-011-1056-2>.

Baulch, J. E. et al. (2015), "Persistent oxidative stress in human neural stem cells exposed to low fluences of charged particles Redox biology, Vol. 5, Elsevier, Amsterdam, <https://doi.org/10.1016/j.redox.2015.03.001>.

Belkacémi, Y. et al. (2001), "Lens epithelial cell protection by aminothiol WR-1065 and anetholedithiolethione from ionizing radiation", International journal of cancer, Vol. 96, John Wiley & Sons, Ltd., Hoboken, <https://doi.org/10.1002/ijc.10346>.

Cabrera M., R. Chihuailaf and F. Wittwer Menge (2011), "Antioxidants and the integrity of ocular tissues", Veterinary medicine international, Vol. 2011, Hindawi, London, <https://doi.org/10.4061/2011/905153>.

Cadet, J. et al. (2012), "Oxidatively generated complex DNA damage: tandem and clustered lesions", Cancer letters, Vol. 327, Elsevier, Amsterdam, <https://doi.org/10.1016/j.canlet.2012.04.005>.

Cencer, C. et al. (2018), "PARP-1/PAR activity in cultured human lens epithelial cells exposed to low levels of UVB light", Photochemistry and photobiology, Vol. 94, John Wiley & Sons, Ltd., Hoboken, <https://doi.org/10.1111/php.12814>.

Cervelli, T. et al. (2017), "A New Natural Antioxidant Mixture Protects against Oxidative and DNA Damage in Endothelial Cell Exposed to Low-Dose Irradiation",

Oxidative medicine and cellular longevity, Vol. 2017, Hindawi, London, <https://doi.org/10.1155/2017/9085947>.

Chen, Y. et al. (2021), "Effects of neutron radiation on Nrf2-regulated antioxidant defence systems in rat lens", Experimental and therapeutic medicine, Vol. 21/4, Spandidos Publishing Ltd, Athens, <https://doi.org/10.3892/etm.2021.9765>.

Chien, L. et al. (2015) "Low-dose ionizing radiation induces mitochondrial fusion and increases expression of mitochondrial complexes I and III in hippocampal neurons", Oncotarget, Vol. 6/31, Impact Journals, Orchard Park, <https://doi.org/10.18632/oncotarget.5790>

Chitchumroonchokchai, C. et al. (2004), "Xanthophylls and α -tocopherol decrease UVB-induced lipid peroxidation and stress signaling in human lens epithelial cells", The Journal of Nutrition, Vol. 134/12, American Society for Nutritional Sciences, Bethesda, <https://doi.org/10.1093/jn/134.12.3225>.

Collins-Underwood, J. R. et al. (2008), "NADPH oxidase mediates radiation-induced oxidative stress in rat brain microvascular endothelial cells", Free radical biology & medicine, Vol. 45/6, Elsevier, Amsterdam, <https://doi.org/10.1016/j.freeradbiomed.2008.06.024>.

de Jager, T.L., Cockrell, A.E., Du Plessis, S.S. (2017), "Ultraviolet Light Induced Generation of Reactive Oxygen Species", in Ultraviolet Light in Human Health, Diseases and Environment. Advances in Experimental Medicine and Biology, Springer, Cham, https://doi.org/10.1007/978-3-319-56017-5_2

Demir, E. et al. (2020), "Nigella sativa oil and thymoquinone reduce oxidative stress in the brain tissue of rats exposed to total head irradiation", International journal of radiation biology, Vol. 96/2, Informa, London, <https://doi.org/10.1080/09553002.2020.1683636>.

Eaton, J. W. (1994), "UV-mediated cataractogenesis: A radical perspective", Documenta ophthalmologica, Vol. 88, Springer, London, <https://doi.org/10.1007/BF01203677>.

Fatma, N. et al. (2005), "Impaired homeostasis and phenotypic abnormalities in Prdx6-/- mice lens epithelial cells by reactive oxygen species: Increased expression and activation of TGF β ", Cell death and differentiation, Vol. 12, Nature Portfolio, London, <https://doi.org/10.1038/sj.cdd.4401597>.

Fletcher, A. E (2010), "Free radicals, antioxidants and eye diseases: evidence from epidemiological studies on cataract and age-related macular degeneration", Ophthalmic Research, Vol. 44, Karger International, Basel, <https://doi.org/10.1159/000316476>.

Ganea, E. and J. J. Harding (2006), "Glutathione-related enzymes and the eye", Current eye research, Vol. 31/1, Informa, London, <https://doi.org/10.1080/02713680500477347>.

Giblin, F. J. et al. (2002), "UVA light in vivo reaches the nucleus of the guinea pig lens and produces deleterious, oxidative effects", Experimental eye research, Vol. 75/4, Elsevier, Amsterdam, <https://doi.org/10.1006/exer.2002.2039>.

Giedzinski, E. et al. (2005), "Efficient production of reactive oxygen species in neural precursor cells after exposure to 250 MeV protons", Radiation research, Vol. 164/4, Radiation Research Society, Bozeman, <https://doi.org/10.1667/rr3369.1>.

Hamada, N. et al. (2014), "Emerging issues in radiogenic cataracts and cardiovascular disease", Journal of radiation research, Vol. 55/5, Oxford University Press, Oxford, <https://doi.org/10.1093/jrr/rru036>.

Hatoum, O. A. et al. (2006), "Radiation induces endothelial dysfunction in murine intestinal arterioles via enhanced production of reactive oxygen species", Arteriosclerosis, Thrombosis, and Vascular Biology, Vol. 26/2, Lippincot Williams & Wilkins, Philadelphia, <https://doi.org/10.1161/01.ATV.0000198399.40584.8C>.

Hightower, K. and J. McCready (1992), "Mechanisms involved in cataract development following near-ultraviolet radiation of cultured lenses", Current eye research, Vol. 11/7, Informa, London, <https://doi.org/10.3109/02713689209000741>.

Hightower, K. R. (1995), "The role of the lens epithelium in development of UV cataract", Current eye research, Vol. 14/1, Informa, London, <https://doi.org/10.3109/02713689508999916>.

Hua, H. et al. (2019), "Protective effects of lanosterol synthase up-regulation in UV-B-induced oxidative stress", Frontiers in pharmacology, Vol. 10, Frontiers Media SA, Lausanne, <https://doi.org/10.3389/fphar.2019.00947>.

Huang, L. et al. (2006), "Oxidation-induced changes in human lens epithelial cells 2. Mitochondria and the generation of reactive oxygen species", Free radical biology & medicine, Vol. 41/6, Elsevier, Amsterdam, <https://doi.org/10.1016/j.freeradbiomed.2006.05.023>.

Huang, B. et al. (2019), "Amifostine suppresses the side effects of radiation on BMSCs by promoting cell proliferation and reducing ROS production", Stem Cells International, Vol. 2019, Hindawi, London, <https://doi.org/10.1155/2019/8749090>.

Huang, B. et al. (2018), "Sema3a inhibits the differentiation of raw264.7 cells to osteoclasts under 2gy radiation by reducing inflammation", PLoS ONE, Vol. 13/7, PLOS, San Francisco, <https://doi.org/10.1371/journal.pone.0200000>.

ICRU (1998), "ICRU report 57: conversion coefficients for use in radiological protection against external radiation", Journal of the ICRU, Vol. 29/2, SAGE Publishing

Ismail, A. F. and S. M. El-Sonbaty (2016), "Fermentation enhances Ginkgo biloba protective role on gamma-irradiation induced neuroinflammatory gene expression and stress hormones in rat brain", *Journal of photochemistry and photobiology. B, Biology*, Vol. 158, Elsevier, Amsterdam, <https://doi.org/10.1016/j.jphotobiol.2016.02.039>.

Ji, Y. et al. (2015), "The mechanism of UVB irradiation induced-apoptosis in cataract", *Molecular and cellular biochemistry*, Vol. 401, Springer, London, <https://doi.org/10.1007/s11010-014-2294-x>.

Jiang, Q. et al. (2006), "UV radiation down-regulates Dsg-2 via Rac/NADPH oxidase-mediated generation of ROS in human lens epithelial cells", *International Journal of Molecular Medicine*, Vol. 18/2, Spandidos Publishing Ltd, Athens, <https://doi.org/10.3892/ijmm.18.2.381>.

Jurja, S. et al. (2014), "Ocular cells and light: harmony or conflict?", *Romanian Journal of Morphology & Embryology*, Vol. 55/2, Romanian Academy Publishing House, Bucharest, pp. 257–261.

Kang, L. et al. (2020), "Ganoderic acid A protects lens epithelial cells from UVB irradiation and delays lens opacity", *Chinese journal of natural medicines*, Vol. 18/12, Elsevier, Amsterdam, [https://doi.org/10.1016/S1875-5364\(20\)60037-1](https://doi.org/10.1016/S1875-5364(20)60037-1).

Karam, H. M. and R. R. Radwan (2019), "Metformin modulates cardiac endothelial dysfunction, oxidative stress and inflammation in irradiated rats: A new perspective of an antidiabetic drug", *Clinical and Experimental Pharmacology and Physiology*, Vol. 46/12, Wiley-Blackwell, Hoboken, <https://doi.org/10.1111/1440-1681.13148>.

Karimi, N. et al. (2017), "Radioprotective effect of hesperidin on reducing oxidative stress in the lens tissue of rats", *International Journal of Pharmaceutical Investigation*, Vol. 7/3, Phcog Net, Bengaluru, https://doi.org/10.4103/jphi.JPHI_60_17.

Kłuciński, P. et al. (2008), "Erythrocyte antioxidant parameters in workers occupationally exposed to low levels of ionizing radiation", *Annals of Agricultural and Environmental Medicine*, Vol. 15/1, pp. 9-12.

Kook, S. H. et al. (2015), "Irradiation inhibits the maturation and mineralization of osteoblasts via the activation of Nrf2/HO-1 pathway", *Molecular and Cellular Biochemistry*, Vol. 410/1-2, Springer, London, <https://doi.org/10.1007/s11010-015-2559-z>.

Kubo, E. et al. (2010), "Protein expression profiling of lens epithelial cells from Prdx6-depleted mice and their vulnerability to UV radiation exposure", *American Journal of Physiology*, Vol. 298/2, American Physiological Society, Rockville, <https://doi.org/10.1152/ajpcell.00336.2009>.

Lee, J. et al. (2004), "Reactive oxygen species, aging, and antioxidative nutraceuticals", *Comprehensive reviews in food science and food safety*, Vol. 3/1, Blackwell Publishing Ltd, Oxford, <http://doi.org/10.1111/j.1541-4337.2004.tb00058.x>.

Limoli, C. L. et al. (2007), "Redox changes induced in hippocampal precursor cells by heavy ion irradiation", *Radiation and environmental biophysics*, Vol. 46/2, Springer, London, <https://doi.org/10.1007/s00411-006-0077-9>.

Limoli, C. L. et al. (2004), "Radiation response of neural precursor cells: linking cellular sensitivity to cell cycle checkpoints, apoptosis and oxidative stress", *Radiation research*, Vol. 161/1, Radiation Research Society, Bozeman, <https://doi.org/10.1667/rr3112>.

Liu, F. et al. (2019), "Transcriptional response of murine bone marrow cells to total-body carbon-ion irradiation", *Mutation Research - Genetic Toxicology and Environmental Mutagenesis*, Vol. 839, Elsevier, Amsterdam, <https://doi.org/10.1016/j.mrgentox.2019.01.014>.

Liu, Y. et al. (2018), "Protective effects of α 2macroglobulin on human bone marrow mesenchymal stem cells in radiation injury", *Molecular Medicine Reports*, Vol. 18/5, Spandidos Publishing Ltd, Athens, <https://doi.org/10.3892/mmr.2018.9449>.

Manda, K. et al. (2007), "Melatonin attenuates radiation-induced learning deficit and brain oxidative stress in mice", *Acta neurobiologiae experimentalis*, Vol. 67/1, Nencki Institute of Experimental Biology, Warsaw, pp. 63–70.

Manda, K., M. Ueno and K. Anzai (2008), "Memory impairment, oxidative damage and apoptosis induced by space radiation: ameliorative potential of alpha-lipoic acid", *Behavioural brain research*, Vol. 187/2, Elsevier, Amsterdam, <https://doi.org/10.1016/j.bbr.2007.09.033>.

Mansour, H. H. (2013), "Protective effect of ginseng against gamma-irradiation-induced oxidative stress and endothelial dysfunction in rats", *EXCLI Journal*, Vol. 12, Leibniz Research Centre for Working Environment and Human Factors, Dortmund, pp. 766-777.

Marshall, J. (1985), "Radiation and the ageing eye", *Ophthalmic & physiological optics*, Vol. 5, Wiley-Blackwell, Hoboken, <https://doi.org/10.1111/j.1475-1313.1985.tb00666.x>.

Padgaonkar, V. A. et al. (2015) "Thioredoxin reductase activity may be more important than GSH level in protecting human lens epithelial cells against UVA light", *Photochemistry and photobiology*, Vol. 91/2, Wiley-Blackwell, Hoboken, <https://doi.org/10.1111/php.12404>.

Pendergrass, W. et al. (2010), "X-ray induced cataract is preceded by LEC loss, and coincident with accumulation of cortical DNA, and ROS; similarities with age-related cataracts", *Molecular Vision*, Vol. 16, Emory University, Atlanta, pp. 1496-513.

Philipp, J. et al. (2020), "Radiation Response of Human Cardiac Endothelial Cells Reveals a Central Role of the cGAS-STING Pathway in the Development of Inflammation", *Proteomes*, Vol. 8/4, Multidisciplinary Digital Publishing Institute, Basel, <https://doi.org/10.3390/proteomes8040030>.

Quan, Y. et al. (2021), "Connexin hemichannels regulate redox potential via metabolite exchange and protect lens against cellular oxidative damage", *Redox biology*, Vol. 46, Elsevier, Amsterdam, <https://doi.org/10.1016/j.redox.2021.102102>.

Ramadan, R. et al. (2020), "Connexin43 Hemichannel Targeting With TAT-Gap19 Alleviates Radiation-Induced Endothelial Cell Damage", *Frontiers in Pharmacology*, Vol. 11, Frontiers Media SA, Lausanne, <https://doi.org/10.3389/fphar.2020.00212>

Rehman, M. U. et al. (2016), "Comparison of free radicals formation induced by cold atmospheric plasma, ultrasound, and ionizing radiation", *Archives of biochemistry and biophysics*, Vol. 605, Elsevier, Amsterdam, <https://doi.org/10.1016/j.abb.2016.04.005>.

Rogers, C. S. et al. (2004), "The effects of sub-solar levels of UV-A and UV-B on rabbit corneal and lens epithelial cells", *Experimental eye research*, Vol. 78, Elsevier, Amsterdam, <https://doi.org/10.1016/j.exer.2003.12.011>.

Rong, X. et al. (2019), "TRIM69 inhibits cataractogenesis by negatively regulating p53", *Redox biology*, Vol. 22, Elsevier, Amsterdam, <https://doi.org/10.1016/j.redox.2019.101157>.

Rugo, R. E. and R. H. Schiestl (2004), "Increases in oxidative stress in the progeny of X-irradiated cells", *Radiation research*, Vol. 162/4, Radiation Research Society, Bozeman, <https://doi.org/10.1667/rr3238>.

Santos, A. L., S. Sinha, and A. B. Linder (2018), "The good, the bad, and the ugly of ROS: New insights on aging and aging-related diseases from eukaryotic and prokaryotic model organisms", *Oxidative medicine and cellular longevity*, Vol. 2018, Hindawi, London, <https://doi.org/10.1155/2018/1941285>.

Schoenfeld, M. P. et al. (2012), "A hypothesis on biological protection from space radiation through the use of new therapeutic gases as medical counter measures", *Medical gas research*, Vol. 2/8, BioMed Central Ltd, London, <https://doi.org/10.1186/2045-9912-2-8>.

Sharma, U. C. et al. (2018), "Effects of a novel peptide Ac-SDKP in radiation-induced coronary endothelial damage and resting myocardial blood flow", *Cardio-oncology*, Vol. 4, BioMed Central Ltd, London, <https://doi.org/10.1186/s40959-018-0034-1>.

Shen, Y. et al. (2018), "Transplantation of bone marrow mesenchymal stem cells prevents radiation-induced artery injury by suppressing oxidative stress and inflammation", *Oxidative Medicine and Cellular Longevity*, Vol. 2018, Hindawi, London, <https://doi.org/10.1155/2018/5942916>.

Slezak, J. et al. (2017), "Potential markers and metabolic processes involved in the mechanism of radiation-induced heart injury", *Canadian journal of physiology and pharmacology*, Vol. 95/10, Canadian Science Publishing, Ottawa, <https://doi.org/10.1139/cjpp-2017-0121>.

Soloviev, A. I. and I.V. Kizub (2019), "Mechanisms of vascular dysfunction evoked by ionizing radiation and possible targets for its pharmacological correction", *Biochemical pharmacology*, Vol. 159, Elsevier, Amsterdam, <https://doi.org/10.1016/j.bcp.2018.11.019>.

Soltani, B. (2016), "Nanoformulation of curcumin protects HUVEC endothelial cells against ionizing radiation and suppresses their adhesion to monocytes: potential in prevention of radiation-induced atherosclerosis", *Biotechnology Letters*, Vol. 38, Springer, London, <https://doi.org/10.1007/s10529-016-2189-x>.

Soucy, K. G. et al. (2011), "HZE 56Fe-Ion Irradiation Induces Endothelial Dysfunction in Rat Aorta: Role of Xanthine Oxidase", *Radiation Research*, Vol. 176/4, Radiation Research Society, Bozeman, <https://doi.org/10.1667/RR2598.1>.

Soucy, K. G. et al. (2010), "Dietary inhibition of xanthine oxidase attenuates radiation-induced endothelial dysfunction in rat aorta", *Journal of Applied Physiology*, Vol. 108/5, American Physiological Society, Rockville, <https://doi.org/10.1152/japplphysiol.00946.2009>.

Spector, A. (1990), "Oxidation and aspects of ocular pathology", *The CLAO journal*, Vol. 16, Contact Lens Association of Ophthalmologists, Colorado, pp. S8-10.

Stohs, S. (1995), "The role of free radicals in toxicity and disease", *Journal of Basic and Clinical Physiology and Pharmacology*, Vol. 6/3-4, Walter de Gruyter GmbH, Berlin, pp. 205-228.

Suman, S. et al. (2013), "Therapeutic and space radiation exposure of mouse brain causes impaired DNA repair response and premature senescence by chronic oxidant production", *Aging*, Vol. 5/8, Impact Journals, Orchard Park, <https://doi.org/10.18632/aging.100587>.

Tahimic, C. G. T., and R. K. Globus (2017), "Redox signaling and its impact on skeletal and vascular responses to spaceflight", *International Journal of Molecular Sciences*, Vol. 18/10, Multidisciplinary Digital Publishing Institute, Basel, <https://doi.org/10.3390/ijms18102153>.

Tangvarasittichai, O. and S. Tangvarasittichai (2018), "Oxidative stress, ocular disease and diabetes retinopathy", *Current pharmaceutical design*, Vol. 24/40, Bentham Science Publishers, Sharjah, <https://doi.org/10.2174/1381612825666190115121531>.

Taysi, S. et al. (2012), "Zinc administration modulates radiation-induced oxidative injury in lens of rat", *Pharmacognosy Magazine*, Vol. 8/2, <https://doi.org/10.4103/0973-1296.103646>

Tian, Y. et al. (2017), "The Impact of Oxidative Stress on the Bone System in Response to the Space Special Environment", *International Journal of Molecular Sciences*, Vol. 18/10, Multidisciplinary Digital Publishing Institute, Basel, <https://doi.org/10.3390/ijms18102132>.

AOP482

Tseng, B. P. et al. (2014), "Functional consequences of radiation-induced oxidative stress in cultured neural stem cells and the brain exposed to charged particle irradiation", *Antioxidants & redox signaling*, Vol. 20/9, Mary Ann Leibert Inc., Larchmont, <https://doi.org/10.1089/ars.2012.5134>.

Turner, N. D. et al. (2002), "Opportunities for nutritional amelioration of radiation-induced cellular damage", *Nutrition*, Vol. 18/10, Elsevier Inc, New York, [http://doi.org/10.1016/S0899-9007\(02\)00945-0](http://doi.org/10.1016/S0899-9007(02)00945-0).

Ungvari, Z. et al. (2013), "Ionizing Radiation Promotes the Acquisition of a Senescence-Associated Secretory Phenotype and Impairs Angiogenic Capacity in Cerebromicrovascular Endothelial Cells: Role of Increased DNA Damage and Decreased DNA Repair Capacity in Microvascular Radiosensitivity", *The Journals of Gerontology Series A: Biological Sciences and Medical Sciences*, Vol. 68/12, Oxford University Press, Oxford, <https://doi.org/10.1093/gerona/glt057>.

Varma, S. D. et al. (2011), "Role of ultraviolet irradiation and oxidative stress in cataract formation-medical prevention by nutritional antioxidants and metabolic agonists", *Eye & contact lens*, Vol. 37/4, Lippincot Williams & Wilkins, Philadelphia, <https://doi.org/10.1097/ICL.0b013e31821ec4f2>.

Venkatesulu, B. P. et al. (2018), "Radiation-Induced Endothelial Vascular Injury: A Review of Possible Mechanisms", *JACC: Basic to Translational Science*, Vol. 3/4, Elsevier, Amsterdam, <https://doi.org/10.1016/j.jacbs.2018.01.014>.

Veeraraghavan, J. et al. (2011), "Low-dose gamma-radiation-induced oxidative stress response in mouse brain and gut: regulation by NF κ B-MnSOD cross-signaling", *Mutation research*, Vol. 718/1-2, Elsevier, Amsterdam, <https://doi.org/10.1016/j.mrgentox.2010.10.006>.

Wang, C. et al. (2016), "Protective effects of cerium oxide nanoparticles on MC3T3-E1 osteoblastic cells exposed to X-ray irradiation", *Cellular Physiology and Biochemistry*, Vol. 38/4, Karger International, Basel, <https://doi.org/10.1159/000443092>.

Wang, H. et al. (2019a), "Radiation-induced heart disease: a review of classification, mechanism and prevention", *International Journal of Biological Sciences*, Vol. 15/10, Ivyspring International Publisher, Sydney, <https://doi.org/10.7150/ijbs.35460>.

Wang, H. et al. (2019b), "Gamma Radiation-Induced Disruption of Cellular Junctions in HUVECs Is Mediated through Affecting MAPK/NF- κ B Inflammatory Pathways", *Oxidative Medicine and Cellular Longevity*, Vol. 2019, Hindawi, London, <https://doi.org/10.1155/2019/1486232>.

Wegener, A. R. (1994), "In vivo studies on the effect of UV-radiation on the eye lens in animals", *Documenta ophthalmologica*, Vol. 88, Springer, London, <https://doi.org/10.1007/BF01203676>.

Weinreb O. and A. Dovrat (1996), "Transglutaminase involvement in UV-A damage to the eye lens", *Experimental eye research*, Vol. 63/5, Elsevier, London, <https://doi.org/10.1006/exer.1996.0150>.

Yang, H. et al. (2020), "Cytoprotective role of humanin in lens epithelial cell oxidative stress-induced injury", *Molecular medicine reports*, Vol. 22/2, Spandidos Publishing Ltd, Athens, <https://doi.org/10.3892/mmr.2020.11202>.

Yao, K. et al. (2008), "The flavonoid, fisetin, inhibits UV radiation-induced oxidative stress and the activation of NF- κ B and MAPK signaling in human lens epithelial cells", *Molecular Vision*, Vol. 14, Emory University, Atlanta, pp. 1865-1871.

Yao, J. et al. (2009), "UVB radiation induces human lens epithelial cell migration via NADPH oxidase-mediated generation of reactive oxygen species and up-regulation of matrix metalloproteinases", *International Journal of Molecular Medicine*, Vol. 24/2, Spandidos Publishing Ltd, Athens, https://doi.org/10.3892/ijmm_00000218.

Yves, C. (2000), "Oxidative stress and Alzheimer disease", *The American Journal of Clinical Nutrition*, Vol. 71/2 <https://doi.org/10.1093/ajcn/71.2.621s>.

Zhang, J. et al. (2012), "Ultraviolet radiation-induced cataract in mice: The effect of age and the potential biochemical mechanism", *Investigative ophthalmology & visual science*, Vol. 53, Association for Research in Vision and Ophthalmology, Rockville, <https://doi.org/10.1167/iovs.12-10482>.

Zhang, L. et al. (2020), "Amifostine inhibited the differentiation of RAW264.7 cells into osteoclasts by reducing the production of ROS under 2 Gy radiation", *Journal of Cellular Biochemistry*, Vol. 121/1, John Wiley & Sons, Ltd., Hoboken, <https://doi.org/10.1002/jcb.29247>.

Zhang, L. et al. (2018), "Astragalus polysaccharide inhibits ionizing radiation-induced bystander effects by regulating MAPK/NF- κ B signaling pathway in bone mesenchymal stem cells (BMSCs)", *Medical Science Monitor*, Vol. 24, International Scientific Information, Inc., Melville, <https://doi.org/10.12659/MSM.909153>.

Zigman, S. et al. (2000), "Effects of intermittent UVA exposure on cultured lens epithelial cells", *Current Eye Research*, Vol. 20/2, Informa UK Limited, London, [https://doi.org/10.1076/0271-3683\(200002\)2021:DFT095](https://doi.org/10.1076/0271-3683(200002)2021:DFT095).

Zigman, S. et al. (1995), "Damage to cultured lens epithelial cells of squirrels and rabbits by UV-A (99.9%) plus UV-B (0.1%) radiation and alpha tocopherol protection", *Molecular and cellular biochemistry*, Vol. 143, Springer, London, <https://doi.org/10.1007/BF00925924>.

Relationship: 2716: Oxidative Stress leads to Increase, Cell death

AOPs Referencing Relationship

AOP Name	Adjacency	Weight of Evidence	Quantitative Understanding
----------	-----------	--------------------	----------------------------

AOP Name	Adjacency	Weight of Evidence	Quantitative Understanding																
Deposition of energy leading to occurrence of bone loss	adjacent	Moderate	Low																
Evidence Supporting Applicability of this Relationship																			
Taxonomic Applicability																			
<table> <thead> <tr> <th>Term</th><th>Scientific Term</th><th>Evidence</th><th>Links</th></tr> </thead> <tbody> <tr> <td>human</td><td>Homo sapiens</td><td>Low</td><td>NCBI</td></tr> <tr> <td>mouse</td><td>Mus musculus</td><td>Moderate</td><td>NCBI</td></tr> <tr> <td>rat</td><td>Rattus norvegicus</td><td>Moderate</td><td>NCBI</td></tr> </tbody> </table>				Term	Scientific Term	Evidence	Links	human	Homo sapiens	Low	NCBI	mouse	Mus musculus	Moderate	NCBI	rat	Rattus norvegicus	Moderate	NCBI
Term	Scientific Term	Evidence	Links																
human	Homo sapiens	Low	NCBI																
mouse	Mus musculus	Moderate	NCBI																
rat	Rattus norvegicus	Moderate	NCBI																
Life Stage Applicability																			
<table> <thead> <tr> <th>Life Stage</th><th>Evidence</th></tr> </thead> <tbody> <tr> <td>Adult</td><td>Moderate</td></tr> <tr> <td>Juvenile</td><td>Moderate</td></tr> </tbody> </table>				Life Stage	Evidence	Adult	Moderate	Juvenile	Moderate										
Life Stage	Evidence																		
Adult	Moderate																		
Juvenile	Moderate																		
Sex Applicability																			
<table> <thead> <tr> <th>Sex</th><th>Evidence</th></tr> </thead> <tbody> <tr> <td>Male</td><td>Moderate</td></tr> <tr> <td>Female</td><td>Moderate</td></tr> </tbody> </table>				Sex	Evidence	Male	Moderate	Female	Moderate										
Sex	Evidence																		
Male	Moderate																		
Female	Moderate																		
<p>The evidence for the taxonomic applicability to humans is low as majority of the evidence is from in vitro human-derived cells and in vitro animal-derived cells. The relationship is supported by mice and rat models using male and female animals. The relationship is plausible at any life stage. However, most studies have used adolescent and adult animal models.</p>																			
Key Event Relationship Description																			
<p>Oxidative stress can cause cellular damage and activate signaling cascades that result in programmed cell death, including apoptosis and autophagy. Increased production of free radicals, such as reactive oxygen species (ROS) and reactive nitrogen species (RNS), collectively RONS, and a weakened antioxidant defence system can be detrimental. When free radicals overwhelm antioxidants, the resulting oxidative stress can cause damage to DNA, including base damage; strand breaks; and mutation, as well as damage to vital cellular components, such as lipid peroxidation within the cellular and mitochondrial membranes. Sufficient oxidative damage to the cell can result in programmed cell death (Pacheco and Stock, 2013; Tian et al., 2017). Overwhelming DNA damage from oxidative stress can result in cell damage and death.</p>																			
Evidence Supporting this KER																			
<p>Overall weight of evidence: Moderate</p>																			
Biological Plausibility																			
<p>High concentrations of ROS induce cell death by activating apoptosis pathways and causing oxidative damage to lipids, proteins, and DNA, including base damage, strand breaks, and mutations. In addition, ROS cause damage to vital cellular components, including the mitochondria and cellular membrane, resulting in programmed cell death (Pacheco and Stock, 2013; Valko et al., 2007). When the hydroxyl radical interacts with DNA it can cause damage to both purine and pyrimidine bases, as well as the deoxyribose backbone. A common DNA lesion that has been extensively researched is the bonding of hydroxyl radicals to the guanine nucleotide base, known as the 8-hydroxyguanine (8-OH-G) bond (Glasauer & Chandel, 2013; Halliwell & Gutteridge, 1999; Valko et al., 2007; Valko et al., 2006). ROS can damage the cellular membrane by oxidizing the polyunsaturated fatty acids residues of the phospholipid bilayer, in a process known as lipid peroxidation. The final product of lipid peroxidation is malondialdehyde (MDA), a common marker of oxidative stress. Another aldehyde product of lipid peroxidation is 4-hydroxyonenal (4-HNE) (Siems, Grune, & Esterbauer, 1995; Valko et al., 2007). Proteins undergo oxidative damage through the interaction of ROS with its amino acid monomers. All amino acid side chains can be oxidized by RONS, with cysteine and methionine being particularly susceptible. A common measure of oxidative damage to proteins is the concentration of carbonyl groups (Stadtman, 2004; Valko et al., 2007).</p>																			
<p>Programmed cell death is regulated by the balance of positive signals involved in cell survival, such as growth factors, and negative signals that can harm to the cell, including increased RONS concentration and oxidative damage to DNA (Hengartner, 2000; Valko et al., 2007). The redox environment of cells is regulated in large part by the intracellular concentration of the antioxidant, glutathione (GSH). When GSH drops below a certain level, the cellular environment becomes too oxidizing, and apoptosis occurs. Apoptosis begins to occur after moderate oxidation, with overwhelming oxidation resulting in necrosis (Cai & Jones, 1998; Evans, 2004; Valko et al., 2007; Voehringer et al., 2000). Intracellular damage to the cell via oxidative stress causes Bcl-2 to activate the pro-apoptotic Bcl-2 associated protein x (Bax) (Jezek et al., 2019; Memme et al., 2021; Pistilli, Jackson, & Alway, 2006; Philchenkov et al., 2004; Valko et al., 2007). Alternatively, ROS accumulation in the mitochondria can cause the mitochondrial permeability transition pore (mPTP) to open, allowing for an influx of solutes to enter the mitochondria, creating a hypotonic environment, and subsequently inducing apoptosis (Bauer & Murphy, 2020; Memme et al., 2021).</p>																			
<p>Accumulation of ROS in the mitochondria can also lead to activation of the ion channel, transient receptor potential cation channel (TRPML1), which facilitates the release of Ca²⁺ from the lysosome into the cytosol, resulting in swelling of the endo-lysosomal structures and stimulation of transcription factor EB (TFEB)-mediated signaling cascade that culminates in increased autophagy (Erkhembaatar et al., 2017; Johnson et al., 2020; Todkar, Ilamathi, & Germain, 2017). Alternatively, an accumulation of NADPH oxidase (NOX)-generated ROS in endosomal compartments can lead to activation of autophagy. NOX2 enzymes, found in the endosome, induce oxidative damage to mitochondrial and nuclear DNA through reduction of NADPH, resulting in apoptosis. NOX-generated ROS can also increase signaling from endocytosed receptors that are responsible for inducing mitochondrial dysfunction induced-apoptosis (Davis Volk & Moreland, 2014; Harrison et al., 2018; Johnson et al., 2020; Karunakaran et al., 2019; Li et al., 2015; Ran et al., 2016; Tsubata, 2020).</p>																			
Empirical Evidence																			
<p>The empirical evidence for this KER provides moderate support for a linkage between increased oxidative stress and increased cell death. Most of the evidence supporting this relationship come from studies that examine the effects of low linear energy transfer (LET) radiation, such as X-rays and gamma rays. However, one study examined the effects of high LET carbon ions and another exposed its model to simulated microgravity conditions. These studies observed dose and time concordant responses (Huang et al., 2019; Huang et al., 2018; Kondo et al., 2010; Li et al., 2020; Li et al., 2018; Liu et al., 2019; Liu et al., 2018; Yoo, Han & Kim, 2016).</p>																			
Incidence Concordance																			
<p>Few studies demonstrate a greater oxidative stress than cell death following a stressor. Human bone marrow-derived mesenchymal stem cells (hBMMSCs) irradiated with 8 Gy demonstrated greater increases to ROS levels than to apoptosis (Li et al., 2020). Similarly, rats irradiated with 35 Gy showed greater increases to ROS levels than to osteocyte apoptosis (Li et al., 2018).</p>																			
Dose Concordance																			
<p>Current literature on the impact of oxidative stress on cell death provides moderate evidence for a dose concordant link between the two key events. Studies that examined the effects of ionizing radiation (IR) and microgravity conditions on bone cells have observed both stressors induce significant increases in ROS and oxidative stress markers, as well as decreases in antioxidants, followed by subsequent increases in markers of cell death.</p>																			

Studies that apply IR to their experimental models provide the strongest support for dose concordance as they clearly demonstrate variances in oxidative stress and cell death following exposure to a range of doses. Oxidative stress was observed at the same or lower doses than cell death across all studies. Kondo et al. (2010) irradiated C57BL/6J mice with 1 or 2 Gy of 137Cs gamma rays and observed significant increases to ROS production and the oxidative stress markers, MDA and 4-HNE, at 1 Gy, while apoptosis only experienced a significant increase at 2 Gy. Bai et al. (2020) irradiated the bone marrow derived mesenchymal cells (bmMSCs) of Sprague-Dawley rats with 2, 5, and 10 Gy of 137Cs gamma rays and observed significant changes to levels of ROS, superoxide dismutase (SOD)1 and catalase (CAT)2, as well as cell viability at ≥ 2 Gy. The one study that applied high LET radiation, in this case 2 Gy of calcium ions, observed more significant increases to oxidative stress and cell death on average than studies that applied 2 Gy of a lower LET radiation type. Liu et al. (2019) observed ~ 2.2 -, ~ 5.4 -, and ~ 4.2 -fold increases to ROS levels, early apoptosis, and late apoptosis/necrosis, respectively, after exposure to 2 Gy of carbon ions (LET=31.6 KeV/ μ m), while other studies that applied 2 Gy of lower LET radiation types, including X-rays and gamma rays, observed increases of ~ 1.2 -fold to ~ 2.5 -fold in ROS levels and increases of ~ 1.6 -fold to 5.26-fold in apoptosis (Huang et al., 2019; Huang et al., 2018; Kondo et al., 2010; Liu et al., 2019). Furthermore, microgravity as a stressor also supports the relationship between oxidative stress and cell death. Yoo, Han & Kim (2016) did observe significant increases to both oxidative stress and cell death after exposing MC3T3-E1 murine pre-osteoblast cells to microgravity conditions.

Time Concordance

There is moderate evidence in the current literature to support a time concordant relationship between oxidative stress and cell death. All of the studies that measured oxidative stress and cell death endpoints at multiple time points observed significant changes to oxidative stress earlier or at the same time as changes to cell death (Huang et al., 2018; Kondo et al., 2010; Li et al., 2020; Li et al., 2018). Huang et al. (2018) irradiated murine RAW264.7 osteoclast precursor cells with 2 Gy of gamma rays and observed a significant increase in ROS levels at 2 hours post-irradiation, while increases to apoptosis were not reported until 24 hours. Kondo et al. (2010) irradiated C57BL/6J mice with 1 and 2 Gy of 137Cs gamma rays and observed significant increases to both ROS levels and apoptosis by day 3 post-irradiation. Li et al. (2020) irradiated hBMMSCs with 8 Gy of radiation and observed significant increases to both ROS levels and cell apoptosis by 24 hours post-exposure. Li et al. (2018) observed significant increases to ROS activity, as well as significant decreases to SOD activity, at 1 day post-irradiation, while significant increases to empty lacunae were not reported until 4 months post-irradiation. Lastly, Wang et al. (2016) irradiated murine MC3T3-E1 cells with 6 Gy of X-rays and observed significant increases to ROS production at 24 hours post exposure and extracellular hydrogen peroxide levels at 3 hours post exposure, while significant decreases to cell viability did not occur until day 4.

Essentiality

Several studies have investigated the essentiality of the relationship, where the blocking or attenuation of the upstream KE causes a change in frequency of the downstream KE. The increase in oxidative stress can be modulated by certain drugs and antioxidants. Treatment with α -2-macroglobulin (α 2M) decreased SOD activity and reduced the rate of apoptosis and autophagy in human bone marrow mesenchymal stem cells hBMMSCs (Liu et al., 2018). This countermeasure also showed the same influence on SOD activity and a decrease in osteocyte apoptosis (Li et al., 2018). Sema3a was found to reduce ROS and promote the apoptosis of the Raw264.7 cells post-radiation (Huang et al., 2018). Treatment with Amifostine (AM) reversed the radiation-induced effects on ROS levels and reduced the percentage of apoptotic cells and DNA damage (Huang et al., 2019; Zhang et al., 2020). Cerium oxide (CeO₂) nanoparticles significantly reduced increases to ROS production and hydrogen peroxide, as well as causing cell viability to recover significantly by day 4 post-irradiation (Wang et al., 2016). Lastly, the antioxidant melatonin was shown to reverse the effect of microgravity on Bcl-2, Bax, Cu/Zn-SOD and manganese superoxide dismutase (Mn-SOD) to control levels (Yoo, Han & Kim, 2016).

Uncertainties and Inconsistencies

- When MC3T3-E1 murine preosteoblast cells underwent microgravity conditions in a 3D clinostat, CAT expression increased by ~ 1.25 -fold. This response was the opposite of the other antioxidants that were measured and is contrary to the decrease in antioxidant expression normally seen after microgravity exposure (Yoo, Han & Kim, 2016).
- Kondo et al. (2010) did not observe any significant effects to MDA+4-HNE levels or apoptosis after subjecting their C57BL/6J mice to hindlimb unloading.

Quantitative Understanding of the Linkage

The following are a few examples of quantitative understanding of the relationship. All reported findings are statistically significant at various alpha levels as listed in the original sources

Response-response relationship

Dose/Incidence Concordance

Reference	Experiment Description	Result
Liu et al., 2018	In vitro. hBMMSCs were irradiated with 8 Gy of X-rays at a rate of 1.24 Gy/min. SOD activity and MnSOD protein expression levels were measured to assess oxidative stress. hBMMSCs were stained for Annexin V to determine cell death.	SOD activity decreased by ~ 0.5 -fold compared to the non-irradiated control at 24 hours post-irradiation. MnSOD protein expression decreased by ~ 0.4 -fold. This decrease in antioxidant defense resulted in a ~ 3 -fold increase in the rate of apoptosis.
Huang et al., 2018	In vitro. Murine RAW264.7 macrophage cells were irradiated with 2 Gy of gamma rays at a rate of 0.83 Gy/min. ROS levels were measured to assess oxidative stress. Levels of Annexin binding was measured to determine cell death.	ROS levels had a maximum increase of ~ 2.5 -fold compared to the non-irradiated control at 2 hours post-irradiation. This increase in oxidative stress was accompanied by a 5.26-fold increase in apoptotic cells (from 1.86% to 9.78%) at 24 hours post-irradiation.
Liu et al., 2019	In vivo. 8-10-week-old, female, SPF BALB/c mice underwent whole-body irradiation with 2 Gy of carbon ions (LET=31.6 KeV/ μ m in water) at a rate of 1 Gy/min. Femoral bone marrow mononuclear cells were then extracted and ROS levels were measured to assess oxidative stress, while Annexin binding was used to measure the number of apoptotic cells.	ROS levels increased by ~ 2.2 -fold, compared to the non-irradiated control. This increase in oxidative stress was accompanied by a ~ 5.4 -fold increase in early apoptosis and a ~ 4.2 -fold increase in late apoptosis/necrosis.
Huang et al., 2019	Ex-vivo. A single 2 Gy dose of 60Co gamma radiation was administered to bmSCs of Sprague Dawley rats at a rate of 0.83 Gy/min. ROS production was measured to assess oxidative stress and apoptosis was determined by Annexin V staining.	ROS production increased by ~ 2 -fold compared to the non-irradiated control. This increase in oxidative stress was accompanied by a ~ 4 -fold increase in osteoblast apoptosis.
Kondo et al., 2010	In vivo. Male C57BL/6J mice at 17 weeks of age were hindlimb unloaded or normally loaded, 4 days later they were exposed to 1 or 2 Gy of 137Cs gamma rays or sham-irradiated. Intracellular ROS and apoptotic cell numbers in the bone marrow cells of the right femora were assessed to determine oxidative stress and cell death, respectively. To assess oxidative damage MDA and 4-HNE were measured.	Following irradiation under normal loading, ROS production increased by ~ 1.3 -fold at 1 Gy by day 3 post-irradiation and a ~ 1.2 -fold at 2 Gy by day 3. The cumulative levels of MDA and 4-HNE increased by ~ 2 -fold under exposure to both 1 and 2 Gy by day 10. This increase in oxidative stress was associated with a ~ 1.6 -fold increase in bone marrow cell apoptosis at 2 Gy by day 3.

Wang et al., 2016	In vitro. Murine MC3T3-E1 osteoblast-like cells were irradiated with 6 Gy of X-rays. Intracellular ROS production and extracellular hydrogen peroxide levels were measured to assess oxidative stress and cell viability was measured to assess cell death.	Intracellular ROS production and extracellular hydrogen peroxide levels increased by ~1.75-fold at 24 hours post-irradiation and ~1.5-fold at 3 hours post-irradiation, respectively, compared to the non-irradiated control. This increase in oxidative stress was accompanied by a significant ~0.3-fold decrease in cell viability at 4 days post-irradiation (no significant decrease at 1 day)..
Bai et al., 2020	Ex vivo. bmMSCs were taken from 4-week-old, male Sprague-Dawley rats. After extraction, cells were then irradiated with 2, 5, and 10 Gy of 137Cs gamma rays. Intracellular ROS levels and relative mRNA expression of the antioxidants, SOD1, SOD2, and CAT2, were measured to assess the extent of oxidative stress induced by IR. Cell death was measured by a viability assay.	Cellular ROS levels increased significantly in a dose-dependent manner from 0-10 Gy. Compared to sham-irradiated controls, ROS levels increased by ~15%, ~55%, and ~105% after exposure to 2, 5, and 10 Gy, respectively. Antioxidant mRNA expression decreased in a dose-dependent manner from 0-10 Gy, with significant decreases seen at doses as low as 2 Gy for SOD1 and CAT2 and 5 Gy for SOD2. Compared to sham-irradiated controls, SOD1 expression decreased by ~9%, ~18%, and ~27% after exposure to 2, 5, and 10 Gy, respectively. SOD2 expression decreased by ~31% and ~41% after exposure to 5 and 10 Gy, respectively. CAT2 expression decreased by ~15%, ~33%, and ~58% after exposure to 2, 5, and 10 Gy, respectively. This increase in oxidative stress was associated with decreases in cell viability of ~33% and ~44% after 1 day post-exposure to 5 and 10 Gy, respectively, and ~3%, ~45%, and ~65% after 3 days post-exposure to 2, 5, and 10 Gy.
Li et al., 2020	In vitro. hBMMSCs were exposed to 8 Gy of X-ray radiation at a rate of 2.75 Gy/min. To assess IR-induced oxidative stress, ROS levels were measured. hBMMSC apoptosis was then measured using terminal deoxynucleotidyl transferase dUTP nick end labeling (TUNEL) staining and an Annexin V-FITC/PI apoptosis detection kit to assess cell subsequent cell death.	At 24 hours post-irradiation, ROS levels increased by ~3.3-fold and ~1.5-fold when measured with fluorescent microscopy and flow cytometry, respectively. At 24 hours post-irradiation, cell apoptosis increased by ~1.8-fold. TUNEL-positive cells experienced a maximum increase of ~1.75-fold compared to the non-irradiated control at 7 days post-irradiation.
Li et al., 2018	In vivo. The mandibles of Sprague-Dawley rats were exposed to a cumulative dose of 35 Gy of X-ray radiation fractionated into 7 Gy daily for 5 days. ROS activity was measured along with SOD activity to assess oxidative stress and empty lacunae were measured to assess cell death among osteocytes.	ROS activity increased significantly at days 1, 14, and 28, with a maximum increase of ~5-fold at day 28. SOD activity decreased significantly at days 1 and 14, with a maximum decrease of ~0.66-fold at day 1. The % of empty lacunae increased ~1.8-fold compared to the non-irradiated control at 4 months post-irradiation.
Yoo, Han & Kim, 2016	In vitro. MC3T3-E1 murine pre-osteoblast cells underwent microgravity conditions in a 3D clinostat. The expression of the antioxidants, Cu/Zn-SOD; Mn-SOD; and CAT, were measured to assess oxidative stress. The expression of the apoptosis/autophagy regulators, Bax and Bcl-2, were measured along with the autophagy marker, LC3 II, to assess IR-induced cell death	After 72 hours, expression of Cu/Zn-SOD and Mn-SOD decreased by ~0.25-fold and ~0.6-fold, respectively, while CAT expression increased by ~1.25-fold. LC3 II levels increased by ~2.25-fold compared to the normally loaded control. Bax levels increased by ~2.4-fold, while Bcl-2 levels decreased by ~0.6-fold.

Time-scale**Time Concordance**

Reference	Experiment Description	Result
Huang et al., 2018	In vitro. Murine RAW264.7 macrophage cells were irradiated with 2 Gy of gamma rays (60Co isotope) at a rate of 0.83 Gy/min. ROS levels were measured to assess oxidative stress. Levels of Annexin binding was measured to determine the effects of IR on cell death.	ROS levels increased by ~2.5-fold at 2 hours post-irradiation and ~2-fold at 8 hours. The increase in oxidative stress was followed by a ~5.26-fold increase in apoptotic cells (from 1.86% to 9.78%) at 24 hours post-irradiation.
Kondo et al., 2010	In vivo. Male C57BL/6J mice at 17 weeks of age were hindlimb unloaded or normally loaded, 4 days later they were exposed to 1 or 2 Gy of 137Cs gamma rays or sham-irradiated. Intracellular ROS and apoptotic cell numbers in the bone marrow cells of the right femora were assessed to determine oxidative stress and cell death, respectively. To assess oxidative damage, MDA and 4-HNE levels were measured.	Following irradiation under normal loading, ROS production increased by ~1.3-fold at 1 Gy by day 3 post-irradiation and a ~1.2-fold at 2 Gy by day 10. The cumulative levels of MDA and 4-HNE increased by ~2-fold under exposure to both 1 and 2 Gy by day 10. This increase in oxidative stress was associated with a ~1.6-fold increase in bone marrow cell apoptosis at 2 Gy by day 3.
Li et al., 2020	In vitro. hBMMSCs were exposed to 8 Gy of radiation. To assess IR-induced oxidative stress, ROS levels were measured. hBMMSC apoptosis was then measured using TUNEL staining and Annexin V-FITC/PI staining to assess cell subsequent cell death.	ROS levels increased significantly at 24 hours post-irradiation. Cell apoptosis also increased significantly at 24 hours post-irradiation. IR-induced changes to the % of TUNEL-positive cells decreased over time, with increases of ~1.75-fold compared to the non-irradiated control at 7 days post-irradiation, ~1.35-fold at 14 days, and ~1.33-fold at 28 days.
Li et al., 2018	In vivo. The mandibles of Sprague-Dawley rats were exposed to a cumulative dose of 35 Gy of radiation fractionated into 7 Gy daily for 5 days. Empty lacunae were measured to assess cell death among osteocytes and ROS activity was measured along with SOD activity to assess oxidative stress.	ROS activity increased by ~4.9-fold compared to the non-irradiated control at day 1 post-irradiation, ~3.7-fold at day 14, and ~5-fold at day 28. SOD activity experienced a maximum decrease of ~0.66-fold at day 1 and recovered over time with a ~0.78-fold decrease at day 14, and a non-significant increase at day 28. The % of empty lacunae increased significantly compared to the non-irradiated control at 4 months post-irradiation.
Wang et al., 2016	In vitro. Murine MC3T3-E1 osteoblast-like cells were irradiated with 6 Gy of X-rays. Intracellular ROS production and extracellular hydrogen peroxide levels were measured to assess oxidative stress and cell viability was measured to assess cell death.	ROS production increased by ~1.75-fold at 24 hours post-irradiation and hydrogen peroxide levels increased by ~1.5-fold at 3 hours post-irradiation, while cell viability did not decrease significantly until 4 days post-exposure (~0.3-fold).

Known modulating factors

Modulating Factor	Details	Effects on the KER	References
Drug	α 2M	Treatment reversed the radiation-induced effects on SOD activity, reduced autophagy, reduced osteocyte cell death, and reduced the rate of apoptosis in hBMMSCs.	Liu et al., 2018; Li et al., 2018
Drug	Sema3a	Treatment with 50 ng/mL partially reduced ROS levels and promoted Raw264.7 cell apoptosis after irradiation.	Huang et al., 2018
Drug	AMI	Treatment with 30 mg/kg reversed the radiation-induced effects on ROS levels and reduced the percentage of apoptotic cells and DNA damage.	Huang et al., 2019

Nanoparticle	CeO2	Cerium oxide acts can switch between a fully reduced and fully oxidized state, allowing it to mimic antioxidants to mediate oxidative stress. Treatment with 100nM significantly attenuated IR-induced increases to ROS production and extracellular hydrogen peroxide, as well as causing cell viability to significantly recover.	Wang et al., 2016
Drug	Melatonin (antioxidant)	Treatment with 200nM melatonin reversed the effect of microgravity on Bcl-2, Bax, Cu/Zn-SOD and Mn-SOD to control levels.	Yoo, Han & Kim, 2016

Known Feedforward/Feedback loops influencing this KER

None identified

References

Bai, J. et al. (2020), "Irradiation-induced senescence of bone marrow mesenchymal stem cells aggravates osteogenic differentiation dysfunction via paracrine signaling", American Journal of Physiology - Cell Physiology, Vol. 318/5, American Physiological Society, Rockville, <https://doi.org/10.1152/ajpcell.00520.2019>.

Bauer, T.M. and Murphy, E. (2020), "Role of Mitochondrial Calcium and the Permeability Transition Pore in Regulating Cell Death", Circ. Res., Vol. 126/2, Lippincott Williams & Wilkins, doi:10.1161/CIRCRESAHA.119.316306.

Cai, J. Y., and Jones, D. P. (1998), "Communication - superoxide in apoptosis - mitochondrial generation triggered by Cytochrome c loss", J. Biol. Chem., Vol. 273/19, doi: 10.1074/jbc.273.19.11401.

Erkhembaatar, M. et al. (2017), "Lysosomal Ca²⁺ Signaling Is Essential for Osteoclastogenesis and Bone Remodeling", J. Bone Miner. Res., Vol. 32/2, doi: 10.1002/jbmr.2986.

Evans, A. M. (2004), "Motexafin gadolinium: A redox-active tumor selective agent for the treatment of cancer", Curr. Opin. Oncol., Vol. 16/2, Lippincott Williams & Wilkins, doi: 10.1097/01.cco.0000142073.29850.98

Glasauer, A. and Chandel, N. S. (2013), "ROS", CURBIO, Vol. 23/3, Elsevier, Amsterdam, <https://doi.org/10.1016/j.cub.2012.12.011>

Halliwell, B. and Gutteridge, J. M. C. (1999), Free radicals in biology and medicine (3rd ed.), Oxford University Press, Oxford.

Harrison, I.P. et al. (2018), "Nox2 Oxidase Expressed in Endosomes Promotes Cell Proliferation and Prostate Tumour Development", Oncotarget, Vol. 9/83, Impact Journals LLC, doi: 10.18632/oncotarget.26237.

Hengartner, M. O. (2000), "The biochemistry of apoptosis", Nature, Vol. 407/6805, Nature Publishing Group.

Huang, B. et al. (2018), "Sema3a inhibits the differentiation of raw264.7 cells to osteoclasts under 2gy radiation by reducing inflammation", PLoS ONE, Vol. 13/7, PLOS, San Francisco, <https://doi.org/10.1371/journal.pone.0200000>.

Huang, B. et al. (2019), "Amifostine suppresses the side effects of radiation on BMSCs by promoting cell proliferation and reducing ROS production", Stem Cells International, Vol. 2019, Hindawi, <https://doi.org/10.1155/2019/8749090>.

Johnson, I. R. D. et al. (2020), "Implications of Altered Endosome and Lysosome Biology in Space Environments", International Journal of Molecular Sciences, Vol. 21/21, MDPI, Basel, <https://doi.org/10.3390/ijms21218205>.

Jezek, J. et al. (2019), "Mitochondrial translocation of cyclin C stimulates intrinsic apoptosis through Bax recruitment", EMBO Rep., Vol. 20/9, Blackwell Publishing Ltd, <https://doi.org/10.15252/embr.201847425>.

Karunakaran, U. et al. (2019), "Cd36 Dependent Redoxosomes Promotes Ceramide-Mediated Pancreatic Beta-Cell Failure Via P66shc Activation", Free Radic. Biol. Med., Vol. 134, Elsevier, Amsterdam, <https://doi.org/10.1016/j.freeradbiomed.2019.02.004>.

Kondo, H. et al. (2010), "Oxidative stress and gamma radiation-induced cancellous bone loss with musculoskeletal disuse", Journal of Applied Physiology, Vol. 108/1, American Physiological Society, <https://doi.org/10.1152/japplphysiol.00294.2009>.

Kook, S. H. et al. (2015), "Irradiation inhibits the maturation and mineralization of osteoblasts via the activation of Nrf2/HO-1 pathway", Molecular and Cellular Biochemistry, Vol. 410/1-2, Springer, London, <https://doi.org/10.1007/s11010-015-2559-z>.

Kozbenko, T. et al. (2022), "Deploying elements of scoping review methods for adverse outcome pathway development: a space travel case example", International Journal of Radiation Biology, Vol. 98/12. <https://doi.org/10.1080/09553002.2022.2110306>

Li, J. et al. (2020), "Effect of α 2-macroglobulin in the early stage of jaw osteoradionecrosis", International Journal of Oncology, Vol. 57/1, Spandidos Publications, <https://doi.org/10.3892/ijo.2020.5051>

Li, J. et al. (2018), "Protective role of α 2-macroglobulin against jaw osteoradionecrosis in a preclinical rat model", Journal of Oral Pathology and Medicine, 48/2, Wiley, <https://doi.org/10.1111/jop.12809>

Li, L. et al. (2015), "Ros and Autophagy: Interactions and Molecular Regulatory Mechanisms", Cell Mol. Neurobiol., Vol. 35/5, Springer, New York, doi: 10.1007/s10571-015-0166-x.

Liu, F. et al. (2019), "Transcriptional Response of Murine Bone Marrow Cells to Total-Body Carbon-Ion Irradiation", Mutation Research - Genetic Toxicology and Environmental Mutagenesis, Vol. 839, Elsevier, Amsterdam, <https://doi.org/10.1016/j.mrgentox.2019.01.014>.

Liu, Y. et al. (2018), "Protective Effects of α -2-Macroglobulin on Human Bone Marrow Mesenchymal Stem Cells in Radiation Injury", Molecular Medicine Reports, Vol. 18/5, Spandidos Publications, <https://doi.org/10.3892/mmr.2018.9449>.

Memme, J. M. et al. (2021), "Mitochondrial Bioenergetics and Turnover during Chronic Muscle Disuse", International journal of molecular sciences, Vol. 22/10, MDPI, Basel, <https://doi.org/10.3390/ijms22105179>.

Pacheco, R. and H. Stock. (2013), "Effects of Radiation on Bone", Current Osteoporosis Reports, Vol.11, Springer Nature, <https://doi.org/10.1007/s11914-013-0174-z>

Philchenkov, A. et al. (2004), "Caspases and cancer: Mechanisms of inactivation and new treatment modalities", Exp. Oncol., Vol. 26/2.

Pistilli, E.E., Jackson, J.R., and Alway, S.E. (2006) "Death receptor-associated pro-apoptotic signaling in aged skeletal muscle", Apoptosis, Vol. 11/12, Springer, doi: 10.1007/s10495-006-0194-6.

Ran, F. et al. (2016), "Simulated Microgravity Potentiates Generation of Reactive Oxygen Species in Cells", Biophys. Rep., Vol. 2/5-6, Springer, doi: 10.1007/s41048-016-0029-0.

Sasi, S. P. et al. (2015), "Particle Radiation-Induced Nontargeted Effects in Bone-Marrow-Derived Endothelial Progenitor Cells", Stem Cells International, Vol. 2015, Hindawi, London, <https://doi.org/10.1155/2015/496512>.

Siems, W. G., Grune, T., and Esterbauer, H. (1995), "4-Hydroxynonenal formation during ischemia and reperfusion of rat small-intestine", Life Sci., Vol. 57/8, Elsevier, Amsterdam, doi: 10.1016/0024-3205(95)02006-5.

Stadtman, E. R. (2004), "Role of oxidant species in aging", Curr. Med. Chem., Vol. 11/9, doi: 10.2174/0929867043365341.

Tian, Y. et al. (2017), "The impact of oxidative stress on the bone system in response to the space special environment", International Journal of Molecular Sciences, Vol. 18/10, MDPI, Basel, <https://doi.org/10.3390/ijms18102132>

Todkar, K., Ilamathi, H.S., and Germain, M. (2017), "Mitochondria and Lysosomes: Discovering Bonds", Front. Cell Dev. Biol., Vol. 5, Frontiers Research Foundation, doi: 10.3389/fcell.2017.00106.

Tsubata, T. (2020), "Involvement of Reactive Oxygen Species (Ros) in Bcr Signaling as a Second Messenger", Adv. Exp. Med. Biol., Vol. 1254, Springer, doi:

10.1007/978-981-15-3532-1_3.

Valko, M. et al. (2007), "Free radicals and antioxidants in normal physiological functions and human disease", *The International Journal of Biochemistry & Cell Biology*, Vol. 39/1, <https://doi.org/10.1016/j.biocel.2006.07.001>

Valko, M. et al. (2006), "Free radicals, metals and antioxidants in oxidative stress-induced cancer", *Chem. Biol. Interact.*, Vol.160/1, Elsevier, doi: 10.1016/j.cbi.2005.12.009.

Voehringer, D. W. et al. (2000), "Gene microarray identification of redox and mitochondrial elements that control resistance or sensitivity to apoptosis", *Proc. Natl. Acad. Sci. U.S.A.*, Vol. 97/6, National Academy of Sciences of the United States of America, doi: 10.1073/pnas.97.6.2680.

Volk, A.P.D and Moreland, J.G. (2014), "Ros-Containing Endosomal Compartments: Implications for Signaling", *Methods Enzymol.*, Vol. 535, <https://doi.org/10.1016/B978-0-12-397925-4.00013-4>.

Wang, C. et al. (2016), "Protective effects of cerium oxide nanoparticles on MC3T3-E1 osteoblastic cells exposed to X-ray irradiation", *Cellular Physiology and Biochemistry*, Vol. 38/4, Karger International, Basel, <https://doi.org/10.1159/000443092>.

Willey, J. S. et al. (2011), "Ionizing Radiation and Bone Loss: Space Exploration and Clinical Therapy Applications", *Clinical Reviews in Bone and Mineral Metabolism*, Vol. 9, *Nature*, <https://doi.org/10.1007/s12018-011-9092-8>.

Yoo, Y. M., T. Y. Han and H. S. Kim. (2016), "Melatonin suppresses autophagy induced by clinostat in preosteoblast MC3T3-E1 cells", *International Journal of Molecular Sciences*, Vol. 17/4, MDPI, Basel, <https://doi.org/10.3390/ijms17040526>

[Relationship: 3319: Oxidative Stress leads to Altered cell differentiation signaling](#)

AOPs Referencing Relationship

AOP Name	Adjacency	Weight of Evidence	Quantitative Understanding
Deposition of energy leading to occurrence of bone loss	adjacent	High	Low

Evidence Supporting Applicability of this Relationship

Taxonomic Applicability

Term	Scientific Term	Evidence	Links
human	Homo sapiens	Low	NCBI
mouse	Mus musculus	High	NCBI
rat	Rattus norvegicus	High	NCBI
Pig	Pig	Moderate	NCBI

Life Stage Applicability

Life Stage Evidence

Juvenile	High
Adult	Moderate

Sex Applicability

Sex	Evidence
Male	High
Female	Low
Unspecific	Low

Based on the prioritized studies presented here, the evidence of taxonomic applicability is low for humans despite there being strong plausibility as the evidence only includes *in vitro* human cell-derived models. The taxonomic applicability for mice and rats is considered high as there is much available data using *in vivo* rodent models that demonstrate the concordance of the relationship. In terms of sex applicability, all *in vivo* studies that indicated the sex of the animals used male animals, therefore, the evidence for males is high and females is considered to be low for this KER. The majority of studies used adolescent animals, with a few using adult animals. Preadolescent animals were not used to support the KER; however, the relationship in preadolescent animals is still plausible.

Key Event Relationship Description

Oxidative stress arises when the generation of free radicals surpasses the ability of cellular antioxidant defenses to neutralize them (Cabrera & Chihuaif, 2011). Both reactive oxygen species (ROS) and reactive nitrogen species (RNS) are types of free radicals that can lead to oxidative stress (Ping et al., 2020); however, ROS are more frequently studied than RNS (Nagane et al., 2021). ROS can cause oxidative damage to biomacromolecules by reacting with DNA, proteins, and lipids, leading to functional alterations in these molecules (Ping et al., 2020). For instance, ROS interacting with lipids results in lipid peroxidation (Cabrera & Chihuaif, 2011).

Cell differentiation pathways are the processes through which unspecialized cells, such as stem cells, develop into specialized cells with distinct functions (Soumelis and Liu, 2006). Disruptions in cell differentiation pathways can occur due to various mechanisms, including ROS production. Persistent activation or inhibition of these pathways can lead to aberrant cell fate decisions (Kharrazian, 2021). ROS plays a crucial role in inducing cell differentiation by modulating signaling pathways and influencing transcription, and excessively high or low amounts of ROS can hinder cell differentiation. For instance, the oxidation of specific cysteine residues in signaling proteins can alter their activity, leading to aberrant activation or inhibition of pathways such as Wnt, Notch, or TGF- β , which are essential for maintaining proper cell differentiation. The disrupted signaling can cause cells to deviate from their intended differentiation path, leading to abnormal cell states or even contributing to pathological conditions. For example, ROS plays crucial role in regulating bone remodeling and repair, impacting osteoblasts and osteoclast activities. Under healthy conditions, ROS generated by osteoclasts activate and balance bone resorption with bone reformation. Exogenous ROS, such as H2O2 and superoxide's initiate RANK signaling in macrophages and endogenous ROS activates TNF receptor associated factor 6, NOX1, and the transcription factors NFkB and nuclear factor of activated T-cells (Rieger et al., 2023). These disruptions can have significant consequences, contributing to various diseases (Wu et al., 2023). An increase of ROS can cause osteocyte apoptosis, leading to bone resorption through osteoclastogenic RANKL and additionally impair Wnt/b-catenin signaling (Rieger et al., 2023). The MAPK family pathway, crucial in regulating molecular processes such as cell differentiation, is activated in response to ROS production through calcium-induced phosphorylation of several kinases (Sinkala et al., 2021). ROS can activate the JAK/STAT pathway through oxidation of glutathione, a pathway which affects cell differentiation (Hu et al., 2023; Villalpando-Rodriguez & Gibson, 2021). Oxidative stress in bone cells can lead to increased expression of the receptor activator of nuclear factor kappa B ligand (RANKL) and Nrf2 activation (Tahimic & Globus, 2017; Tian et al., 2017). Following activation, Nrf2 then interferes with the activation of runt-related transcription factor 2 (Runx2), and depending on the level of oxidative stress, this may result in altered bone cell function (Kook et al., 2015).

Evidence Supporting this KER

Overall weight of evidence: Moderate

Biological Plausibility

Many reviews describe the role of oxidative stress in cell differentiation signaling. The mechanisms through which oxidative stress can contribute to cell differentiation signaling via changes in signaling pathways are well-described. For example, oxidative stress can directly alter various pathways through protein oxidation (Ping et al., 2020; Schmidt-Ullrich et al., 2000; Valerie et al., 2007). Oxidation of cysteine and methionine residues, which are particularly sensitive to

oxidation, can cause conformational change, protein expansion, and degradation, leading to changes in the protein levels of pathways involved in cell differentiation (Ping et al., 2020). Furthermore, oxidation of key residues in signaling proteins can alter their function, resulting in cell differentiation signaling. For example, oxidation of methionine 281 and 282 in the Ca2+/calmodulin binding domain of Ca2+/calmodulin-dependent protein kinase II (CaMKII) leads to constitutive activation of its kinase activity and subsequent downstream alterations in cell differentiation signaling. (Li et al., 2013; Ping et al., 2020). Similarly, during oxidative stress, tyrosine phosphatases can be inhibited by oxidation of a catalytic cysteine residue, resulting in increased phosphorylation of proteins in various cell differentiation signaling pathways (Schmidt-Ullrich et al., 2000; Valerie et al., 2007). Particularly relevant to this are the MAPK pathways. For example, the extracellular signal-regulated kinase (ERK) pathway is activated by upstream tyrosine kinases and relies on tyrosine phosphatases for deactivation (Lehtinen & Bonni, 2006; Valerie et al., 2007).

Furthermore, oxidative stress can indirectly influence cell differentiation signaling through oxidative DNA damage which can lead to mutations or changes in the gene expression of proteins in signaling pathways (Ping et al., 2020; Schmidt-Ullrich et al., 2000; Valerie et al., 2007). DNA damage surveillance proteins like ATM telangiectasia mutated (ATM) kinase and ATM/Rad3-related (ATR) protein kinase phosphorylate over 700 proteins, leading to changes in downstream signaling (Nagane et al., 2021; Schmidt-Ullrich et al., 2000; Valerie et al., 2007). For example, ATM, activated by oxidative DNA damage, phosphorylates many proteins in the ERK, p38, and Jun N-terminal kinase (JNK) MAPK pathways, leading to various downstream effects (Nagane et al., 2021; Schmidt-Ullrich et al., 2000).

The response of oxidative stress on cell differentiation signaling has been studied extensively in disease. Here presented are examples relevant to a few cell types related to bone loss. Many other pathways are plausible but available research has highlighted these to be critical to disease.

Oxidative stress can induce signaling changes in the Wnt/β-catenin pathway, the RANK/RANKL pathway, the Nrf2/HO-1 pathway, and the MAPK pathways (Domazetovic et al., 2017a; Manolagas & Almeida, 2007; Tian et al., 2017).

The mechanisms of oxidative stress leading to cell differentiation signaling may be different for each pathway. For example, ROS-induced MAPK activation can be initiated through Ras-dependent signaling. Firstly, oxygen radicals mediate the phosphorylation of upstream epidermal growth factor receptors (EGFRs) on tyrosine residues, resulting in increased binding of growth factor receptor-bound protein 2 (Grb2) and subsequent activation of Ras signaling (Lehtinen & Bonni, 2006). Direct inhibition of MAPK phosphatases with hydroxyl radicals also activates this pathway (Li et al., 2013). In another mechanism, ROS competitively inhibit the Wnt/β-catenin pathway through the activation of forkhead box O (FoxO), which are involved in the antioxidant response and require binding of β-catenin for transcriptional activity (Tian et al., 2017).

Empirical Evidence

A few studies demonstrate greater changes to oxidative stress than to altered signaling. Microgravity exposure to preosteoblast cells showed a 0.24-fold decrease to the antioxidant Cu/Zn-superoxide dismutase (SOD) and a 0.36-fold decrease to p-Akt (Yoo et al., 2016). Bai et al. (2020) also demonstrated with multiple endpoints that ROS levels increased, and antioxidant enzyme levels decreased more than signaling pathways were altered.

Dose Concordance:

Many studies demonstrate dose concordance for this relationship, at the same doses. After simulated microgravity, changes to signaling pathways, increased ROS and MDA, and decreased antioxidants were found both in *in vitro* mouse-derived bone cells and in *in vivo* rat femurs. In Bone marrow mesenchymal stem cells (BM-MSCs) exposed to 0, 6 and 16 Gy of Co-60 gamma rays, ROS levels increased concurrently with decreased β-catenin expression levels when compared to controls (Zuo et al. 2019). Increased ROS levels and decreased antioxidants were found with changes in the RANK/RANKL pathway, Wnt/β-catenin pathway, Runx2, and MAPK pathways (Diao et al., 2018; Sun et al., 2013; Xin et al., 2015; Yoo et al., 2016). Osteocyte-like cells (MLO-Y4) treated with 20, 40 and 80 μM of ferric ammonium citrate (FAC) had increased ROS levels of 1.5-folds, 2-folds and 2.5-folds compared to the control respectively, and increased RANKL/β-actin expression levels (~1.8, 3.5 and 5.5-folds compared to the control respectively) (Ma et al. (2022)).

A few studies also find that oxidative stress often occurs at lower doses than altered cell differentiation signaling. Bai et al. (2020) measured oxidative stress, shown by increased ROS and decreased antioxidant expression, at 2, 5, and 10 Gy of gamma rays. They also found Runx2 increased at the same doses, but the p53/p21 pathway was only significantly altered at 5 and 10 Gy (Bai et al., 2020). At similar doses, X-ray irradiated mouse osteoblast-like cell line MC3T3-E1 cells showed increased ROS and decreased antioxidants both 4 and 8 Gy (Kook et al., 2015). While HO-1 also increased at both 4 and 8 Gy, Nrf2 and Runx2 were measured altered at 8 Gy (Kook et al., 2015).

Time Concordance

Limited evidence shows that oxidative stress leads to altered signaling pathways in a time-concordance manner. When irradiated with X-rays and MC3T3-E1 osteoblast-like cells show increase in ROS or levels of protein carbonylation, or a decrease in the levels of superoxide dismutase (SOD), catalase (CAT), GSTO1 or glutathione (GSH) at earlier timepoints than alterations in the signaling molecules p16, p21, Ceramide, Runx2, and HO-1 (Kook et al., 2015). The molecular-level changes occur quickly after irradiation. In human osteoblast-like SaOS-2 cells treated with various concentrations of butionine sulfoximine (BSO), GSH levels showed a significant decrease compared to the control 0, 3 and 6 days post treatment. The treated cells concurrently demonstrated a significant decrease of RANKL/OPG levels at 0, 3 and 6 days post treatment (Romagnoli et al., 2013). In another study, starved MLO-Y4 osteocyte-like cells demonstrated that both H2O2 and RANKL significantly increased 24 hours post starvation treatment when compared to controls (Fontani et al. (2015)).

Essentiality

Several studies have investigated the essentiality of the relationship, where the blocking or attenuation of the upstream KE causes a change in frequency of the downstream KE. Antioxidants (N-acetyl cysteine, curcumin) were shown to restore or reduce ROS levels closer to control levels following radiation or microgravity exposure, respectively. Signaling proteins in the RANKL/osteoprotegerin (OPG) ratio were decreased and brought closer to control levels (Kook et al., 2015; Xin et al., 2015). Hydrogen rich medium showed reduced ROS with restoration of RANKL signaling levels to controls (Sun et al., 2013). Polyphenol S3 (60 mg/kg/d) treatment was found to reverse the effect of microgravity on CAT, SOD and MDA, returning the levels to near control values. Meanwhile, Runx2 mRNA levels and β-catenin/β-actin levels increased following treatment (Diao et al., 2018). It was observed when treated with butionine sulfoximine (BSO), a specific inhibitor of γ-glutamylcysteine synthetase, GSH levels were significantly decreased for all days compared to the control and RANKL/OPG were significantly increased for all days (0, 3, 6 days) relative to the control (Romagnoli et al. 2013).

Uncertainties and Inconsistencies

- MAPK pathways can exhibit varied responses after exposure to oxidative stress. The expected response is an increase in the activity of the ERK, JNK, and p38 pathways as protein phosphatases, involved in the inactivation of MAPK pathways, are deactivated by oxidative stress (Valerie et al., 2007). Although some studies show a decrease (Yoo et al., 2016).
- The assays employed in studies to assess the KEs may lead to variations in the quantitative understanding of observations.

Quantitative Understanding of the Linkage

The table below provides some representative examples of quantitative linkages between the two key events. It was difficult to identify a general trend across all the studies due to differences in experimental design and reporting of the data. All reported findings are statistically significant at various alpha levels as listed in the original sources

Response-response relationship

Dose/Incidence Concordance

Reference	Experiment Description	Result
Kook et al., 2015	In vitro. MC3T3-E1 osteoblast-like cells were irradiated with 2, 4, and 8 Gy of X-rays (1.5 Gy/min). ROS were measured with a fluorescent probe, and SOD, CAT, and GSH antioxidant activities were determined with assay kits. Protein levels in the Nrf2/HO-1 signaling pathway were determined by either western blot or RT-PCR.	ROS increased linearly at 2 and 4 Gy up to 1.4-fold at 8 Gy (significant changes at 4 Gy and 8 Gy). GSH and SOD were decreased 0.7-fold at 4 Gy and 0.5-fold at 8 Gy (insignificant increases at 2 Gy). CAT was also decreased but not significantly. HO-1 increased 3.3-fold after 4 Gy and 4.9-fold after 8 Gy (insignificant increase at 2 Gy). Nrf2 increased 2.3-fold after 8 Gy. Runx2 mRNA was decreased 0.5-fold after 8 Gy.

Bai et al., 2020	In vitro. Rat-derived bone marrow-derived mesenchymal stem cells (bmMSCs) were irradiated with 2, 5, and 10 Gy of ^{137}Cs gamma rays. Mitochondrial and cellular ROS levels were determined with fluorescent probes. RT-qPCR was performed to measure antioxidant enzyme expression. Protein expression in various signaling pathways was measured by western blot.	Mitochondrial ROS increased 1.6-fold at 2 Gy (non-significant), 2-fold at 5 Gy, and 2.3-fold at 10 Gy. Cellular ROS increased 1.2-fold at 2 Gy, 1.5-fold at 5 Gy, and 2.1-fold at 10 Gy. Antioxidants SOD1, SOD2, and CAT all decreased about 0.9-fold (ns for SOD2) after 2 Gy, 0.8- to 0.7-fold at 5 Gy, and 0.7- to 0.4-fold at 10 Gy. Runx2 decreased 0.9-fold at 2 and 5 Gy and 0.6-fold at 10 Gy. p21 increased 1.6-fold at 5 Gy and 2.5-fold at 10 Gy. p53 increased 1.6-fold at 5 Gy and 1.7-fold at 10 Gy. p16 remained unchanged.
Xin et al., 2015	In vitro and in vivo. In vitro. MC3T3-E1 osteoblast-like cells were exposed to microgravity for 96 hours. ROS were determined with a fluorescent probe and the RANK/RANKL pathway was measured using RANKL and OPG assay kits. In vivo. Male 8-week-old Sprague-Dawley rats were exposed to hind-limb suspension for 6 weeks. Femur and plasma MDA and femur sulphydryl levels were measured with assay kits and the RANK/RANKL pathway was measured in the femur using RANKL and OPG assay kits.	In vitro. ROS increased 1.5-fold and the RANKL/OPG ratio increased 1.6-fold. In vivo. Serum and femur MDA increased 1.4-fold and femur sulphydryl decreased 0.6-fold. The RANKL/OPG ratio increased 3.5-fold.
Sun et al., 2013	In vitro. MC3T3-E1 osteoblast-like cells were exposed to microgravity (0.01G) for 96 hours. ROS production was measured by a fluorescent probe. The RANKL/OPG ratio was determined by assay kit and Runx2 mRNA expression was determined by RT-qPCR	ROS increased 1.5-fold. The RANKL/OPG ratio increased 1.6-fold. Runx2 expression decreased 0.4-fold.
Yoo et al., 2016	In vitro. Preosteoblast MC3T3-E1 cells were exposed to microgravity conditions by a 3D clinostat at a speed from 1-10 rpm. Oxidative stress was measured by Cu/Zn-SOD, Mn-SOD and catalase activity. Signaling molecules, phosphorylation of the mechanistic target of rapamycin p-(mTOR), and p-ERK were measured by western blot.	Following microgravity exposure, Cu/Zn-SOD and Mn-SOD levels decreased by 0.24 and 0.65-fold, respectively. Signaling molecules p-mTOR and p-ERK decreased by 0.58-fold.
Diao et al., 2018	In vivo. The left femur of rats was studied after exposure to simulated microgravity. Oxidative stress was measured by MDA, SOD, and CAT levels. RANK/RANKL signaling pathway was measured in rat femur by enzyme-linked immunoassay detection of OPG/RANKL molecules. Signaling molecule, Runx2, mRNA levels were measured by quantitative real time PCR. The Wnt/ β -catenin pathway was measured by western blot for β -catenin protein levels.	MDA increased by 1.4-fold. SOD and CAT levels decreased by 0.4-fold. OPG/RANKL decreased by 0.6-fold. Runx2 mRNA levels decreased 0.04-fold (Fig 8d). β -catenin decreased 0.6-fold.
Ma et al., 2022	In vitro. MLO-Y4 osteocyte-like cells were treated with ferric ammonium citrate (FAC) at concentration of 20, 40 and 80 μM . ROS levels were measured with flow cytometry. RANKL/ β -actin levels were assessed with western blotting.	ROS levels increased 1.5-folds, 2-folds and 2.5-folds with each increasing dose of FAC (20, 40, 80 μM) compared to the control. RANKL/ β -actin expression levels increased approximately 1.8-folds, 3.5-folds and 5.5-folds with each increasing dose of FAC (20, 40, 80 μM) compared to the control.
Zuo et al., 2019	Ex vivo. Bone marrow mesenchymal stem cells (BM-MSCs) were isolated from 3-month-old female rats exposed to 0, 6 and 16 Gy of Co-60 gamma rays at 0.56 Gy/min. Cellular ROS was measured with a 2',7'-dichlorodihydrofluorescein diacetate (DCF-DA) stain and examined by flow cytometry. β -catenin expression levels were measured with quantitative real-time PCR, western blot and immunochemistry.	ROS levels increased significantly after 6 Gy of radiation compared to the control. β -catenin expression levels decreased after 6 Gy of radiation compared to the control.

Time-scale**Time Concordance**

Reference	Experiment Description	Result
Kook et al., 2015	In vitro. MC3T3-E1 osteoblast-like cells were irradiated with X-rays (1.5 Gy/min). ROS were measured with a fluorescent probe, and SOD, CAT, and GSH antioxidant activities were determined with assay kits. Protein levels in the Nrf2/HO-1 signaling pathway were determined by either western blot or RT-PCR.	After 1 day and 8 Gy, ROS increased 1.4-fold, GSH decreased 0.5-fold, and SOD decreased 0.5-fold. CAT was also decreased but not significantly. After 1 day and 8 Gy, Nrf2 increased 2.3-fold. After 2 days and 8 Gy, HO-1 increased 4.9-fold. After 3 days and 8 Gy, Runx2 mRNA was decreased 0.5-fold.
Romagnoli et al., 2013	In vitro. Human osteoblast-like SaOS-2 cells were treated with concentrations butionine sulfoximine (BSO). Cellular GSH protein levels were measured using bicinchoninic acid. RANKL/OPG markers were assessed with Quantitative real-time PCR.	Cells treated with BSO showed significant progressive decrease of GSH levels over the course of 6 days compared to the control group. Concurrently, levels of RANKL/OPG significantly increased with increasing days (0, 3, 6 days) compared to the control.
Fontani et al., 2015	In vitro. MLO-Y4 osteocyte-like cells were starved. Intracellular H ₂ O ₂ was measured by cell-permeant 2',7'-dichlorodihydrofluorescein diacetate, a chemically reduced form of fluorescein and analyzed by fluorescence spectrophotometric analysis. RANKL was measured using quantitative sandwich enzyme immunoassay kits.	H ₂ O ₂ significantly increased 24 hours post starvation treatment when compared to controls. Concurrently, RANKL increased significantly 24 hours post treatment when compared to controls.

Known modulating factors

Modulating factor	Details	Effects on the KER	References
Drug	N-acetyl cysteine (antioxidant)	Treatment of osteoblast-like cells with 5 mM restored ROS levels, SOD activity, and the level of proteins in the Nrf2/HO-1 pathway.	Kook et al., 2015
Drug	Curcumin (antioxidant)	Treatment of osteoblast-like cells with 4 μM reduced ROS levels and the RANKL/OPG ratio. Treatment of rats with 40 mg/kg of body weight reduced oxidative stress and the RANKL/OPG ratio.	Xin et al., 2015
Media	Hydrogen-rich (antioxidant)	Osteoblasts in a medium consisting of 75% H ₂ , 20% O ₂ , and 5% CO ₂ (vol/vol/vol) showed a reduction in ROS production and restoration of normal signaling.	Sun et al., 2013
Drug	Melatonin (antioxidant)	Treatment with 200 nM melatonin reversed the effect of microgravity on Cu/Zn-SOD and Mn-SOD to control levels.	Yoo et al., 2016
Drug	Polyphenol S3	Polyphenol S3 treatment reverses the effect of microgravity on CAT, SOD and MDA, returning the levels to near control values when S3 is used at high dose (60mg/kg/d). β -catenin/ β -actin levels increased following treatment and simulated microgravity.	Diao et al., 2018

Known Feedforward/Feedback loops influencing this KER

ROS can upregulate protein kinase C, which stimulates the production of ceramide from sphingomyelinase. Ceramide activates NADPH oxidase, which can then produce more ROS (Soloviev & Kizub, 2019). Lastly, the MAPK pathway also exhibits a feedback loop. ERK can regulate ROS levels indirectly through p22phox, which increases ROS and upregulates antioxidants by Nrf2 activation. JNK activation can lead to FoxO activation, thereby resulting in antioxidant production (Arfin et al., 2021; Essers et al., 2004).

References

Arfin, S. et al. (2021), "Oxidative Stress in Cancer Cell Metabolism", *Antioxidants* 2021, Vol. 10/5, MDPI, Basel <https://doi.org/10.3390/ANTIOX10050642>

Bai, J. et al. (2020), "Irradiation-induced senescence of bone marrow mesenchymal stem cells aggravates osteogenic differentiation dysfunction via paracrine

signaling", American Journal of Physiology - Cell Physiology, Vol. 318/5, American Physiological Society, <https://doi.org/10.1152/ajpcell.00520.2019>

Cabrera, M. P. and R. H. Chihualaf (2011), "Antioxidants and the integrity of ocular tissues", Veterinary medicine international, Vol. 2011, <https://doi.org/10.4061/2011/905153>

Diao, Y. et al. (2018), "Polyphenols (S3) isolated from Cone Scales of *Pinus koraiensis* Alleviate Decreased Bone Formation in Rat under Simulated Microgravity", Scientific Reports, Vol. 8/1, Nature, <https://doi.org/10.1038/s41598-018-30992-8>

Domazetovic, V. et al. (2017a), "Oxidative stress in bone remodeling: role of antioxidants", Clinical cases in mineral and bone metabolism, Vol. 14/2, <https://doi.org/10.11138/ccmbm/2017.14.1.209>

Fontani, F. et al. (2015), "Glutathione, N-acetylcysteine and lipoic acid down-regulate starvation-induced apoptosis, RANKL/OPG ratio and sclerostin in osteocytes: involvement of JNK and ERK1/2 signalling", Calcified tissue international, Vol. 96/4, Springer, London, <https://doi.org/10.1007/s00223-015-9961-0>

Hu, Q. et al. (2023), "JAK/STAT pathway: Extracellular signals, diseases, immunity, and therapeutic regimens", Frontiers in bioengineering and biotechnology, Vol. 11, Frontiers Media, Lausanne, <https://doi.org/10.3389/fbioe.2023.1110765>

Kharazian D. (2021), "Exposure to Environmental Toxins and Autoimmune Conditions", Integrative medicine (Encinitas, Calif.), Vol. 20/2.

Kook, S. H. et al. (2015), "Irradiation inhibits the maturation and mineralization of osteoblasts via the activation of Nrf2/HO-1 pathway", Molecular and Cellular Biochemistry, Vol. 410/1-2, Springer Nature, London, <https://doi.org/10.1007/s11010-015-2559-z>

Lehtinen, M. and A. Bonni. (2006), "Modeling Oxidative Stress in the Central Nervous System", Current Molecular Medicine, Vol. 6/8, <https://doi.org/10.2174/156652406779010786>.

Li, J. et al. (2013), "Oxidative Stress and Neurodegenerative Disorders", International Journal of Molecular Sciences, Vol. 14/12, <https://doi.org/10.3390/ijms141224438>.

Ma, J. et al. (2022), "Iron overload induced osteocytes apoptosis and led to bone loss in Hepcidin-/ mice through increasing sclerostin and RANKL/OPG", Bone, Vol. 164, Elsevier, Amsterdam, <https://doi.org/10.1016/j.bone.2022.116511>

Manolagas, S. C. and M. Almeida. (2007), "Gone with the Wnts: β -Catenin, T-Cell Factor, Forkhead Box O, and Oxidative Stress in Age-Dependent Diseases of Bone, Lipid, and Glucose Metabolism", Molecular Endocrinology, Vol. 21/11, Oxford University Press, Oxford, <https://doi.org/10.1210/me.2007-0259>

Essers, M. A. et al. (2004), "FOXO transcription factor activation by oxidative stress mediated by the small GTPase Ral and JNK". The EMBO journal, Vol. 23/24, EMBO, <https://doi.org/10.1038/sj.emboj.7600476>

Nagane, M. et al. (2021), "DNA damage response in vascular endothelial senescence: Implication for radiation-induced cardiovascular diseases", Journal of Radiation Research, Vol. 62/4, Oxford University Press, Oxford, <https://doi.org/10.1093/jrr/rrab032>

Ping, Z. et al. (2020), "Oxidative Stress in Radiation-Induced Cardiotoxicity", Oxidative Medicine and Cellular Longevity, Vol. 2020, Hindawi, London, <https://doi.org/10.1155/2020/3579143>

Ramadan, R. et al. (2021), "The role of connexin proteins and their channels in radiation-induced atherosclerosis", Cellular and Molecular Life Sciences, Vol. 78, Nature, <https://doi.org/10.1007/s00018-020-03716-3>

Riegger, Jana et al. (2023) "Oxidative stress as a key modulator of cell fate decision in osteoarthritis and osteoporosis: a narrative review", Cellular & molecular biology letters, Vol. 28/1 doi:10.1186/s11658-023-00489-y

Romagnoli, C. et al. (2013), "Role of GSH/GSSG redox couple in osteogenic activity and osteoclastogenic markers of human osteoblast-like SaOS-2 cells", The FEBS journal, Vol. 280/3, Wiley, Hoboken, <https://doi.org/10.1111/febs.12075>

Schmidt-Ullrich, R. K. et al. (2000), "Signal transduction and cellular radiation responses.", Radiation research, Vol. 153/3, BioOne [https://doi.org/10.1667/0033-7587\(2000\)153\[0245:stacr\]2.0.co:2](https://doi.org/10.1667/0033-7587(2000)153[0245:stacr]2.0.co:2)

Sinkala, M. et al. (2021), "Integrated molecular characterisation of the MAPK pathways in human cancers reveals pharmacologically vulnerable mutations and gene dependencies", Communications biology, Vol. 4/1, Springer, London, <https://doi.org/10.1038/s42003-020-01552-6>

Solov'ev, A. I. and I. V. Kizub. (2019), "Mechanisms of vascular dysfunction evoked by ionizing radiation and possible targets for its pharmacological correction", Biochemical Pharmacology, Vol. 159, Elsevier, Amsterdam, <https://doi.org/10.1016/j.bcp.2018.11.019>

Soumelis, V. and Y. J. Liu (2006), "From plasmacytoid to dendritic cell: morphological and functional switches during plasmacytoid pre-dendritic cell differentiation", European journal of immunology, Vol. 36/9, Wiley, Hoboken, <https://doi.org/10.1002/eji.200636026>

Sun, Y. et al. (2013), "Treatment of hydrogen molecule abates oxidative stress and alleviates bone loss induced by modeled microgravity in rats", Osteoporosis International, Vol. 24/3, Nature, <https://doi.org/10.1007/s00198-012-2028-4>

Tahimic, C. G. T. and R. K. Globus. (2017), "Redox Signaling and Its Impact on Skeletal and Vascular Responses to Spaceflight", International Journal of Molecular Sciences, Vol. 18/10, MDPI, Basel, <https://doi.org/10.3390/IJMS18102153>

Tian, Y. et al. (2017), "The impact of oxidative stress on the bone system in response to the space special environment", International Journal of Molecular Sciences, Vol. 18/10, MDPI, Basel, <https://doi.org/10.3390/ijms18102132>

Valerie, K. et al. (2007), "Radiation-induced cell signaling: inside-out and outside-in", Molecular Cancer Therapeutics, Vol. 6/3, American Association for Cancer Research, <https://doi.org/10.1158/1535-7163.MCT-06-0596>

Villalpando-Rodriguez, G. E. and S. B. Gibson (2021), "Reactive Oxygen Species (ROS) Regulates Different Types of Cell Death by Acting as a Rheostat", Oxidative medicine and cellular longevity, Vol. 2021, John Wiley & Sons, Hoboken, <https://doi.org/10.1155/2021/9912436>

Wu, H. et al., (2023), "Molecular mechanisms of environmental exposures and human disease. Nature reviews" Genetics, Vol. 24/5, Springer, London, <https://doi.org/10.1038/s41576-022-00569-3>

Xin, M. et al. (2015), "Attenuation of hind-limb suspension-induced bone loss by curcumin is associated with reduced oxidative stress and increased vitamin D receptor expression", Osteoporosis International, Vol. 26/11, Nature, <https://doi.org/10.1007/s00198-015-3153-7>

Yoo, Y. M., T. Y. Han and H. S. Kim. (2016), "Melatonin suppresses autophagy induced by clinostat in preosteoblast MC3T3-E1 cells", International Journal of Molecular Sciences, Vol. 17/4, MDPI, Basel, <https://doi.org/10.3390/ijms17040526>

Zuo, R. et al. (2019), "BM-MSC-derived exosomes alleviate radiation-induced bone loss by restoring the function of recipient BM-MSCs and activating Wnt/ β -catenin signaling", Stem cell research & therapy, Vol. 10/1, Springer, London, <https://doi.org/10.1186/s13287-018-1121-9>

Relationship: 2842: Increase, Cell death leads to Altered Bone Cell Homeostasis

AOPs Referencing Relationship

AOP Name	Adjacency	Weight of Evidence	Quantitative Understanding
Deposition of energy leading to occurrence of bone loss	adjacent	High	Low

Evidence Supporting Applicability of this Relationship

Taxonomic Applicability

Term	Scientific Term	Evidence	Links
human	Homo sapiens	Low	NCBI
mouse	Mus musculus	Moderate	NCBI
rat	Rattus norvegicus	Moderate	NCBI

Life Stage Applicability**Life Stage Evidence**

Adult	Moderate
Juvenile	Low
Sex Applicability	
Sex	Evidence
Male	Low
Female	Low
Unspecific	Moderate

The evidence for the taxonomic applicability to humans is low as majority of the evidence is from *in vitro* human-derived cells. The relationship is supported by mice and rat models using male and female animals. The relationship is plausible at any life stage. However, most studies have used adult animal models.

Key Event Relationship Description

With respect to bone, an increase in cell apoptosis can overwhelm bone homeostasis leading to the release of pro-inflammatory factors, such as tumor necrosis factor (TNF)- α , interleukin (IL)-6, and IL-1, that can promote disbalance of bone homeostasis (Fadeel & Orrenius, 2005). For example, increased apoptosis of osteocytes can lead to increased bone resorption and decreased bone deposition. Although the exact mechanism is still debated, it is believed that apoptotic osteocytes release various osteoclast stimulatory factors, such as the receptor activator of nuclear factor kappa B ligand (RANKL), upon death. Neighbouring viable osteocytes also release signals to recruit macrophages/pre-osteoclasts to stimulate osteoclastogenesis, leading to increased bone resorption locally (Jilka, Noble, and Weinstein, 2013; Komori et al., 2013; Plotkin, 2014). Additionally, some studies suggest osteoblast apoptosis may augment bone resorption as the pool of active osteoblasts is reduced and unable to counteract the activity of osteoclasts (Xiong et al., 2013).

Evidence Supporting this KER

Overall weight of evidence: High

Biological Plausibility

The biological rationale for the connection of cell death and altered bone cell homeostasis is well-supported in the literature. Bone homeostasis is regulated by the balanced action of bone-forming osteoblasts and bone-resorbing osteoclasts and by the action of osteocytes, the "mechano-sensing cells" in the compact bone. Research has shown that osteocyte apoptosis-induced bone resorption plays a role in regulating bone homeostasis/bone mass (Komori, 2013). Briefly, apoptotic osteocytes release of osteoclast stimulatory factors that recruit pre-/osteoclasts locally to the apoptotic cell (Jilka, Noble, and Weinstein, 2013; Komori, 2013; O'Brien, Nakashima, and Takayanagi, 2013; Plotkin, 2014; Xiong and O'Brien, 2012). Further osteoblast death may impair bone formation as the pool of active bone-forming osteoblasts decreases.

Regardless of if cells undergo apoptosis or autophagy, death is completed with the removal of the cells through engulfment by scavengers. In these cases, the cells are quietly removed without inflammation, because the integrity of the cytoplasmic membranes is maintained when phagocytosis occurs. In the case of apoptotic osteocytes, scavengers cannot reach osteocytes that are embedded in the compact bone and, thus, any type of osteocyte death will end in the rupture of the cytoplasmic membrane (Komori, 2013). After cell rupture, immunostimulatory factors are released to the bone surface and vascular channels and facilitate the recruitment and activation of macrophages, thereby promoting the production of proinflammatory cytokines that in turn facilitates osteoclastogenesis and bone resorption (Komori, 2013). The relationship between osteocyte apoptosis and increased local bone resorption has been verified by studies showing co-localization of apoptotic osteocytes and recruited osteoclasts, blockade of osteocyte apoptosis reduced bone resorption, and osteocyte apoptosis preceding osteoclast recruitment (Jilka, Noble, and Weinstein, 2013; O'Brien, Nakashima, and Takayanagi, 2013; Plotkin, 2014; Xiong et al., 2013). However, the exact mechanism how apoptotic osteocytes recruit osteoclasts is still debated.

It has been shown that after rupture of the plasma membrane of dead osteocytes immunostimulatory factors such as high-mobility group box 1 (HMGB1) are released, facilitating the recruitment and activation of macrophages, thereby promoting the production of proinflammatory cytokines such as TNF- α , IL-6 and IL-1. IL-6 and IL-1 induce RANKL expression, that in turn facilitates osteoclastogenesis and bone resorption (Jilka, Noble, and Weinstein, 2013; Komori, 2013). Other studies, however, propose that apoptotic osteocytes signal to viable osteocytes in their vicinity to express high ratios of RANKL/OPG (RANKL being the main stimulator of osteoclastogenesis and OPG, osteoprotegerin, its inhibitor) and other pro-osteoclastogenic factors that directly stimulate osteoclast recruitment and enhance the production of mature osteoclasts (O'Brien, Nakashima, and Takayanagi, 2013; Plotkin, 2014).

Autophagy is part of the regulation process of osteoclast differentiation and function and thus linked to bone resorption. Regarding bone resorption, osteoclasts encounter a low oxygen tension in their local environment as they are living at the surface and interior parts of the bone (Shapiro et al., 2014). Different studies have reported that hypoxia via activation of HIF-1 α (hypoxia inducing factor-1 α) enhances osteoclast differentiation and activity along with autophagic flux (Knowles and Athanasou, 2009). HIF-1 α induces the expression of its downstream target BNIP3, which stimulates Beclin-1 release, increases the expression level of autophagic-related genes such as ATG5 and ATG12, recruits LC3 to autophagosome, and enhances the expression of osteoclast genes (nuclear factor of activated T cells 1 (NFATc1), tartrate-resistant acid phosphatase (TRAP), Cathepsin K (CTSK), and matrix-metalloproteinases (MMPs)) (Zhao et al., 2012). It also has been shown that upon activation of the osteoclast receptor RANK, by osteoblast-secreted and osteocyte-secreted RANKL, leads to the recruitment of TRAF6 and an increase of Beclin-1 and ATG5/7/12 with enhanced activation of LC3. Further, formed autophagosomes and lysosomes are directed to the ruffled border where bone resorption takes place (Chatziravdeli et al., 2019; Lacombe, Karsenty, and Ferron, 2013).

Empirical Evidence

The empirical data obtained for this KER strongly supports a link between apoptosis and altered bone cell homeostasis. This evidence comes from studies examining the effects of microgravity exposure and various forms of ionizing radiation, including gamma rays and X-rays, which directly induced apoptosis of bone cells and resulted in a dose-dependent increase in bone resorption and a dose-dependent decrease in bone formation (Aguirre et al., 2009; Chandra et al., 2017; Chandra et al., 2014; Huang et al., 2019; Huang et al., 2018; Li et al., 2020; Li et al., 2015; Liu et al., 2018; Wright et al., 2015).

Incidence concordance

There is some evidence that cell death increases more than bone cell homeostasis is altered following a stressor. *In vivo* osteoblast apoptosis in rats increased 7-fold while osteoblast numbers decreased 0.25-fold after irradiation with 8 Gy of X-rays (Chandra et al., 2014). Similarly, mice irradiated with 8 Gy of X-rays showed a 4-fold increase in osteoblast apoptosis and a 0.5-fold decrease in osteoblast number (Chandra et al., 2017). *In vitro*, human bone marrow-derived mesenchymal stem cells (hBMSCs, osteoblast precursors) irradiated with 8 Gy of X-rays showed a 3-fold increase in apoptosis and osteoblasts subsequently had a 0.5-fold decrease in alkaline phosphatase (ALP) activity (Liu et al., 2018). Huang et al. (2019) showed very similar results in rats with a 4-fold increase in osteoblast apoptosis and a 0.3-fold decrease in ALP activity after irradiation with 2 Gy of gamma rays. Osteoblast irradiated with gamma rays at 10 Gy showed a 3-fold increase in caspase-3 and a 0.7-fold decrease in ALP activity (Li et al., 2015).

Dose Concordance

Current literature provides evidence suggesting a dose concordance relationship between cell death of bone cells and altered bone cell homeostasis. Studies examining the effects of microgravity exposure on osteocytes *in vivo* have found a significantly increased number of empty lacunae suggesting significantly enhanced osteocyte apoptosis; which coincided with increased osteoclast number/activity and decreased osteoblast number/activity (Aguirre et al., 2009; Yang et al., 2020).

A similar trend was observed in radiation studies of 2-10 Gy X-rays, finding dose-dependent increases in empty lacunae, indicating enhanced osteocyte apoptosis under radiation exposure. The increased apoptosis of osteocytes was accompanied by significant dose-dependent increases in measures of osteoclastogenesis and decreased measures of osteoblastogenesis (Chandra et al., 2014; Wright et al., 2015).

Many studies also examine the dose-concordance relationship between apoptosis of osteoblasts/osteoclasts and altered bone cell homeostasis under microgravity and radiation exposure. Evidence from microgravity exposures, although limited, also support the relationship. Studies show profound increases in osteoblast apoptosis in vitro, as examined by various measures, including Annexin V with FITC/PI and terminal deoxynucleotidyl transferase dUTP nick end labeling (TUNEL) stain, as well as significant increases in cleaved caspases, in-situ nick-end labeling (ISEL) or the ratio of B-cell lymphoma (Bcl)-2 to Bcl-2 associated X protein (Bax). Following microgravity, an increase in cell death in addition to an increase in osteoclast number (Aguirre et al., 2006) or TRAP-positive cells (Wu et al., 2020) and a decrease in ALP activity, a marker of bone deposition, as well as increases in measures of osteoclast bone resorption were observed (Yang et al., 2020). Data on gamma and X-ray radiation-induced osteoblast apoptosis is plentiful, with most studies examining the effects of high doses of ionizing radiation (> 2 Gy). Murine models exposed to high-dose X-ray radiation have shown increased osteoblast apoptosis under 8-12 Gy with accompanying decreased osteoblast and increased osteoclast activity (Chandra et al., 2017; Chandra et al., 2014; Liu et al., 2018). Relatively lower dose studies (0.25-4 Gy) have found significant increases in osteoblast apoptosis resulting in a decrease in ALP activity (Huang et al., 2019; Li et al., 2020; Li et al., 2015).

One study of osteoclast apoptosis under radiation exposure has also revealed interesting results, observing significantly increased apoptosis of osteoclasts, but with enhanced osteoclast activity and bone resorption (Huang et al., 2018). It is proposed that osteoclast apoptosis results in the recruitment macrophages that release inflammatory molecules that directly activate osteoclasts and induce RANK-L expression, ultimately increasing the overall pool of osteoclasts in bone (Huang et al., 2018).

A study performed in osteoblasts observed significant increases in autophagy induction under ionizing radiation exposure, with decreased osteoblast activity (Li et al., 2020).

Time Concordance

A moderate amount of evidence exists in the current literature suggesting a time concordance relationship between apoptosis and altered bone cell homeostasis. Increases in osteoblast and osteocyte apoptosis has been observed as early as 24-72 hours post-irradiation, and as early as day 3 of microgravity exposure. The resulting effects on bone cell homeostasis under microgravity exposure have been observed by days 3-7, and under radiation exposure as early as 3 days post-exposure, indicating a slight delay in the loss of homeostasis after onset of apoptosis (Aguirre et al., 2006; Li et al., 2020; Wright et al., 2015; Yang et al., 2020).

Essentiality

Studies examining the effects of various countermeasures to apoptosis and autophagy of osteoblasts, osteoclasts, and osteocytes suggest a strong relationship between the occurrence of cell death and altered bone cell homeostasis. 1-34 amino-terminal fragment of parathyroid hormone (PTH)1-34 is used to treat osteoporosis by stimulating both osteoblast and osteoclast activity, but with greater stimulation of osteoblasts; it can increase bone deposition by suppressing apoptosis of mature osteoblasts. In a study of the effects of PTH1-34 treatment in mouse tibial bones exposed to 8 Gy X-ray radiation, PTH1-34 was found to fully reverse the effect of radiation on both osteoblast and osteocyte cell death and enhance overall osteoblast number under radiation exposure to vehicle-treated unirradiated controls (Chandra et al., 2014).

α -2-macroglobulin (α 2M) is a macromolecular glycoprotein found in plasma that possesses a wide range of biological functions, including radioprotective and anti-inflammatory effects. Treatment of 12 Gy X-ray irradiated hBMMSCs (osteoblast precursors), with 0.25-0.5 mg/mL of α 2M was found to dose-dependently decrease cell apoptosis rate of hBMMSCs, as well as dose-dependently increased ALP activity, indicating increased induction of osteoblastogenesis in these cells, and bone deposition, as demonstrated by Alizarin red staining for calcium nodule formation (Liu et al., 2018). Another radioprotective compound known to promote healing in bone fractures is Amifostine (AMI), which protects cells from radiation-induced DNA damage by preventing interaction with reactive oxygen species. In vitro research with bone marrow-derived mesenchymal stem cells (bmMSCs) found that treatment with AMI fully reversed apoptosis induction under 2 Gy gamma radiation, as measured by Annexin V FITC/PI double staining, and ultimately restored ALP activity and calcium deposition by osteoblasts to control levels (Huang et al., 2019).

Glucocorticoids (GCs) are known to induce devastating effects on bone mass and density by decreasing bone remodeling; the mechanism by which this occurs is through suppression of osteoblast differentiation and induction of osteoblast apoptosis. In a study examining transgenic mice, blocking GC signaling of hindlimb unloaded mice was found to fully reverse the effect of microgravity on osteoblast and osteocyte apoptosis, as well as decreasing the production of RANK-L by osteocytes. GC signaling blockade was also found to fully protect the decrease in osteoblast number observed in unloading and restore markers of osteoblast activity, as well as diminish markers of osteoclastogenesis and osteoclast number (Yang et al., 2020).

MicroRNAs (miRNA) are a well-known tool for epigenetically modifying gene expression; many studies have shown that miRNAs may be implicated in bone cell differentiation and suppression of disease osteopenia through various mechanisms. MiR-655-3p is a miRNA that has been proposed to prevent the induction of osteopenia in simulated microgravity. Inhibition of miR-655-3p was found to profoundly enhance osteoblast apoptosis and decrease ALP activity; microgravity-exposed cells treated with miR-655-3p were fully protected against microgravity-induced apoptosis, and had ALP activity fully restored, indicating microgravity-induced apoptosis of osteoblasts may play a role in decreased bone deposition (Wang et al., 2020b).

One study found that inhibition of autophagy after microgravity reduces osteoclast activity. Both 4-acetylantroquinonol B (4-AAQB) and 3-methyladenine (3-MA) can inhibit autophagy induction. Treatment of osteoclasts with these autophagy inhibitors results in reduced osteoclast activity (Wu et al., 2020).

Treatment of irradiated osteoblasts with doxycycline, an antibiotic compound that inhibits autophagy, was found to fully reverse the increased expression of autophagy proteins ATG5, Beclin-1, and LC3-II/LC3-I, while also substantially increasing ALP activity under 0.25-4 Gy radiation (Li et al., 2020). Similarly, treatment with α -2-macroglobulin, a glycoprotein with diverse cellular functions, was found to reverse radiation-induced autophagy induction and increase ALP activity, restoring them to near-control levels (Liu et al., 2018). These results suggest autophagy induction in osteoblasts may also play a role in the suppression of bone deposition observed under radiation exposure.

Uncertainties and Inconsistencies

- The exact mechanism by which apoptotic osteocytes recruit osteoclasts is disputed. Some studies support the notion that apoptotic osteocytes in bone cannot be engulfed by phagocytes, due to physical restriction, and thus allow for rupture of the cell membrane; this allows for the release of a variety of osteoclast stimulatory factors that directly enhance bone resorption (Jilka, Noble, and Weinstein, 2013; Komori et al., 2013). Other studies, however, propose that dying osteocytes signal to viable osteocytes in their vicinity to release osteoclast stimulatory molecules, which then enhance osteoclast activity (O'Brien, Nakashima, and Takayanagi, 2013; Plotkin, 2014). Further research in this area may aid in elucidating the mechanisms of osteoclast recruitment directed to apoptotic osteocytes.

Quantitative Understanding of the Linkage

The following are a few examples of quantitative understanding of the relationship. All data is statistically significant unless otherwise indicated.

Response-response relationship

Dose/Incidence Concordance- Apoptosis

Reference	Experiment Description	Result
Aguirre et al., 2006	In vivo. Female Swiss Webster mice (C57BL/6 genetic background) were suspended via their tail to stimulate microgravity conditions. Bone resorption was determined by evaluating osteoclast number. Osteocyte and osteoblast apoptosis were detected.	Following tail suspension of mice, significant increases in osteocyte and osteoblast apoptosis were observed by day 3. There was a maximum increase of ~2.3-fold and ~1.8-fold in cortical and cancellous osteocyte apoptosis, respectively, on day 7. A ~2.6-fold increase in osteoblast apoptosis was measured at day 3 and sustained until day 7. This was associated with a significant 0.53-fold decrease in osteoblast number on day 3, which was restored to above controls on day 18 as it increased by 1.9-fold compared to the group without tail suspension. A 4.6-fold increase was observed in osteoclast number on day 18 relative to controls.

Yang et al., 2020	In vitro. Male 14-week-old wildtype and transgenic mice (CD1 background) were unloaded using tail suspension. Apoptosis was measured by TUNEL staining. Bone blood serum markers were measured via enzyme-linked immunosorbent assay (ELISA) for osteocalcin (OCN) as an indicator for bone formation, and TRAP-5b as an indicator for bone resorption. In bone sections, osteoclasts and osteoblasts were identified by hematoxylin, eosin and TRAP staining.	Hindlimb unloaded wildtype mice had an overall ~2.7-fold increase in osteocyte apoptosis, as well as a 3-fold increase in osteoblast apoptosis after 7 days of unloading. At day 7 and 28, significantly reduced number of osteoblasts (~0.3-fold and ~0.7-fold) was found in conjunction with reduced ALP (~0.4-fold and ~0.6-fold) gene expression. Further, serum marker OCN was significantly reduced (~0.5-fold and ~0.6-fold) at both time points indicating impaired bone formation. In contrast, at day 7 and 28, significantly increased number of osteoclasts (~13-fold and ~2.1-fold) was found in conjunction with increased cathepsin K (~8-fold and ~4.3-fold) gene expression. Further, serum marker TRAP5b was significantly increased (~3.5-fold and ~2-fold, respectively) at day 7 and 28 indicating increased bone resorption.
Wright et al., 2015	In vivo. The right hindlimbs of 20-week-old male C57Bl/6 mice were irradiated with 2 Gy of X-rays at a rate of 1.6 Gy/min. Apoptotic osteocytes were measured by TUNEL. Osteoclast number was determined by TRAP stain.	In vivo. 2 Gy X-ray exposure resulted in a 2.5-fold increase in percentage of apoptotic osteocytes in trabecular bone. Osteoclast number increased significantly by ~1.8-fold after 2 Gy irradiation in the right hindlimb.
	In vitro. Osteocyte-like cells (MLO-Y4) and osteoblast cells (MC3T3) were irradiated with 0-20 Gy X-rays. Annexin V was used as a marker of cellular apoptosis.	In vitro, exposure to increasing doses of radiation from 0-20 Gy led to a linear dose-dependent increase in osteocyte apoptosis (MLO-Y4 cell culture) up to ~13.7-fold above controls at 20 Gy. Osteoblast apoptosis (MC3T3 cell culture) similarly increased in a dose-dependent fashion from 4-20 Gy, with a maximum increase of ~2.5-fold at 20 Gy (only significant increase). Osteoclasts increased significantly in MLO-Y4 coculture at 8 Gy, and calvarial osteoblasts decreased by ~0.5-fold at 10 Gy.
Chandra et al., 2014	In vivo. 4-month-old female rats were irradiated with 16 Gy of small animal radiation research platform (SARRP) X-rays, fractionated into two 8 Gy doses at a rate of 1.65 Gy/min. TUNEL staining in tibial trabecular bone was performed to determine osteoblast apoptosis. Osteoblast number was determined using static histomorphometry.	Exposure to 16 Gy X-rays increases osteoblast apoptosis by ~7-fold and resulted in a ~0.25-fold decrease in osteoblast number. A significant decrease in osteoclast surface was also observed and is inconsistent with other radiation studies. The authors suggest the imbalance of radiation effects may lead to relatively higher osteoclast activity compared to osteoblast activity, leading to overall bone resorption.
Chandra et al., 2017	In vivo. Male C57BL/6 mice (8-10 weeks) were exposed to 8 Gy X-ray radiation at a rate of 1.65 Gy/min. Apoptosis was determined with a TUNEL assay. Osteoblast number was determined by static histomorphometry.	8 Gy radiation exposure led to a ~3.9-fold increase in the number of TUNEL-positive osteoblasts and a ~0.5-fold decrease in osteoblast number.
Liu et al., 2018	In vitro. hBMSCs were irradiated with 8 Gy of X-rays at a rate of 1.24 Gy/min. Apoptosis was measured with using an Annexin V-FITC staining kit. ALP activity was determined with a kit, and bone deposition was determined by Alizarin red staining.	Apoptosis rate of osteoblast precursor cells (hBMSCs) exposed to 8 Gy X-ray radiation increased ~3-fold, resulting in a ~0.5-fold decrease in ALP activity and bone deposition, as measured by optical density of calcium nodules.
Huang et al., 2019	Ex vivo. bmMSCs from the tibiae and femur of rats were irradiated with 2 Gy of 60Co gamma rays at a rate of 0.83 Gy/min. Apoptosis was determined with Annexin V staining. bmMSCs were analyzed for changes in bone cell function following irradiation through measuring levels of ALP.	Exposure to 2 Gy gamma radiation resulted in a ~4-fold increase in osteoblast apoptosis and led to a significant ~0.3-fold decrease in ALP activity.
Li et al., 2020	In vitro. Osteoblastic MC3T3-E1 cells of mice were irradiated with 0.25, 0.5, 1, 2, or 4 Gy of X-ray radiation. Apoptosis was determined by the Bcl-2/Bax ratio through western blot as well as caspase-3 activity with an assay kit. ALP activity was determined with an assay kit.	X-ray radiation exposure resulted in a significant, dose-dependent decrease in the Bcl-2/Bax ratio at 0-4 Gy with a maximum decrease of ~0.6-fold below controls at 4 Gy, indicating a significant shift of osteoblasts towards apoptosis. There was also a dose-dependent increase in caspase-3 activity at 0.5-4 Gy with significant increases at 0.5 Gy and greater and a maximum increase of 1.6-fold above controls at 4 Gy. This was accompanied by a dose dependent linear decrease in ALP activity with significant decreases at 0.5 Gy and greater, and a maximum decrease of ~0.3-fold below controls at 4 Gy.
Li et al., 2015	In vitro. Calvarial osteoblasts of Male rats were irradiated using 0, 1, 2, 5, 10 Gy of 137Cs gamma rays at a rate of 0.76 Gy/min. Reverse transcription quantitative polymerase chain reaction (RT-qPCR) was used to determine caspase-3 levels and apoptosis was measured by Annexin v fluorescence. ALP activity was determined to measure osteoblastogenesis.	Osteoblasts exposed to 1-10 Gy radiation observed an exponential dose-dependent increase in caspase-3 with significant increases at 5 and 10 Gy and a maximum increase of 3-fold above controls at 10 Gy. A maximum increase in osteoblast apoptosis was observed under 2 Gy at ~1.6-fold above control, with the first significant increase at 1 Gy. This resulted in a roughly inverse-exponential dose-dependent decrease in ALP activity down to ~0.7-fold below controls at 10 Gy, with the first significant increase at 5 Gy.
Huang et al., 2018	In vitro. Murine RAW264.7 macrophage cells were irradiated with 2 Gy of gamma rays at a rate of 0.83 Gy/min. Annexin V-FITC/PI was used as a measure for apoptosis. TRAP staining was used to determine osteoclast differentiation.	Exposure of RAW264.7 osteoclast cells to 2 Gy gamma radiation had a 5.26-fold increase in apoptosis percentage, from 1.86% to 9.78%. This resulted in a 2-fold increase in TRAP-stained cell number and 2.4-fold increase in total resorption area.

Dose/Incidence concordance- Autophagy

Reference	Experiment Description	Result
Li et al., 2020	In vitro. Osteoblastic MC3T3-E1 cells of mice were irradiated with 0.25, 0.5, 1, 2, and 4 Gy of X-ray radiation. Autophagy markers were determined by western blot. ALP activity was determined by an assay kit.	X-ray irradiation of osteoblasts linearly and dose-dependently increased LC3II/LC3I protein expression up to ~2.5-fold above controls under 1 Gy, after which it remained consistently elevated under 2 and 4 Gy. There were also dose-dependent increases in ATG5 and Beclin-1 up to ~1.75- and 3-fold above controls under 4 Gy, respectively. These increases in markers of autophagy induction were accompanied by substantial, dose-dependent inverse-exponential decrease in ALP activity down to 0.3-fold below control levels under 2 Gy.

Time-scale**Time Concordance**

Reference	Experiment Description	Result
Aguirre et al., 2009	In vivo. Female Swiss Webster mice (C57BL/6 genetic background) were suspended via their tail to stimulate microgravity conditions. Bone homeostasis (biomechanical testing, bone histomorphometry) was assessed in lumbar vertebra (L1-L5). Bone resorption was determined by evaluating osteoclast number. Osteocyte and osteoblast apoptosis were detected by ISEL.	Hindlimb unloading of mice led to significant increase in cortical and trabecular osteocyte apoptosis and osteoblast apoptosis on day 3 of unloading, which remained increased up to day 18. Control mice had an increase in osteoblast apoptosis on day 18 such that the increased apoptosis under unloading conditions was non-significant on that day. Osteoblast number was significantly decreased by day 3 of unloading, returned to control levels by day 7, and surpassed controls by 2-fold on day 18. Significantly increased osteoclast number was not observed until day 18 of unloading.

Yang et al., 2020	In vitro. Male 14-week-old wildtype and transgenic mice (CD1 background) were unloaded using tail suspension. The tibia were scanned via micro-CT at 28 days after un-loading. Apoptosis was measured by TUNEL staining. Bone blood serum markers were measured via ELISA for OCN as indicator for bone formation, and TRAP-5b as indicator for bone resorption. In bone sections osteoclasts and osteoblasts were identified by hematoxylin, eosin and TRAP staining.	On day 7 of unloading, ALP decreased ~0.4-fold and OCN decreased ~0.5-fold, while TRAP-5b increased ~3.5-fold, indicating enhanced osteoclast activity and decreased osteoblast activity. This was further shown by a ~13-fold increase in osteoclast number and 3.7-fold decrease in osteoblast number on day 7 of unloading. On day 28 of unloading, there were further decreases in osteoblastogenesis markers (~0.6-fold decrease in ALP activity and 0.6-fold decrease in OCN expression), and an overall 3-fold decrease in osteoblast number.
Wright et al., 2015	In vivo. The right hindlimbs of 20-week-old male C57Bl/6 mice were irradiated with 2 Gy of X-rays at a rate of 1.6 Gy/min. Apoptotic osteocytes were measured by TUNEL. Osteoclasts and osteoblasts as measures of altered bone cell homeostasis were determined by TRAP. In vitro. Osteocyte-like cells (MLO-Y4) and osteoblast cells (MC3T3) were irradiated with 2-20 Gy X-rays. Annexin V was used as a marker of cellular apoptosis.	Osteocyte and osteoblast apoptosis under in vitro simulated microgravity was increased by ~2-3-fold by day 7 of unloading. Significant decreases in several markers of osteoblastogenesis were observed on day 7, which were attenuated relative to contemporaneous controls on day 28. A similar trend was observed for osteoclastogenesis. In vitro radiation exposure of osteocytes (MLO-Y4) resulted in significant increases in apoptosis by 24 hours post-exposure, which increased several-fold by 48 hours. Osteoblast (MC3T3) apoptosis was also increased by 24 hours post-irradiation and remained increased up to 48 hours. Calvarial osteocyte apoptosis was not increased until 10 days post-irradiation. In vivo radiation exposure resulted in significant increase in hindlimb trabecular osteocyte apoptosis at 7 days post-irradiation. Significantly increased osteoclast number was observed at around the same time at 1 week post-irradiation, however, no significant changes in osteoblast number were observed.
Li et al., 2020	In vitro. Osteoblastic MC3T3-E1 cells of mice were irradiated with 0.25, 0.5, 1, 2, or 4 Gy of X-ray radiation. Apoptosis was determined by the Bcl-2/Bax ratio through western blot as well as caspase-3 activity with an assay kit. ALP activity was determined with an assay kit. All endpoints were measured 72h post-irradiation.	X-ray radiation exposure from 0.25-4 Gy led to a dose-dependent decrease in the Bcl-2/Bax ratio down to 40% below controls, indicating a significant shift of osteoblasts towards apoptosis. There was also a dose-dependent increase in caspase-3 activity from 0.5-4 Gy up to 1.6-fold above controls. This was accompanied by a dose dependent linear decrease in ALP activity down to 0.3-fold below controls under 4 Gy.
Chandra et al., 2014	In vivo. 3-month-old female rats were irradiated with 16 Gy of SARRP X-rays, fractionated into two 8 Gy doses at a rate of 1.65 Gy/min. TUNEL staining in tibial trabecular bone was performed to determine osteoblast apoptosis. Osteoblast number was determined using static histomorphometry.	Exposure to 16 Gy X-rays increases osteoblast apoptosis by ~7-fold at 2 weeks post-irradiation and resulted in a ~0.25-fold decrease in osteoblast number by day 28 post-irradiation. A significant decrease in osteoclast surface was also observed on day 28 post-irradiation and is inconsistent with other radiation studies. The authors suggest the imbalance of radiation effects may lead to relatively higher osteoclast activity compared to osteoblast activity, leading to overall bone resorption.
Chandra et al., 2017	In vivo. An experiment was conducted on male C57BL/6 mice (8-10 weeks) exposed to 8 Gy X-ray radiation at a rate of 1.65 Gy/min. Apoptosis was determined with a TUNEL assay. Osteoblast number was determined by static histomorphometry.	8 Gy radiation exposure led to a ~3.9-fold increase in the number of TUNEL-positive osteoblasts 2 weeks after irradiation and a 0.5-fold decrease in osteoblast number 4 weeks after irradiation.
Liu et al., 2018	In vitro. hBMMSCs were irradiated with 12 Gy of X-rays at a rate of 1.24 Gy/min. Apoptosis was measured using an Annexin V-fluorescein isothiocyanate staining kit. ALP activity was determined with a kit, and bone deposition was determined by Alizarin red staining.	Apoptosis rate of osteoblast precursor cells (human bone marrow mesenchymal stem cells) exposed to 12 Gy X-ray radiation increased 3-fold after 24h, resulting in a 0.5-fold decrease in ALP activity after 1 week and bone deposition after 3 weeks, as measured by optical density of calcium nodules.

Known modulating factors

Modulating factor	Details	Effects on the KER	References
Genotype	Transgenic mice showed no effect of microgravity on apoptosis.	Microgravity effect on TRAP-5b was partially reversed in transgenic mice. Microgravity effect on OCN activity was fully reversed in transgenic mice.	Yang et al., 2020
Drug	α 2M	Treatment at 0.25 and 0.5 mg/mL slightly restored ALP activity and decreased the rate of apoptosis.	Liu et al., 2018
Drug	Amifostine	Treatment returned both apoptosis and ALP activity to control levels.	Huang et al., 2018
Drug	Doxycycline autophagy inhibitor	Treatment slightly reduced the increase in apoptosis and autophagy and slightly increased ALP activity.	Li et al., 2020
Drug	Sem3a	Treatment after 2 Gy irradiation stimulated an increase in cell apoptosis and decreased bone resorption.	Huang et al., 2018
Drug	4-AAQb	Treatment reduced autophagy and decreased the number of TRAP+ cells.	Wu et al., 2020

Known Feedforward/Feedback loops influencing this KER

Not Identified

References

Aguirre, J. I. et al. (2006), "Osteocyte apoptosis is induced by weightlessness in mice and precedes osteoclast recruitment and bone loss", *Journal of Bone and Mineral Research*, Vol. 21/4, Wiley, <https://doi.org/10.1359/jbmr.060107>.

Bang, C., and Thum, T. (2012), "Exosomes: New players in cell-cell communication", *The International Journal of Biochemistry & Cell Biology*, Vol. 44, Elsevier, Amsterdam, <https://doi.org/10.1016/j.biocel.2012.08.007>

Chandra, A. et al. (2017), "Suppression of Sclerostin Alleviates Radiation-Induced Bone Loss by Protecting Bone-Forming Cells and Their Progenitors Through Distinct Mechanisms", *Journal of Bone and Mineral Research*, Vol. 32/2, Wiley, <https://doi.org/10.1002/jbmr.2996>.

Chandra, A. et al. (2014), "PTH1-34 Alleviates Radiotherapy-induced Local Bone Loss by Improving Osteoblast and Osteocyte Survival", *Bone*, Vol. 67/1, Elsevier, Amsterdam, <https://doi.org/10.1016/j.bone.2014.06.030>. Chatziravdeli, V., G. N. Katsaras and G. I. Lambrou. (2019), "Gene Expression in Osteoblasts and Osteoclasts Under Microgravity Conditions: A Systematic Review", *Current Genomics*, Vol. 20/3, Bentham Science Publishers, <https://doi.org/10.2174/1389202920666190422142053>. Debnath, J., E. H. Baehrecke and G. Kroemer. (2005), "Does Autophagy Contribute To Cell Death?", *Autophagy*, Vol. 1/2, Informa, London, <https://doi.org/10.4161/auto.1.2.1738>. Donaubauer, A. J. et al. (2020), "The influence of radiation on bone and bone cells—differential effects on osteoclasts and osteoblasts", *International Journal of Molecular Sciences*, Vol. 21/17, MDPI, Basel, <https://doi.org/10.3390/ijms21176377>. Fadeel, B. and Orrenius, S. (2005), "Apoptosis: a basic biological phenomenon with wide-ranging implications in human disease", *Journal of Internal Medicine*, Vol. 258/6, Wiley, <https://doi.org/10.1111/j.1365-2796.2005.01570.x>. Fan, Y., and Zong, W. (2013), "The cellular decision between apoptosis and autophagy", *Chinese Journal of Cancer*, Vol. 32/3, Department of Molecular Genetics and Microbiology, <https://doi.org/10.5732/cjc.012.10106>. Huang, B. et al. (2019), "Amifostine suppresses the side effects of radiation on BMSCs by promoting cell proliferation and reducing ROS production", *Stem Cells International*, Vol. 2019, Hindawi, <https://doi.org/10.1155/2019/8749090>.

AOP482

Huang, B. et al. (2018), "Sema3a inhibits the differentiation of raw264.7 cells to osteoclasts under 2gy radiation by reducing inflammation", PLoS ONE, Vol. 13/7, PLOS, San Francisco, <https://doi.org/10.1371/journal.pone.0200000>.

Jilka, R. L., B. Noble and R. S. Weinstein. (2013), "Osteocyte Apoptosis", Bone, Vol. 54/2, Elsevier, Amsterdam, <https://doi.org/10.1016/j.BONE.2012.11.038>.

Knowles, H. J., and Athanasou, N. A. (2009), "Acute hypoxia and osteoclast activity: A balance between enhanced resorption and increased apoptosis", Journal of Pathology, Vol. 218/2, Wiley, <https://doi.org/10.1002/PATH.2534>

Kobayashi, S. (2015), "Choose Delicately and Reuse Adequately: The Newly Revealed Process of Autophagy". Biological and Pharmaceutical Bulletin, Vol. 38/8, J- ST.

Komori, T. (2013), "Functions of the osteocyte network in the regulation of bone mass", Cell and Tissue Research, Vol. 352, Nature, <https://doi.org/10.1007/s00441-012-1546-x>.

Kozbenko, T. et al. (2022), "Deploying elements of scoping review methods for adverse outcome pathway development: a space travel case example", International Journal of Radiation Biology, Vol. 98/12. <https://doi.org/10.1080/09553002.2022.2110306>

Lacombe, J., G. Karsenty and M. Ferron. (2013), "Regulation of lysosome biogenesis and functions in osteoclasts", Cell Cycle, Vol. 12/17, Informa, London, <https://doi.org/10.4161/cc.25825>.

Levine, B. and G. Kroemer. (2008), "Autophagy in the Pathogenesis of Disease", Cell, Vol. 132/1, Elsevier, Amsterdam, <https://doi.org/10.1016/j.cell.2007.12.018>.

Li, R. et al. (2020), "Effect of autophagy on irradiation-induced damage in osteoblast-like MC3T3-E1 cells", Molecular Medicine Reports, Spandidos Publications, <https://doi.org/10.3892/mmr.2020.11425>

Li, X. F. et al. (2015), "Inhibitory effects of autologous γ -irradiated cell conditioned medium on osteoblasts in vitro", Molecular Medicine Reports, Vol. 12/1, Spandidos Publications, <https://doi.org/10.3892/mmr.2015.3354>.

Liu, Y. et al. (2018), "Protective Effects of a-2-Macroglobulin on Human Bone Marrow Mesenchymal Stem Cells in Radiation injury", Molecular Medicine Reports, Vol. 18/5, Spandidos Publications, <https://doi.org/10.3892/mmr.2018.9449>.

Liu, W. et al. (2015), "Osteoprotegerin Induces Apoptosis of Osteoclasts and Osteoclast Precursor Cells via the Fas/Fas Ligand Pathway", PLOS ONE, Vol. 10/11, PLOS, San Francisco, <https://doi.org/10.1371/journal.pone.0142519>

Medina, D. L. et al. (2011), "Transcriptional Activation of Lysosomal Exocytosis Promotes Cellular Clearance", Vol. 21/3, Elsevier, Amsterdam, <https://doi.org/10.1016/j.devcel.2011.07.016>

Mizushima, N., and Komatsu, M. (2011), "Autophagy: Renovation of Cells and Tissues", Cell, Vol. 147/4, Elsevier, Amsterdam, <https://doi.org/10.1016/j.cell.2011.10.026>

Mizushima, N., Yoshimori, T., and Levine, B. (2010), "Methods in Mammalian Autophagy Research", Cell, Vol. 140/3, Elsevier, Amsterdam, <https://doi.org/10.1016/j.cell.2010.01.028>

Nakamura, T. et al. (2007), "Estrogen Prevents Bone Loss via Estrogen Receptor α and Induction of Fas Ligand in Osteoclasts", Cell, Vol 130/5, Elsevier, Amsterdam, <https://doi.org/10.1016/j.cell.2007.07.025>

O'Brien, C. A., T. Nakashima and H. Takayanagi. (2013), "Osteocyte Control of Osteoclastogenesis", Bone, Vol. 54/2, Elsevier, Amsterdam, <https://doi.org/10.1016/j.bone.2012.08.121>.

Plotkin, L. I. (2014), "Apoptotic osteocytes and the control of Targeted Bone Resorption", Current Osteoporosis Reports, Vol. 12/1, Nature, <https://doi.org/10.1007/s11914-014-0194-3>.

Shapiro, I. et al. (2014), "Boning up on autophagy The role of autophagy in skeletal biology", Autophagy, Vol. 10/1, Landes Bioscience, <https://doi.org/10.4161/auto.26679>

Soysa, N. S. and N. Alles. (2019), "Positive and negative regulators of osteoclast apoptosis", Bone Reports, Vol 11, Elsevier, Amsterdam, <https://doi.org/10.1016/j.bonr.2019.100225>

Wang, S. et al. (2020a), "The Role of Autophagy and Mitophagy in Bone Metabolic Disorders", International journal of biological sciences, Vol. 16/14, IIVyspring International Publisher, <https://doi.org/10.7150/ijbs.46627>

Wang, Y. et al. (2020b), "Targeted Overexpression of the Long Noncoding RNA ODSM can Regulate Osteoblast Function In Vitro and In Vivo", Cell Death and Disease, Vol. 11, Springer Nature, Berlin, <https://doi.org/10.1038/s41419-020-2325-3>

Wright, L. E. et al. (2015), "Single-Limb Irradiation Induces Local and Systemic Bone Loss in a Murine Model", Journal of Bone and Mineral Research, Vol. 30/7, Wiley, <https://doi.org/10.1002/jbmr.2458>.

Wu, C. H. et al. (2020), "4-Acetylantroquinonol B Inhibits Osteoclastogenesis By Inhibiting the Autophagy Pathway in a Simulated Microgravity Model", International Journal of Molecular Sciences, Vol. 21/18, MDPI, Basel, <https://doi.org/10.3390/ijms21186971>.

Xiong, J. and C. A. O'Brien. (2012), "Osteocyte RANKL: New Insights into the Control of Bone Remodeling", Journal of Bone Mineral Research, Vol. 27/3, Wiley, <https://doi.org/10.1002/jbmr.1547>

Yang, J. et al. (2020), "Blocking Glucocorticoid Signaling in Osteoblasts and Osteocytes Prevents Mechanical Unloading-Induced Cortical Bone Loss", Bone, Vol. 130, Elsevier, Amsterdam, <https://doi.org/10.1016/j.bone.2019.115108>.

Zhao, Y. et al. (2012), "Autophagy regulates hypoxia-induced osteoclastogenesis through the HIF-1 α /BNIP3 signaling pathway", Journal of Cellular Physiology, Vol. 227/2, Wiley, <https://doi.org/10.1002/JCP.22768>

Relationship: 3320: Altered cell differentiation signaling leads to Altered Bone Cell Homeostasis

AOPs Referencing Relationship

AOP Name	Adjacency	Weight of Evidence	Quantitative Understanding
Deposition of energy leading to occurrence of bone loss	adjacent	High	Moderate

Evidence Supporting Applicability of this Relationship

Taxonomic Applicability

Term	Scientific Term	Evidence	Links
human	Homo sapiens	Low	NCBI
mouse	Mus musculus	High	NCBI
rat	Rattus norvegicus	Moderate	NCBI

Life Stage Applicability

Life Stage Evidence

Juvenile	Moderate
Adult	Moderate

Sex Applicability

Sex	Evidence
-----	----------

Unspecific	High
Male	High
Female	Low

The evidence for the taxonomic applicability to humans is low as majority of the evidence is from *in vitro* human-derived cells and *in vivo* animal models. The relationship is supported primarily by studies from mice models and rat models. The relationship has been shown in both male and female animal models and plausible at any life stage. However, majority of studies use preadolescence and adolescence animal models.

Key Event Relationship Description

Signaling pathways involved in cellular differentiation are important in the maintenance of bone cell homeostasis. This process refers to the deposition and resorption of bone matrix by osteoblasts and osteoclasts, respectively. The Wnt/β-catenin pathway is activated in osteoblasts and the receptor activator of nuclear factor kappa B ligand/osteoprotegerin (RANK-L/OPG) pathway regulates osteoclast differentiation. Osteoclasts originate from hematopoietic stem cells, RANK-L stimulates these progenitor cells to differentiate into pre-osteoclasts (Donaubauer et al., 2020; Smith, 2020b). Binding of RANK-L to its receptor on the osteoclast surface, RANK, triggers the expression of genes associated with osteoclastic bone resorption (Donaubauer et al., 2020). Newly formed mature osteoclasts are multi-nucleated and secrete resorptive proteins and molecules, including hydrochloric acid, tartrate-resistant acid phosphatase (TRAP), Cathepsin K (CTSK), and matrix metalloproteinase (MMP), among others, which degrade bone tissue and can be used as indicators of osteoclast activity (Smith, 2020b). As such, pathways involved in RANK-L activation are important to increased bone resorption.

Mesenchymal stem cells (MSCs) are the precursors to osteoblasts and these cells differentiate upon stimulation by signaling molecules such as tumor growth factor (TGF)-β, Wnt, and bone morphogenic protein (BMP) (Chen, Deng and Li, 2012; Maeda et al., 2019). Alterations in these signaling pathways result in altered differentiation of MSCs and pre-osteoblasts. Early maturation of osteoblasts is regulated by runt-related transcription factor 2 (Runx2) as well as the Wnt/β-catenin signaling pathway; altered signaling in these pathways ultimately leads to decreased production of osteoblast markers of bone deposition, including alkaline phosphatase (ALP), osteocalcin (OCN), and collagen, among others (Chatziravdeli, Katsaras and Lambrou, 2019; Manolagas and Almeida, 2007).

Tight regulation of osteoblast and osteoclast differentiation as well as bone deposition and resorption are crucial to homeostatic bone turnover. Under stress the aforementioned signaling pathways become dysregulated both internally and by external signals, resulting in altered bone cell homeostasis as measured by production of bone depositing/resorbing proteins and their by-products leading to increased osteoclast number and activity and a decrease in osteoblast number (Chatziravdeli, Katsaras and Lambrou, 2019; Donaubauer et al., 2020; Smith, 2020a; Smith, 2020b; Tian et al., 2017).

Evidence Supporting this KER

Overall weight of evidence: High

Biological Plausibility

The biological rationale for linking altered cell differentiation signaling to altered bone cell homeostasis is strongly supported by a number of review articles published on the subject. A recent review by Donaubauer et al. (2020) discusses internal and external signaling pathways in osteoblasts and osteoclasts that are influenced from exposure to a multitude of stressors. A number of reviews also discuss signaling pathways affecting osteoblast and osteoclast differentiation as well as the integral role osteoblasts play in the differentiation of osteoclasts through the RANK-L/OPG pathway (Arfat et al., 2014; Bellido, 2014; Boyce and Xing, 2007; Chatziravdeli, Katsaras and Lambrou, 2019; Chen, Deng and Li, 2012; Donaubauer et al., 2020; Maeda et al., 2019; Manolagas and Almeida, 2007; Smith, 2020a; Smith, 2020b; Willey et al., 2011).

The RANK/RANK-L pathway plays a central role in the differentiation of osteoclasts, as both RANK-L and OPG, an inhibitor of RANK-L, are secreted by osteoblasts and osteocytes (Boyce and Xing, 2007; Donaubauer et al., 2020). The upregulation of RANK-L and downregulation of OPG secretion by osteoblasts indirectly affect osteoclasts and ultimately increase the resorption of bone matrix (Chatziravdeli, Katsaras and Lambrou, 2019; Donaubauer et al., 2020).

RANK-L, upon binding to its receptor on the osteoclast surface, RANK, internally activates cytokine NF-κB in osteoclasts, as well as growth and survival signaling cascades of extracellular signal-regulated kinase (ERK), TNF, and IL-6, preventing apoptosis and promoting differentiation of osteoclasts (Donaubauer et al., 2020; Tian et al., 2017). Over-expression of RANK-L will over-stimulate these downstream pathways leading to the activation of the master transcription factor of osteoclasts, nuclear factor of activated T cells 1 (NFATc1). NFATc1 is responsible for the transcription of genes specific to osteoclastic bone resorption including TRAP and CTSK (Donaubauer et al., 2020; Smith, 2020b). Overexpression of RANK-L results in increased transcription of TRAP and CTSK genes and ultimately, increased bone resorption.

Osteoblastogenesis itself is also tightly regulated by external signals, of which Wnt (activator of Wnt/β-catenin pathway) is often discussed in the literature (Arfat et al., 2014; Chen, Deng and Li, 2012; Maeda et al., 2019; Smith, 2020b). The canonical Wnt/β-catenin pathway plays a central role in osteoblast differentiation, as Wnt stimulation preserves β-catenin from ubiquitination/ degradation, allowing it to translocate to the nucleus and induce expression of key osteoblast genes (Maeda et al., 2019; Manolagas and Almeida, 2007). Dysregulation of key components in this pathway result in significantly depressed protein expression/activity of ALP and OCN, implicating this pathway in the depression of osteoblastic bone deposition (Arfat et al., 2014; Maeda et al., 2019; Manolagas and Almeida, 2007; Tian et al., 2017). As such, Wnt signaling is of paramount importance for preservation of bone mass, as β-catenin commits precursors to the osteoblast lineage (Manolagas and Almeida, 2007; Tian et al., 2017). Runx2 and Osterix (OSX), among others, are also key transcription factors involved in the early maturation osteoblasts, as they advance the progressive differentiation of MSCs and coordinate the expression of key proteins essential to osteoblast function; downregulation of Runx2 and OSX in osteoblasts is concordant with decreases in ALP and OCN activity (Arfat et al., 2014; Chatziravdeli, Katsaras and Lambrou, 2019).

Although less direct, altered osteocyte signaling also plays a key role in the loss of homeostasis among bone cells as osteocytes are the most abundant cell type in bones and are key regulators of bone metabolism. Osteocytes can stimulate osteoclastogenesis by increasing production and release of high mobility group box 1 (HMGB1) and elevating the RANK-L/OPG ratio, inducing the maturation of osteoclast precursors and promoting bone resorption (Arfat et al., 2014; Donaubauer et al., 2020; He et al., 2019). Further, osteocytes with increased expression of Dkk1 and sclerostin result in potent antagonization of bone morphogenic proteins (BMPs) and diversion of LRP5/6 (coreceptors in the Wnt pathway) from Wnt signaling, ultimately inhibiting osteoblast differentiation (Bellido, 2014; Chandra et al., 2017).

Empirical Evidence

The empirical data obtained for this KER strongly supports a link of altered cell differentiation signaling leading to altered bone cell homeostasis. The majority of empirical evidence is derived from research using various stressors including X-rays and gamma rays as well as microgravity. These exposures are both known to directly/indirectly induce alterations in relevant signaling pathways of bone cells leading to the deposition and resorption of bone in a dose-dependent manner (Bai et al., 2020; Chandra et al., 2017; Chen et al., 2020; Goyden et al., 2015; He et al., 2019; He et al., 2020; Kook et al., 2015; Li et al., 2020; Liu et al., 2018; Rucci et al., 2007; Sambandam et al., 2016; Saxena et al., 2011; Yang et al., 2019; Zhang et al., 2019).

Incidence concordance

There is some evidence that signaling pathways demonstrate greater changes following a stressor than altered bone cell homeostasis. He et al. (2019) demonstrated this in osteocytes irradiated with 4 and 8 Gy of gamma rays through increases to HMGB1 and the RANK-L/OPG ratio that were greater than the increases to osteoclast numbers. X-ray irradiation of mice at 16 Gy resulted in a 2.5-fold increase in sclerostin (Wnt/β-catenin pathway inhibitor) and a 0.5-fold decrease in osteoblast number (Chandra et al., 2017). After 8 Gy of X-ray irradiation of human bone marrow mesenchymal stem cells (hBMMSCs) Sox2 and Nanog decreased to less than 0.1-fold, while ALP activity decreased 0.5-fold (Liu et al., 2018). Microgravity exposure to mice increased the RANK-L/OPG ratio 3.5-fold while osteoblast markers decreased a maximum of 0.3-fold and osteoclast markers increased a maximum of 2-fold (He et al., 2020). Microgravity exposure to rats also led to decreases in osteoblast signaling molecules between 0.4- and 0.1-fold and a 5-fold increase in the RANK-L/OPG ratio (Li et al., 2018). This led to a 0.5-fold decrease in osteoblast markers and a 1.5-fold increase in osteoclast markers (Li et al., 2018). Also under microgravity, osteoclast cells showed 6-fold increased TRAF6 and 14.5-fold increased TRAIL, while the osteoclast marker TRAP increased 1.7-fold (Sambandam et al., 2016).

Dose Concordance

Strong evidence exists in the current literature suggesting a dose concordance between alterations of signaling pathways and altered bone cell homeostasis. Exposure to radiation (X-rays and gamma rays) ranging from 0.25-12 Gy and microgravity in mice, rat, and osteoblast cell models shows significant linear dose-dependent diminishment of signaling molecules essential to osteoblast differentiation, including Runx2, Sox2/Nanog, H2S and β-catenin. Studies observing diminishment of these signaling molecules present significant dose-dependent linear decreases in ALP and OCN activity/expression as well, indicating depressed osteoblast function as a result (Bai et al., 2020; Chen et al., 2020; Li et al., 2020; Liu et al., 2018). Further signaling changes in osteoblasts occur under low-to-high dose radiation (0.25 to >2 Gy) and microgravity, with significant increases in osteoblast production of sclerostin, inhibitor of the Wnt/β-catenin pathway. These

changes result in significant linear dose-dependent decreases in ALP activity and osteoblast number at radiation doses greater than 0.25 Gy and/or microgravity exposure (Chandra et al., 2017; Goyden et al., 2015; Li et al., 2020).

One study showed dysregulation of the nuclear factor erythroid 2-related factor/heme oxygenase-1 (Nrf2/HO-1) pathway and downstream effects on bone metabolism. Dose-dependent increases in protein expression of both Nrf2 and HO-1 were observed following high doses of radiation exposure (>2 Gy) with linear dose-dependent decreases in ALP activity in osteoblasts (Kook et al., 2015). Another study examined hydrogen sulfide level, a known gasotransmitter (a class of neurotransmitters) serving many physiological and pathophysiological functions. Decreased levels of this transmitter by microgravity exposure similarly reduced OCN activity and ALP expression in osteoblasts (Yang et al., 2019).

Osteoblasts and osteocytes have also been shown to upregulate the production of cytokines (interleukin (IL)-6 and RANK-L, an osteoclastogenic cytokine) following low and high doses of radiation or microgravity exposure. Alterations in these signaling molecules resulted in upregulation in bone resorption and expression of TRAP (He et al., 2019; He et al., 2020; Rucci et al., 2007). Further, production of OPG, a RANK-L inhibitor, by osteoblasts is significantly diminished under radiation and microgravity exposure, strengthening the stimulatory effect of RANK-L on osteoclasts leading to enhanced expression of TRAP and bone resorption pit area (He et al., 2019; He et al., 2020; Rucci et al., 2007; Yang et al., 2019).

Osteocytes irradiated with gamma rays >2 Gy showed significant linear dose-dependent upregulation in HMGB1, a signaling molecule released by apoptotic osteocytes involved in osteoclast recruitment. Upregulation of HMGB1 resulted in a similar dose-dependent increase in osteoclast count, along with upregulation in the RANK-L/OPG ratio indicating increased resorptive activity (He et al., 2019). Osteoclastogenesis pathways downstream to RANK-L-induced activation also show significant dysregulation under microgravity or ionizing radiation exposure. Microgravity exposure resulted in the upregulation of tumor necrosis factor receptor-associated factor 6 (TRAF6), an osteoclastogenic signaling molecule activated by RANK, and tumor necrosis factor-related apoptosis inducing ligand (TRAIL), an inhibitor of OPG, resulting in significantly enhanced osteoclast count and osteoclastogenesis (Sambandam et al., 2016). Osteoclasts exposed to microgravity, or 2 Gy X-rays show significant upregulation in NFATc1, the master transcription factor for osteoclastogenesis, and nuclear factor kappa B (NF- κ B), an inducible cytokine transcription factor. Upregulation of NFATc1 and NF- κ B results in severely enhanced TRAP expression, osteoclast area, and resorption pit area, indicating increased bone resorption (Saxena et al., 2011; Zhang et al., 2019). Further, phosphorylation of intracellular signaling components, ERK and phospholipase C (PLC γ 2), involved in cell survival and proliferation are upregulated in microgravity-exposed osteoclasts. Enhanced ERK and PLC γ 2 results in an enhanced count of TRAP-positive multinucleated osteoclasts, indicating increased bone resorption (Saxena et al., 2011).

With the exception of the study by Rucci et al. (2007), studies that examined the effects of a range of doses of radiation on a single model found that significant changes to signaling pathways occurred at lower or equal doses than increases in altered bone cell homeostasis, thus providing evidence for dose concordance between the upstream and downstream KEs (Bai et al., 2020; He et al., 2019; Kook et al., 2015; Li et al., 2020). For example, Bai et al. (2020) showed *in vitro* that both signaling molecule Runx2 and osteoblast activity significantly decreased at all doses from 2-10 Gy of gamma irradiation. Similarly, osteocytes irradiated with gamma rays showed changes in the expression of multiple signaling molecules after 4 and 8 Gy but not after 2 Gy, while TRAP-positive osteoclasts increased at 4 and 8 Gy as well, but also not after 2 Gy (He et al., 2019). Kook et al. (2015) used X-rays at the same doses and found altered signaling at 4 and 8 Gy but not at 2 Gy. Osteoblast activity decreased at 4 and 8 Gy, but not at 2 Gy (Kook et al., 2015). Using slightly lower doses, Li et al. (2020) found that altered expression of signaling molecule Runx2 and decreased osteoblast activity both occurred at the same dose of 0.5 Gy, but neither changed at 0.25 Gy.

Time Concordance

Many studies using *in vitro* mouse and human as well as *in vivo* mouse models exposed to microgravity and X-ray irradiation from 2 to 8 Gy show that bone cell altered bone cell homeostasis occurs at the same time or after altered signaling in a time-course. Altered signaling molecules including Runx2, RANK-L, OPG and Nrf2 were mostly found altered 1 to 3 days after a stressor (Goyden et al., 2015; Kook et al., 2015; Li et al., 2020; Liu et al., 2018). Bone cell markers were frequently found decreased weeks after a stressor (Kook et al., 2015; Li et al., 2020; Liu et al., 2018; Zhang et al., 2019).

Essentiality

Studies examining the inhibition or knock-down of signaling molecules strongly support the relationship between altered cell differentiation signaling and bone cell altered bone cell homeostasis. In one study, treatment with OPG, an inhibitor for RANK-L, reversed the effect of microgravity on osteoclast activity, decreasing it to well-below control levels, suggesting a role for RANK-L in microgravity-induced osteoclastogenesis (Rucci et al., 2007). Treatment with doxycycline, known to inhibit autophagy in osteoclasts, reversed the effect of irradiation on the osteoblastogenic transcription factor Runx2, ultimately restoring ALP activity at X-ray doses of 0.25-4 Gy completely to control levels (Li et al., 2020).

Sclerostin is a protein known to inhibit the Wnt/ β -catenin canonical pathway by competing for the Wnt receptor. Chandra et al. (2017) observed that sclerostin knock-out increased osteoblast activity and decreased osteoclast activity, by replenishing β -catenin protein expression, thereby strongly favouring osteoblastogenesis. Further, overexpression of β -catenin in osteoblasts has been shown to reverse the effect of simulated microgravity on β -catenin protein expression, and partially reversing its effect on ALP staining area; β -catenin knockdown had the opposite effect under microgravity (Chen et al., 2020). Knockdown of TRAIL, which induces osteoclastogenesis by sequestering the RANK-L inhibitor OPG, reversed the effect of microgravity on osteoclast numbers (Sambandam et al., 2016). HMGB1 is a protein released by apoptotic osteocytes that mediates RANK-L-induced osteoclastogenesis by interacting with receptor for advanced glycation end-products (RAGE); He and associates confirmed this under gamma radiation-induced osteoclastogenesis, as treatment with HMGB1 antibody fully reversed the effect of radiation on osteoclast count (He et al., 2019; Zhou et al., 2008). A role for hydrogen sulfide in osteoblast and osteoclast differentiation under microgravity has also been suggested, as treatment with H2S donor GYY4137 leads to decreased RANK-L/OPG production ratio by osteoblasts and increased ALP activity (Yang et al., 2019).

α -macroglobulin (α 2M) is a glycoprotein known to exert radioprotective effects on cells, and treatment of osteoblasts with α 2M was shown to significantly reverse the effect of radiation on protein expression of transcription factors Runx2 and Sox2, and osteoglycin (OGN), while also reversing its effect on ALP activity, returning the values to control levels (Liu et al., 2018). A significant role for iron in the induction of osteoclastogenesis under both radiation and non-radiation conditions was posited, as treatment with iron chelator deferoxamine mesylate (DFO) fully decreased serum ferritin and iron levels, while also decreasing osteoclast and resorption pit area by 100% in both irradiated and non-irradiated groups (Zhang et al., 2019).

Exposure to pulsed electromagnetic fields (PEMFs) has also shown promise in improving the effects of modeled microgravity on measures of bone cell function. In one study, PEMF exposure together with hindlimb suspension of rats showed significant improvement in protein expression related to bone cell function, with increased expression of Runx2 and OSX (involved in early osteoblast maturation), and BMP-2 (an osteoblast stimulatory molecule), along with significant decrease in the RANK-L/OPG ratio (osteoclast stimulatory molecule and its inhibitor) relative to the hindlimb suspension alone group. A role of the sAC/cAMP/PKA/CREB signaling pathway was also implicated in these improvements, as phosphorylation of its key components, including protein kinase A (PKA) and (cAMP response element-binding protein) CREB, and expression of soluble adenylyl cyclases (sAC) and cAMP were significantly improved in comparison to the hindlimb suspended group. These changes were ultimately accompanied by significant improvements in bone deposition markers osteocalcin and propeptide of type I procollagen (PIP α) and decreases in bone resorption markers TRAP5b and collagen C-terminal telopeptide (CTX)-1 (Li et al., 2018).

Uncertainties and Inconsistencies

- Some studies suggest radiation exposure at doses at or below 2 Gy result in no significant changes in osteoblast and osteoclast activity, as measured by ALP and TRAP expression, respectively (Kook et al., 2015; He et al., 2019). These studies, however, are inconsistent with other studies examining the effects of radiation doses from 0.25-2 Gy, which report significant, dose-dependently diminished ALP activity, and enhanced count of TRAP-positive osteoclasts (Li et al., 2020; Zhang et al., 2019). Further research is needed to elucidate the effects of lower doses of ionizing radiation on osteoblasts and osteoclasts, as well as their dose-dependent effects.

Quantitative Understanding of the Linkage

The following are a few examples of quantitative understanding of the relationship. All reported findings are statistically significant at various alpha levels as listed in the original sources

Response-response relationship

Dose/Incidence Concordance

Reference	Experiment Description	Result
Li et al., 2020	<i>In vitro</i> . Mouse pre-osteoblastic MC3T3-E1 was irradiated with X-rays at 0.25, 0.5, 1, 2, and 4 Gy. Runx2 transcription factor was measured to determine signaling. ALP5 activity was measured to determine osteoblastogenesis.	All endpoints changed dose-dependently. Runx2 expression and ALP5 activity both decreased a maximum of 0.4-fold after 4 Gy. Runx2 expression and ALP activity both first decreased significantly at 0.5 Gy.

Zhang et al., 2019	<i>In vivo</i> . 4-week-old male C57BL/6J mice were irradiated with 2 Gy X-rays at 0.23 Gy/s. Levels of NFATc1 and NF-κB transcription factors in the RANK-L/RANK pathway of osteoclastogenesis were determined. A TRAP stain was performed to determine osteoclast area.	NFATc1 increased 2.9-fold and NF-κB increased 1.5-fold after 2 Gy. TRAP-positive surface area increased 2.3-fold after 2 Gy.
He et al., 2019	<i>In vitro</i> . Osteocyte-like MLO-Y4 cells were irradiated with 137Cs gamma rays at 2, 4, and 8 Gy. HMGB1 and the RANK-L/OPG ratio (OPG inhibits RANK-L) protein and mRNA levels were determined to measure altered signaling. Osteoclast differentiation was measured in preosteoclast RAW264.7 cells co-cultured with irradiated MLO-Y4 cells using TRAP staining.	No significant changes were observed at 2 Gy. HMGB1 protein and mRNA levels both increased, with protein levels increasing 2.5-fold at 4 Gy and 4-fold after 8 Gy. RANK-L increased and OPG decreased shown by both protein and mRNA levels, with the RANK-L/OPG ratio of mRNA levels increasing 1.8-fold at 4 Gy and 2.5-fold at 8 Gy. The number of TRAP-positive cells increased 1.3-fold at 4 Gy and 1.8-fold at 8 Gy.
Chandra et al., 2017	<i>In vivo</i> . An experiment was conducted on male C57BL/6 mice (8–10 weeks) exposed to 16 Gy X-ray radiation at a rate of 1.65 Gy/min. Sclerostin, an inhibitor of the Wnt/β-catenin pathway. Osteoblast number was determined.	16 Gy radiation exposure led to a 2.5-fold increase in sclerostin and a 0.5-fold decrease in osteoblast number.
Bai et al., 2020	<i>In vitro</i> . Bone marrow derived MSCs (bmMSCs), osteoblast precursors from 4-week-old male Sprague–Dawley rats were irradiated with 2, 5, and 10 Gy of 137Cs gamma rays. The Runx2 transcription factor part of osteoblastogenic pathways was measured. ALP (osteoblastogenesis marker) activity was measured.	Runx2 decreased significantly after 2, 5, and 10 Gy, reaching a maximum 0.6-fold decrease at 10 Gy. ALP activity decreased significantly at 2, 5, and 10 Gy, following a linear trend to a maximum decrease of 48.2% (from 218 U/mg protein to 113 U/mg protein) at 10 Gy.
Liu et al., 2018	<i>In vitro</i> . hBMMSCs were irradiated with 8 Gy of X-rays at 1.24 Gy/min. The Runx2 transcription factor part of osteoblastogenic pathways and OGN (inhibits osteoclasts) were measured. Sox2 and Nanog (cytokine markers of stem cell pluripotency) were measured. ALP (osteoblastogenesis marker) activity was measured.	Runx2 and OGN both decreased about 0.5-fold at 8 Gy. Sox2 and Nanog both decreased more than 0.1-fold at 8 Gy. ALP activity decreased about 0.5-fold at 8 Gy.
Kook et al., 2015	<i>In vitro</i> . MC3T3-E1 osteoblast cells were irradiated with 2, 4, and 8 Gy of X-rays at 1.5 Gy/min. The Runx2 transcription factor mRNA levels as well as proteins in the Nrf2/HO-1 pathway were measured. ALP activity was measured to determine osteoblast function.	Runx2 mRNA decreased 0.5-fold after 8 Gy. HO-1 was increased 3-fold after 4 Gy and 5-fold after 8 Gy (non-significant increase at 2 Gy). Nrf2 increased 2.3-fold after 8 Gy. ALP activity decreased 0.3-fold after 8 Gy (non-significant decrease at 2 Gy).
Goyden et al., 2015	<i>In vitro</i> . The MC3T3-E1 pre-osteoblast cells were subject to microgravity. RANK-L, OPG, and sclerostin mRNA levels were measured to determine altered signaling. OCN and collagen α1 mRNA levels (osteoblast markers) were measured.	RANK-L was increased 1.3-fold, OPG decreased 0.8-fold, and sclerostin increased 1.7-fold. OCN and collagen α1 were decreased 0.6-fold.
He et al., 2020	<i>In vivo</i> and <i>in vitro</i> . Male 10-week-old C57BL/6J mice were subject to hindlimb suspension. MC3T3-E1 cells were exposed to modeled microgravity. The RANK-L/OPG ratio of signaling molecules was determined. ALP and OCN for osteoblasts and TRAP for osteoclasts were determined.	In the hind-limb suspended mice, RANK-L/OPG ratio increased 3.5-fold, ALP decreased 0.3-fold, OCN decreased 0.5-fold, TRAP increased 2-fold. In MC3T3-E1 cells, RANK-L expression was increased 75% and OPG decreased 33%. This was accompanied by a ~50% in ALP mRNA expression and a 0.4-fold decrease in ALP activity.
Li et al., 2018	<i>In vivo</i> . Female 3-month-old Wistar rats were subjected to microgravity for 4 weeks. Runx2, OSX, BMP-2, RANK-L, OPG signaling proteins and components of the sAC/cAMP/PKA/CREB signaling pathway were measured. OCN and PIPN were measured for osteoblastogenesis and TRAP5b and CTX-1 were measured for osteoclastogenesis in serum.	Runx2 decreased 0.3-fold, OSX 0.4-fold, BMP-2 0.1-fold, OPG/RANK-L 0.2-fold. Phosphorylated PKA and CREB both decreased more than 0.5-fold. Osteoblast markers decreased about 0.5-fold, while osteoclast markers increased about 1.5-fold.
Rucci et al., 2007	<i>In vitro</i> . Calvaria and primary osteoclasts from 7-day-old CD1 mice were differentiated into osteoblasts and osteoclasts, respectively, and exposed to microgravity at 0.08 G or 0.008 G for 24 h. The RANK-L/OPG ratio was determined. ALP activity (osteoblast marker) and TRAP level (osteoclast marker) were determined.	The RANK-L/OPG ratio showed a nonsignificant 1.4-fold increase after 0.08 G and a 4-fold increase after 0.008 G. TRAP increased 2.4-fold after 0.08 G and 5.6-fold after 0.008 G. ALP activity and expression did not significantly change.
Saxena et al., 2011	<i>In vitro</i> . RAW264.7 murine macrophage cells and mouse bone marrow macrophage precursors were exposed to microgravity. All cells were cultured with RANK-L. The signaling molecules ERK, p38, NFATc1, and PLCy2 were measured. TRAP and CTSK mRNA levels (osteoclast markers) were measured.	Phosphorylated ERK, PLCy2, and p38 as well as NFATc1 were increased after microgravity. TRAP and CTSK increased 3.5-fold in RAW264.7 cells. TRAP increased 3-fold and CTSK increased 7.5-fold in mouse bone marrow macrophages.
Yang et al., 2019	<i>In vivo</i> and <i>in vitro</i> . Rats were exposed to microgravity conditions by hindlimb suspension. An <i>in vitro</i> model used MC3T3-E1 (osteoblast-like cells) in a bone cell differentiation media exposed to microgravity conditions. RANK-L and OPG were measured as part of RANK signaling pathway. Plasma H2S concentration, a gasotransmitter serving many physiological/pathophysiological roles, and endogenous H2S produced by osteoblasts were monitored. Osteoblastogenesis was measured by serum OCN and ALP.	Concentration of RANK-L increased significantly by 1.5-fold, while OPG concentration decreased by 0.71-fold. Endogenous H2S production by osteoblasts and concentration in plasma were decreased 0.66-fold. ALP activity decreased 0.53-fold after microgravity simulation in rats. OCN levels in sera of rats exposed to hindlimb suspension decreased 0.6-fold. Rats experienced a 3-fold increase in tibia IL-6, while osteoblasts supernatant had a 4-fold increase in IL-6.
Chen et al., 2020	<i>In vivo</i> and <i>in vitro</i> . 2-month-old mice were subject to hindlimb unloading to simulate microgravity. An <i>in vitro</i> model of primary osteoblasts isolated from murine femurs were exposed to microgravity for 48-hours. β-catenin mRNA and protein expression were determined. ALP, an osteoblast marker, and collagen type 1 alpha-1 were measured as osteoblastogenesis markers.	Following hindlimb unloading, PCR analysis of β-catenin showed decreased expression by 0.45-fold in both <i>in vivo</i> mice after 28 days and <i>in vitro</i> primary osteoblasts after 48 h. <i>In vitro</i> β-catenin protein expression decreased by 0.5-fold. The mRNA expressions of ALP and collagen type 1 alpha-1 were downregulated by 93.9% and 62.4%, respectively, <i>in vivo</i> , and were both downregulated by 60% <i>in vitro</i> .
Sambandam et al., 2016	<i>In vitro</i> . Osteoclast cells were taken from the bone marrow of 6- to 8-week-old C57BL/6 mice and exposed to 0.008 G for 24h. The mRNA of TRAF6 signaling molecule downstream of RANK was measured. The mRNA of TRAIL (proliferative signaling molecule) was also measured. TRAP staining was performed to measure osteoclastogenesis. Western blots were also performed to confirm changes in mRNA levels.	Following 0.008G, signaling molecules TRAF6 and TRAIL increased 6-fold and 14.5-fold, respectively. TRAP increased 1.7-fold after 0.008G.

Time-scale**Time Concordance**

Reference	Experiment Description	Result
Li et al., 2020	<i>In vitro</i> . Mouse pre-osteoblastic MC3T3-E1 was irradiated with X-rays at various doses. Runx2 transcription factor was measured to determine signaling. ALP5 activity was measured to determine osteoblastogenesis.	Runx2 and ALP5 activity both decreased a maximum of 0.4-fold after 72 h. ALP5 activity was also observed decreased the same amount after 1 and 2 weeks.
Zhang et al., 2019	<i>In vivo</i> . 4-week-old male C57BL/6J mice were irradiated with 2 Gy X-rays at 0.23 Gy/s. Levels of NFATc1 and NF-κB transcription factors in the RANK-L/RANK pathway of osteoclastogenesis were determined. A TRAP stain was performed to determine osteoclast area.	NFATc1 increased 2.9-fold and NF-κB increased 1.5-fold after 28 days. TRAP-positive surface area increased 2.3-fold after 28 days.
Liu et al., 2018	<i>In vitro</i> . hBMMSCs were irradiated with 8 Gy of X-rays at 1.24 Gy/min. The Runx2 transcription factor was measured. Sox2 and Nanog (cytokine markers of stem cell pluripotency) were measured. ALP (osteoblastogenesis marker) activity was measured.	Sox2 and Nanog both decreased more than 0.1-fold after 24h. Runx2 decreased about 0.5-fold at 1 week. ALP activity decreased about 0.5-fold at 1 week.

Kook et al., 2015	<i>In vitro</i> . MC3T3-E1 osteoblast cells were irradiated with X-rays at 1.5 Gy/min. The mRNA of Runx2 transcription factor as well as proteins in the Nrf2/HO-1 pathway were measured. ALP activity and mRNA level were measured to determine osteoblast function.	Runx2 mRNA decreased 0.5-fold at 1-3 days after 8 Gy irradiation. HO-1 was increased 4.5-fold at 2 days. Nrf2 increased 2.3-fold at 1 day. ALP activity decreased 0.3-fold after 7 days.
Goyden et al., 2015	<i>In vitro</i> . The MC3T3-E1 pre-osteoblast cells were subject to microgravity at 0 G. The mRNA of RANK-L, OPG, and sclerostin was measured to determine altered signaling. The mRNA of OCN and collagen α 1 (osteoblast markers) was measured to determine osteoblast function.	RANK-L was increased 1.3-fold, OPG decreased 0.8-fold, and sclerostin increased 1.7-fold after 48 h of microgravity. OCN and collagen α 1 were decreased 0.6-fold after 48 h of microgravity. IL-6 increased 2-fold after 48 h, where the maximum change in OCN was observed, but not after 12 h.

Known modulating factors

Modulating factor	Details	Effects on the KER	References
Drug	Doxycycline (autophagy inhibitor)	Treatment partially restored the radiation-induced decreases in autophagy markers as well as increased Runx2 signaling protein and ALP5 (osteoblastogenesis marker) levels.	Li et al., 2020
Drug	Anti-HMGB1 neutralizing antibody	Treatment with 0.5 μ g/ml completely prevented the increased RANK-L/OPG ratio and the increased osteoclastogenesis.	He et al., 2019
Drug	α 2M	Treatment with 0.25 and 0.5 mg/mL slightly restored all endpoints of altered signaling as well as ALP activity.	Liu et al., 2018
Drug	N-acetyl cysteine (antioxidant)	Treatment reduced Nrf1 and HO-1 levels and restored Runx2 levels and ALP activity.	Kook et al., 2015
Drug	GYY4137 (25mg/kg per day)	Treatment on rats exposed to hindlimb suspension found increased levels of osteocalcin close to control levels.	Yang et al., 2019
Pulsed electromagnetic field	50 Hz, 0.6 mT pulsed electromagnetic field for 1.5 h/day during hind-limb suspension	Treatment restored signaling pathways as well as osteoblast markers to control levels.	Li et al., 2018
Drug	1 nM r-irisin	Treatment after simulated microgravity slightly restored ALP and collagen type 1 alpha-1 α 1 levels.	Chen et al., 2020
Drug	DFO	Can completely inhibit osteoclast formation and bone resorption <i>in vitro</i> .	Zhang et al., 2019
Genetic	IL-6 knockdown	IL-6 knockdown with an IL-6 antibody partially reversed microgravity effect on all parameters of signaling pathways, osteoblastogenesis, and osteoclastogenesis	He et al., 2020

Known Feedforward/Feedback loops influencing this KER

Not Identified

References

Arfat, Y. et al. (2014), "Physiological Effects of Microgravity on Bone Cells", *Calcified Tissue International*, Vol. 94/6, *Nature* <https://doi.org/10.1007/s00223-014-9851-x>

Bai, J. et al. (2020), "Irradiation-induced senescence of bone marrow mesenchymal stem cells aggravates osteogenic differentiation dysfunction via paracrine signaling", *American Journal of Physiology - Cell Physiology*, Vol. 318/5, *American Physiological Society*, <https://doi.org/10.1152/ajpcell.00520.2019>

Bellido, T. (2014), "Osteocyte-Driven Bone Remodeling", *Calcified Tissue International*, Vol. 94/1, *Nature*, <https://doi.org/10.1007/s00223-013-9774-y>.

Boyce, B. F. and L. Xing. (2007), "The RANKL/RANK/OPG pathway", *Current Osteoporosis Reports*, Vol. 5/3, *Nature* <https://doi.org/10.1007/s11914-007-0024-y>

Chandra, A. et al. (2017), "Suppression of Sclerostin Alleviates Radiation-Induced Bone Loss by Protecting Bone-Forming Cells and Their Progenitors Through Distinct Mechanisms", *Journal of Bone and Mineral Research*, Vol. 32/2, *Wiley*, <https://doi.org/10.1002/bmr.2996>.

Chatziravdeli, V., G. N. Katsaras and G. I. Lambrou. (2019), "Gene Expression in Osteoblasts and Osteoclasts Under Microgravity Conditions: A Systematic Review", *Current Genomics*, Vol. 20/3, *Bentham Science Publishers*, <https://doi.org/10.2174/1389202920666190422142053>.

Chen, G., C. Deng and Y.-P. Li. (2012), "TGF- β and BMP Signaling in Osteoblast Differentiation and Bone Formation", *International Journal of Biological Sciences*, Vol. 8/2, *Ivyspring International Publisher* <https://doi.org/10.7150/ijbs.2929>.

Chen, Z. et al. (2020), "Recombinant irisin prevents the reduction of osteoblast differentiation induced by stimulated microgravity through increasing β -catenin expression", *International Journal of Molecular Sciences*, Vol. 21/4, *MDPI, Basel*, <https://doi.org/10.3390/ijms21041259>.

Donaubauer, A. J. et al. (2020), "The influence of radiation on bone and bone cells—differential effects on osteoclasts and osteoblasts", *International Journal of Molecular Sciences*, Vol. 21/17, *MDPI, Basel*, <https://doi.org/10.3390/ijms21176377>

Goyden, J. et al. (2015), "The effect of OSM on MC3T3-E1 osteoblastic cells in simulated microgravity with radiation", *PLoS ONE*, Vol. 10/6, *PLOS, San Francisco*, <https://doi.org/10.1371/journal.pone.0127230>.

He, B. et al. (2020), "Blockade of IL-6 alleviates bone loss induced by modelled microgravity in mice", *Canadian Journal of Physiology and Pharmacology*, Vol. 98/10, *Canadian Science Publishing*, <https://doi.org/10.1139/cjpp-2019-0632>.

He, F. et al. (2019), "Irradiation-Induced Osteocyte Damage Promotes HMGB1-Mediated Osteoclastogenesis In Vitro", *Journal of Cellular Physiology*, Vol. 234/10, *Wiley, New York City*, <https://doi.org/10.1002/jcp.28351>.

Kook, S. H. et al. (2015), "Irradiation inhibits the maturation and mineralization of osteoblasts via the activation of Nrf2/HO-1 pathway", *Molecular and Cellular Biochemistry*, Vol. 410/1-2, *Nature*, <https://doi.org/10.1007/s11010-015-2559-z>.

Li, R. et al. (2020), "Effect of autophagy on irradiation-induced damage in osteoblast-like MC3T3-E1 cells", *Molecular Medicine Reports*, Vol. 22/4, *Spandidos Publications*, <https://doi.org/10.3892/mmr.2020.11425>.

Li, W. Y. et al. (2018), "Pulsed electromagnetic fields prevented the decrease of bone formation in hindlimb-suspended rats by activating sAC/cAMP/PKA/CREB signaling pathway", *Bioelectromagnetics*, Vol. 39/8, *Wiley*, <https://doi.org/10.1002/bem.22150>.

Liu, Y. et al. (2018), "Protective Effects of α -2-Macroglobulin on Human Bone Marrow Mesenchymal Stem Cells in Radiation Injury", *Molecular Medicine Reports*, Vol. 18/5, *Spandidos Publications*, <https://doi.org/10.3892/mmr.2018.9449>.

Maeda, K. et al. (2019), "The Regulation of Bone Metabolism and Disorders by Wnt Signaling", *International Journal of Molecular Sciences*, Vol. 20/22, <https://doi.org/10.3390/ijms20225525>.

Manolagas, S. C. and M. Almeida. (2007), "Gone with the Wnts: β -Catenin, T-Cell Factor, Forkhead Box O, and Oxidative Stress in Age-Dependent Diseases of Bone, Lipid, and Glucose Metabolism", *Molecular Endocrinology*, Vol. 21/11, *MDPI, Basel*, <https://doi.org/10.1210/me.2007-0259>.

Rucci, N. et al. (2007), "Modeled microgravity stimulates osteoclastogenesis and bone resorption by increasing osteoblast RANKL/OPG ratio", *Journal of Cellular Biochemistry*, Vol. 100/2, *Wiley*, <https://doi.org/10.1002/jcb.21059>.

Sambandam, Y. et al. (2016), "Microgravity Induction of TRAIL Expression in Preosteoclast Cells Enhances Osteoclast Differentiation", *Scientific Reports*, Vol. 6, *Nature*, <https://doi.org/10.1038/srep25143>.

Saxena, R. et al. (2011), "Modeled microgravity and hindlimb unloading sensitize osteoclast precursors to RANKL-mediated osteoclastogenesis", *Journal of Bone and Mineral Metabolism*, Vol. 29/1, *Nature*, <https://doi.org/10.1007/s00774-010-0201-4>.

Smith, J. K. (2020a), "Microgravity, Bone Homeostasis, and Insulin-Like Growth Factor-1", *Applied Sciences*, Vol. 10/13, *MDPI, Basel*, <https://doi.org/10.3390/app10134433>.

Smith, J. K. (2020b), "Osteoclasts and microgravity", *Life*, Vol. 10/9, MDPI, Basel, <https://doi.org/10.3390/life10090207>.

Tian, Y. et al. (2017), "The impact of oxidative stress on the bone system in response to the space special environment", *International Journal of Molecular Sciences*, Vol. 18/10, MDPI, Basel, <https://doi.org/10.3390/ijms18102132>.

Willey, J. S. et al. (2011), "Ionizing Radiation and Bone Loss: Space Exploration and Clinical Therapy Applications", *Clinical Reviews in Bone and Mineral Metabolism*, Vol. 9, *Nature*, <https://doi.org/10.1007/s12018-011-9092-8>.

Yang, M. et al. (2019), "Treatment with hydrogen sulfide donor attenuates bone loss induced by modeled microgravity", *Canadian Journal of Physiology and Pharmacology*, Vol. 97/7, Canadian Science Publishing, <https://doi.org/10.1139/cjpp-2018-0521>.

Zhang, J. et al. (2019), "Lowering iron level protects against bone loss in focally irradiated and contralateral femurs through distinct mechanisms", *Bone*, Vol. 120/October 2018, Elsevier, Amsterdam, <https://doi.org/10.1016/j.bone.2018.10.005>.

Zhou, Z. et al. (2008), "HMGB1 Regulates RANKL-Induced Osteoclastogenesis in a Manner Dependent on RAGE", *Journal of Bone and Mineral Research*, Vol. 23/7, Wiley, <https://doi.org/10.1359/jbmr.080234>.

Relationship: 2844: Altered Bone Cell Homeostasis leads to Bone Remodeling

AOPs Referencing Relationship

AOP Name	Adjacency	Weight of Evidence	Quantitative Understanding
Deposition of energy leading to occurrence of bone loss	adjacent	Moderate	Low

Evidence Supporting Applicability of this Relationship

Taxonomic Applicability

Term	Scientific Term	Evidence	Links
human	Homo sapiens	Low	NCBI
mouse	Mus musculus	High	NCBI
rat	Rattus norvegicus	High	NCBI

Life Stage Applicability

Life Stage Evidence

Adult	High
Juvenile	Moderate

Sex Applicability

Sex	Evidence
Male	High
Female	Moderate
Unspecific	Low

Considerable evidence is available in mice and rats. The relationship has been demonstrated *in vivo* for both males and females, with more available evidence for males. *In vivo* evidence is derived from adolescents and adult models, with considerable evidence for adults.

Key Event Relationship Description

The bone microenvironment is defined as a complex structural and biological system containing mesenchymal cells from different lineages; bone resident cells, such as osteoclasts, osteoblasts, and osteocytes; and the bone extracellular matrix. For bone structure to remain at a homeostatic level, osteoclasts and osteoblasts must act in unison so that bone resorption does not outpace bone formation, and vice versa. Osteoblasts differentiate from mesenchymal stem cells (MSCs) into pre-osteoblasts, then pre-osteoblasts migrate to the site of bone resorption where they become fully functioning osteoblasts capable of depositing new bone matrix (Donaubauer et al., 2020). Osteoclasts originate from hematopoietic stem cells (HSCs) in the bone marrow and their differentiation into pre-osteoclasts is stimulated by the release of cytokines by osteocytes, osteoblasts, and immune cells (Donaubauer et al., 2020). Imbalances in the regulation of osteoblast and osteoclast differentiation and proliferation results in altered bone cell homeostasis and consequent disruption to bone remodeling (Chatziravdeli et al., 2019; Donaubauer et al., 2020; Smith, 2020a; Smith, 2020b; Tian et al., 2017).

Altered bone cell homeostasis can be defined by an increase in osteoclast number and activity and a decrease in osteoblast number and activity, resulting in an imbalance in bone formation and resorption. Altered cell processes can increase osteoclast activity and decrease osteoblast activity and the production of the organic and inorganic components of the bone matrix. As a result of altered bone cell homeostasis, bone remodeling processes may be impacted. Each remodeling event, known as a basic multicellular unit (BMU), consists of osteoclasts, bone resorption cells, osteoblasts, and bone-forming cells (Raggatt & Partridge; Slyfield et al., 2012; Frost, 1966). The BMU activity can be assessed by examining parameters of dynamic bone histomorphometry. The structural model index (SMI) of bone tissue, which measures the proportion of rods and plates in trabecular bone, also serves as an important marker of bone structural changes (Shahnazari et al., 2012). A disruption in the activity of bone remodeling cells, such as bone MSCs, osteoblasts and osteoclasts, leads to dysfunction of bone cells and downstream altered bone remodeling (Wright et al., 2015; Zhang et al., 2018). The strict regulation of differentiation pathways that define osteoblast/osteoclastogenesis is essential for the maintenance of osteogenic balance and functioning of bone cells to bone remodeling.

Evidence Supporting this KER

Overall weight of evidence: Moderate

Biological Plausibility

The biological basis for linking the loss of homeostasis among bone cells to bone remodeling is well-supported by literature, as illustrated by multiple review articles on the subject. (Bartell et al., 2014; Donaubauer et al., 2020; Manolagas et al., 2007; Maeda et al., 2019; Tahimic and Globus, 2017; Tian et al., 2017).

Under normal conditions, osteoblasts make new bone by secreting collagen and proteoglycans, which make up the unmineralized organic bone matrix, and hydroxyapatite crystals, which form the mineralized, inorganic component. As osteoblasts are responsible for bone formation and mineralization, a reduction in osteoblast numbers has been shown to decrease bone formation rate and mineral apposition rate, which are important measures of bone remodeling (Bikle and Halloran, 1999; Donaubauer et al., 2020; Morey-Holton and Arnaud, 1991).

Disrupted bone cell function includes activation of osteoclasts by upregulation of HSC differentiation, resulting in promotion of bone resorption (Donaubauer et al., 2020). The osteoclast-specific gene, tartrate-resistant acid phosphatase (TRAP)-5b, is expressed during osteoclastogenesis and is commonly used as a marker of osteoclast activity due to its role in osteoclast function (Donaubauer et al. 2020; Willey et al., 2011; Smith, 2020b). Osteoclasts break down the bone matrix by attaching to the surface of the bone, forming a sealed resorption pit, and secreting hydrochloric acid to dissolve hydroxyapatite crystals, as well as proteases such Cathepsin K (CTSK) and matrix metalloproteinases (MMP9 and MMP14) to degrade matrix proteins (Smith, 2020b; Stavnicuk et al., 2020). The removal and resorption of organic matrix derivatives and mineral components, such as calcium and phosphorus, from the bone surface results in increased demineralization and resorption of bone matrix. (Bikle and Halloran, 1999; Morey-Holton and Arnaud, 1991). High levels of osteoclasts in the bone microenvironment results in increased bone resorption rate and decreased bone formation rate (BFR) and mineral apposition rate (MAR) (Donaubauer et al., 2020; Smith, 2020a; Willey et al., 2011; Xiao et al., 2016). Review papers on bone remodeling during spaceflight cite numerous studies indicating that a loss of homeostasis in bone cells towards resorption is a factor leading to impaired bone remodeling (Bikle and Halloran, 1999; Morey-Holton and Arnaud, 1991).

Empirical Evidence

The empirical data relevant to this KER provides strong support for the linkage between altered bone cell homeostasis and bone remodeling. The majority of the evidence supporting this relationship is derived from studies examining the effect of microgravity and radiation, on the skeletal system. Both stressors induce a dose- and time-dependent loss of homeostasis in bone cells towards disrupted bone remodeling (Chandra et al., 2017; Chandra et al., 2014; Hui et al., 2014; Lloyd et al., 2015; Matsumoto et al. 1998; Shahnazari et al., 2012; Wright et al. 2015; Wronski et al., 1987).

Incidence Concordance

There is moderate support in current literature for an incidence concordance relationship between altered bone cell homeostasis and disrupted bone remodeling. Seven of the primary research studies used to support this AOP demonstrated an average change to endpoints of altered bone cell homeostasis that was greater or equal to that of bone remodeling (Chandra et al., 2017; Wright et al., 2015; Yang et al., 2020; Lloyd et al., 2015; Shahnazari et al., 2012; Dehoriy et al., 1999; Wronski et al., 1987).

Dose Concordance

The evidence for a dose-dependent relation between altered bone cell homeostasis and bone remodeling is moderate. Studies on the effects of space-related stressors such as ionizing radiation and microgravity on bone development have found that these stressors produce significant changes in bone cell function, which are linked to subsequent bone remodeling. Microgravity exposure, whether through simulated methods like hindlimb unloading and tail suspension or authentic means like spaceflight, resulted in significant reductions in bone formation markers. Examples include a 40-50% reduction in osteocalcin (OCN) and significant increases in bone resorption markers, such as a 3-4-fold increase in TRAP-5b (Yang et al., 2020; Lloyd et al., 2015; Yotsumoto, Takeoka, and Yokoyama, 2010). Microgravity also has been shown to result in significant dose dependent changes in bone remodeling markers such as MS, MAR, and BFR. Studies on mice and rats exposed to microgravity for 1-5 weeks found dramatic reductions in bone remodeling parameters compared to control or baseline values, ranging from 33-80% for BFR, 23-75% for MAR, and 29% for mineralizing surface (MS/BS). (Dehoriy et al., 1999; Iwaniec et al., 2005; Lloyd et al., 2015; Matsumoto et al. 1998; Shahnazari et al., 2012; Wronski et al., 1987; Yang et al., 2020; Yotsumoto, Takeoka, and Yokoyama, 2010).

Studies that use ionizing radiation provide the best support for dose-dependence, as they support the relationship at a range of radiation doses. Studies that examined the effects of low doses (≤ 2 Gy) of low linear energy transfer (LET) radiation (X-rays and protons) on mice found that there was a dose-dependent relationship between osteoblast and osteoclast markers and bone remodeling markers. 2 Gy of low LET radiation resulted in a significant linear decrease in levels of osteoblast markers, such as OCN by 52% and ALP by 75%, and increased levels of osteoclast markers, such as osteoclast number by 44% and TRAP-5b levels by 14%. As a result, bone remodeling factors, such as BFR and MS/BS, were decreased after exposure to 2 Gy (Bandstra et al., 2008; Wright et al., 2015). Studies with higher doses (> 8 Gy) of low LET radiation have shown the similar linear relationship; however, the changes to markers of osteoblasts, osteoclasts, and bone remodeling were more significant (Chandra et al., 2017; Chandra et al., 2014; Hui et al., 2014).

Time Concordance

There is limited evidence for a time-dependent link between altered bone cell homeostasis and bone remodeling in the existing literature. Few research articles examined the long-term consequences of microgravity or ionizing radiation-induced losses in bone cell homeostasis on bone remodeling (Dehoriy et al., 1999; Hui et al., 2014; Shahnazari et al., 2012). Hui et al. (2014) irradiated mice with 16 Gy and found C-terminal telopeptide (CTX), a marker of osteoclast activity, to increase 3 days post-irradiation, while MAR was measured increased 12 to 29 days post-irradiation. Shahnazari et al. (2012) showed that hindlimb unloading for 2 and 4 weeks increased TRAP-positive osteoclasts after 1 week, while decreasing the BFR/BS in DBA/2 mice. Similarly, Dehoriy et al. (1999) found that osteoblast surface decreased starting at 1 week of microgravity, while BFR was decreased when measured over 0-2 weeks of microgravity. Mice exposed to 0.5, and 1 Gy of X-radiation showed a significant decrease in osteoblast colony numbers and significant increase in osteoclasts when compared to controls 3 days post-irradiation. In the same time frame, the mice also showed a significantly decreased BFR (Lima et al., 2017).

Essentiality

No study was found that blocked bone cell homeostasis following a stressor and observed the resulting effects on bone remodeling.

Uncertainties and Inconsistencies

None identified

Quantitative Understanding of the Linkage

The following are a few examples of quantitative understanding of the relationship. All reported findings are statistically significant at various alpha levels as listed in the original sources.

Response-response relationship**Dose/Incidence Concordance**

Reference	Experiment Description	Result
Chandra et al., 2017	<i>In vivo</i> . An experiment was conducted on male C57BL/6 mice (8-10 weeks old) exposed to 8 Gy X-ray radiation at a rate of 1.65 Gy/min to analyze suppression of Sclerostin on irradiated bones. Osteoblast number over bone surface (Ob.N/BS), and structural model index (SMI) (bone remodeling markers) were measured.	The group without the sclerostin with a monoclonal antibody (Scl-Ab) injections experienced a 52% decrease in osteoblast number, and 26% increase in SMI.
Chandra et al., 2014	<i>In vivo</i> . 3-month-old female rats were irradiated with 16 Gy of X-rays, fractionated into two 8 Gy doses at a rate of 1.65 Gy/min. To analyze the effects of ionizing radiation-induced bone remodeling, histometric measurements of Ob.N/BS and osteoclast number over bone surface (Oc.N/BS) and BFR, MAR, and SMI (bone remodeling markers) were measured.	Ob.N/BS and Oc.N/BS was 75% and 50% lower in the irradiated group compared to the non-irradiated group, respectively. Ionizing radiation exposure also resulted in a ~100% decrease in both BFR and MAR, as well as a ~20% increase in SMI, at 28 days post-irradiation relative to non-irradiated controls.
Hui et al., 2014	<i>In vivo</i> . 20-week-old adult female mice were exposed to a single 16 Gy dose of X-rays. CTX (osteoclast marker), OCN (osteoblast marker) and MAR (bone remodeling marker) of the distal femurs of irradiated mice were measured.	Compared to the non-irradiated controls, CTX levels increased 38.2% by 3 days after radiation and OCN levels increased by 18.3% by 30 days after radiation. Mice experiencing a 16% decrease per day in MAR by 12-29 days post irradiation.
Wright et al., 2015	<i>In vivo</i> . The right hindlimbs of 20-week-old male C57BL/6 mice were irradiated with 2 Gy of X-rays at a rate of 1.6 Gy/min. Ob.N/BS and Oc.N/BS were measured to assess altered bone cell homeostasis and osteoid volume (OV/BV), osteoid surface (OS/BS), BFR, and MS/BS were measured to assess bone remodeling.	Compared to the control group, and contralateral group, bone marrow adiposity was increased in the irradiated group. Mineralized bone surface decreased in the irradiated group and unmineralized osteoid surface area was increased. Irradiation led to 46% increase in Oc.N/BS, a (n.s.) 15% increase in Ob.N/BS, a 33% decrease in BFR and a 20% decrease in MS/BS. In irradiated femurs OV/BV and OS/BS were increased compared to controls.
Yang et al., 2020	<i>In vivo</i> . Male 14-week-old transgenic mice were unloaded using tail suspension. The tibia of wildtype and transgenic mice were scanned at 28 days after un-loading. Bone cell markers including ALP activity, OCN, and TRAP-5b levels and bone remodeling markers such as MAR, BFR, and MS/BS were measured.	Analysis showed a 50% decrease in ALP activity, 47.5% decrease in OCN activity, and 4-fold increase in TRAP-5b by day 7. This was accompanied by a 23% decrease in MAR, a 33% decrease in BFR, and a 50% decrease in MS/BS under microgravity relative to control.

Lloyd et al., 2015	<i>In vivo</i> . 77-day-old female C57BL/6 mice were exposed to 12 days of microgravity conditions during spaceflight. Histological measurements were taken from the femur and proximal tibiae of the mice to study the effects of microgravity. These measurements consisted of indicators of bone cell function such as TRAP-5b and OCN and bone remodeling markers including MS/BS, MAR, BFR, and SMI	OCN was decreased by 40% in control groups and by nearly 50% in the spaceflight group. TRAP-5b levels were unchanged in the control group and were increased by 200% in the spaceflight group. There was a 33% decrease in periosteal BFR, a 32% decrease in periosteal MS/BS, and a 40% decrease in endocortical BFR, a 29% decrease in endocortical MS/BS, and a 33% decrease in endocortical MAR. Lastly, there was a 50% decrease in trabecular BFR and a 6% increase in SMI.
Shahnazari et al., 2012	<i>In vivo</i> . 6-month-old adult male C57BL/6 and DBA/2 mice underwent hindlimb unloading for 1, 2, and 4 weeks to simulate the effects of microgravity. Measurements of calcified nodules and histological parameters were taken from cultured bone marrow cells and murine femurs, respectively. Levels of TRAP-positive cells (osteoclast marker) and BFR, MAR, MS/BS, and SMI (bone remodeling markers) were analyzed.	Compared to normally loaded controls, TRAP-positive osteoclasts increased by ~3.5-fold by week 1 of unloading and became non-significant after a week. By 1 week of unloading, there was a 70% and 60% decrease in calcified nodules in C57BL/6 and DBA/2 mice, respectively. While there was no significant change to BFR/BS in C57BL/6 mice, there was a ~33% decrease in DBA/2 mice at 2 weeks post-exposure. After 2 and 4 weeks, DBA/2 mice experienced significant decreases in MS/BS and MAR. SMI did not significantly change following unloading in either model.
Yotsumoto, Takeoka, and Yokoyama, 2010	<i>In vivo</i> . Eight-week-old male mice were tail-suspended. Deoxypyridinoline (DPD, osteoclast marker) and MAR, and BFR (bone remodeling markers) were measured to determine the effects of microgravity on bone remodeling.	Tail suspension resulted in a 50% decrease in OCN and 25% increase in DPD. This was accompanied by a 75% decrease in MAR and a 50% decrease in BFR under tail suspension.
Dehority et al., 1999	<i>In vivo</i> . Fifty-six 6-month-old virgin male Sprague-Dawley rats were unloaded using the hindlimb elevation model for 5 weeks. Osteoblast surface, BFR, and MAR (bone remodeling markers) levels were measured.	After 1 week of unloading, there was a 62.5% decrease in osteoblast surface, accompanied by an 80% decrease in BFR at the tibiofibular junction and a 33% decrease in MAR in the tibia after 2 weeks of unloading.
Matsumoto et al., 1998	<i>In vivo</i> . 6-week-old juvenile male rats underwent tail suspension for 14 days to simulate microgravity conditions. Histological measurements including osteoclast number, osteoblast surface and bone remodeling marker, MAR, of the femur and tibiae were measured.	Osteoclast number was 30% higher after tail suspension relative to controls at the same time point. Osteoblast surface was ~28% lower after tail suspension relative to controls. Tail suspension also resulted in a 48% decrease in periosteal MAR in the femur compared to baseline levels.
Wronski et al., 1987	<i>In vivo</i> . 84-day-old adult male, five large and six small, rats were exposed to microgravity conditions for 7 days during spaceflight. Osteoblast and osteoclast surface were measured along with BFR to assess altered bone cell homeostasis and bone remodeling, respectively.	Osteoclast surface increased 22% and osteoblast surface decreased 51% in large rats after spaceflight relative to controls. This was associated with a 34% decrease in BFR compared to the ground controls.
Bandstra et al., 2008	<i>In vivo</i> . 58-day-old, female, juvenile, C57BL/6 mice were exposed to whole-body irradiation with 0.5, 1, and 2 Gy of 250 MeV protons at a rate of 0.7 Gy/min. Histological measurements, including TRAP-5b, OCN (osteoclast markers) and periosteal BFR (Ps.BFR) and endosteal BFR (Ec.BFR) (bone remodeling marker) were measured.	All IR-induced changes to serum OCN and TRAP levels, along with BFR were non-significant compared to the control. TRAP-5b levels decreased in the 0.5 and 1 Gy group by 6% and 10%, respectively, and increased in the 2 Gy group by 2%. OCN levels were the same in the 1 Gy group and decreased in the 0.5 Gy and 2 Gy groups by 4%, and 18%, respectively. Ps.BFR increased by 5% and 14% after 0.5 and 1 Gy radiation, respectively; however, it remained unchanged post-2 Gy exposure. Ec.BFR decrease by 19%, 27%, and 21% after 0.5, 1, and 2 Gy, respectively.
Iwaniec et al., 2005	<i>In vivo</i> . 70-day-old female C56BL/6 F1 and DBA/2 mice underwent 1 week of hindlimb unloading to simulate microgravity conditions. Histological measurements were taken from the distal femur to study the effects of microgravity-induced bone remodeling. These measurements include BFR, an indicator of bone remodeling, and osteoblast and osteoclast surface, indicators of altered bone cell homeostasis.	Osteoclast surface was increased by 48% and osteoblast surface was decreased by 17% after hindlimb unloading. This was associated with a 43% decrease in BFR in wild type mice compared to control groups.

Time-scale**Time Concordance**

Reference	Experiment Description	Result
Shahnazari et al., 2012	<i>In vivo</i> . 6-month-old adult male C57BL/6 and DBA/2 mice underwent hindlimb unloading for 1, 2, and 4 weeks to simulate the effects of microgravity. Measurements of calcified nodules and histological parameters were taken from cultured bone marrow cells and murine femurs, respectively. Levels of TRAP-positive cells (osteoclast marker) and BFR, MAR, and MS (bone remodeling markers) were analyzed.	Compared to normally loaded controls, TRAP-positive osteoclasts increased by ~3.5-fold at week 1 of unloading but became non-significant after a week. Calcified nodule formation in both unloaded mouse models decreased significantly at all time points but progressively recovered from 1 to 4 weeks. C57BL/6 and DBA/2 mice saw maximum decreases of ~69% and ~61%, respectively, at 1 week of unloading. DBA/2 mice only experienced a significant decrease in BFR/BS at 2 weeks. BFR/BS in C57BL/6 mice did not change significantly at any time point. MS/BS and MAR both showed significant decreases in DBA/2 mice at 2 and 4 weeks.
Dehority et al., 1999	<i>In vivo</i> . Fifty-six 6-month-old male Sprague-Dawley rats were unloaded using the hindlimb elevation model for 5 weeks. Osteoblast surface (osteogenesis indicator), BFR, and MAR (bone remodeling markers) levels were measured.	Initial decrease in osteoblast surface at week 1 followed by a slight recovery at week 3 in unloaded rats; controls remained constant. At week 5 control rats showed a decrease in osteoblast surface and unloaded rats decreased to week 1 levels. BFR showed maximal decrease at week 2 of unloading and remained constant until week 4.
Hui et al., 2014	<i>In vivo</i> . 20-week-old adult female mice were exposed to a single 16 Gy dose of X-rays. CTX (osteoclast marker), OCN (osteoblast marker) and MAR (bone remodeling marker) of the distal femurs of irradiated mice were measured.	Compared to non-irradiated controls, CTX levels increased by 38.2% by 3 days after radiation. Irradiation resulted in the mice experiencing a 16% decrease per day in MAR by 12-29 days post irradiation.
Lima et al., 2017	<i>In vivo</i> . 4-month-old female BALB/CByJ mice were administered 0, 0.17, 0.5, and 1 Gy of X-rays. Osteoclast numbers were measured using a tartrate-resistant acid phosphatase (TRAP+) staining kit. Marrow aspirate was used to determine osteoblast colony-forming unit. Histomorphometry analysis and fluorochrome labeling was used to measure BFR.	3 days following radiation exposure, there was a significant increase in osteoclasts when compared to the control group. Osteoblast colony numbers were significantly decreased in the 0.5 Gy and the 1 Gy irradiated groups when compared to the control group 3 days post-exposure. 1 Gy and 0.5 Gy of radiation also significantly decreased BFR 3 days post-irradiation.

Known modulating factors

Modulating Factors	Details	Effects on the KER	References
Drug	Sclerostin (Wnt antagonist) suppression	Sclerostin, a Wnt antagonist, expression in adults is primarily restricted to osteocytes. The suppression of sclerostin was examined using Scl-Ab. Scl-Ab was found to completely reverse the effects of radiation on bone tissue. Scl-Ab injections not only blocked any structural deterioration, but also increased bone mass and improved bone quality in the radiated area to the same levels as in a non-radiated area with Scl-Ab treatment.	Chandra et al., 2017
Drug	Parathyroid hormone (PTH)1-34	Rats were given daily injections of human recombinant PTH (PTH1-34) to avoid the effects of ionizing radiation after being exposed to 16 Gy of X-rays. Compared to the irradiated group, rats treated with PTH1-34 had a 70.6% decrease in apoptotic osteoblasts (from 34 percent to 10 percent) and a 53% decrease in apoptosis in osteocytes.	Chandra et al., 2014

Age	Old age	Lower estrogen at old age is thought to contribute to higher osteoclast activity and increased bone resorption.	Pacheco and Stock, 2013
-----	---------	---	-------------------------

Known Feedforward/Feedback loops influencing this KER

Not Identified

References

Bandstra, E. R. et al. (2008), "Long-term dose response of trabecular bone in mice to proton radiation", *Radiation Research*, Vol. 169/6, BioOne, <https://doi.org/10.1667/RR1310.1>.

Bartell, S. M., et al. (2014), "FoxO proteins restrain osteoclastogenesis and bone resorption by attenuating H2O2 accumulation", *Nature communications*, Vol. 5. *Nature*, <https://doi.org/10.1038/ncomms4773>

Bikle, D. D. and B. P. Halloran. (1999), "The response of bone to unloading", *Journal of Bone and Mineral Metabolism*, Vol. 17/4, *Nature*, <https://doi.org/10.1007/s007740050090>.

Chandra, A. et al. (2017), "Suppression of Sclerostin Alleviates Radiation-Induced Bone Loss by Protecting Bone-Forming Cells and Their Progenitors Through Distinct Mechanisms", *Journal of Bone and Mineral Research*, Vol. 32/2, Wiley, <https://doi.org/10.1002/jbmr.2996>.

Chandra, A. et al. (2014), "PTH1-34 Alleviates Radiotherapy-induced Local Bone Loss by Improving Osteoblast and Osteocyte Survival", *Bone*, Vol. 67/1, Elsevier, Amsterdam, <https://doi.org/10.1016/j.bone.2014.06.030.PTH1-34>

Chatziravdeli, V., G. N. Katsaras and G. I. Lambrou. (2019), "Gene Expression in Osteoblasts and Osteoclasts Under Microgravity Conditions: A Systematic Review", *Current Genomics*, Vol. 20/3, Bentham Science Publishers, <https://doi.org/10.2174/1389202920666190422142053>.

Dehority, W. et al. (1999), "Bone and hormonal changes induced by skeletal unloading in the mature male rat", *American Journal of Physiology - Endocrinology and Metabolism*, Vol. 276/1, American Physiological Society, <https://doi.org/10.1152/ajpendo.1999.276.1.e62>.

Donaubauer, A. J. et al. (2020), "The influence of radiation on bone and bone cells—differential effects on osteoclasts and osteoblasts", *International Journal of Molecular Sciences*, Vol. 21/17, MDPI, Basel, <https://doi.org/10.3390/ijms21176377>.

Frost H. M. (1966), "Bone dynamics in metabolic bone disease" *The Journal of bone and joint surgery. American volume*, 48(6), 1192-1203.

Hui, S. K. et al. (2014), "The Influence of Therapeutic Radiation on the Patterns of Bone Remodeling in Ovary-Intact and Ovariectomized Mice", *Calcified Tissue International*, Vol. 23/1, *Nature*, <https://doi.org/10.1007/s00223-012-9688-0>

Iwaniec, U. T. et al. (2005), "Effects of disrupted β 1-integrin function on the skeletal response to short-term hindlimb unloading in mice", *Journal of Applied Physiology*, Vol. 98/2, American Physiological Society, <https://doi.org/10.1152/japplphysiol.00689.2004>.

Kozbenko, T. et al. (2022), "Deploying elements of scoping review methods for adverse outcome pathway development: a space travel case example", *International Journal of Radiation Biology*, Vol. 98/12, <https://doi.org/10.1080/09553002.2022.2110306>

Lima, F. et al. (2017), Exposure to Low-Dose X-Ray Radiation Alters Bone Progenitor Cells and Bone Microarchitecture. *Radiation Research*, 188(4.1), 433-442. <http://www.jstor.org/stable/26428489>

Lloyd, S. A. et al. (2015), "Osteoprotegerin is an effective countermeasure for spaceflight-induced bone loss in mice", *Bone*, Vol. 81, Elsevier, Amsterdam, <https://doi.org/10.1016/j.bone.2015.08.021>.

Matsumoto, T. et al. (1998), "Effect of mechanical unloading and reloading on periosteal bone formation and gene expression in tail-suspended rapidly growing rats", *Bone*, Vol. 22/5, Elsevier, Amsterdam, [https://doi.org/10.1016/S8756-3282\(98\)00018-0](https://doi.org/10.1016/S8756-3282(98)00018-0).

Morey-Holton, E. and S. B. Arnaud. (1991), "NASA Technical Memorandum 103890".

Pacheco, R. and H. Stock. (2013), "Effects of Radiation on Bone", *Current Osteoporosis Reports*, Vol. 11/4, *Nature*, <https://doi.org/10.1007/s11914-013-0174-z>

Raggatt, L. J., and Partridge, N. C. (2010), "Cellular and Molecular Mechanisms of Bone Remodeling", *Journal of Biological Chemistry*, Vol. 285/33, Elsevier, Amsterdam, <https://doi.org/10.1074/jbc.R109.041087>

Shahnazari, M. et al. (2012), "Simulated spaceflight produces a rapid and sustained loss of osteoprogenitors and an acute but transitory rise of osteoclast precursors in two genetic strains of mice", *American Journal of Physiology - Endocrinology and Metabolism*, Vol. 303/11, American Physiological Society, <https://doi.org/10.1152/ajpendo.00330.2012>.

Slyfield, C. R., et al. (2012), "Three-dimensional dynamic bone histomorphometry", *Journal of bone and mineral research*, Vol. 27/2, Wiley, <https://doi.org/10.1002/jbmr.553>.

Smith, J.K. (2020a), "Microgravity, Bone Homeostasis, and Insulin-Like Growth Factor-1", *Applied Sciences*, Vol. 10/13, MDPI, Basel, <https://doi.org/10.3390/app10134433>

Smith, J.K. (2020b), "Osteoclasts and Microgravity", *Life*, Vol. 10/9, MDPI, Basel, <https://doi.org/10.3390/life10090207>.

Stavnichuk, M., et al. (2020), "A systematic review and meta-analysis of bone loss in space travelers", *NPJ microgravity*, Vol. 6, *Nature*, <https://doi.org/10.1038/s41526-020-0103-2>.

Tahimic, C. G. T. and R. K. Globus. (2017), "Redox signaling and its impact on skeletal and vascular responses to spaceflight", *International Journal of Molecular Sciences*, Vol. 18/10, MDPI, Basel, <https://doi.org/10.3390/ijms18102153>.

Tian, Y. et al. (2017), "The Impact of Oxidative Stress on the Bone System in Response to the Space Special Environment", *International Journal of Molecular Sciences*, Vol. 18/10, MDPI, Basel, <https://doi.org/10.3390/ijms18102132>.

Willey, J. S. et al. (2011), "Ionizing Radiation and Bone Loss: Space Exploration and Clinical Therapy Applications", *Clinical Reviews in Bone and Mineral Metabolism*, Vol. 9, *Nature*, <https://doi.org/10.1007/s12018-011-9092-8>

Wright, L. E. et al. (2015), "Single-Limb Irradiation Induces Local and Systemic Bone Loss in a Murine Model", *Journal of Bone and Mineral Research*, Vol. 30/7, Wiley, <https://doi.org/10.1002/jbmr.2458>.

Wronski, T. J. et al. (1987), "Histomorphometric analysis of rat skeleton following spaceflight", *American Journal of Physiology - Regulatory Integrative and Comparative Physiology*, Vol. 252/2, <https://doi.org/10.1152/ajpregu.1987.252.2.r252>.

Xiao, W. et al. (2016), "Bone Remodeling under Pathological Conditions", *Frontiers of Oral Biology*, Vol. 18/April 2016, <https://doi.org/10.1159/000351896>.

Yang, J. et al. (2020), "Blocking Glucocorticoid Signaling in Osteoblasts and Osteocytes Prevents Mechanical Unloading-Induced Cortical Bone Loss", *Bone*, Elsevier, Amsterdam, <https://doi.org/10.1016/j.bone.2019.115108>.

Yotsumoto, N., M. Takeoka and M. Yokoyama. (2010), "Tail-suspended mice lacking calponin H1 experience decreased bone loss.", *The Tohoku journal of experimental medicine*, Vol. 221/3, Tohoku University Medical Press, Tohoku, <https://doi.org/10.1620/tjem.221.221>.

Zhang, J., et al. (2018), "Therapeutic ionizing radiation induced bone loss: a review of in vivo and in vitro findings", *Connective tissue research*, Vol. 59/6, Informa, London, <https://doi.org/10.1080/03008207.2018.1439482>

Relationship: 2845: Bone Remodeling leads to Bone Loss

AOPs Referencing Relationship

AOP Name	Adjacency	Weight of Evidence	Quantitative Understanding
Deposition of energy leading to occurrence of bone loss	adjacent	Moderate	Low

Evidence Supporting Applicability of this Relationship**Taxonomic Applicability**

Term	Scientific Term	Evidence	Links
rhesus monkeys	Macaca mulatta	Moderate	NCBI
human	Homo sapiens	Low	NCBI
mouse	Mus musculus	High	NCBI
rat	Rattus norvegicus	High	NCBI

Life Stage Applicability**Life Stage Evidence**

Adult	High
Juvenile	High

Sex Applicability**Sex Evidence**

Male	High
Female	High

Evidence for this relationship has been demonstrated *in vivo* for monkeys, mice, and rats, with considerable evidence from mice and rats. The relationship has been demonstrated *in vivo* for both males and females, with considerable evidence for both. There is *in vivo* evidence in adolescent and adult animals, with considerable evidence for both. However, less evidence supports a decrease in bone formation in mature animal models or humans.

Key Event Relationship Description

An imbalance in bone remodeling towards increased resorption of the organic and inorganic components of the bone matrix can lead to an increase in bone loss. Bone remodeling can facilitate bone loss through either stimulating the natural process of resorbing bone matrix back into the blood to facilitate vital processes, or by decreasing the deposition of replacement bone matrix, both of which result in increased bone loss. Changes to bone structure and the subsequent loss of bone results in changes to the portion of bone surface that is actively being mineralized (mineralizing surface, MS/BS). This can lead to measurable changes in the rate at which osteoid seams are mineralized (mineral apposition rate, MAR), and the amount of new bone formed per unit time in relation to the mineralizing surface (bone formation rate, BFR) (Dempster et al., 2013). The structural model index (SMI) of bone tissue, which measures the proportion of rods and plates in trabecular bone, is an important indicator of bone restructuring, with increased rod-like geometry being associated with reduced bone strength (Shahnazari et al., 2012). The resulting bone loss from dysregulated bone remodeling is characterized by deteriorated bone matrix, which is evident in measures of bone structure, including trabecular microarchitecture, cortical microarchitecture, and other measures of static bone histomorphometry, as well as measures of bone strength.

Evidence Supporting this KER

Overall weight of evidence: Moderate

Biological Plausibility

The biological plausibility supporting the link between bone remodeling and bone loss is highly supported and described well in review papers on the subject (Bikle and Halloran, 1999; Donaubauer et al., 2020; Morey-Holton and Arnaud, 1991; Smith, 2020; Tian et al., 2017). Bone loss is the result of inducing a decrease in bone formation and/or an increase in bone resorption by bone remodeling cells (Willey et al., 2011; Zhang et al., 2008). Osteoblasts generate new bone by secreting collagen and proteoglycans to form the unmineralized, organic bone matrix, and hydroxyapatite crystals to form the mineralized, inorganic component of the matrix (Donaubauer et al., 2020). The organic matrix, or osteoid, contribute strength and stability to bone, while hydroxyapatite crystals provide stiffness (Morey-Holton and Arnaud, 1991). Osteoclasts degrade bone matrix by attaching to the bone surface, forming a sealed resorption pit, and secreting hydrochloric acid to dissolve the hydroxyapatite crystals, as well as proteases such as Cathepsin K (CTSK) and matrix metalloproteinases (MMP9 and MMP14), to degrade the matrix proteins (Smith, 2020; Stavnickuk et al., 2020). Increased demineralization and resorption of bone matrix results in bone mineral density decreasing as organic matrix derivatives and mineral components, such as calcium and phosphorus, are stripped from the bone surface and resorbed into the blood stream (Bikle and Halloran, 1999; Morey-Holton and Arnaud, 1991).

Empirical Evidence

The empirical data relevant to this KER provides strong support for the linkage between bone remodeling and bone loss. Most of the evidence supporting this relationship comes from studies examining the effect of microgravity and X-ray radiation on the skeletal system. Both stressors induce a dose- and time-dependent imbalance in bone remodeling towards increased resorption that results in bone loss (Chandra et al., 2017; Chandra et al., 2014; Hefferan et al., 2003; Hu et al., 2020; Hui et al., 2014; Iwaniec et al., 2005; Iwasaki et al., 2002; Lloyd et al., 2015; Matsumoto et al., 1998; Shahnazari et al., 2012; Wang et al., 2020; Wright et al., 2015; Wronski et al., 1987; Zerath et al., 2002; Zerath et al., 2000).

Incidence Concordance

There is moderate support in current literature for an incidence concordance relationship between bone remodeling and bone loss. Many studies demonstrate an average change to endpoints of bone remodeling that are greater than or equal to that of bone loss (Chandra et al., 2017; Chandra et al., 2014; Hefferan et al., 2003; Hu et al., 2020; Hui et al., 2014; Ishijima et al., 2001; Iwaniec et al., 2005; Lloyd et al., 2015; Willey et al., 2010; Wright et al., 2015; Wronski et al., 1987; Yotsumoto, Takeoka, and Yokoyama, 2010; Zerath et al., 2002; Zerath et al., 2000).

Dose Concordance

Current literature on bone deterioration provides moderate evidence that bone remodeling occurs at lower or the same doses as bone loss. Studies that examine imbalances in bone remodeling caused by space-related stressors, namely ionizing radiation and microgravity, have observed both stressors induce significant decreases in bone formation that are associated with subsequent increases in bone loss. Exposure to microgravity conditions through simulated means, such as hindlimb unloading and tail suspension, or through authentic means, such as spaceflight, resulted in significant decreases in MS, MAR, and BFR, associated with diminished bone volume fraction (BV/TV) and bone mineral density (BMD). Studies that examined the effects of 1-4 weeks of microgravity exposure on mice observed significant decreases in bone remodeling parameters compared to control or baseline levels, from 33-75% for BFR, 33-90% for MAR, and 29% for MS/BS, as well as increases of 0-6% to SMI. These decreases in bone formation were accompanied by degradation to bone structure, as demonstrated by reduced BV/TV (26-82%) and volumetric BMD (vBMD) (12-28%) (Hu et al., 2020; Ishijima et al., 2001; Iwaniec et al., 2005; Lloyd et al., 2015; Shahnazari et al., 2012; Wang et al., 2020; Yotsumoto, Takeoka, and Yokoyama, 2010). Studies that examined microgravity-induced changes in rats after 1-4 weeks of exposure observed decreased MS/BS (70%), BFR (34-80%), MAR (20-50%), as well as increased SMI (9%). These decreases in bone formation were accompanied by bone loss, including 11-69% less BV/TV and 25-45% less BMD (Hefferan et al., 2003; Iwasaki et al., 2002; Matsumoto et al., 1998; Wronski et al., 1987; Zerath et al., 2000).

Studies that utilize ionizing radiation provide the best support for dose-dependence, as they show the variances in bone remodeling and bone loss when exposed to a range of radiation doses. Chandra et al. (2017; 2014) observed significant increases in SMI (~20% and 26%) following irradiation with 8 and 16 Gy of small animal

radiation research platform (SARRP) X-rays, indicating a shift in trabecular geometry towards the weaker rod-like trabeculae. This change in the proportion of plates and rods in trabecular bone was associated with decreases to BMD (30% and 14.3%), BV/TV (31% and 17.7%), and trabecular number (Tb.N) (13% and 17.7%), as well as increases in trabecular separation (Tb.Sp) (19% and ~25%), indicating that rod-like trabeculae are more susceptible to bone loss (Chandra et al., 2017; Chandra et al., 2014).

Time Concordance

In the current literature there is limited evidence for a time-dependent relationship between bone remodeling and bone loss. Certain studies examined the effects of microgravity or ionizing radiation-induced bone remodeling on bone loss over a span of time (Hui et al., 2014; Shahnazari et al., 2012). Each study found that changes to their measurement of interest generally increased over time. When examining MAR Hui et al. (2014) observed a decrease by 15.7% per day when measured 12-29 days post-irradiation. They also found a significant decrease in BV/TV at day 30 after exposure to 16 Gy of ionizing radiation (Hui et al., 2014).

After hindlimb unloading, Shahnazari et al. (2012) found that their C57BL/6 and DBA/2 mice both displayed a linear, time-dependent decrease in BV/TV when measured at 1, 2, and 4 weeks, with C57BL/6 mice also exhibiting the same trend in total bone mineral density (BMD/TV). Both bone loss and remodeling showed the first significant decrease after 2 weeks of microgravity (Shahnazari et al., 2012). Bone remodeling and bone loss generally occur at similar time points, with bone remodeling being observed to substantially decrease as early as 1 week of exposure, as demonstrated by the reduction in calcium nodule formation (Hui et al., 2014; Shahnazari et al., 2012). Lima et al. (2017) observed a significant decrease of BFR in 1 Gy irradiated mice 3 days post irradiation. 21 days post irradiation, mice also showed a significant decrease in cancellous bone volume fraction along with a 21% decrease in trabecular bone volume.

Essentiality

Few studies were found that blocked bone remodeling following a stressor and observed the resulting effects on bone loss. Mice exposed to microgravity showed reduced bone formation through decreased MAR and BFR as well as bone loss through decreased BV/TV (Ishijima et al., 2001). Bone remodeling blocked by knockout of osteopontin, a protein that mediates bone remodeling following mechanical stress, resulted in restoration of bone formation and BV/TV (Ishijima et al., 2001). Similarly, inhibition of Calponin h1, a negative regulator of bone formation, restored the indices of bone formation and subsequently increased BMD following microgravity (Yotsumoto, Takeoka, and Yokoyama, 2010).

Uncertainties and Inconsistencies

- Following exposure to 16 Gy of radiation, mice experienced a significant increase in trabecular BV/TV on day 8 post-irradiation relative to the non-irradiated controls, contrary to the expected outcome of decreased BV/TV (Hui et al., 2014).
- Mice exposed to 4.4cGy of X-rays experienced significant decrease in the SMI and a significant increase in trabecular BV/TV compared to the non-irradiated controls, contrary to the expected outcomes of decreased BV/TV and increased SMI (Karim and Judex, 2014).

Quantitative Understanding of the Linkage

The following are a few examples of quantitative understanding of the relationship. All data represented is statistically significant unless otherwise indicated.

Response-response relationship

Dose/Incidence Concordance

Reference	Experiment Description	Result
Chandra et al., 2017	<i>In vivo</i> . The femoral metaphyseal osteoblasts and osteocytes of 8- to 10-week-old male mice were irradiated with 8 Gy of focal SARRP X-ray radiation at a rate of 1.65 Gy/min. Histomorphometric parameters including MS, BFR, and SMI for bone remodeling and vBMD, BV/TV, Tb.N, and trabecular separation (Tb.Sp) for bone loss were measured.	Irradiated mice experienced an 86% decrease in MS, a 100% decrease in BFR, and a 26% increase in SMI. The reduction in bone formation and increase in bone resorption was accompanied by a 30% decrease in vBMD, a 31% decrease in BV/TV, a 13% decrease in Tb.N, and a 19% increase in Tb.Sp.
Chandra et al., 2014	<i>In vivo</i> . 3-month-old female rats were irradiated with 16 Gy of SARRP X-rays, fractionated into two 8 Gy doses at a rate of 1.65 Gy/min. Measurements in rat tibiae consisted of indicators of bone remodeling, including MS, BFR, and SMI, and indicators of bone loss, including BMD, BV/TV, Tb.N, and Tb.Sp.	Ionizing radiation exposure resulted in a ~100% decrease in both BFR and MAR, as well as a ~20% increase in SMI, at 28 days post-irradiation relative to non-irradiated controls. The reduction in bone formation was accompanied by a 14.3% decrease in BMD, a 17.7% decrease in BV/TV, a 17.7% decrease Tb.N, and a ~25% increase in Tb.Sp.
Hui et al., 2014	<i>In vivo</i> . 20-week-old adult female mice were irradiated with a single dose of 16 Gy. Measurements in the distal femur included MAR, an indicator of bone remodeling, as well as BV/TV and cortical thickness (Ct.Th), indicators of bone loss.	X-ray irradiation resulted in the mice experiencing a 15.7%/day decrease in MAR from day 12-29 post-irradiation compared to non-irradiated controls. The reduction in bone formation was accompanied by a 0.5-fold decrease in trabecular BV/TV by day 30.
Wright et al., 2015	<i>In vivo</i> . The hindlimbs of 20-week-old adult male mice were irradiated with 2 Gy of X-rays at a rate of 1.6 Gy/min, respectively. Measurements in the tibia and femur consisted of indicators of bone remodeling, including MS and BFR, and the indicator of bone loss, BV/TV.	By 1-week post-irradiation, there was a ~30% and ~52% decrease in BFR and MS, respectively. The decrease in bone formation was accompanied by a 14% and 22% decrease in BV/TV in the distal femur and proximal tibia, respectively, compared to baseline levels.
Willey et al., 2010	<i>In vivo</i> . 20-week-old, adult, female, C57BL/6 mice were exposed to whole body irradiation with 2 Gy of 140 kVp X-rays at a rate of 1.36 Gy/min. Histological measurements were taken from the tibiae to examine the effects of bone remodeling on bone loss. These measurements included BFR, indicator of bone remodeling, and BV/TV, connectivity density (Conn.D), Tb. N, trabecular thickness (Tb. Th), Tb. Sp, vBMD, and Marrow volume (Ma.V), indicators of bone loss.	Following irradiation, the BFR decreased dramatically by 92% after 1 week of irradiation. However, it reached 50% below baseline levels after 3 weeks. This reduction in bone formation was accompanied by a 13% decrease in Tb. N after 1 week, a 15% increase in Tb. Sp after 1 week, and a 21% decrease in vBMD after 3 weeks. There was no significant change in Tb. Th. Additionally, 30% decrease in BV/TV and a 53% decrease in Conn.D in the proximal tibiae after 3 weeks. Ma.V was decreased by 5% at the end of week 3 (non-significant).
Wang et al., 2020	<i>In vivo</i> . 6-month-old male C57BL/6J mice were subjected to 3 weeks of hindlimb unloading. Histological measurements were taken from the distal femurs of the mice to study the effects bone remodeling on bone loss. These measurements included MAR, an indicator of bone remodeling, and BV/TV, an indicator of bone loss.	Following hindlimb unloading, mice experienced a 67% decrease in MAR compared to 1G controls. The decrease in bone formation was accompanied by a 75% decrease in BV/TV.
Hu et al., 2020	<i>In vivo</i> . 6-month-old adult male mice underwent hindlimb unloading for 3 weeks to simulate the effects of microgravity. Histological measurements were taken from the femurs of the mice to study the effects of bone remodeling on bone loss. These measurements consisted of indicators for bone remodeling, including MAR and BFR, and indicators for bone loss, including BMD and BV/TV.	Following hindlimb unloading, mice experienced a ~90% decrease in MAR and a ~75% decrease in BFR compared to baseline levels. The decrease in bone formation was accompanied by a ~28% decrease in BMD and a ~82% decrease in BV/TV.
Lloyd et al., 2015	<i>In vivo</i> . 77-day-old female C57BL/6J mice were exposed to 12 days of spaceflight. Histological measurements were taken from the femur and proximal tibiae of the mice to study the effects of bone remodeling on bone loss. These measurements consisted of indicators of bone remodeling, including MS, MAR, BFR, and SMI, and indicators of bone loss, including BV/TV, cortical volume (Ct.V), and vBMD.	The histology of the spaceflight group was compared against the control and the authors found there was a 33% decrease in periosteal BFR, a 32% decrease in periosteal MS/BS, and a 40% decrease in periosteal MAR. There was also a 40% decrease in endocortical BFR, a 29% decrease in endocortical MS/BS, and a 33% decrease in endocortical MAR. Lastly, there was a 50% decrease in trabecular BFR and a 6% increase in SMI. This reduction in bone formation was accompanied by a 26% decrease in BV/TV, a 7% decrease in femur Ct.V, and a 12% decrease in vBMD.

Shahnazari et al., 2012	<i>In vivo</i> . 6-month-old adult male C57BL/6 and DBA/2 mice underwent hindlimb unloading for 1, 2, and 4 weeks to simulate the effects of microgravity. Measurements of calcified nodules and histological parameters were taken from cultured bone marrow cells and murine femurs, respectively, to study the effects of bone remodeling on bone loss. These histological measurements consisted of indicators of bone remodeling, including BFR, MAR, MS, and SMI, and indicators of bone loss, including BMD, Ct.V, and BV/TV.	While there was no significant change to BFR in C57BL/6 mice, there was a ~33% decrease in DBA/2 mice at 2 weeks post-exposure. After 2 and 4 weeks, DBA/2 mice experienced significant decreases in MS/BS and MAR. SMI did not significantly change following unloading in either model. This reduction in bone formation was accompanied by a progressive decrease in BV/TV, with maximum decreases of 44% and 35% in C57BL/6 and DBA/2 mice, respectively, and significant decreases of ~25% and ~20% at 2 weeks in C57BL/6 and DBA/2 mice, respectively. There was no significant change to Ct.V following unloading.
Iwaniec et al., 2005	<i>In vivo</i> . 70-day-old female C56BL/6 F1 and DBA/2 mice underwent 1 week of hindlimb unloading to simulate microgravity conditions. Histological measurements were taken from the distal femur to study the effects of bone remodeling on bone loss. These measurements included BFR, an indicator of bone remodeling, and bone volume, an indicator of bone loss.	Hindlimb unloading resulted in wild type mice experiencing a 43% decrease in BFR compared to control groups. The decrease in bone formation was accompanied by a 33% decrease in cancellous bone volume.
Hefferan et al., 2003	<i>In vivo</i> . 6-month-old adult rats underwent 14 days of hindlimb unloading to simulate the microgravity conditions. Histological measurements were taken from the tibiae to study the effects of bone remodeling on bone loss. These measurements included BFR and MAR, indicators of bone remodeling, as well as BV/TV and cortical area, indicators of bone loss.	Following hindlimb unloading, there was a ~50% and 33% decrease in MAR in female and male rats, respectively, compared to control groups. There was an 80% decrease in BFR in both male and female rats. This reduction in bone formation was accompanied by an 11% and 18% decrease in BV/TV in female and male mice, respectively. There was no significant change to cortical area between unloaded and ground controls in either male or female rats.
Zerath et al., 2002	<i>In vivo</i> . 3- to 4-year-old male rhesus monkeys spent 14 days in spaceflight. Histological measurements of their iliac bone were taken upon landing to study the effects of bone remodeling on bone loss. These measurements consisted of indicators of bone remodeling, including BFR, MAR, and MS, and cancellous bone volume, an indicator of bone loss.	Following microgravity exposure, the monkeys experienced a 33% decrease in MAR, a 53% decrease in BFR, and a 32% decrease in MS/BS compared to pre-flight values. This reduction in bone formation was accompanied by a 35% decrease in BV/TV.
Iwasaki et al., 2002	<i>In vivo</i> . 13-week-old adult male rats underwent 4 weeks of tail suspension to simulate microgravity conditions. Histological measurements were taken from the tibiae of the rats to study the effects of bone remodeling on bone loss. These measurements consisted of indicators of bone remodeling, including BFR and MAR, and indicators of bone loss, including BV/TV and BMD.	Following tail suspension, there was a 20% decrease in MAR and a 39% decrease in BFR in rat tibiae compared to non-suspended controls. This reduction in bone formation was accompanied by a 45% decrease in tibiae BMD and a 69% decrease in BV/TV.
Zerath et al., 2000	<i>In vivo</i> . 9-week-old juvenile male rats were exposed to 17 days of spaceflight and histological measurements were taken from pelvic tissue upon landing to study the effects of bone remodeling on bone loss. These measurements included BFR and MAR, indicators of bone remodeling, and BV/TV, an indicator of bone loss.	Microgravity exposure resulted in a 52% decrease in BFR and a 34% decrease in MAR compared to the animal enclosure model (AEM) ground control. This reduction in bone formation was accompanied by a 12% decrease in BV/TV compared to the AEM ground control.
Matsumoto et al., 1998	<i>In vivo</i> . 6-week-old juvenile male rats underwent tail suspension for 14 days to simulate microgravity conditions. Histological measurements of the femur and tibiae were taken to study the effects of bone remodeling on bone loss. These measurements included MAR, an indicator of bone remodeling, as well as BMD and BV/TV, indicators of bone loss.	Tail suspension resulted in a 48% decrease in periosteal MAR in the femur compared to baseline levels. This reduction in bone formation was accompanied by a 67% decrease in tibial BV/TV compared to baseline levels. The average of BMD levels across multiple regions of the femur were also significantly reduced.
Wronski et al., 1987	<i>In vivo</i> . 84-day-old adult male rats were exposed to 7 days of spaceflight and histological measurements were taken from their tibiae to study the effect of bone remodeling on bone loss. These measurements included periosteal BFR, an indicator of bone remodeling, and trabecular bone volume, an indicator of bone loss.	Microgravity resulted in a 34% decrease compared to the ground controls. The reduction in bone formation was accompanied by a 28% decrease in trabecular bone volume compared to ground controls.
Yang et al., 2020	<i>In vivo</i> . Male 14-week-old transgenic mice were unloaded using tail suspension. The tibia of wildtype and transgenic mice were scanned at 28 days after un-loading. Bone remodeling markers such as MAR, BFR, and MS/BS were measured. BV/TV was used as a bone loss marker.	Following hindlimb unloading, there was a 23% decrease in MAR, a 33% decrease in BFR, and a 50% decrease in MS/BS under microgravity relative to control. This was accompanied by a 58% decrease in BV/TV.
Yotsumoto, Takeoka, and Yokoyama, 2010	<i>In vivo</i> . Eight-week-old male mice were tail-suspended. MAR, and BFR as bone remodeling markers and BV/TV and BMD as bone loss markers were measured.	75% decrease in MAR and 50% decrease in BFR under tail suspension was accompanied by a 50% decrease in BV/TV and a 25% decrease in BMD.
Ishijima et al., 2001	<i>In vivo</i> . Female 12-week-old mice were tail-suspended. MAR, and BFR as bone remodeling markers and BV/TV as bone loss marker were measured.	68% decrease in BFR and a 40% decrease in MAR in tail-suspended mice. This was accompanied by a 50% decrease in BV/TV.

Time-scale**Time Concordance**

References	Experiment Description	Result
Hui et al., 2014	<i>In vivo</i> . 16-week-old adult female mice were irradiated with a single dose of 16 Gy. Histological measurements of the distal femurs of the mice were taken to study the effects of bone remodeling on bone loss. These measurements included MAR, an indicator of bone remodeling (upstream KE), and BV/TV, an indicator of bone loss (downstream KE).	X-ray irradiation resulted in the mice experiencing a 15.7%/day decrease in MAR from day 12-29 post-irradiation compared to non-irradiated controls. Trabecular BV/TV decreased 0.5-fold at day 30.
Shahnazari et al., 2012	<i>In vivo</i> . 6-month-old adult male C57BL/6 and DBA/2 mice underwent hindlimb unloading for 1, 2, and 4 weeks to simulate the effects of microgravity. Measurements of calcified nodules and histological parameters were taken from cultured bone marrow cells and murine femurs, respectively, to study the effects of bone remodeling on bone loss. The histological measurements consisted of indicators of bone remodeling, including BFR, MAR, and MS, and indicators of bone loss, including BMD and BV/TV.	DBA/2 mice only experienced a significant decrease in BFR at 2 weeks. BFR in C57BL/6 mice did not change significantly at any time point. MS/BS and MAR both showed significant decreases in DBA/2 mice at 2 and 4 weeks. Both BV/TV and BMD/TV decreased in a linear, time-dependent manner in C57BL/6 mice with significant decreases at 2 and 4 weeks. Reductions in the BV/TV of DBA/2 mice also followed a linear, time-dependent trend, with significant decreases at 2 and 4 weeks. DBA/2 mice only saw a significant decrease in BMD/TV at 2 weeks.
Lima et al., 2017	<i>In vivo</i> . 4-month-old female BALB/cBYJ mice were administered 0, 0.17, 0.5, and 1 Gy of X-ray radiation. Histomorphometry analysis and fluorochrome labeling was used to measure BFR. BV/TV was analyzed using micro-computed tomography (micro-CT).	1 Gy of radiation significantly decreased bone formation rate 3 days post-irradiation. At 21 days post-irradiation, a significant decrease in cancellous bone volume fraction occurred, along with a 21% decrease in trabecular bone volume.

Known modulating factors

Modulating factor	Details	Effects on the KER	References
Genetic	Sclerostin knockout	Sclerostin knockout mice blocked structural deterioration and improved bone quality after radiation.	Chandra et al., 2017
Drug	Parathyroid hormone1-34	Treatment led to a full recovery of all static bone histomorphometric parameters after irradiation.	Chandra et al., 2014
Drug	ODSM	Treatment partially recovered MAR and BV/TV in tibia.	Wang et al., 2020
Drug	Antagomir-132	Partially reversed MAR, BFR and BV/TV and completely reversed BMD.	Hu et al., 2020
Drug	Osteoprotegerin	Treatment reversed spaceflight-induced bone loss.	Lloyd et al., 2015

Genetic	Calponin h1 knockout	Calponin h1 knockout mice showed attenuated bone loss and no significant changes in bone remodeling markers under tail suspension.	Yotsumoto, Takeoka, and Yokoyama, 2010
Genetic	Osteopontin knockout	Osteopontin knockout mice showed no significant changes in bone loss and bone remodeling markers when exposed to a tail suspension model.	Ishijima et al., 2001
Age	Old age	Lower estrogen at old age is thought to contribute to the detrimental effects of radiotherapy on bone loss in elderly patients.	Pacheco and Stock, 2013

Known Feedforward/Feedback loops influencing this KER

Not Identified

References

Bikle, D. D. and B. P. Halloran. (1999), "The response of bone to unloading", *Journal of Bone and Mineral Metabolism*, Vol. 17/4, *Nature*, <https://doi.org/10.1007/s007740050090>.

Chandra, A. et al. (2017), "Suppression of Sclerostin Alleviates Radiation-Induced Bone Loss by Protecting Bone-Forming Cells and Their Progenitors Through Distinct Mechanisms", *Journal of Bone and Mineral Research*, Vol. 32/2, Wiley, <https://doi.org/10.1002/jbmr.2996>.

Chandra, A. et al. (2014), "PTH1-34 Alleviates Radiotherapy-induced Local Bone Loss by Improving Osteoblast and Osteocyte Survival", *Bone*, Vol. 67/1, Elsevier, Amsterdam, [https://doi.org/10.1016/j.bone.2014.06.030.PTH1-34](https://doi.org/10.1016/j.bone.2014.06.030).

Donaubauer, A. J. et al. (2020), "The influence of radiation on bone and bone cells—differential effects on osteoclasts and osteoblasts", *International Journal of Molecular Sciences*, Vol. 21/17, MDPI, Basel, <https://doi.org/10.3390/ijms21176377>.

Frost H. M. (1966), "Bone dynamics in metabolic bone disease" *The Journal of bone and joint surgery. American volume*, 48(6), 1192-1203.

Hefferan, T. E. et al. (2003), "Effect of gender on bone turnover in adult rats during simulated weightlessness", *Journal of Applied Physiology*, Vol. 95/5, American Physiological Society, <https://doi.org/10.1152/japplphysiol.00455.2002>.

Hu, Z. et al. (2020), "Targeted silencing of miRNA-132-3p expression rescues disuse osteopenia by promoting mesenchymal stem cell osteogenic differentiation and osteogenesis in mice", *Stem Cell Research and Therapy*, Vol. 11/1, *Nature*, <https://doi.org/10.1186/s13287-020-1581-6>.

Hui, S. K. et al. (2014), "The Influence of Therapeutic Radiation on the Patterns of Bone Remodeling in Ovary-Intact and Ovariectomized Mice", *Calcified Tissue International*, Vol. 23/1, *Nature*, <https://doi.org/10.1007/s00223-012-9688-0>.

Ishijima, M. et al. (2001), "Enhancement of Osteoclastic Bone Resorption and Suppression of Osteoblastic Bone Formation in Response to Reduced Mechanical Stress Do Not Occur in the Absence of Osteopontin", *The Journal of Experimental Medicine*, Vol. 193/3, <https://doi.org/10.1084/jem.193.3.399>.

Iwaniec, U. T. et al. (2005), "Effects of disrupted $\beta 1$ -integrin function on the skeletal response to short-term hindlimb unloading in mice", *Journal of Applied Physiology*, Vol. 98/2, American Physiological Society, <https://doi.org/10.1152/japplphysiol.00689.2004>.

Iwasaki, Y. et al. (2002), "Maintenance of trabecular structure and bone volume by vitamin K 2 in mature rats with long-term tail suspension", *Journal of Bone and Mineral Metabolism*, Vol. 20/4, *Nature*, <https://doi.org/10.1007/s007740200031>.

12. Karim, L. and S. Judex. (2014), "Low level irradiation in mice can lead to enhanced trabecular bone morphology", *Journal of bone and mineral metabolism*, Vol. 32/5, 476-483. <https://doi.org/10.1007/s00774-013-0518-x>

13. Lima, F. et al. (2017). Exposure to Low-Dose X-Ray Radiation Alters Bone Progenitor Cells and Bone Microarchitecture. *Radiation Research*, 188(4.1), 433-442. <http://www.jstor.org/stable/26428489>

Lloyd, S. A. et al. (2015), "Osteoprotegerin is an effective countermeasure for spaceflight-induced bone loss in mice", *Bone*, Vol. 81, Elsevier, <https://doi.org/10.1016/j.bone.2015.08.021>.

Matsumoto, T. et al. (1998), "Effect of mechanical unloading and reloading on periosteal bone formation and gene expression in tail-suspended rapidly growing rats", *Bone*, Vol. 22/5, Elsevier, [https://doi.org/10.1016/S8756-3282\(98\)00018-0](https://doi.org/10.1016/S8756-3282(98)00018-0).

Morey-Holton, E. and S. B. Arnaud. (1991), "NASA Technical Memorandum 103890".

Pacheco, R. and H. Stock. (2013), "Effects of Radiation on Bone", *Current Osteoporosis Reports*, Vol. 11/4, *Nature* <https://doi.org/10.1007/s11914-013-0174-z>

Shahnazari, M. et al. (2012), "Simulated spaceflight produces a rapid and sustained loss of osteoprogenitors and an acute but transitory rise of osteoclast precursors in two genetic strains of mice", *American Journal of Physiology - Endocrinology and Metabolism*, Vol. 303/11, American Physiological Society, <https://doi.org/10.1152/ajpendo.00330.2012>.

Slyfield, C. R., et al. (2012), "Three-dimensional dynamic bone histomorphometry", *Journal of bone and mineral research*, Vol. 27/2, Wiley, <https://doi.org/10.1002/jbmr.553>.

Smith, J. K. (2020), "Osteoclasts and microgravity", *Life*, Vol. 10/9, MDPI, Basel, <https://doi.org/10.3390/life10090207>.

Stavnichuk, M., et al. (2020), "A systematic review and meta-analysis of bone loss in space travelers", *NPJ microgravity*, Vol. 6, *Nature*, <https://doi.org/10.1038/s41526-020-0103-2>.

Tian, Y. et al. (2017), "The Impact of Oxidative Stress on the Bone System in Response to the Space Special Environment", *The International Journal of Molecular Sciences*, Vol. 18/10, MDPI, Basel, <https://doi.org/10.3390/ijms18102132>.

Wang, Y. et al. (2020), "Targeted Overexpression of the Long Noncoding RNA ODSM can Regulate Osteoblast Function In Vitro and In Vivo", *Cell Death and Disease*, Vol. 11, Springer Nature, Berlin, <https://doi.org/10.1038/s41419-020-2325-3>.

Willey, J. S. et al. (2011), "Ionizing Radiation and Bone Loss: Space Exploration and Clinical Therapy Applications", *Clinical Reviews in Bone and Mineral Metabolism*, Vol. 9, *Nature*, <https://doi.org/10.1007/s12018-011-9092-8>.

Willey, J. S. et al. (2010), "Risedronate prevents early radiation-induced osteoporosis in mice at multiple skeletal locations", *Bone*, Vol. 46/1, Elsevier, <https://doi.org/10.1016/j.bone.2009.09.002>.

Wright, L. E. et al. (2015), "Single-Limb Irradiation Induces Local and Systemic Bone Loss in a Murine Model", *Journal of Bone and Mineral Research*, Vol. 30/7, Wiley, <https://doi.org/10.1002/jbmr.2458>

Wronski, T. J. et al. (1987), "Histomorphometric analysis of rat skeleton following spaceflight", *American Journal of Physiology - Regulatory Integrative and Comparative Physiology*, Vol. 252/2, American Physiological Society, <https://doi.org/10.1152/ajpregu.1987.252.2.r252>.

Yang, J. et al. (2020), "Blocking Glucocorticoid Signaling in Osteoblasts and Osteocytes Prevents Mechanical Unloading-Induced Cortical Bone Loss", *Bone*, Elsevier, Amsterdam, <https://doi.org/10.1016/j.bone.2019.115108>.

Yotsumoto, N., M. Takeoka and M. Yokoyama. (2010), "Tail-suspended mice lacking calponin H1 experience decreased bone loss.", *The Tohoku journal of experimental medicine*, Vol. 221/3, Tohoku University Medical Press, Tohoku, <https://doi.org/10.1620/tjem.221.221>.

Zérath, E. et al. (2002), "Spaceflight affects bone formation in rhesus monkeys: A histological and cell culture study", *Journal of Applied Physiology*, Vol. 93/3, American Physiological Society, <https://doi.org/10.1152/japplphysiol.00610.2001>.

Zerath, E. et al. (2000), "Spaceflight inhibits bone formation independent of corticosteroid status in growing rats", *Journal of Bone and Mineral Research*, Vol. 15/7, Wiley, <https://doi.org/10.1359/bmr.2000.15.7.1310>.

Zhang, P. et al. (2008), "A brief review of bone adaptation to unloading." *Genomics, proteomics and bioinformatics*, Vol. 6/1, Elsevier, Amsterdam,

[https://doi.org/10.1016/S1672-0229\(08\)60016-9](https://doi.org/10.1016/S1672-0229(08)60016-9)

List of Non Adjacent Key Event Relationships

Relationship: 2846: Oxidative Stress leads to Altered Bone Cell Homeostasis

AOPs Referencing Relationship

AOP Name	Adjacency	Weight of Evidence	Quantitative Understanding
Deposition of energy leading to occurrence of bone loss	non-adjacent	Moderate	Low

Evidence Supporting Applicability of this Relationship

Taxonomic Applicability

Term	Scientific Term	Evidence	Links
human	Homo sapiens	Low	NCBI
mouse	Mus musculus	High	NCBI
rat	Rattus norvegicus	Moderate	NCBI

Life Stage Applicability

Life Stage	Evidence
Adult	Moderate
Juvenile	Moderate

Sex Applicability

Sex	Evidence
Male	Moderate
Female	Low

The evidence for the taxonomic applicability to humans is low as majority of the evidence is from *in vitro* human-derived cells. The relationship is supported by mice and rat models using male and female animals. The relationship is plausible at any life stage. However, most studies have used adolescent and adult animal models.

Key Event Relationship Description

The tight regulation of differentiation pathways leading to bone-forming osteoblasts (osteoblastogenesis) and bone-resorbing osteoclasts (osteoclastogenesis) is essential for the maintenance of osteogenic balance, i.e., the deposition and resorption of bone matrix. As such, perturbations by the overproduction of reactive oxygen species (ROS) during oxidative stress can have devastating effects on the delicate balance of bone cell (i.e., osteocyte, osteoclast, and osteoblast) differentiation and function.

Oxidative stress disrupts the homeostatic balance of osteoblastic bone deposition and osteoclastic bone resorption by altering the osteoblastogenic/osteoclastogenic differentiation pathways through the overproduction of ROS (Agidigbi and Kim, 2019; Tian et al., 2017). Briefly, ROS produced in pre-osteoblasts and pre-osteoclasts will affect the activities of different signaling molecules in the respective cell types. In osteoblasts, ROS naturally upregulate expression of the transcription factor forkhead box O (FoxO) which enhances cell antioxidant status. FoxO requires β -catenin binding, which sequesters β -catenin from the main osteoblast differentiation pathway, the Wnt/ β -catenin pathway, ultimately downregulating osteoblastogenesis and the expression of alkaline phosphatase (ALP) and osteocalcin (OCN) (Manolagas and Almeida, 2007; Tian et al., 2017). Further, ROS upregulate the receptor activator of nuclear factor kappa B ligand (RANK-L), which is the main regulator of osteoclastogenesis. By increasing RANK-L production, ROS inhibits osteoclast apoptosis and promotes osteoclastogenesis and the expression of tartrate-resistant acid phosphatase (TRAP), Cathepsin K (CTSK), and HCl (Tian et al., 2017).

Evidence Supporting this KER

Overall weight of evidence: Moderate

Biological Plausibility

The biological rationale for connection of increased oxidative stress to altered bone cell homeostasis is well-supported by research. Tian et al. (2017) reviewed the influence of oxidative stress on osteoblasts and osteoclasts by the increased production of ROS and its resulting effect on bone resorption and deposition in the space environment. Several other papers evaluated the impact of oxidative stress on osteoclastogenesis and osteoblastogenesis and the crucial role of ROS in up and downregulation of bone resorption and deposition (Agidigbi and Kim, 2019; Bartell et al., 2014; Donaubauer et al., 2020; Maeda et al., 2019; Manolagas et al., 2007; Tahimic and Globus, 2017).

Increased ROS production during oxidative stress plays crucial and opposing roles in osteoclast and osteoblast differentiation, activation and inhibition, respectively. Cells use FoxO transcription factors to defend against oxidative stress by upregulating production of antioxidant enzymes. In osteoblasts, FoxO-mediated transcription differs between mature osteoblasts and differentiating osteoblasts precursors (Almeida 2011). In mature osteoblasts FoxO directly regulates the transcription of genes involved in cell survival and proliferation (Almeida 2011). During differentiation of osteoblasts precursors FoxO requires binding of β -catenin before translocating into the nucleus and regulating gene expression (Almeida 2011). β -catenin is also a well-known component of the Wnt/ β -catenin signaling pathway which is essential to osteoblast differentiation. Thus, increased FoxO production under oxidative stress divert β -catenin, directly downregulating osteoblast differentiation and deposition of bone matrix (Maeda et al., 2019; Manolagas et al., 2007; Tian et al., 2017).

The opposite effect was found in osteoclasts. Increased ROS production in osteoblasts enhances the production of RANK-L, a ligand for RANK, the main regulator of osteoclast differentiation. Upon RANK-RANK-L interaction, transcription and translation of osteoclast-specific genes involved in bone matrix resorption by nuclear factor of activated T cells 1 (NFATc1), the master transcription factor for osteoclastogenesis, occurs (Donaubauer et al., 2020; Tahimic and Globus, 2017; Tian et al., 2017). Further, RANK-RANKL interaction suppresses FoxO transcription in osteoclasts feeding osteoclastogenesis (Bartell et al., 2014). Accumulation of H2O2, the most abundant form of ROS, is pivotal for osteoclastogenesis as it stimulates osteoclast progenitor proliferation and prolongs survival of mature osteoclasts; the enhanced production of RANK-L by ROS feeds into this by suppressing FoxO transcriptional activity, thereby preventing ROS-scavenging by antioxidant enzymes and creating a positive feedback loop for osteoclast stimulation (Bartell et al., 2014).

Empirical Evidence

Empirical data obtained for this KER moderately supports the link of increased oxidative stress resulting in altered bone cell homeostasis. Most of the evidence is derived from work in bone cells or rodent animal models studying multiple space-relevant radiation sources and microgravity, indicating a direct induction of oxidative stress in bone cells and increase resorption and decrease deposition of bone matrix in a dose-dependent manner (Diao et al., 2018; Huang et al., 2018; Huang et al., 2019; Kondo et al., 2009; Kook et al., 2015; Liu et al., 2018; Sun et al., 2013; Wang et al., 2016; Xin et al., 2015; Zhang et al., 2020).

Incidence concordance

Limited studies demonstrate that oxidative stress increases more than bone cell homeostasis is altered. A few studies demonstrate equal changes to both KEs following gamma irradiation *in vitro* (Huang et al., 2018; Xin et al., 2015; Zhang et al., 2020). *In vivo*, it was shown that rats subject to microgravity had 0.3- to 0.4-fold decreases in antioxidant enzyme activities and a 1.5-fold increase in malondialdehyde (MDA), while osteoclast markers increased a maximum of 1.3-fold (Diao et al., 2018).

Dose Concordance

Moderate evidence exists in the current literature for dose concordance between oxidative stress and altered bone cell homeostasis. Studies have shown that oxidative stress occurs at the same radiation doses as altered bone cell homeostasis (Huang et al., 2019; Huang et al., 2018; Kook et al., 2015; Liu et al., 2018; Wang et al., 2016; Zhang et al., 2020). Very few studies find oxidative stress at lower doses than altered bone cell homeostasis. Mice showed increased ROS at 1 Gy, while osteoclast numbers were only measured increased at 2 Gy (Kondo et al., 2010).

Moderate documentation are available documenting effects of microgravity on oxidative stress-induced changes in osteoblast/osteoclast activity. Mouse and rat models of microgravity, often simulated via hindlimb suspension, have shown significant increases in ROS production and down-regulation of the antioxidant defense system, resulting in decreased osteoblast activity and increased osteoclast activity (Diao et al., 2018; Sun et al., 2013; Xin et al., 2015). However, only limited data exists on dose-dependent effects of microgravity on oxidative stress response and altered bone cell homeostasis. A study by Almeida et al. (2007) showed a 25% decrease in osteoblast differentiation measured as Alkaline phosphatase (AP) activity, after a dose of 50 μ M of H₂O₂ in Wnt3a-induced cells. A greater decrease (50%) in AP was observed after 100 μ M of H₂O₂ in Wnt3a-induced cells compared to the control.

Time Concordance

A moderate amount of evidence in the current literature suggests a time response between oxidative stress and altered bone cell homeostasis *in vivo* and *in vitro*. Increased production of ROS in cells can be observed as early as 1-2 hours post-irradiation with a sustained response for several days; significant changes in osteoblast and osteoclast activity measures are generally observed later than this, often a few days post-irradiation (Huang et al., 2018; Kondo et al., 2010; Kook et al., 2015; Liu et al., 2018). Cao et al observed increased free radical production in the left distal femur from 1 to 4 weeks following 4 Gy irradiation in mice (Cao et al. 2011). In the same timeframe, decreased osteoblast numbers were observed in the distal femora following 4 Gy irradiation.

Essentiality

The strong relationship between increased oxidative stress and altered bone cell homeostasis is further verified by studies examining the use of antioxidants to inhibit oxidative stress in bone cells. Radiation studies with bone cells pre-treated with antioxidants such as N-acetyl cysteine, Amifostine (AM), α -2-macroglobulin (α 2M) and cerium (IV) oxide showed full reversals of the radiation effect on oxidative stress response and led to partial reversals on altered bone cell homeostasis (Huang et al., 2019; Kook et al., 2015; Liu et al., 2018; Wang et al., 2016; Zhang et al., 2020). One study showed that pre-treatment with curcumin, a strong antioxidant, of osteoblast/osteoclast cell models and rodent animal model undergoing microgravity exposure, resulted in a full reversal of both oxidative stress response and altered bone cell homeostasis (Xin et al., 2015). Another study showed that treatment of osteoblast/osteoclast cell models with hydrogen water simultaneously to microgravity exposure, inhibited microgravity-induced ROS formation and cell differentiation in osteoblastic cells while aggravated ROS production and differentiation/function was found in osteoclastic cells (Sun et al., 2013). The same study showed in a rodent animal model, alleviated microgravity-induced reduction of bone mass with hydrogen water in conjunction with improved bone formation and inhibited bone resorption. These data indicate that full removal of oxidative stress via treatment with antioxidants results in partial-to-full reversal of radiation- and microgravity-induced changes of osteoblast and osteoclast activity.

Uncertainties and Inconsistencies

- One study suggests X-ray radiation results in a dose-dependent increase in oxidative stress and bone resorption parameters only at doses above 2 Gy (Kook et al., 2015). This, however, is inconsistent with other studies performed at doses of 1-2 Gy, which indicate a significant effect of radiation on ROS production, TRAP expression, and ALP activity at lower doses (\leq 2 Gy) (Huang et al., 2018; Huang et al., 2019; Kondo et al., 2010; Zhang et al., 2020). Further research is needed to elucidate the effects of low doses, as well as the dose-dependent effect of increasing doses of ionizing radiation (IR).
- Another study's findings show that absorbic acid treatment to RAW 264.7 cells result in significant increase in oxidative stress (H₂O₂) production. This increase in H₂O₂ concentration resulted in a significant decrease in osteoclast formation (Le Nihouann et al., 2010) This is inconsistent with other studies which show that increased levels of endpoints related to oxidative stress result in increased amounts of osteoclast production.

Quantitative Understanding of the Linkage

The following are a few examples of quantitative understanding of the relationship. All reported findings are statistically significant at various alpha levels as listed in the original sources

Response-response relationship

Dose/Incidence concordance

Reference	Experiment Description	Result
Huang et al., 2018	<i>In vitro</i> . A single dose of 2 Gy ⁶⁰ Co gamma radiation by linear accelerator was administered to murine RAW264.7 osteoclast-like cells at a rate of 0.83 Gy/min. ROS production was measured to assess oxidative stress and TRAP staining was used to measure subsequent osteoclastogenic changes.	2-fold increase in ROS production accompanied by a ~2-fold increase in the number of TRAP-positive cells in cells exposed to 2 Gy ⁶⁰ Co gamma radiation relative to controls.
Huang et al., 2019	<i>Ex vivo</i> . A single dose of 2 Gy ⁶⁰ Co gamma radiation was administered to bone marrow stromal stem cells of Sprague-Dawley rats at a rate of 0.83 Gy/min. ROS production was measured to assess oxidative stress and ALP activity was measured to determine subsequent imbalances in osteoblastogenesis.	~2-fold increase in ROS production with a 0.33-fold decrease in ALP activity in cells exposed to 2 Gy ⁶⁰ Co gamma rays relative to unirradiated controls.
Zhang et al., 2020	<i>In vitro</i> . RAW264.7 cells were irradiated with 2 Gy of ⁶⁰ Co gamma radiation at rate of 0.83 Gy/min was administered. ROS production was measured to assess oxidative stress and TRAP staining was used to measure subsequent changes to osteoclastogenesis.	2-fold increase in ROS production in RAW264.7 cells and a 2-fold increase in the number of TRAP-positive osteoclasts when exposed to 2 Gy gamma radiation.
Kondo et al., 2010	<i>In vivo</i> . Male C57BL/6J mice at 17 weeks of age were hindlimb unloaded or normally loaded, 4 days later they were exposed to 1 or 2 Gy of ¹³⁷ Cs or sham irradiated. Oxidative stress markers including, ROS production, MDA, and 4-hydroxynonenal (4-HNE) were measured along with tibial osteoclast surface.	In normally loaded mice, there was a ~1.3-fold increase in ROS at 1 Gy by day 3 and a ~1.2-fold increase in ROS at 2 Gy by day 10. There was a 2-fold increase in MDA and 4-HNE under exposure to either 1 or 2 Gy gamma radiation relative to control in normally loaded models by day 10. There was a 46%, 47% and 64% increase in tibiae osteoclast surface as a result of 2 Gy irradiation, hindlimb unloading and the combination of irradiation and hindlimb unloading, respectively.
Kook et al., 2015	<i>In vitro</i> . MC3T3-E1 cells were exposed to various doses of X-ray irradiation (0-8 Gy) at a rate of 1.5 Gy/min. Levels of ROS, superoxide dismutase (SOD), and glutathione (GSH) were measured to assess oxidative stress and ALP activity was measured to assess subsequent changes in osteoblastogenesis.	Roughly linear dose-dependent increase from 0-8 Gy (significant increases at 4 and 8 Gy) in intracellular ROS accumulation up to 1.39-fold of the control at 8 Gy. Dose dependent decrease from 2-8 Gy (significant decreases at 4 Gy and 8 Gy) in SOD and GSH activity to half at 8 Gy. Following 8 Gy of IR, OCN mRNA expression decreased 48% compared to the non-irradiated control. Irradiation at 4 Gy showed similar decrease in OCN mRNA expression. Mouse bone marrow stromal cell ALP activity saw a significant, 0.62-fold decrease following 8 Gy irradiation.
Liu et al., 2018	<i>In vitro</i> . Human bone marrow-derived mesenchymal cells (hBMMSCs) were irradiated with X-rays at a dose of 2, 4, 8 and 12 Gy and a dose rate of 1.24 Gy/min. SOD levels were measured to assess oxidative stress. ALP activity, calcium deposition and hBMMSCs proliferation were determined.	Following irradiation at 8 Gy, there was a ~0.5-fold decrease in osteoblast SOD activity. There was a dose-dependent decrease in hBMMSC proliferation following irradiation with 2, 4, 8, and 12 Gy, compared to the non-irradiated control. Changes in cell proliferation became significant at doses \geq 8 Gy, with a maximum decrease of ~0.60-fold at 1 week-post irradiation with 12 Gy. 8 Gy of IR resulted in a 0.46 decrease in both ALP activity and calcium deposition compared to non-irradiated controls.

Wang et al., 2016	<i>In vitro</i> . MC3T3-E1 cells were exposed to X-ray irradiation at a dose of 6 Gy. Levels of ROS and H2O2 were measured along with ALP activity and calcium deposition.	1.5-fold increase in H2O2 accumulation and 1.75-fold increase in ROS staining intensity under 6 Gy X-rays. Measured at 1-week post-irradiation, following 6 Gy of IR, there was a 0.54-fold decrease in ALP activity compared to the non-irradiated controls. Measured at 3 weeks post-irradiation, Alizarin Red staining revealed a ~0.1-fold decrease in calcium deposition following exposure to 6 Gy of IR.
Xin et al., 2015	<i>In vivo</i> and <i>in vitro</i> . Sprague-Dawley rats (8 weeks old) were hindlimb suspended and after six weeks, oxidative stress markers and altered bone cell homeostasis were measured. MC3T3-E1 cells and RAW264.7 cells were exposed to modeled microgravity in the NASA rotating wall vessel bioreactor (RWVB). Intracellular ROS and ALP and TRAP levels were measured.	Rat femur MDA increased by ~1.4-fold. Rat femurs showed a ~2.5-fold increase in TRAP mRNA and a ~0.5-decrease in OCN mRNA. MC3T3-E1 cells found a ~1.3-fold increase in ROS formation and a ~0.75-fold decrease in ALP activity. RAW264.7 found a 2-fold increase in intracellular ROS and a 2-fold increase in TRAP positive osteoclasts.
Sun et al., 2013	<i>In vivo</i> and <i>in vitro</i> . Male Sprague-Dawley rats were subjected to hindlimb suspension for 6 weeks. RAW264.7 and MC3T3-E1 cells were exposed to modeled microgravity by RWVB (0.01xg). Femoral peroxynitrite (OONO-), MDA, and intracellular ROS were measured to assess oxidative stress and deoxypyridinoline (DPy), ALP levels, and TRAP-positive cells were subsequently measured to assess bone cell function.	Rats exposed to microgravity via unloading of hindlimbs showed a 2.5-fold increase in femoral peroxynitrite (OONO-) and a 1.3-fold increase in femoral MDA. This was accompanied by a roughly 1.8-fold increase in DPy excretion (biomarker of bone resorption) and 0.4-fold decrease in femoral ALP expression. Exposure to modeled microgravity in MC3T3-E1 (osteoblast cell line) led to a ~1.4-fold increase in intracellular ROS and a 0.75-fold decrease in osteoblast ALP activity. RAW264.7 (preosteoclast cell line) found a ~2-fold increase in ROS and a ~5-fold increase in TRAP mRNA expression.
Diao et al., 2018	<i>In vivo</i> . 50 Male Sprague-Dawley rats (6 weeks) were hindlimb suspended for 72 hours. SOD, catalase (CAT), and MDA were measured to assess oxidative stress and TRAP-5b, OCN and N-terminal type 1 collagen telopeptide (NTX) were measured to assess subsequent bone cell function.	Rats under hindlimb suspension showed a ~0.4-fold decrease in SOD, ~0.3-fold decrease in CAT activity, and a ~1.5-fold increase in MDA relative to unloaded controls in rat femur. This was accompanied by ~1.14-fold increase in serum TRAP-5b and ~1.3-fold increase in NTX. Relative mRNA OCN levels and mRNA collagen I alpha 1 in rat femur decreased significantly.
Almeida et al., 2007	<i>In vitro</i> . C2C12 cells were pre-treated with vehicle or with H2O2 (oxidative stress environment), and maintained for 24 h with or without Wnt3a (50 ng/ml). Osteoblast differentiation was measured as Alkaline phosphatase (AP) activity.	A 25% decrease in AP was observed after a dose of 50 μ M of H2O2 in Wnt3a-induced cells compared to the control. A decrease of more than 50% was observed after 100 μ M of H2O2 in Wnt3a-induced cells compared to the control.

Time-scale**Time concordance**

Reference	Experiment Description	Result
Huang et al., 2018	<i>In vitro</i> . A single dose of 2Gy 60 Co gamma radiation was administered to murine RAW264.7 osteoclast-like cells at a rate of 0.83 Gy/min. ROS production was measured to assess oxidative stress and TRAP staining was used to measure subsequent changes in osteoclastogenesis.	2-fold increase in ROS production after 2h accompanied by a ~2-fold increase in the number of TRAP-positive cells after 7 days in cells exposed to 2 Gy gamma radiation relative to controls.
Kondo et al., 2010	<i>In vivo</i> . Male C57BL/6J at 17 weeks of age were hindlimb unloaded or normally loaded, 4 days later they were exposed to 1 or 2 Gy of 137 Cs or sham irradiated. Oxidative stress markers including, ROS production, MDA, and 4-HNE were measured along with tibial osteoclast surface.	In normally loaded mice, at day 3, ROS in the 1 Gy group increased significantly. By day 10, however, ROS in the 1 Gy group had dropped relative to day 3, while ROS in the 2 Gy group reached significant levels compared to the control. Also, by day 10, MDA and 4-HNE increased ~2-fold in normally loaded mice. This was accompanied by a 46% increase in tibiae osteoclast surface due to irradiation at day 3.
Kook et al., 2015	<i>In vitro</i> . MC3T3-E1 cells were exposed to various doses of X-ray radiation (0-8 Gy) at a rate of 1.5 Gy/min. Levels of ROS, SOD, and GSH were measured to assess oxidative stress and ALP activity was measured to assess subsequent changes in osteoblastogenesis.	Roughly linear dose-dependent increase (after 2 Gy X-ray radiation) in intracellular ROS accumulation up to 1.39-fold of the control at 8 Gy after 1 day. Dose dependent decrease (after 2 Gy) in SOD and GSH activity to half at 8 Gy after 1 day. Markers for altered bone cell homeostasis were measured at 7 days post-irradiation. Following 8 Gy of IR, OCN mRNA expression decreased 48% compared to the non-irradiated control. Irradiation at 4 Gy showed similar decrease in OCN mRNA expression. Mouse bone marrow stromal cell ALP activity saw a significant, 0.62-fold decrease following 8 Gy irradiation.
Liu et al., 2018	<i>In vitro</i> . hBMMSCs were irradiated with X-rays at dose of 2, 4, 8 and 12 Gy, and a dose rate of 1.24 Gy/min. SOD levels were measured to assess oxidative stress. ALP activity, calcium deposition and hBMMSCs proliferation were determined.	0.5-fold decrease in osteoblast SOD activity after 1 day with 0.46-fold decrease in ALP activity after 1 week.
Cao et al., 2011	<i>In vivo</i> . C57BL/6J (wild type) mice were irradiated with a 13 mA beam current, at a total dose of 20 Gy, and a dose rate of 4 Gy per minute/min. Free radical levels were measured to assess oxidative stress using thiobarbituric acid reactive substances (TBARS) assay. Osteoblast numbers were measured in the distal femora as number of osteoblasts per bone perimeter using the CFU-Ob assay.	Free radical levels were increased threefold at 1 week post irradiation and remained increased at 4 weeks in the distal femora. Osteoblast numbers were decreased in the distal femora at both 1 week and 4 weeks following irradiation.

Known modulating factors

Modulating factor	Details	Effects on the KER	References
Drug	α 2M	Treatment reversed the radiation-induced effects on ALP and SOD activity	Liu et al., 2018
Drug	N-acetyl cysteine	2.5 and 5 mM reversed the effects of 8 Gy radiation on ROS levels and ALP activity	Kook et al., 2015
Drug	AMI	Treatment with 30 mg/kg reversed the radiation-induced effects on ROS levels, ALP activity and TRAP-5b levels	Huang et al., 2019; Zhang et al., 2020
Drug	CeO ₂	Treatment with 100 nM lowered dihydroethidium (DHE) and H ₂ O ₂ levels and partially restored Alizarin red optical density	Wang et al., 2016
Drug	Sema3a	Treatment with 50 ng/mL partially reduced ROS levels and reversed TRAP stain to below controls	Huang et al., 2018
Drug	Curcumin (antioxidant)	Fully reversed all oxidative stress and altered bone cell homeostasis	Xin et al., 2015
Drug	Hydrogen water	Reversed microgravity-induced effects on oxidative stress and altered bone cell homeostasis	Sun et al., 2013
Drug	Polyphenol S3	Fully reversed microgravity-induced oxidative stress, osteoblastogenesis and osteoclastogenesis	Diao et al., 2018

Known Feedforward/Feedback loops influencing this KER

Not Identified

ReferencesAgidigbi, T. S., C. Kim. (2019), "Reactive Oxygen Species in Osteoclast Differentiation and Possible Pharmaceutical Targets of ROS-Mediated Osteoclast Diseases." International journal of molecular sciences, Vol. 20/14, Multidisciplinary Digital Publishing Institute, <https://doi.org/10.3390/ijms20143576>Almeida, M. et al. (2007), "Oxidative stress antagonizes Wnt signaling in osteoblast precursors by diverting beta-catenin from T cell factor- to forkhead box O-mediated transcription", The Journal of biological chemistry, Vol. 282/37, 27298-27305. <https://doi.org/10.1074/jbc.M702811200>

AOP482

Almeida, M. (2011), "Unraveling the role of FoxOs in bone--insights from mouse models." *Bone* vol. 49,3: 319-27. <https://doi.org/10.1016/j.bone.2011.05.023>

Bartell, S. M. et al. (2014), "FoxO proteins restrain osteoclastogenesis and bone resorption by attenuating H2O2 accumulation", *Nature Communications*, Vol. 5/1, *Nature*, <https://doi.org/10.1038/ncomms4773><https://doi.org/10.1038/ncomms4773>.

Cao, X. et al (2011). Irradiation induces bone injury by damaging bone marrow microenvironment for stem cells. *Proceedings of the National Academy of Sciences of the United States of America*, 108(4), 1609-1614. <https://doi.org/10.1073/pnas.1015350108>

Diao, Y. et al. (2018), "Polyphenols (S3) Isolated from Cone Scales of *Pinus koraiensis* Alleviate Decreased Bone Formation in Rat under Simulated Microgravity", *Scientific Reports*, Vol. 8/1, *Nature* <https://doi.org/10.1038/s41598-018-30992-8>.

Donaubauer, A.-J. et al. (2020), "The Influence of Radiation on Bone and Bone Cells—Differential Effects on Osteoclasts and Osteoblasts", *International Journal of Molecular Sciences*, Vol. 21/17, MDPI, Basel, <https://doi.org/10.3390/ijms21176377>.

Huang, B. et al. (2019), "Amifostine suppresses the side effects of radiation on BMSCs by promoting cell proliferation and reducing ROS production", *Stem Cells International*, Vol. 2019, Hindawi, <https://doi.org/10.1155/2019/8749090>.

Huang, B. et al. (2018), "Sema3a inhibits the differentiation of raw264.7 cells to osteoclasts under 2gy radiation by reducing inflammation", *PLoS ONE*, Vol. 13/7, PLOS, San Francisco, <https://doi.org/10.1371/journal.pone.0200000>.

Kondo, H. et al. (2010), "Oxidative stress and gamma radiation-induced cancellous bone loss with musculoskeletal disuse", *Journal of Applied Physiology*, Vol. 108/1, American Physiological Society, <https://doi.org/10.1152/japplphysiol.00294.2009>.

Kook, S. H. et al. (2015), "Irradiation inhibits the maturation and mineralization of osteoblasts via the activation of Nrf2/HO-1 pathway", *Molecular and Cellular Biochemistry*, Vol. 410/1-2, *Nature*, <https://doi.org/10.1007/s11010-015-2559-z>.

Le Nihouannen et al. (2010) "Ascorbic acid accelerates osteoclast formation and death" *Bone*, Vol 5, <https://doi.org/10.1016/j.bone.2009.11.021>.

Liu, Y. et al. (2018), "Protective Effects of α -2-Macroglobulin on Human Bone Marrow Mesenchymal Stem Cells in Radiation Injury", *Molecular Medicine Reports*, Vol. 18/5, Spandidos Publications, <https://doi.org/10.3892/mmr.2018.9449>.

Maeda, K. et al. (2019), "The Regulation of Bone Metabolism and Disorders by Wnt Signaling", *International Journal of Molecular Sciences*, Vol. 20/22, MDPI, Basel, <https://doi.org/10.3390/ijms20225525>.

Manolagas, S. C. and M. Almeida. (2007), "Gone with the Wnts: β -Catenin, T-Cell Factor, Forkhead Box O, and Oxidative Stress in Age-Dependent Diseases of Bone, Lipid, and Glucose Metabolism", *Molecular Endocrinology*, Vol. 21/11, Oxford University Press, Oxford, <https://doi.org/10.1210/me.2007-0259>.

Sun, Y. et al. (2013), "Treatment of hydrogen molecule abates oxidative stress and alleviates bone loss induced by modeled microgravity in rats", *Osteoporosis International*, Vol. 24/3, *Nature*, <https://doi.org/10.1007/s00198-012-2028-4>.

Tahimic, C. G. T. and R. K. Globus. (2017), "Redox signaling and its impact on skeletal and vascular responses to spaceflight", *International Journal of Molecular Sciences*, Vol. 18/10, MDPI, Basel, <https://doi.org/10.3390/ijms18102153>.

Tian, Y. et al. (2017), "The impact of oxidative stress on the bone system in response to the space special environment", *International Journal of Molecular Sciences*, Vol. 18/10, MDPI, Basel, <https://doi.org/10.3390/ijms18102132>.

Wang, C. et al. (2016), "Protective effects of cerium oxide nanoparticles on MC3T3-E1 osteoblastic cells exposed to X-ray irradiation", *Cellular Physiology and Biochemistry*, Vol. 38/4, Karger, Basel, <https://doi.org/10.1159/000443092>.

Xin, M. et al. (2015), "Attenuation of hind-limb suspension-induced bone loss by curcumin is associated with reduced oxidative stress and increased vitamin D receptor expression", *Osteoporosis International*, Vol. 26/11, *Nature*, <https://doi.org/10.1007/s00198-015-3153-7>.

Zhang, L. et al. (2020), "Amifostine inhibited the differentiation of RAW264.7 cells into osteoclasts by reducing the production of ROS under 2 Gy radiation", *Journal of Cellular Biochemistry*, Vol. 121/1, Wiley, <https://doi.org/10.1002/jcb.29247>.

[Relationship: 2847: Energy Deposition leads to Altered Bone Cell Homeostasis](#)

AOPs Referencing Relationship

AOP Name	Adjacency	Weight of Evidence	Quantitative Understanding
Deposition of energy leading to occurrence of bone loss	non-adjacent	High	Low

Evidence Supporting Applicability of this Relationship

Taxonomic Applicability

Term	Scientific Term	Evidence	Links
human	<i>Homo sapiens</i>	Moderate	NCBI
mouse	<i>Mus musculus</i>	Moderate	NCBI
rat	<i>Rattus norvegicus</i>	Moderate	NCBI

Life Stage Applicability

Life Stage Evidence

Adult	Moderate
Juvenile	Low

Sex Applicability

Sex	Evidence
Male	Moderate
Female	Moderate

The evidence for the taxonomic applicability to humans is moderate as majority of the evidence is from *in vitro* human-derived cells, but one study performed a meta-analysis of astronauts. The relationship is supported *in vivo* mainly by mouse models with a few studies looking at rat models. The relationship has been shown in both male and female animal models. The relationship is plausible at any life stage. However, majority of studies have used adult animal models.

Key Event Relationship Description

Energy deposition in the form of ionizing radiation (IR) exposure can result in a loss of homeostasis among the osteocyte, osteoclast, and osteoblast bone cells. The severity of the irradiation effects is influenced by dose, dose rate, and the level of linear energy transfer (LET) between IR and bone tissue. The energy deposited into cells causes ionization events that can lead to oxidative stress, which may induce cell death and alter signaling pathways in the bone microenvironment that regulate the differentiation and activity of bone remodeling cells (Willey et al., 2011). Bone cells can be dysregulated by deposited energy from a variety of IR types, including X-rays, gamma rays, and heavy ions, and has been observed at a wide range of doses from 0-30 Gy. IR-induced changes to bone cell homeostasis are defined by progenitor cell proliferation, markers for osteoblast and osteoclast activity, and the number and surface area of both cell types on a sample.

Evidence Supporting this KER

Overall weight of evidence: High

Biological Plausibility

The biological rationale for linking direct deposition of energy to altered bone cell homeostasis is strongly supported in the literature, as documented by several review articles published on the subject (Donaubauer et al., 2020; Pacheco and Stock, 2013; Smith, 2020; Willey et al., 2011). These articles are of particular relevance, as they discuss the effects of environmental perturbations in the form of deposition of energy on osteoblast and osteoclast differentiation pathways. Deposition of energy in the form of IR has been shown to have a wide range of effects on osteoclasts, ranging from increased to decreased number and activity. Irradiated bone has an increased amount and activity of osteoclasts when compared to osteoblasts. Recent research suggests that low-dose (<1Gy) radiation can cause osteoclastogenesis in the acute phase due to inflammatory cytokines that stimulate osteoclastogenesis in the surrounding irradiated tissue. Increased bone resorption and increased bone turnover occur from increased osteoclast and decreased osteoblast activity (Pacheco and Stock, 2013; Sakurai et al., 2007; Willey et al., 2011; Willey et al., 2010).

Deposition of energy into bone cells results in osteoclast activation by upregulating the differentiation of precursors and increasing bone resorption. Osteoclast precursors are recruited to bone remodeling units (BRUs) to differentiate into mature osteoclast by binding macrophage colony-stimulating factor (M-CSF) and receptor activator of nuclear factor kappa B ligand (RANKL) secreted in the bone microenvironment by osteoblasts and osteocytes (Donaubauer et al., 2020; Smith, 2020). Upregulation of osteoclastogenesis signaling pathways downstream to RANKL and M-CSF by radiation significantly enhanced osteoclast activity. Deposition of energy can also induce osteocyte apoptosis, resulting in proinflammatory signaling that upregulates the recruitment of osteoclasts to the area. *In vitro* experiments on osteoblast/osteoclast activity have shown enhanced osteoclastogenesis under exposures to radiation, as the deposition of energy in osteoblasts and osteocytes decreased their secretion of osteoprotegerin (OPG), a RANKL inhibitor, ultimately enhancing osteoclast stimulation (Donaubauer et al., 2020; Smith, 2020). The RANKL/OPG ratio is necessary for normal osteoclast activity, as increasing the proportion of RANKL to its inhibitor, OPG, results in stimulation of osteoclastogenesis. In addition, deposition of energy in bone cells results in upregulation of osteoclast stimulatory molecules, such as interleukin (IL)-6, high mobility group box 1 (HMGB1), and TNF- α , leading to enhanced osteoclast formation. Enhanced osteoclast formation leads to enhanced bone resorption (Donaubauer et al., 2020; Pacheco and Stock, 2013; Smith, 2020; Willey et al., 2011).

Radiation-induced damage to osteoblasts and osteocytes within the bone microenvironment is considered a significant factor and an exemplary instance of the effect of deposition of energy on bone cell function. Both *in vivo* and *in vitro* data suggest that radiation reduces osteoblast proliferation and differentiation, causing cell cycle arrest, reducing collagen production, and increasing apoptotic sensitivity. Radiation-induced oxidative stress likely damages osteoblast precursors, reducing cell viability and differentiation. Under energy deposition, osteoblast numbers and activity remain relatively unchanged, while significant bone degradation occurs, therefore, suggesting enhanced osteoclast activity as part of the altered bone cell homeostasis observed (Willey et al., 2011). Directly irradiated bone shows reduced mesenchymal stem cell (MSC) numbers and reduced colony formation when directed to bone cell precursors, which delays the recovery of damaged osteoblasts (Willey et al., 2011). Osteoclasts can degrade the bone matrix through the release of amino acids such as hydroxyproline (HP), fragments of collagen type I, including C- and N-terminal telopeptides (CTX and NTX), pyridinoline (PYD) and deoxypyridinoline (DPD) as well as proteases, including Cathepsin K (CTSK) and matrix metalloproteinases (MMP9 and MMP14) (Smith, 2020; Stavnicuk et al., 2020). Bone morphogenic protein 2 (BMP-2), a transcription factor regulating osteoblast differentiation can indicate impaired osteoblast differentiation following irradiation (Sakurai et al., 2007).

Empirical Evidence

The empirical data relevant to this KER provides strong support for the linkage between deposition of energy and altered bone cell homeostasis. The evidence supporting this link comes from literature on radiation exposure directly or indirectly increasing osteoclast activity and decreasing osteoblast activity in a dose and/or time concordant manner. Radiation-specific studies examined the effects of irradiation with doses ranging from 0-30 Gy of X-rays, gamma rays, and heavy ions irradiation (da Cruz Vegan et al., 2020; Huang et al., 2019; Kook et al., 2015; Li et al., 2020; Liu et al., 2018; Sakurai et al., 2007; Wang et al., 2016; Willey et al., 2008; Willey et al., 2010; Wright et al., 2015; Zhang et al., 2020).

Dose Concordance

Current literature on the effects of radiation on bone cell function provided strong evidence for a dose concordance relationship between deposition of energy and altered bone cell homeostasis. Once energy is deposited into matter at all doses, follow-on downstream events are immediately initiated. In humans after spaceflight, where the time of flight is used as proxy for the dose of radiation received, osteoclast markers increased hyperbolically with a t1/2 of 11 days and a plateau at 113% increased, while osteoblast markers increased linearly at 7% per month (Stavnicuk et al., 2020). In mice after spaceflight, compared to ground controls, an increase of osteoclasts numbers in the bone surface by 197% was observed. The surface of the bone covered by osteoclasts also increased by 154% (Blaber et al., 2013). Relevant primary research shows that indicators of osteoblastogenesis, including osteoblast number and surface area, MSC proliferation, alkaline phosphatase (ALP) and osteocalcin (OCN) expression, and levels of calcium deposition, all decrease in response to IR exposure (Huang et al., 2019; Kook et al., 2015; Li et al., 2020; Liu et al., 2018; Sakurai et al., 2007; Wang et al., 2016; Wright et al., 2015). Studies also show that indicators of osteoclastogenesis, including osteoclast number and surface area as well as tartrate-resistant acid phosphatase (TRAP) expression increase in response to IR exposure (da Cruz Vegan et al., 2020; Kondo et al., 2009; Li et al., 2020; Willey et al., 2008; Willey et al., 2010; Wright et al., 2015; Zhang et al., 2020). At an irradiation dose less than or equal to 2 Gy X-rays or gamma rays, various models consistently showed a significant increase in the number of osteoclasts/mm² of bone surface, as well as the bone surface area covered by osteoclasts (Kondo et al., 2009; Willey et al., 2008; Willey et al., 2010; Wright et al., 2015; Zhang et al., 2020). A few studies also reported a decrease in osteoblasts following a 2 Gy irradiation dose (Sakurai et al., 2007; Wright et al., 2015). IR-induced changes in osteoclast histology appear to be dose-dependent, as Kondo et al. (2009) found that 3 days after irradiation with gamma rays there was a greater increase in the number of osteoclasts in samples exposed to 2 Gy of gamma rays than to 1 Gy. Li et al. (2020) observed that exposure to 8 Gy resulted in a greater increase in osteoclast number than that to lower dose. At higher doses, such as a total dose of 30 Gy, an even greater fold increase in TRAP was observed (Da Cruz Vegan et al., 2020). This dose-dependent relationship between IR and altered bone cell homeostasis is further supported by measurements of osteoblast markers across a range of radiation doses. Studies that analyzed ALP levels across multiple doses of X-rays, found that expression decreased in a dose-dependent manner (Kook et al., 2015; Sakurai et al., 2007). Kook et al. (2015) also observed a dose dependent decrease in the osteoblast marker, OCN, following exposure to 0-8 Gy of X-rays. Following irradiation with 2, 4, 8, and 12 Gy of X-rays, Liu et al. (2018) found that human bone marrow MSC (hBMSC) proliferation experienced a dose-dependent decrease. Lastly, OCN and osteoblast differentiation decreased 2-fold with each increasing dose (15 and 20 Gy) relative to control (Jia et al., 2011).

Time Concordance

Moderate evidence exists in the current literature suggesting a time concordance relationship between the deposition of energy and altered bone cell homeostasis. When energy is deposited into biological models it immediately causes ionization events which directly lead to downstream events occurring at later time points. In general, data collected from experiments show that overall changes in osteoblast and osteoclast activity occur primarily in the first week post-exposure. At 3 days post-exposure, osteoblast surface was decreased (Willey et al., 2008), TRAP levels increased (Swift et al., 2015; Willey et al., 2008; Zhang et al., 2020) and osteoclast number and surface were increased (Willey et al., 2008). OCN levels decreased on day 3 after radiation exposure, indicating a decrease in osteoblast markers (Swift et al., 2015).

10 days post-exposure revealed decreased osteoblasts in calvarial bone that was not significantly shown at earlier timepoints (Wright et al., 2015). Increased osteoclast surface and number was observed at 3 days, 1 week, and 10 days after irradiation (Kondo et al., 2009; Willey et al., 2010; Willey et al., 2008), however no further changes occurred after 2 and 3 weeks (Willey et al., 2010).

Da Cruz Vegan et al. (2020) found that both TRAP and OCN levels increased at day 3 post-irradiation of rats with a total of 30 Gy gamma rays. Chen et al. (2014) found that OCN protein levels increased at day 10 and continued onto day 14 in the 0.5 Gy MC3T3-E1 cells irradiated group. MC3T3-E1 cells irradiated with 0.5 or 5 Gy X-rays revealed an increase in ALP level at day 7 and day 10, then decreased at day 14 (Chen et al., 2014). As well, the *in vivo* models showed decreased osteoclast number as early as day 7, increased OCN protein levels at day 14 in the 5 Gy group (Chen et al., 2014). Oest et al. (2015) observed increased osteoclast numbers correlated temporally with trabecular resorption, most pronounced 2 weeks post-irradiation (5 Gy and 4X5Gy of X-rays). Mice irradiated with 5 Gy of gamma radiation showed significant increase in osteoblast activity 10 days following irradiation when compared to the control (Green et al. 2021). A single 50 Gy dose of electron beam energy to the proximal tibia of rabbits showed late onset decrease in the number of viable osteocytes (52 weeks) (Sugimoto et al., 1993).

Essentiality

Studies examining the effects of different methods of prevention or treatment of bone resorption under IR suggest a strong relationship between deposition of energy and altered bone cell homeostasis. Altered bone cell homeostasis mainly occurs in the bone tissue directly receiving radiation. Contralateral bone tissue (bone tissue that was shielded from radiation but was removed from irradiated rats) was extracted and compared to bone tissue that was directly exposed to radiation in several studies. Analysis of the shielded bone tissue indicated changes in osteoblast and osteoclast markers such as ALP and TRAP5b were less significant in contralateral bone compared to irradiated bone tissue (Wright et al., 2015).

Uncertainties and Inconsistencies

- Not all radiation qualities and doses of radiation will alter bone cell homeostasis in the same way. Low doses (<1 Gy) of low LET electromagnetic radiation (X-rays and gamma rays) are shown to increase osteoblasts and decrease osteoclasts, while high doses do the opposite (Donaubauer et al., 2020). This is in contrast with particle irradiation, where osteoblasts are decreased and osteoclasts are increased at low and high doses (Donaubauer et al., 2020).
- There are differences in the mechanisms of altered bone cell homeostasis between humans and animals during spaceflight. In humans, increased osteoclast activity is the main cause of bone loss, while in rats, resorption was unchanged (Fu et al., 2021; Stavnickuk et al., 2020). However, microgravity is also a stressor in this case and not just radiation, and there are differences in how this is measured between humans and animals.
- At 3 days post-irradiation, da Cruz Vegian et al. (2020) found that, in addition to an IR-induced increase in TRAP levels (osteoclastogenesis marker), rats that underwent 30 Gy irradiation also experienced a significant, ~8-fold increase in levels of the osteoblastogenesis marker, OCN, compared to non-irradiated controls. In addition, TRAP levels experienced a time-dependent decrease. This is contrary to the increase in osteoclastogenesis and decrease in osteoblastogenesis generally seen post-irradiation.
- Chen et al. (2014) showed increased OCN mRNA expression and protein activity after 0.5 or 5 Gy X-ray irradiation, which is contrary to the decrease in osteoblastogenesis following irradiation observed in other studies. This may be explained by the survival strategy of osteoblasts to retain cell division for DNA repair as opposed to undergoing programmed death (Chen et al., 2014).
- Mice receiving 6 Gy of radiation showed a significant increase in the osteoblasts and osteoclast-lined bone perimeter, as opposed to a decrease in osteoblast after a high dose of radiation (Turner et al., 2013).
- Cao et al. (2010) observed decreased osteoclast numbers in the distal femora four weeks following 4 Gy irradiation, which is contrary to the increase in osteoclast observances found in other studies.

Quantitative Understanding of the Linkage

The following are a few examples of quantitative understanding of the relationship. All reported findings are statistically significant at various alpha levels as listed in the original sources

Response-response relationship

Dose Concordance

Reference	Experiment Description	Result
Stavnickuk et al., 2020	<i>In vivo</i> . A meta-analysis that extracted biochemical markers in 124 astronauts from articles from 1971 to 2019. The longer the spaceflight, the higher dose of ionizing radiation the astronauts received, although ionizing radiation was not the only stressor that the astronauts would have received. Markers for osteoblast activity included serum ALP and C-terminal cleaved collagen type 1 propeptide (PICP). Markers for osteoclast activity included urine HP, NTX, CTX, and DPD.	Early increases in resorption markers and early decreases in formation markers were observed, with late increases in formation markers. Bone resorption markers increased hyperbolically with a t1/2 of 11 days and a plateau at 113%. Formation markers increased linearly at 7% per month. Resorption markers dropped to pre-flight levels after flight, while formation markers continued to increase at 84% per month for 3-5 months.
Kook et al., 2015	<i>In vitro</i> . Mouse bone marrow stromal cells and the MC3T3-E1 murine osteoblast cell line were both irradiated with 0.8 Gy of X-rays at a rate of 1.5 Gy/min. Levels of the osteoblast mineralization proteins, ALP and OCN, were measured 7 days post-irradiation to observe changes to osteoblast activity.	Following 8 Gy of IR, OCN mRNA expression decreased 48% compared to the non-irradiated control. Irradiation at 4 Gy showed similar decrease in OCN mRNA expression. Mouse bone marrow stromal cell ALP activity saw a significant, 0.62-fold decrease following 8 Gy irradiation.
da Cruz Vegian et al., 2020	<i>In vivo</i> . Sixty male Wistar rats were implanted with grade V titanium femur implants and were separated into four groups: (a) no-irradiation group (N-Ir); (b) early-irradiation group (E-Ir); (c) late-irradiation group (L-Ir); and (d) previous-irradiation group (P-Ir). The animals in the E-Ir, L-Ir, and P-Ir groups were irradiated in two fractional stages of 15 Gy of ⁶⁰ Co gamma rays for a total of 30 Gy. Blood samples were collected at the time of euthanasia. Cells were measured for TRAP and OCN levels.	At 3-days post-irradiation, rats observed significant, ~8-fold increase in TRAP levels compared to the non-irradiated control.
Zhang et al., 2020	<i>In vitro and in vivo</i> . Male Sprague-Dawley rats and the RAW264.7 cell line were irradiated with 2 Gy of ⁶⁰ Co gamma rays at a rate of 0.83 Gy/60 seconds. TRAP staining was used to determine changes to osteoclast numbers following IR exposure.	Following exposure to IR, there was a ~2-fold and ~2.7-fold increase in the number of TRAP-positive osteoclasts in RAW264.7 and rat femur samples, respectively, compared to the non-irradiated control.
Huang et al., 2019	<i>In vitro</i> . Bone marrow MSCs (bmMSCs) from the tibiae and femur of rats were irradiated with 2 Gy of ⁶⁰ Co gamma rays at a rate of 0.83 Gy/min. bmMSCs were analyzed for changes in bone cell function through measuring levels of ALP, calcium deposition and proliferation of the bmMSCs.	Following IR exposure, there was a ~0.6-fold decrease in bmMSC proliferation compared to non-irradiated controls. Levels of ALP activity and calcium deposition saw a 0.33-fold 0.66-fold decrease, respectively, from 0 Gy to 2 Gy.
Liu et al., 2018	<i>In vitro</i> . hBMMSCs were irradiated with 2, 4, 8, and 12 Gy of X-rays at a rate of 1.24 Gy/min. Cells were analyzed for progenitor cell proliferation, ALP activity, and calcium deposition to determine the effect of IR on osteoblast function.	There was a dose-dependent decrease in hBMMSC proliferation following irradiation with 2, 4, 8, and 12 Gy, compared to the non-irradiated control. Changes in cell proliferation became significant at doses >8 Gy, with a maximum decrease of ~0.60-fold at 1 week-post irradiation with 12 Gy. 8 Gy of IR resulted in a 0.46 decrease in both ALP activity and calcium deposition compared to non-irradiated controls.
Li et al., 2020	<i>In vitro</i> . hBMMSCs were exposed to 8 Gy of X-rays. To determine the effects of IR on bone cell function, TRAP staining was used to determine the number of osteoclasts/mm ² of bone surface and the CCK-8 assay was used to measure hBMMSC proliferation.	Following exposure to 8 Gy of IR, there was a ~3-fold increase in osteoclast number at 7 days post-irradiation, compared to the non-irradiated control. There was a 0.77-fold decrease in hBMMSC proliferation after 72 hours post-irradiation, compared to the non-irradiated control.
Wang et al., 2016	<i>In vitro</i> . The MC3T3-E1 osteoblast-like cell line was irradiated with 6 Gy of X-rays. Following irradiation, ALP activity and calcium deposition were measured to determine the effects of IR on osteoblast activity.	Measured at 1-week post-irradiation, 6 Gy of IR resulted in a 0.54-fold decrease in ALP activity compared to the non-irradiated controls. Measured at 3 weeks post-irradiation, Alizarin Red staining revealed a ~0.1-fold decrease in calcium deposition following exposure to 6 Gy of IR.
Wright et al., 2015	<i>In vivo and ex vivo</i> . the right hindlimbs of 20-week-old male C57Bl/6 mice were irradiated with 2 Gy of X-rays at a rate of 1.6 Gy/min. In addition, the calvariae of 4-day-old Swiss White mice were extracted and irradiated with 2 and 10 Gy of X-rays at a rate of 0.244 Gy/min. The number of TRAP5b-positive osteoclasts and osteoblasts/ mm ² of bone surface were measured in models. <i>In vitro</i> . Osteocyte-like cells (MLO-Y4) and osteoblast cells (MC3T3) were irradiated with 0-20 Gy X-rays.	Following <i>in vivo</i> irradiation of the right hindlimb of C57Bl/6 mice with 2 Gy of IR, there was a ~1.7-fold increase in osteoclast number over bone surface compared to the non-irradiated control. There was no significant difference in osteoblast number following irradiation. While 2 Gy of IR did not lead to a significant change in osteoblast number, exposure to 10 Gy eventually resulted in a significant, ~0.4-fold decrease in calvarial bone-derived osteoblasts at 10 days post-irradiation, compared to the non-irradiated control.
Willey et al., 2008	<i>In vivo</i> . Thirty-two 13-week-old C57BL/6 mice were either irradiated by 2 Gy X-rays or served as controls. Osteoclast surface, osteoblast surface, osteoclast number and TRAP-5b levels were measured after 3 days to determine the effects of IR on bone cell function.	The stained bone sections of the irradiated mice showed a 44% increase in the number of osteoclasts/mm ² of bone surface, a 14% increase in serum levels of TRAP5b, and a 213% increase in osteoclast-covered bone surface area compared to the control. The irradiated bone sections were also tested for changes in serum levels of OCN (osteoblast activity marker), showing a non-significant radiation-induced decrease.

Willey et al., 2010	<i>In vivo.</i> 20-week-old female C57BL/6 mice were irradiated with 2 Gy X-rays, and left/right hind limbs, along with the vertebral column trabecular bone was analyzed, in addition to blood samples taken for serum analysis. Osteoblast marker OCN and osteoclast marker TRAP-5b was measured with enzyme-linked immunosorbent assay (ELISA). Osteoblast and osteoclast surfaces were determined as well.	Osteoblast surface did not change, but osteoclast surface increased 1.6-fold. Analysis of blood serum samples showed a 21% increase in the serum levels of TRAP-5b at 1 week post-irradiation compared to the control group. Serum levels of OCN were also measured, but no significant differences were found at 1, 2, or 3 weeks post-irradiation. Osteoclast number relative to bone surface increased 218% in the irradiated group, compared to the non-irradiated group.
Kondo et al., 2009	<i>In vivo.</i> 17-week-old male mice were exposed to 1 and 2 Gy of ^{137}Cs gamma-rays and their trabecular bone tissue was analyzed at 3- and 10-days post-irradiation. The number of osteoclasts was measured with TRAP staining.	At 3 days post-irradiation, the number of osteoclasts/square mm of bone surface area was ~2-fold higher than the control (0 Gy) under 1 Gy of radiation and ~2.5-fold higher under 2 Gy of radiation. At 10 days post-irradiation, the number of osteoclasts was ~3-fold higher than the control under 1 Gy of radiation and ~2.5-fold higher under 2 Gy of radiation.
Sakurai et al., 2007	<i>In vitro.</i> To evaluate the effects of radiation on osteoblast differentiation, murine C2C12 myoblast cells (osteoblast-like cells) were irradiated <i>in vitro</i> with 2 and 4 Gy of X-rays, differentiation was induced with BMP-2 and heparin over the course of 3 days. Collagen type 1 and ALP were used as markers of osteoblast differentiation.	When exposed X-rays, ALP activity of the C2C12 cells showed a significant, dose-dependent response. C2C12 cells experienced a ~0.3-fold decrease in ALP activity from 0 Gy to 4 Gy, and a 0.5-fold decrease from 0 Gy to 2 Gy. Collagen type I was significantly reduced at both doses.
Blaber et al., 2013	<i>In vivo.</i> 16-week-old female mice were subjected to 15-days of spaceflight. The quantity of osteoclasts of the right proximal femur were measured with TRAP staining.	Following spaceflight, there was a 197% increase in osteoclast numbers in the bone surface compared to the ground controls. The bone surface covered by osteoclasts also increased by 154% in microgravity.
Jia et al., 2011	<i>In vivo</i> and <i>Ex vivo</i> . 10 to 12 -weeks-old male mice were exposed to 0, 15 and 20 Gy of X-ray. Serum levels of the bone formation marker osteocalcin (OCN) were analyzed with the Mouse Osteocalcin EIA Kit. Osteoblast forming cells of the left tibia and left femur were counted based on the formation of alkaline phosphatase (ALP)-positive osteoblastic colonies.	

Time-scale**Time Concordance**

Reference	Experiment Description	Result
da Cruz Vegian et al., 2020	<i>In vivo.</i> Sixty male Wistar rats were implanted with grade V titanium femur implants and were separated into four groups: (a) N-Ir; (b) E-Ir; (c) L-Ir; and (d) P-Ir. The animals in the E-Ir, L-Ir, and P-Ir groups were irradiated in two fractional stages of 15 Gy 60Co gamma radiation for a total of 30 Gy. Blood samples were collected at the time of euthanasia. Cells were measured for TRAP and OCN levels.	OCN levels in the irradiated groups increased greater than non-irradiated levels at 3 days. By the second week, only P-Ir OCN levels were greater than the N-Ir group. TRAP was greater than N-Ir in all irradiated group at day 3. At week 2, L-Ir TRAP levels fell below control levels, followed by a slight increase in TRAP in all irradiated groups by week 7.
Zhang et al., 2020	<i>In vivo</i> and <i>in vitro</i> . 2 Gy of 60Co gamma rays were given to male rats and the RAW264.7 cell line. To detect changes in osteoclast activity following IR exposure, the number of osteoclasts and levels of TRAP5b were measured 1, 3, 5, and 7 days after exposure.	Samples of blood from rat tail vein were obtained and TRAP5b levels in the serum were measured. In the 2 Gy irradiated group, TRAP5b levels in serum increased 1.7-fold after 3 days and 2.6-fold after 5 days, followed by a slight decrease to a 2.4-fold change at day 7 (Fig. 6).
Willey et al., 2008	<i>In vivo.</i> Thirty-two C57BL/6 mice were either irradiated by 2 Gy X-rays or served as controls. Osteoclast surface, osteoblast surface, osteoclast number and TRAP-5b levels were measured after 3 days to determine the effects of IR on bone cell function.	In the irradiated group, osteoclast surface, osteoclast number, and TRAP-5b level increased after 3 days by 213%, 44%, and 14%, respectively, compared to the control group. Osteoblast surface was decreased by 3% after 3 days compared to the non-irradiated group.
Chen et al., 2014	<i>In vitro</i> and <i>in vivo</i> . <i>In vitro</i> MC3T3-E1 cells were exposed to a single 0.5 Gy or 5 Gy dose of X-ray irradiation at a rate of 200 cGy/min. <i>In vivo</i> male Sprague-Dawley rats were exposed to 0.5 Gy or 5 Gy dose of X-ray irradiation. Rats were euthanized 7, 14, 21 and 28 days after irradiation. Osteoblast differentiation markers, such as OCN and ALP, were measured post-irradiation by western blot. TRAP positive cells were used to determine osteoclast counts.	<i>In vitro.</i> ALP levels in all three groups (control, 0.5 Gy, and 5 Gy) were roughly the same levels relative to each other at day 4 and day 14. Irradiation-induced increases in ALP occurred on day 7 and 10 post-irradiation in both irradiated groups. OCN protein level was increased at day 10 in both irradiated groups, with the increases in the 0.5 Gy group continuing onto day 14 post-irradiation. <i>In vivo.</i> TRAP staining indicated an increase in the number of osteoclasts in the 0.5 Gy irradiated group at day 14, followed by a decrease to below control levels on day 21. Meanwhile, in the 5 Gy irradiated group, number of osteoclasts were decreased as early as 7 days post-irradiation. ALP mRNA expression increased in both irradiated group at day 14 and remained above control levels at day 21 in the 5 Gy group. OCN mRNA expression was increased as early as day 14 and remained increased at day 21 and 28. OCN positive cells in calluses indicated that OCN protein levels increased at day 14 in the 0.5 and 5 Gy groups.
Swift et al., 2015	<i>In vivo.</i> Female, B6D2F1/J mice were divided into 4 groups: Sham (0 Gy), Wound (W; 15% total body surface area), Radiation Injury (RI, 8 Gy 60Co gamma rays), or Combined Injury (CI; RI + W). Mice were euthanized after irradiation at days 3, 7 and 30. The radiation group received a single whole-body dose of 8 Gy gamma rays at a rate of 0.4 Gy/min. Osteoblast surface, osteoclast surface, and osteoclastogenesis markers such as TRAP-5b and OCN were measured post-irradiation to determine the effects of IR on bone cell function.	Irradiated mice showed an increase in TRAP-5b from 38% to 83% from days 3-30. OCN in serum was decreased from -35% to -83% compared to sham mice on day 3.
Kondo et al., 2009	<i>In vivo.</i> 18-week-old male mice were exposed to 1 and 2 Gy of ^{137}Cs gamma rays at a dose of 0.915 Gy/min and their trabecular bone tissue was analyzed at 3- and 10-days post-irradiation. The number of osteoclasts was measured with TRAP staining.	Exposure to 1 Gy led to a ~2-fold increase in osteoclast number at day 3, and ~3-fold increase by day 10 post-irradiation. ~2.5-fold increase in osteoclast number by day 3 which remained constant up to day 10 post-irradiation. A marked ~150% increase in osteoclast number and surface were observed at day 3 and day 10 and at doses 1 and 2 Gy.
Willey et al., 2010	<i>In vivo.</i> 20-week-old female mice were irradiated with 2 Gy of X-rays, and bone and blood samples were taken to analyze levels of markers for osteoclast and osteoblast activity. Osteoblast marker OCN and osteoclast marker TRAP5b were measured with ELISA. Osteoclast and osteoblast surfaces were measured as well.	Osteoblast surface did not change. Osteoclast surface increased 1.6-fold after 1 week, but no change was observed after 2 and 3 weeks. A 21% increase in the levels of TRAP5b was observed within the irradiated group compared to the control group at week 1, but no further differences were observed between the irradiated and non-irradiated groups at weeks 2 and 3. The serum level of OCN did not change. A 218% increase in osteoclast number over bone surface was found at 1-week post-irradiation.
Wright et al., 2015	<i>In vivo</i> and <i>ex-vivo</i> . the right hindlimbs of 20-week-old male C57BL/6 mice were irradiated with 2 Gy of X-rays at a rate of 1.6 Gy/min. In addition, the calvariae of 4-day-old Swiss White mice were extracted and irradiated with 2 and 10 Gy of X-rays at a rate of 0.244 Gy/min. The number of TRAP5b-positive osteoclasts and osteoblasts/ mm ² of bone surface were measured in models. <i>In vitro.</i> Osteocyte-like cells (MLO-Y4) and osteoblast cells (MC3T3) were irradiated with 0-20 Gy X-rays.	Following irradiation, a significant ~0.4-fold decrease in calvarial bone-derived osteoblasts was found at 10 days post-irradiation compared to the non-irradiated control. Earlier time points, such as day 4 and day 7, showed non-significant decreases in osteoblasts.

Oest et al., 2015	In vivo. 12-week-old female mice were irradiated with a single 5 Gy of X-ray or 4 fractions of 5 Gy of X-ray. The number of osteoclasts were enumerated over the distal 5 mm of each femur and stained with TRAP. They were evaluated histologically at 1, 2, 4, 8, 12, and 26 weeks post-irradiation.	1 week after irradiation, a 2-fold increase for the 5 Gy total osteoclasts compared to the control and 4x5Gy groups was observed. 2 weeks post-irradiation, the number of osteoclasts increased more than a 2-fold for both doses of 5 Gy and 4x5Gy compared to the control.
Green et al., 2013	In vivo, eight-week old male C57BL/6 mice were irradiated with gamma irradiation at a total dose of 5 Gy. Osteoclast activity was measured by the serum concentration of tartrate-resistant acid phosphatase (TRAP5b) assay.	At 2 days post-irradiation, a significant increase in osteoblast activity by $43 \pm 35\%$ when compared to the control and remained elevated in compared to control group for 10 days following irradiation.
Lima et al., 2017	In vivo, 4-month-old female BALB/cBYJ mice were administered 0, 0.17, 0.5, and 1 Gy of X-ray radiation. Osteoclast numbers were measured using a tartrate-resistant acid phosphatase (TRAP+) staining kit. Marrow aspirate was used to determine osteoblast colony-forming unit.	3 days following radiation exposure, there was a significant increase in osteoclasts when compared to the control group. Osteoblast colony numbers were significantly decreased in the 0.5 Gy and the 1 Gy irradiated groups when compared to the control group 3 days post exposure.
Sugimoto et al., 1993	In vivo. The proximal tibia of rabbits was exposed to a single dose of 50 Gy of a 14-MeV electron beam generated by a betatron. Osteocytes were quantified by counting silver grains on autoradiographs, using ^{3}H -cytidine as a tracer.	The proximal tibia of rabbits showed late onset decrease in the number of viable osteocytes after 52 weeks after irradiation.

Known modulating factors

Modulating factor	Details	Effects on the KER	References
Drug	Risedronate (osteoporosis drug that blocks osteoclast activity)	Returned TRAP5b levels to near baseline and reduced the osteoclast count after radiation	Willey et al., 2010
Drug	α -2-macroglobulin (α 2M); a radio-protective macromolecule	Treatment at 0.25 and 0.5 mg/mL slightly restored ALP activity.	Liu et al., 2018
Age	Old age	Lower estrogen at old age is thought to increase osteoclast activity, compounding with the effects of radiation.	Pacheco and Stock, 2013

Known Feedforward/Feedback loops influencing this KER

Not Identified

References

1. Blaber, E.A. et al. (2013), "Microgravity induces pelvic bone loss through osteoclastic activity, osteocytic osteolysis, and osteoblastic cell cycle inhibition by CDKN1a/p21", *PLoS One*, Vol. 8/4, e61372. <https://doi.org/10.1371/journal.pone.0061372>
2. Chen, M., et al. (2014), "Low-dose X-ray irradiation promotes osteoblast proliferation, differentiation and fracture healing", *PLoS one*, Vol. 9/8, PLOS, San Francisco, <https://doi.org/10.1371/journal.pone.0104016>
3. da Cruz Vegian, R. M. et al. (2020), "Systemic and local effects of radiotherapy: an experimental study on implants placed in rats", *Clinical Oral Investigations*, Vol. 24, *Nature*, <https://doi.org/10.1007/s00784-019-02946-5>.
4. Donaubauer, A. J. et al. (2020), "The influence of radiation on bone and bone cells—differential effects on osteoclasts and osteoblasts", *International Journal of Molecular Sciences*, Vol. 21/17, *Nature*, <https://doi.org/10.3390/ijms21176377>.
5. Fu, J. et al. (2021), "Bone health in spacefaring rodents and primates: systematic review and meta-analysis", *npj Microgravity* Vol. 7, *Nature*, <https://doi.org/10.1038/s41526-021-00147-7>
6. Green, D. E., Adler, B. J., Chan, M. E., Lennon, J. J., Acerbo, A. S., Miller, L. M., & Rubin, C. T. (2013). Altered composition of bone as triggered by irradiation facilitates the rapid erosion of the matrix by both cellular and physicochemical processes. *PLoS one*, 8(5), e64952. <https://doi.org/10.1371/journal.pone.0064952>
7. Huang, B. et al. (2019), "Amifostine suppresses the side effects of radiation on BMSCs by promoting cell proliferation and reducing ROS production", *Stem Cells International*, Vol. 2019, Hindawi, <https://doi.org/10.1155/2019/8749090>.
8. Jia, D. et al. (2011), "Rapid loss of bone mass and strength in mice after abdominal irradiation", *Radiation research*, Vol. 176/5, 624-635. <https://doi.org/10.1667/rr2505.1>
9. Kondo, H. et al. (2009), "Total-body irradiation of postpubertal mice with 137Cs acutely compromises the microarchitecture of cancellous bone and increases osteoclasts", *Radiation Research*, Vol. 171/3, BioOne, <https://doi.org/10.1667/RR1463.1>.
10. Kook, S. H. et al. (2015), "Irradiation inhibits the maturation and mineralization of osteoblasts via the activation of Nrf2/HO-1 pathway", *Molecular and Cellular Biochemistry*, Vol. 410/1-2, *Nature*, <https://doi.org/10.1007/s11010-015-2559-z>.
11. Li, J. et al. (2020), "Effect of α 2-macroglobulin in the early stage of jaw osteoradionecrosis", *International Journal of Oncology*, Vol. 57/1, Spandidos Publications, <https://doi.org/10.3892/IJO.2020.5051>.
12. Lima, F. et al. (2017). Exposure to Low-Dose X-Ray Radiation Alters Bone Progenitor Cells and Bone Microarchitecture. *Radiation Research*, 188(4.1), 433-442. <http://www.jstor.org/stable/26428489>
13. Liu, Y. et al. (2018), "Protective effects of α -2-macroglobulin on human bone marrow mesenchymal stem cells in radiation injury", *Molecular medicine reports*, Vol. 18/5, Spandidos Publications, <https://doi.org/10.3892/MMR.2018.9449>.
14. Oest, M. E. et al. (2015), "Long-term loss of osteoclasts and unopposed cortical mineral apposition following limited field irradiation", *Journal of orthopaedic research : official publication of the Orthopaedic Research Society*, Vol. 33/3, 334-342. <https://doi.org/10.1002/jor.22761>
15. Pacheco, R. and H. Stock. (2013), "Effects of Radiation on Bone", *Current Osteoporosis Reports*, Vol. 11, *Nature*, <https://doi.org/10.1007/S11914-013-0174-Z>.
16. Sakurai, T. et al. (2007), "Radiation-induced Reduction of Osteoblast Differentiation in C2C12 cells", *Journal of Radiation Research*, Vol. 48/6, Oxford University Press, Oxford, <https://doi.org/10.1269/jrr.07012>.
17. Smith, J. K. (2020), "Osteoclasts and microgravity", *Life*, Vol. 10/9, MDPI, Basel, <https://doi.org/10.3390/life10090207>.
18. Stavnickich, M., et al. (2020), "A systematic review and meta-analysis of bone loss in space travelers", *npj microgravity*, Vol. 6, *Nature*, <https://doi.org/10.1038/s41526-020-0103-2>
19. Sugimoto, M. et al. (1993), "Osteocyte viability after high-dose irradiation in the rabbit", *Clinical orthopaedics and related research*, Vol. 297, 247-252.
20. Swift, J. M., et al. (2015), "Skin wound trauma, following high-dose radiation exposure, amplifies and prolongs skeletal tissue loss", *Bone*, Vol. 81, Elsevier, <https://doi.org/10.1016/j.bone.2015.08.022>
21. Turner, R. T., Iwaniec, U. T., Wong, C. P., Lindenmaier, L. B., Wagner, L. A., Branscum, A. J., Menn, S. A., Taylor, J., Zhang, Y., Wu, H., & Sibonga, J. D. (2013). Acute exposure to high dose γ -radiation results in transient activation of bone lining cells. *Bone*, 57(1), 164-173. <https://doi.org/10.1016/j.jbone.2013.08.002>
22. Wang, C. et al. (2016), "Protective Effects of Cerium Oxide Nanoparticles on MC3T3-E1 Osteoblastic Cells Exposed to X-Ray Irradiation", *Cellular Physiology and Biochemistry*, Vol. 38, Karger, Basel, <https://doi.org/10.1159/000443092>.
23. Willey, J. S. et al. (2011), "Ionizing Radiation and Bone Loss: Space Exploration and Clinical Therapy Applications", *Clinical Reviews in Bone and Mineral Metabolism*, Vol. 9, *Nature*, <https://doi.org/10.1007/s12018-011-9092-8>.

24. Willey, J. S. et al. (2010), "Risedronate prevents early radiation-induced osteoporosis in mice at multiple skeletal locations", *Bone*, Vol. 46/1, Elsevier, <https://doi.org/10.1016/j.bone.2009.09.002>.

25. Willey, J. S. et al. (2008), "Early Increase in Osteoclast Number in Mice after Whole-Body Irradiation with 2 Gy X Rays", *Vol. 170/3, BioOne*, <https://doi.org/10.1667/RR1388.1>

26. Wright, L. E. et al. (2015), "Single-Limb Irradiation Induces Local and Systemic Bone Loss in a Murine Model", *Journal of Bone and Mineral Research*, Vol. 108/2, Wiley, <https://doi.org/10.1002/jbm.2458>

27. Zhang, L. et al. (2020), "Amifostine inhibited the differentiation of RAW264.7 cells into osteoclasts by reducing the production of ROS under 2 Gy radiation", *Journal of Cellular Biochemistry*, Vol. 121/1, Wiley, <https://doi.org/10.1002/jcb.29247>

Relationship: 2848: Energy Deposition leads to Bone Remodeling

AOPs Referencing Relationship

AOP Name	Adjacency	Weight of Evidence	Quantitative Understanding
Deposition of energy leading to occurrence of bone loss	non-adjacent	High	Low

Evidence Supporting Applicability of this Relationship

Taxonomic Applicability

Term	Scientific Term	Evidence	Links
human	Homo sapiens	Low	NCBI
mouse	Mus musculus	High	NCBI
rat	Rattus norvegicus	Moderate	NCBI

Life Stage Applicability

Life Stage Evidence

Adult	High
Juvenile	High
Sex Applicability	
Sex	Evidence

Male	High
Female	Moderate
Unspecific	Low

Supporting evidence for this relationship has been demonstrated *in vivo* for mice and rats, with considerable evidence for mice. The relationship has been demonstrated *in vivo* for both males and females, with considerable evidence for males. *In vivo* evidence is derived from preadolescents, adolescents, and adults, with strong evidence for adolescents and adults.

Key Event Relationship Description

Bone and bone remodeling cells, like all other tissues and cells, are vulnerable to deposited energy, but with varying radiosensitivity. Ionizing radiation (IR) can indirectly disrupt bone remodeling by depositing energy into bone cells, including osteoblasts, osteoclasts, and osteocytes, resulting in ionization events that can lead to oxidative stress and loss of homeostasis in the bone microenvironment. Changes to bone remodeling cell homeostasis are expressed as a decrease in bone formation and an increase in bone resorption. Bone remodeling can be affected by variety of IR sources, including low linear energy transfer (LET) radiation, such as X-rays, gamma rays, and protons, and high LET radiation, such as heavy ions. These changes can be observed through dynamic bone histomorphometry measurements that quantify the destruction of the organic and inorganic bone matrix by osteoclasts and its replacement by osteoblasts (Dempster et al., 2013). As bone tissue is remodeled, shifts in the proportion of stronger, plate-like trabeculae to more brittle, rod-like trabeculae can be observed through changes to the structural model index (SMI) (Shahnazari et al., 2012).

Evidence Supporting this KER

Overall weight of evidence: High

Biological Plausibility

Typically, bone remodeling regulates mineral homeostasis and adapts to everyday stresses by repairing or removing damaged bone to keep it structurally sound (Raggatt & Partridge, 2010). Deposition of energy can indirectly disrupt bone remodeling so that bone resorption and formation do not occur in coordination.

Radiation can cause an imbalance in physiological bone remodeling to favor bone resorption over formation. The activator of nuclear factor kappa B ligand (RANK-L) and Wnt pathways can be influenced by the deposition of energy, leading to increased resorption and decreased formation of bone, respectively (Tian et al., 2017). Irradiated osteocytes contribute to increased bone resorption through the release of osteoclastogenesis-stimulating molecules. Osteocyte apoptosis can also occur due to irradiation of bone, further contributing to increased activity of osteoclasts (Donaubauer et al., 2020). The outcome of these radiation-induced changes is an imbalance in bone remodeling, favoring bone resorption and diminishing bone formation (Donaubauer et al., 2020; Zhang et al., 2018).

In addition to the effects on bone remodeling cells, immune-mediated cytokine response in bone marrow is triggered by IR. IR has been shown to increase the expression of pro-osteoclastogenic proteins such as RANK-L in both mineralized and marrow tissue. Expression of pro-inflammatory and pro-osteoclastogenic factors, such as tumor necrosis factor (TNF), interleukin (IL)-6, and chemoattractant protein (MCP)-1 also induced by IR in bone marrow tissue leading to build-up of osteoclasts in the bone marrow which will stimulate maturation of osteoclasts (Donaubauer et al., 2020).

Empirical Evidence

The empirical data relevant to this KER provides support for the linkage between deposition of energy and bone remodeling. The empirical evidence supporting this KER is gathered from research utilizing *in vivo* models experimenting on radiation exposure and the resulting changes in the SMI, bone formation rate (BFR), mineral apposition rate (MAR) and mineralizing surface normalized to the bone surface (MS/BS). Radiation studies examined these endpoints using X-rays, gamma rays, and heavy ions (Alwood et al., 2010; Bandstra et al., 2008; Chandra et al., 2017; Chandra et al., 2014; Wright et al., 2015; Xu et al., 2014; Zhang et al., 2019).

Dose Concordance

Various studies measure the response of remodeling to a given dose of IR. Once energy is deposited into matter at all doses, follow-on downstream events are immediately initiated. Studies that analyzed the effects of a range of radiation doses on bone remodeling in the same model found that higher doses generally resulted in greater changes to bone remodeling, providing support for a dose-dependent relationship between the two KEs (Alwood et al., 2010; Bandstra et al., 2008; Zhai et al., 2019). Alwood et al. observed significant bone remodeling after exposure to 2 Gy of ^{56}Fe heavy ions and no significant change after 0.5 Gy (Alwood et al., 2010). Zhai et al. observed a similar trend, as there was no significant change to MAR after exposure to 2 Gy of X-rays, but MAR decreased by 50% at 30 days after 3 fractions of 8 Gy (3 x 8 Gy) irradiation (Zhai et al., 2019). MS/BS tends to decrease linearly as the radiation dose increases. Relative to non-irradiated models, MS/BS was shown to decrease up to 80% after exposure to 2 or 8 Gy of X-ray or gamma radiation (Chandra et al., 2017; Kondo et al., 2010; Wright et al., 2015; Zhang et al., 2019). After exposure to high doses (4-16 Gy) of low LET X-rays, SMI increased up to 105.3% (Chandra et al., 2017; Chandra et al., 2014; Xu et al.,

2014), while exposure to 2 Gy of high LET ^{56}Fe ions resulted in a 194% increase in SMI (Alwood et al., 2010). Multiple studies measured changes to the BFR, showing attenuation up to 100% after 8 and 16 Gy and up to 33% after 2 Gy of X-rays (Chandra et al., 2017; Chandra et al., 2014; Wright et al., 2015; Zhang et al., 2019). However, some studies do not show significant changes to the BFR after irradiation but still show a loss of bone volume (Bandstra et al., 2008; Kondo et al., 2010), indicating that the imbalanced bone remodeling is due to increased osteoclast activity instead of decreased osteoblast activity (Kondo et al., 2010).

Time Concordance

Various studies show the response of bone remodeling to deposition of energy over time. When energy is deposited into biological models it immediately causes ionization events which directly lead to downstream events occurring at later time points. Remodeling was found increased after 1 week as well as 1 and 2 months after X-ray and ^{56}Fe irradiation (Alwood et al., 2010; Chandra et al., 2017; Wright et al., 2015; Zhai et al., 2019; Zhang et al., 2019). The highest responses occurred after 1 month, although this could be attributed to the higher LET and dose used when remodeling was measured at this time. Due to the lack of studies on time response there are no trends identified in the changes of bone remodeling markers.

Essentiality

Essentiality is difficult to show with deposition of energy because it is a physical stressor and cannot be modified by chemicals. However, lead shielding used to protect the contralateral limbs of animals demonstrated higher bone remodeling in exposed limbs than contralateral limbs (Wright et al., 2015; Zhai et al., 2019). Wright et al. (2015) irradiated C57BL/6 mice with 2 Gy of X-rays and observed that BFR/BS decreased significantly in the irradiated limb, while the BFR/BS in the shielded contralateral limb decreased by a statistically negligible amount. Thirty days following irradiation of Sprague Dawley rats with 3 fractions of 8 Gy of X-rays, Zhai et al. (2019) observed that MAR in shielded contralateral limbs remained at levels similar to the control, while the irradiated limbs experienced a significant reduction in MAR.

Uncertainties and Inconsistencies

- The BFR, MAR, and MS/BS are measures of bone formation, and therefore are used as endpoints of bone remodeling. However, studies do not directly measure bone resorption as the bone resorption rate cannot be directly measured by dynamic histomorphometry (Dempster et al., 2013). Instead, studies rely on determining the rate of bone resorption indirectly by observing changes to the BFR relative to changes in bone volume. Future work could be done to identify a direct tissue-level measure of the bone resorption rate.
- The MAR of the proximal tibial metaphysis from mice irradiated with 2 Gy X-rays showed significant increase after 1 week as opposed to a decrease (Willey et al., 2010).
- The SMI in the trabecular epiphysis of mice exposed to 4.4 cGy decreased significantly as opposed to an expected increase after ionizing irradiation (Karim and Judex, 2014)
- The MAR in the periosteal, endosteal diaphysis and endosteal metaphysis of mice increased 1-8 weeks after irradiation of 5 Gy and 4x5Gy (Oest et al., 2015).

Quantitative Understanding of the Linkage

The following are a few examples of quantitative understanding of the relationship. All data is statistically significant unless otherwise indicated.

Response-response relationship

Dose Concordance

Reference	Experiment Description	Result
Wright et al., 2015	<i>In vivo</i> . The right hindlimbs of 20-week-old male C57BL/6 mice were irradiated with 2 Gy of X-rays at a rate of 1.6 Gy/min. The bone formation rate normalized to the bone surface (BFR/BS), MS/BS, and MAR were measured 1 week post-irradiation.	Direct radiation with 2 Gy led to a 33% decrease in BFR/BS and a 20% decrease in MS/BS. MAR was decreased by 13% (non-significant).
Chandra et al., 2017	<i>In vivo</i> . The distal metaphyseal region of right femurs of 8- to 10-week-old male mice were irradiated with 8 Gy of X-rays at a rate of 1.65 Gy/min. The SMI, MS, and BFR/BS were measured.	SMI was increased by 26% in irradiated group and MS was decreased by nearly 80% after radiation exposure. BFR/BS levels decreased 100% after irradiation.
Chandra et al., 2014	<i>In vivo</i> . Three-month-old female rats were irradiated at the proximal metaphyseal region of the right tibiae with 16 Gy of X-rays, fractionated into two 8 Gy doses at a rate of 1.65 Gy/min. The SMI, MS/BS, MAR, and BFR/BS were measured.	IR exposure resulted in a 78% decrease in MS/BS and a 100% decrease in both BFR/BS and MAR, as well as a ~20% increase in SMI, at 28 days post-irradiation relative to non-irradiated controls.
Zhang et al., 2019	<i>In vivo</i> . The experiments were performed on 4-week-old male C57BL/6J mice exposed to 2 Gy X-ray radiation at the mid-shaft of the left femur. MS/BS, MAR and BFR/BS were measured.	MS/BS was reduced by 21% in the irradiated group. There was a 22% decrease in BFR/BS in the irradiated group. No changes in MAR, BFR/BS and MS/BS were significant.
Bandstra et al., 2008	<i>In vivo</i> . 58-days old female C57BL/6J mice were exposed to whole-body 0, 0.5, 1, or 2 Gy proton radiation of 250 MeV protons at a rate of 0.7 Gy/min. Endosteal BFR (Ec.BFR) was assessed.	Ec.BFR decreased by 19%, 27%, and 21% after 0.5, 1, and 2 Gy, respectively. However, the changes in BFR were not significant.
Xu et al., 2014	<i>In vivo</i> . 8-week-old male Wistar rats were exposed to whole-body 4 Gy X-ray radiation. SMI was measured in the proximal tibia.	SMI was increased in the irradiated group by 105.3% after 4 Gy of X-ray exposure.
Alwood et al., 2010	<i>In vivo</i> . 4-month-old, adult, male, C57BL/6 mice were exposed to irradiation with 0.5 Gy and 2 Gy of 1 GeV/nucleon ^{56}Fe heavy ions. SMI was measured in the mineralized cancellous bone tissue of the fourth lumbar vertebrae.	SMI was increased by 194% and 31% (non-significant) after exposure to 2 Gy and 0.5 Gy radiation, respectively.
Hui et al., 2014	<i>In vivo</i> . 20-week-old adult female mice were exposed to a single 16 Gy dose of X-rays to the hindlimbs. The MAR of the distal femurs of irradiated mice was measured.	Compared to non-irradiated controls, irradiation resulted in a 16% decrease per day in MAR at 12-29 days after 16 Gy irradiation.
Kondo et al., 2010	<i>In vivo</i> . 17-week-old C57BL/6J mice were exposed to whole-body 1 or 2 Gy ^{137}Cs gamma radiation. Bone remodeling markers such as BFR, MAR, and MS/BS were measured in the proximal tibiae.	Compared to sham-radiated controls, 2 Gy irradiation resulted in a 7% decrease in MS/BS. Changes to BFR and MAR were non-significant.
Zhai et al., 2019	<i>In vivo</i> . 6-week-old male Sprague-Dawley rats were exposed at the left hindlimb to either one single dose of 2 Gy X-ray radiation or fractionated irradiation (3 x 8 Gy) at a dose rate of 185.5 cGy/min. MAR was determined in the irradiated tibia.	MAR did not differ significantly in the 2 Gy irradiated group after 30 and 60 days. MAR was decreased by >50% after 30 days and by 31% (non-significant) after 60 days in the 3 x 8 Gy group.

Time-scale

Time Concordance

Reference	Experiment Description	Result
Wright et al., 2015	<i>In vivo</i> . The right hindlimbs of 20-week-old male C57BL/6 mice were irradiated with 2 Gy of X-rays at a rate of 1.6 Gy/min. BFR/BS, MS/BS, and MAR were measured after 1 week.	Direct radiation with 2 Gy led to a 33% decrease in BFR/BS and a 20% decrease in MS/BS after 1 week. MAR was decreased by 13% (non-significant), also after 1 week.
Chandra et al., 2017	<i>In vivo</i> . The distal metaphyseal region of right femurs of 8- to 10-week-old male mice were irradiated with 8 Gy of X-rays at a rate of 1.65 Gy/min. The SMI, MS, and BFR/BS were measured.	SMI was increased by 26% in the 8 Gy irradiated group and MS was decreased by nearly 80% 4 weeks after radiation exposure. BFR/BS was completely attenuated 4 weeks after irradiation (100% decrease).
Chandra et al., 2014	<i>In vivo</i> . Three-month-old female rats were irradiated at the proximal metaphyseal region of the right tibiae with 16 Gy of X-rays, fractionated into two 8 Gy doses at a rate of 1.65 Gy/min. The SMI, MS/BS, MAR, and BFR/BS were measured.	After 28 days post-irradiation, IR exposure resulted in a 78% decrease in MS/BS and a 100% decrease in both BFR/BS and MAR, as well as a ~20% increase in SMI.

Zhang et al., 2019	<i>In vivo</i> . The experiments were performed on 4-week-old male C57BL/6J mice exposed to 2 Gy X-ray radiation at the mid-shaft of the left femur. MS/BS, MAR and BFR/BS were measured.	MS/BS was reduced by 21% 28 days post-irradiation. There was a 22% decrease in BFR/BS 28 days post-irradiation. No changes in MAR, BFR/BS and MS/BS were significant.
Alwood et al., 2010	<i>In vivo</i> . 4-month-old, adult, male, C57BL/6 mice were exposed to irradiation with 0.5 Gy and 2 Gy of 1 GeV/nucleon ^{56}Fe heavy ions. SMI was measured in the mineralized cancellous bone tissue of the fourth lumbar vertebrae.	SMI was increased by 194% and 31% (non-significant) after exposure to 2 Gy (after 31 days) and 0.5 Gy (after 28 days) radiation, respectively.
Zhai et al., 2019	<i>In vivo</i> . 6-week-old male Sprague-Dawley rats were exposed at the left hindlimb to either one single dose of 2 Gy X-ray radiation or fractionated irradiation (3 x 8 Gy) at a dose rate of 185.5 cGy/min. MAR was determined in the irradiated tibia.	MAR did not differ significantly in the 2 Gy irradiated group after 30 and 60 days. MAR was decreased by >50% after 30 days and by 31% (non-significant) after 60 days in the 3 x 8 Gy group.

Known modulating factors

Modulating Factors	Details	Effects on the KER	References
Drug	Sclerostin (Wnt antagonist) suppression	Chandra et al. (2017) studied the effects of sclerostin on bone remodeling. Sclerostin is a Wnt antagonist, and its expression in adults is primarily restricted to osteocytes. In this experiment, suppression of sclerostin was examined using a monoclonal antibody against sclerostin (Scl-Ab). Data collected from the experiment shows that Scl-Ab completely reverses the effects of radiation on bone tissue. Scl-Ab injections not only blocked any structural deterioration but also increased bone mass and improved bone quality in the irradiated area to the same levels as in a non-irradiated area with Scl-Ab treatment.	Chandra et al., 2017
Age	Old age	Lower estrogen at old age is thought to increase bone resorption, compounding with the effects of radiation.	Pacheco and Stock, 2013

Known Feedforward/Feedback loops influencing this KER

Not Identified

References

Alwood, J. S. et al. (2010), "Heavy ion irradiation and unloading effects on mouse lumbar vertebral microarchitecture, mechanical properties and tissue stresses", *Bone*, Vol. 47/2, Elsevier B.V., <https://doi.org/10.1016/j.bone.2010.05.004>.

Bandstra, E. R. et al. (2008), "Long-term dose response of trabecular bone in mice to proton radiation", *Radiation Research*, Vol. 169/6, BioOne, <https://doi.org/10.1667/RR1310.1>.

Chandra, A. et al. (2017), "Suppression of Sclerostin Alleviates Radiation-Induced Bone Loss by Protecting Bone-Forming Cells and Their Progenitors Through Distinct Mechanisms", *Journal of Bone and Mineral Research*, Vol. 32/2, Wiley, <https://doi.org/10.1002/jbm.2996>.

Chandra, A. et al. (2014), "PTH1-34 Alleviates Radiotherapy-induced Local Bone Loss by Improving Osteoblast and Osteocyte Survival", *Bone*, Vol. 67/1, Elsevier, <https://doi.org/10.1016/j.bone.2014.06.030>

Dempster, D. W. et al. (2013), "Standardized Nomenclature, Symbols, and Units for Bone Histomorphometry: A 2012 Update of the Report of the ASBMR Histomorphometry Nomenclature Committee", *Journal of Bone and Mineral Research*, Vol. 28, Wiley, <https://doi.org/10.1002/jbm.1805>.

Donaubauer, A. J. et al. (2020), "The influence of radiation on bone and bone cells—differential effects on osteoclasts and osteoblasts", *International Journal of Molecular Sciences*, Vol. 21/17, MDPI, Basel, <https://doi.org/10.3390/ijms21176377>.

Frost H. M. (1966), "Bone dynamics in metabolic bone disease" *The Journal of bone and joint surgery*. American volume, 48(6), 1192-1203.

Hui, S. K. et al. (2014), "The Influence of Therapeutic Radiation on the Patterns of Bone Remodeling in Ovary-Intact and Ovariectomized Mice", *Bone*, Vol. 23/1, *Nature*, <https://doi.org/10.1007/s00223-012-9688-0>

Karim, L. and Judex, S. (2014), "Low level irradiation in mice can lead to enhanced trabecular bone morphology", *Journal of bone and mineral metabolism*, Vol. 32/5, 476-483. <https://doi.org/10.1007/s00774-013-0518-x>

Kondo, et al. (2010), "Oxidative stress and gamma radiation-induced cancellous bone loss with musculoskeletal disuse", *Journal of applied physiology*, Vol. 108/1, American Physiological Society, <https://doi.org/10.1152/japplphysiol.00294.2009>

Oest, M. E. et al. (2015), "Long-term loss of osteoclasts and unopposed cortical mineral apposition following limited field irradiation", *Journal of orthopaedic research : official publication of the Orthopaedic Research Society*, Vol. 33/3, 334–342. <https://doi.org/10.1002/jor.22761>

Pacheco, R. and H. Stock (2013), "Effects of radiation on bone", *Current osteoporosis reports*, Vol. 11/4, *Nature*, <https://doi.org/10.1007/s11914-013-0174-z>

Raggatt, L. J., and Partridge, N. C. (2010), "Cellular and molecular mechanisms of bone remodeling", *The Journal of biological chemistry*, Vol. 285/33, <https://doi.org/10.1074/jbc.R109.041087>.

Shahnazari, M. et al. (2012), "Simulated spaceflight produces a rapid and sustained loss of osteoprogenitors and an acute but transitory rise of osteoclast precursors in two genetic strains of mice", *American Journal of Physiology - Endocrinology and Metabolism*, Vol. 303/11, American Physiological Society, <https://doi.org/10.1152/ajpendo.00330.2012>.

Tian, Y. et al. (2017), "The impact of oxidative stress on the bone system in response to the space special environment", *International Journal of Molecular Sciences*, Vol. 18/10, MDPI, Basel, <https://doi.org/10.3390/ijms18102132>

Willey, J. S., Livingston, E. W., Robbins, M. E., Bourland, J. D., Tirado-Lee, L., Smith-Sielicki, H., & Bateman, T. A. (2010). Risedronate prevents early radiation-induced osteoporosis in mice at multiple skeletal locations. *Bone*, 46(1), 101–111. <https://doi.org/10.1016/j.bone.2009.09.002>

Willey, J. S. et al. (2011), "Ionizing Radiation and Bone Loss: Space Exploration and Clinical Therapy Applications", *Clinical Reviews in Bone and Mineral Metabolism*, Vol. 9, *Nature*, <https://doi.org/10.1007/s12018-011-9092-8>.

Wright, L. E. et al. (2015), "Single-Limb Irradiation Induces Local and Systemic Bone Loss in a Murine Model", *Journal of Bone and Mineral Research*, Vol. 30, American Society for Bone and Mineral Research, Washington, <https://doi.org/10.1002/jbm.2458>.

Xu, D., et al. (2014), "The combined effects of X-ray radiation and hindlimb suspension on bone loss", *Journal of radiation research*, Vol. 55/4, Oxford University Press, Oxford, <https://doi.org/10.1093/jrr/rru014>

Zhai, et al. (2019), "Influence of radiation exposure pattern on the bone injury and osteoclastogenesis in a rat model", *International journal of molecular medicine*, Vol. 44/6, Spandidos Publications, <https://doi.org/10.3892/ijmm.2019.4369>

Zhang, J. et al. (2019), "Lowering iron level protects against bone loss in focally irradiated and contralateral femurs through distinct mechanisms", *Bone*, Vol. 120, Elsevier, <https://doi.org/10.1016/j.bone.2018.10.005>.

Zhang, J., et al. (2018), "Therapeutic ionizing radiation induced bone loss: a review of in vivo and in vitro findings", *Connective tissue research*, Vol. 59/6, Informa, London, <https://doi.org/10.1080/03008207.2018.1439482>

Relationship: 2849: Energy Deposition leads to Bone Loss**AOPs Referencing Relationship**

AOP Name	Adjacency	Weight of Evidence	Quantitative Understanding
Deposition of energy leading to occurrence of bone loss	non-adjacent	High	Moderate

Evidence Supporting Applicability of this Relationship**Taxonomic Applicability**

Term	Scientific Term	Evidence	Links
human	Homo sapiens	High	NCBI
mouse	Mus musculus	High	NCBI
rat	Rattus norvegicus	Moderate	NCBI

Life Stage Applicability**Life Stage Evidence**

Adult	High
Juvenile	Moderate

Sex Applicability

Sex	Evidence
Male	High
Female	Moderate
Unspecific	Moderate

Evidence for this relationship is from human, mice, and rat models, with considerable available evidence in mice and humans. The relationship is well supported in both males and females using *in vivo* models. There is *in vivo* evidence from studies conducted using preadolescent, adolescent, and adult rodent models.

Key Event Relationship Description

Energy deposited onto an organism from ionizing radiation (IR) can result in an increase in bone loss. Bone loss refers to a decrease in bone mass or density as observed in a variety of conditions such as osteopenia and osteoporosis (Cummings, Bates, and Black, 2002). Energy deposition can interfere with overall bone integrity and the capacity to withstand mechanical load, leading to an increased risk of fractures (Cummings, Bates, and Black, 2002; Green and Rubin, 2014; Orwoll et al., 2013; Willey et al., 2011; Willey et al., 2013; Wright, 2018). Ionizing energy deposited into an organism is absorbed eliciting breakage of water molecules leading to free radical formation, if this overwhelms the antioxidant capacity, then oxidative stress ensues. If this occurs in bone tissue cells, including osteoblasts, osteoclasts, and osteocytes, it can dysregulate their activity. The subsequent increases in bone resorption and decreases in bone formation culminate in increased bone loss. Bone loss can be induced by a variety of radiation sources, including low linear energy transfer (LET) radiation, such as X-rays, gamma rays, and protons, and high LET radiation, such as heavy ions, at a wide range of doses and dose rates. IR-induced bone loss can be observed through microarchitectural measurements that show the structural deterioration of affected bones.

Evidence Supporting this KER

Overall weight of evidence: High

Biological Plausibility

Extreme stresses, such as energy deposited by IR, can dysregulate bone resorption from osteoclasts and formation from osteoblasts, resulting in bone loss (Donaubauer et al., 2020). Numerous studies have shown that skeletally mature adults exposed to radiotherapy have a greater risk of bone fractures, reduced bone strength, and osteoporosis. Availability of human studies to support this relationship is extensive from both in a clinical and space setting. Bone loss in areas exposed to clinical radiotherapy have been associated with increased fracture risk (Green and Rubin, 2014; Orwoll et al., 2013; Willey et al., 2011, Willey et al., 2013; Wright, 2018). A substantial body of evidence from spaceflight missions demonstrates that the space environment, which consists of IR, induces an imbalance between bone production and resorption (Orwoll et al., 2013; Stavnichuk et al., 2020; Willey et al., 2011). Stavnichuk et al. (2020) performed a meta-analysis using 148 astronauts and found decreased bone density at a rate of 0.8% per month of spaceflight. Even when appropriate nutrition and enhanced physical activity training are implemented, the concentrations of bone resorption indicators increase in astronauts during flight (Farris et al., 2020; Yang et al., 2018).

Irradiated bone has a lower number of osteoblasts than non-irradiated bone. Fewer osteoblasts results in a decrease in the bone formation rate leading to bone loss. This may reduce the synthesis of a new matrix (e.g., collagen) and decrease bone density, which can increase bone loss and the risk of bone fracture (Costa and Reagan, 2019; Farris et al., 2020). Increased osteoclast and decreased osteoblast activity following irradiation results in increased bone resorption and trabecular bone turnover.

Bone marrow is among the most radiosensitive tissues in the body. Another outcome of irradiation on bones is the elimination of red (active, hematopoietic) marrow and the replacement with yellow (or white, inactive, fatty) marrow (ICRP, 2007; Pacheco and Stock, 2013). Yellow marrow is less vascular than red marrow and is therefore more vulnerable to repetitive physiologic skeletal loads (Pacheco and Stock, 2013).

One contributor to bone loss from deposited energy is an increase in reactive oxygen species (ROS), associated DNA damage, and related apoptosis. In bone marrow-derived skeletal cell progenitors, radiation reduced osteoblast development and promoted ROS generation (Willey et al., 2011; Yang et al., 2018). Total body irradiation in rodents increases the production of ROS in marrow cells and accelerates cell death. These findings suggested that irradiation could generate oxidative stress, inhibiting osteoblast development and differentiation while promoting bone resorption. As a result, radiation may influence key bone cell processes by promoting the generation of ROS and suppressing osteoblasts. After gamma irradiation, male C57BL/6 mice showed reduced cancellous BV/TV in the proximal tibia and lumbar vertebrae, higher osteoclast surface in the tibia, and increased ROS generation in marrow cells (Donaubauer et al., 2020; Tian et al., 2017; Willey et al., 2011; Yang et al., 2018).

The degree of bone mineralization and bone density are direct indicators of bone loss in the body that are depleted following irradiation (Farris et al., 2020; Green and Rubin, 2014; Slyfield et al., 2012). Changes to trabecular and cortical parameters also indicate bone loss due to the deposition of energy. Indirect measures of bone loss following radiation can include the incidence of fractures as well as the energy required to fracture the bone (Fonseca et al., 2014; Turner, 2002). In addition, stiffness and the elastic modulus have been shown to positively correlate with the degree of mineralization of bones (Fonseca et al., 2014; Turner, 2002).

Empirical Evidence

The empirical data relevant to this KER provides support for the linkage between deposition of energy and bone loss. The majority of the evidence supporting this relationship comes from studies examining the effect of IR sources, including X-rays, gamma rays, protons, and heavy ions, on the skeletal system. Current literature on the subject explores the deterioration of bone structure under exposure to a wide range of doses (0.05-64 Gy), dose rates (0.1-4 Gy/min), and LET levels (0.23-175 keV/μm). IR exposure consistently resulted in increased bone loss, often in a dose- and time-dependent manner (Alwood et al., 2017; Alwood et al., 2010; Bandstra et al., 2009; Bandstra et al., 2008; Chandra et al., 2017; Chandra et al., 2014; Ghosh et al., 2016; Green et al., 2012; Hamilton et al., 2006; Hui et al., 2014; Lloyd et al., 2012; Nishiyama et al., 1992; Stavnichuk et al., 2020; Willey et al., 2010; Wright et al., 2015; Yumoto et al., 2010).

Dose Concordance

Current literature on the effects of IR on bone tissue provides strong evidence for a dose concordance relationship between energy deposition and bone loss. Once energy is deposited onto matter at all doses, follow-on downstream events are immediately initiated. The models used in these studies, mostly C57BL/6 mice, generally experienced some degree of degradation in one or more parameters of bone structure or quality, including bone mineral density (BMD), bone volume fraction (BV/TV), connectivity density (Conn.D), trabecular number (Tb.N), trabecular separation (Tb.Sp), trabecular thickness (Tb.Th), maximum load, stiffness, the elastic modulus, and the frequency of fractures after irradiation.

A few human studies show the response after a given dose of IR. Patients with uterine cervix carcinoma irradiated with photons (4 MV) showed similar reductions in CaCO₃ content by an average of 55 mg after both 22.4 and 45 Gy (Nishiyama et al., 1992). In astronauts exposed to space radiation, bone density is estimated to be reduced at 0.8% per month in lower limbs and 0.1% per month in upper limbs as longer duration flights lead to a higher dose of IR (Stavnichuk et al., 2020). Short duration flights (<30 days) led to decreased bone density up to 10%, which could be due to an early onset of increased resorption and late onset of increased formation (Stavnichuk et al., 2020). However, astronauts are also exposed to microgravity and not just radiation. A follow-up study of the Stockholm I and II Trials found a significantly increased incidence of femoral neck or pelvic fractures in rectal carcinoma patients receiving 25 Gy of radiotherapy compared to unexposed

patients (Holm et al., 1996). Multiple clinical studies demonstrate that increasing fractionated doses of photons from ~40-60 Gy during radiotherapy lead to an increased incidence of bone fractures, likely due to lower bone mass after higher radiation doses (Dickie et al., 2009; Overgaard, 1988).

Of the studies that examined the effects of irradiation in animal models with low LET sources, such as X-rays, gamma rays, and protons, most found that low doses (<2 Gy) could result in bone loss (Alwood et al., 2017; Bandstra et al., 2008; Lloyd et al., 2012). Similarly, higher LET sources, such as heavy ions, could result in bone loss at doses as low as 0.1 Gy (Alwood et al., 2017; Alwood et al., 2010; Bandstra et al., 2009; Ghosh et al., 2016; Yumoto et al., 2010). However, changes at low doses were often non-significant.

Exposure to high doses (>2 Gy) of IR resulted in statistically significant bone loss in almost all cases, regardless of the radiation type, along with greater changes compared to lower doses (Alwood et al., 2017; Alwood et al., 2010; Bandstra et al., 2008; Chandra et al., 2017; Chandra et al., 2014; Green et al., 2012; Hamilton et al., 2006; Hui et al., 2014; Jia et al., 2011; Willey et al., 2010; Wright et al., 2015; Yumoto et al., 2010). While bone loss was generally significant in all high dose studies, Hamilton et al. (2006) and Alwood et al. (2017) compared the impact that exposure to the same dose of radiation has on bone structure when multiple sources with different LET levels are used. They found that changes in BV/TV and Tb.Th were generally LET-dependent, with higher LET sources consistently inducing greater loss of bone than lower LET sources. However, some measurements, including Tb.N, Tb.Sp, and Conn. D, did not always follow this trend.

Studies that examined the impact of a range of radiation doses on bone structure in the same model provide excellent evidence for a dose-dependent relationship between energy deposition and bone loss. These studies found that high dose radiation generally resulted in more pronounced bone loss than low dose radiation (Alwood et al., 2017; Alwood et al., 2010; Bandstra et al., 2008), except for the study by Yumoto et al. (2010), which observed significant dose-dependent decreases in BV/TV and Conn. D at 0.1 and 0.5 Gy compared to non-irradiated controls, but a non-significant decrease at 2 Gy. Bandstra et al. (2008) observed linear, dose-dependent decreases in BV/TV and volumetric BMD (vBMD) from 0.5-2 Gy, while Tb.Sp similarly increased in a linear, dose-dependent manner at 0.5-2 Gy. Alwood et al. (2017) observed proton and ⁵⁶Fe radiation both induced a decrease in BV/TV and Tb.N at 2 Gy, but not at 0.05 or 0.1 Gy. Alwood et al. (2010) observed significant changes to BV/TV, Tb.Sp, Tb.N, Conn. D, cancellous bone stress, and the elastic modulus after exposure to 2 Gy of ⁵⁶Fe heavy ions, while 0.5 Gy did not result in significant changes to any measures of bone structure. Jia et al. (2011) showed that BMD decreased almost 2-folds with each increasing dose (5, 10, 15, 20 Gy) from 0 Gy. A significant decrease in BV/TV was observed in mice exposed to 5 Gy compared to the control group, while 1 Gy did not result in any significant changes (Pendleton et al., 2021). Mice exposed to 0.5 Gy in a single or fractionated dose (0.17 X3) of high-LET 28 Si ions showed significant reductions in bone volume, respectively, when compared to sham controls (Macias et al. 2017). Additionally, under spaceflight conditions mice were observed to exhibit a 6.23% decrease in BV/TV and a 11.91% decrease Tb.Th in the pelvis compared to the ground control group (Blaber et al., 2013).

Time Concordance

In the current literature, there is limited evidence of a time-concordance relationship between energy deposition and bone loss. When energy is deposited onto biological models it immediately causes ionization events which directly lead to downstream events occurring at later time points. In patients with uterine cervix carcinoma irradiated with protons (4 MV) at 22.5 and 45 Gy, bone CaCO₃ content decreased linearly from 140 mg to 84 mg after 3 months, plateauing at about 70 mg after 6 and 12 months (Nishiyama et al., 1992). A higher incidence of fractures was observed in patients receiving 25 Gy of photons compared to unexposed patients, measured 5 years after exposure (Holm et al., 1996). Current data in animal models suggests that most bone loss occurs in the first few months after exposure. In mice exposed to 5 Gy gamma radiation, significant decline was found in both mineral/bone matrix ratio and bone volume fraction 10 days following exposure (Green et al. 2013). The BV/TV of control mice after 12 weeks decreased 11.5% compared to the 0 Gy at 11 days. After exposure to 5 Gy, BV/TV in mice decreased 23% after 11 days and -21.6% after 12 weeks (Pendleton et al., 2021). At 12 weeks post-exposure to 20 Gy gamma rays, Tb.Sp and the ratio of bone surface to volume (BS/BV) were increased, while BV/TV, Tb.Th, Tb.N, and maximum loading were decreased (Zou et al., 2016). One week to 1 year after exposure resulted in significant decreases in BMD, BV/TV, Tb.N, Conn.D, bending strength, the elastic modulus, and stiffness (Alwood et al., 2017; Green et al., 2012; Hui et al., 2014; Oest et al., 2018; Zhang et al., 2019). Mandair et al. 2020 observed a significant decrease in mineral/matrix ratio in the endosteal and mid-cortical bone 2 weeks following 20 Gy (4 X 5Gy) radiation exposure, with progressive decrease 4- and 8-weeks post exposure (Mandair et al. 2020). In mice exposed to 5 or 20 Gy of x-ray radiation, a significant decrease in bone volume was shown in irradiated mice with both 5 Gy and 20 Gy at 6-, 12- and 26-weeks post irradiation. A significant increase in Trabecular spacing (Tb sp) was also shown in the 20 Gy irradiated mice when compared with control groups up to 13 weeks post-irradiation (Wernle et al. 2010).

Essentiality

In vivo studies show that bone loss mainly occurs in the bone tissue directly receiving radiation. In several experiments, malleable lead shielding was used to protect the contralateral limbs of mice from the effects of IR. Contralateral bone tissue was harvested and was compared to the bone tissue directly receiving radiation. Relative to baseline levels, shielding of contralateral limbs consistently attenuated the effects of IR on all markers of bone loss compared to non-shielded limbs. Shielding reduced the IR-induced changes to various bone loss measures including BV/TV, Conn.D, Tb.N, and Tb.Th (Oest et al., 2018; Wright et al., 2015). Furthermore, Baxter et al. (2005) found that the risk of osteoporotic fractures in humans exposed to radiotherapy increased only at the irradiated site. However, some studies still show bone loss in shielded limbs, possibly due to the abscopal effects of radiation (Zhang et al., 2019; Zou et al., 2016).

Uncertainties and Inconsistencies

- At 8 days post-16 Gy irradiation, there was a significant increase in trabecular BV/TV relative to the non-irradiated controls, contrary to the expected reduction in bone volume usually seen following energy deposition (Hui et al., 2014).
- When exposed to 0.1, 0.5, and 2 Gy of ⁵⁶Fe heavy ions, mice did not follow the expected dose-dependent response. Compared to non-irradiated controls, 0.1 and 0.5 Gy irradiation resulted in significant 16% and 18% decreases in BV/TV, respectively. 2 Gy radiation did not have a significant effect on trabecular BV/TV. 0.1 and 0.5 Gy irradiation similarly decreased Tb.N by 7% and 5%, respectively, while changes following 2 Gy irradiation were non-significant (Yumoto et al., 2010).
- Many clinical studies demonstrate that bone loss occurs following radiotherapy in humans (Willey et al., 2011). However, very few studies specify the dose of radiation used, reducing the availability of human studies and an understanding of dose-effects.
- There was approximately a 2-fold increase in %BV/TV of the distal femur of mice following a 0.5 Gy of ⁵⁶Fe compared to the sham-irradiated group (Bokhari et al., 2019).
- There was a significant increase in trabecular BV/TV, Conn.D and Tb.N after mice were exposed to 4.4 cGy of ionizing radiation (Karim and Judex, 2014).
- Exposure to 0.5 Gy ⁵⁶Fe radiation in WB and 6/G mice improved cancellous bone microarchitecture 21 days after irradiation and continued to improve during recovery period. Additionally, in irradiated WB and G/6 mice, cancellous bone volume of the distal femur was 78% and 5% greater compared to their sham control groups (Bokhari et al. 2019).
- Bone mineral to matrix ratio, which is correlated with mineral density, was significantly increased at 4 weeks post 20 Gy irradiation in mice tibia (Gong et al. 2013). However, at 12 weeks the parameters shifted in the opposite direction with the ratio significantly decreasing in the irradiated group. It is important to note that these findings were done using Raman spectroscopy, which is not a well-established technology for biochemical measurements. In another study, mineral crystallinity which also supports mineral density, was transiently increased from weeks 2 to 4 after irradiation (4x5Gy) (Oest et al., 2016).

Quantitative Understanding of the Linkage

The following are a few examples of quantitative understanding of the relationship. All reported findings are statistically significant at various alpha levels as listed in the original sources.

Response-response relationship

Dose Concordance

Reference	Experiment Description	Result
Overgaard, 1988	In vivo. Patients receiving post-mastectomy photon radiation (8 MV) had the number of rib fractures evaluated with chest radiograms.	The frequency of fractures increased dose-dependently between 40 and 50 Gy (12 fractions) and between 50 and 55 Gy (22 fractions), resulting in a maximum of 48% of patients with rib fractures at 50 Gy.

Holm et al., 1996	In vivo. Rectal carcinoma patients received preoperative radiotherapy with photons at 25 Gy (500 irradiated, 527 control). The source of photons was either 60Co or a 6-21 MV linear accelerator. The incidence of hospitalizations for femoral neck or pelvic fracture was determined at a 5-year follow-up.	Patients irradiated with 25 Gy had an incidence of pelvic fracture of 5.3%, while significantly fewer non-irradiated patients were admitted for fracture (2.4%).
Dickie et al., 2009	In vivo. Lower extremity soft tissue sarcoma patients receiving radiotherapy were divided into patients with lower extremity fractures (n=21) and patients without fractures (n=53). The average dose received was compared between the two groups.	Radiotherapy patients that had a bone fracture received an average dose of 45 Gy. Patients without a fracture had a lower average dose of 37 Gy. In addition, the maximum dose received by patients with a fracture was 64 Gy, while the maximum dose received by non-fractured patients was 59 Gy.
Nishiyama et al., 1992	In vivo. Patients with uterine cervix carcinoma from 1989 to 1990 with or without 4 MV photon irradiation to lumbar vertebrae had bone mineral content (measured in mg CaCO ₃ eq/cm ³) determined. Radiation was given in 1.8 Gy fractions over 5 weeks for a total dose of either 22.5 or 45 Gy to the vertebrae (radiation plan dependent).	The control group did not show a change in bone mineral content. Both 22.5 and 45 Gy reduced bone mineral content by about 55 mg.
Stavnichuk et al., 2020	In vivo. A meta-analysis that extracted the percent change in bone density in 148 astronauts from articles from 1971 to 2019. The longer the spaceflight, the higher dose of IR the astronauts received, although IR was not the only stressor that the astronauts would have received.	In missions from 30 to 250 days, the estimated reduction in bone density was 0.1% per month in upper limbs and 0.8% per month in lower limbs.
Bandstra et al., 2008	In vivo. 58-day-old, female, juvenile, C57BL/6 mice were exposed to whole-body irradiation with 0.5, 1, and 2 Gy of 250 MeV protons at a rate of 0.7 Gy/min. Microarchitectural measurements, including trabecular BV/TV, Tb.Sp, and vBMD, were measured in the proximal tibiae. Three-point bending tests on the left femora were performed to assess mechanical parameters.	Following exposure to 2 Gy of proton radiation, mice showed significant changes in bone structure compared to the non-irradiated controls, including a 20% loss of trabecular BV/TV, an 11% increase in Tb.Sp, and a 19% decrease in trabecular vBMD. BV/TV also decreased by 13% at 1 Gy. 0.5 Gy irradiation did not result in significant changes to trabecular bone structure. BV/TV and vBMD followed a decreasing trend at 1 and 2 Gy, and Tb.Sp similarly showed a linear, dose-dependent increase. No significant changes to mechanical strength were observed at any dose.
Hamilton et al., 2006	In vivo. 9-week-old, juvenile, female, C57BL/6 mice were exposed to 2 Gy whole-body irradiation from different sources, including LET=0.23 keV/μm 60Co gamma rays, LET=0.4 keV/μm protons, LET=13 keV/μm 12C, and LET=148 keV/μm 56Fe. 4 months post-exposure, microarchitectural parameters, including trabecular BV/TV, Tb.Sp, Tb.Th, Tb.N, cortical porosity (Ct.Po), cortical volume (Ct.V), and Conn.D (integrity), were measured in the proximal tibiae.	Compared to non-irradiated controls, mice from all radiation groups experienced significant decreases in trabecular BV/TV following exposure to 2 Gy of IR, including decreases of 29% for gamma rays, 35% for protons, 39% for 12C, and 34% for 56Fe. Tb.Th showed a LET-dependent difference in IR-induced bone loss, with high LET sources (12C and 56Fe) showing significant decreases of 10% and 11%, respectively, while changes caused by low LET sources (gamma rays and protons) were non-significant. Only proton-irradiated mice experienced significant changes in Tb.N, and Tb.Sp, with a 20% decrease in Tb.N and a 22% increase in Tb.Sp. Trabecular Conn.D declined significantly in all radiation groups following exposure, with decreases of 54% for gamma rays, 64% for protons, 54% for 12C, and 46% for 56Fe. Ct.Po and Ct.V did not change significantly compared to the control after exposure to gamma, proton, 12C, or 56Fe radiation.
Willey et al., 2010	In vivo. 20-week-old, adult, female, C57BL/6 mice were exposed to whole body irradiation with 2 Gy of 140 kVp X-rays at a rate of 1.36 Gy/min. Microarchitectural parameters, including BV/TV, Conn.D, Tb.N, Tb.Th, Tb.Sp, Ct.V, Ct.Po, polar moment of inertia (pMOI), the percent eroded surface at the endocortical surface (Ec.ES/Ec.BS), vBMD, and marrow volume (Ma.V) were measured in the tibiae.	The irradiated group experienced a 30% decrease in BV/TV and a 53% decrease in Conn.D in the proximal tibia after 3 weeks. Similar changes occurred in the distal femur and the fifth lumbar vertebrae. Decreases in vBMD and Tb.N and increases in Tb.Sp were observed from 1-3 weeks in the proximal tibia, distal femur, and the fifth lumbar vertebrae. vBMD decreased a maximum of 44%, Tb.N decreased a maximum of 13%, and Tb.Sp increased a maximum of 15%. There was no significant change in Tb.Th. Neither endocortical or periosteal Ct.V, Ct.Po, Ma.V, or pMOI changed significantly after exposure to X-rays. Ec.ES/Ec.BS increased by 68% at week 3.
Ghosh et al., 2016	In vivo. 16-week-old, adult, male C57BL/6 mice were exposed to whole body irradiation with 1 Gy of LET=150 MeV/μm 56Fe heavy ion radiation at a rate of 0.1 Gy/min. Microarchitectural measurements, including BV/TV, Tb.Th, Tb.Sp, and Tb.N, were measured in the cancellous bone of the tibia.	Compared to non-irradiated controls, mice that underwent total body irradiation experienced a 14% decrease in BV/TV, an 11% increase in Tb.Sp, and a 14% decrease in Tb.N. The resulting change in Tb.Th after irradiation was not significant.
Alwood et al., 2010	In vivo. 4-month-old, adult, male, C57BL/6 mice were exposed to irradiation with 0.5 Gy (low dose) and 2 Gy (high dose) of 1 GeV/nucleon 56Fe heavy ions at a rate of 0.45 Gy/min and 0.9 Gy/min, respectively. 1-month post-irradiation, microarchitectural parameters, including BV/TV, Tb.Sp, Tb.N, cortical thickness (Ct.Th), cortical bone area (Ct.BA), and Conn.D, were measured in the mineralized cancellous bone tissue of the fourth lumbar vertebra. Stress transfer was assessed within the fourth lumbar vertebra. The elastic modulus of the cancellous centrum compartment and whole-vertebral body were determined with an axial compression test.	Compared to non-irradiated controls, mice that were exposed to 2 Gy of heavy ions showed a 14% decrease in cancellous BV/TV, a 9% decrease in Tb.N, and an 18% decrease in Conn.D, as well as a 12% increase in Tb.Sp. The average cancellous tissue stress increased by 27% within the centrum following 2 Gy. The centrum elastic modulus (30%) and whole-vertebral body elastic modulus (10%) were decreased at 2 Gy. Mice that received a 0.5 Gy dose did not exhibit a significant degradation in bone structure or mechanical properties. Ct.Th and Ct.BA were not significantly affected.
Green et al., 2012	In vivo. 8- and 16-week-old (young and mature adult) C57BL/6J mice were irradiated with 5 Gy of 137Cs gamma rays at a rate of 0.6 Gy/min. 8 weeks post-irradiation, microarchitectural parameters, including BV/TV, Tb.N, Tb.Sp, and Conn.D, were measured in the proximal tibial bones of the mice.	Compared to non-irradiated controls, mice showed decreases of 45% and 51% for BV/TV, 34% and 21% for Tb.N, and 81% and 85% for Conn.D, as well as a 56% and 28% increase in Tb.Sp, in young and mature adults, respectively.
Bandstra et al., 2009	In vivo. 16-week-old, adult, male, C57BL/6 mice were irradiated with 0.47 Gy of LET=151.4 keV/μm 56Fe heavy ions at a rate of 4 Gy/min. Nine weeks after irradiation, microarchitectural parameters, including BV/TV, Conn. D, Tb.Sp, Tb.Th, Tb.N, Ct.V (excluding marrow volume), cortical total volume (Ct.TV, including marrow volume), Ct.Po, pMOI and vBMD, were measured in the trabecular bone of the proximal humerus.	Compared to non-irradiated controls, mice saw a 17% decrease in BV/TV and a 4% decrease in Tb.Th in the trabecular bone of their proximal humerus. While the changes to BV/TV and Tb.Th were statistically significant, the changes to the other microarchitectural parameters were not significant. After exposure to 0.47 Gy radiation, the proximal humerus experienced a significant decrease in BV (4%), TV (3%), and pMOI (6%), as well as a significant increase in Ct.Po (6%), compared to the control. After exposure to 0.18 Gy radiation, the proximal tibia experienced non-significant changes to all endpoints.
Yumoto et al., 2010	In vivo. 16-week-old, adult, male, C57BL/6 mice were exposed to whole-body irradiation with 0.1, 0.5, and 2 Gy of LET=150 keV/μm 56Fe heavy ions at a rate of 0.2-1 Gy/min. 3 days after irradiation, BV/TV, Tb.Th, Tb.N, and Conn. D were measured in the proximal tibiae of the mice.	Compared to non-irradiated controls, 0.1 and 0.5 Gy irradiation resulted in significant 16% and 18% decreases in BV/TV, respectively. 2 Gy radiation did not have a significant effect on trabecular BV/TV. 0.1 and 0.5 Gy irradiation similarly decreased Tb.N by 7% and 5%, respectively, while changes following 2 Gy irradiation were non-significant. Following 0.1 and 0.5 Gy irradiation, Conn. D decreased by 21% and 24%, respectively. Tb.Th was not affected by IR at any of the measured doses.
Alwood et al., 2017	In vivo. 16-week-old, adult, male, C57BL/6J mice were irradiated with 0.05, 0.1, 0.5, or 2 Gy of either LET>0.52 keV/μm protons or LET>175 keV/μm 56Fe heavy ions. At 5 weeks and 1 year after exposure, microarchitectural parameters, including BV/TV, Tb.N, Tb.Th, Tb.Sp, Ct.BV, and Ct.Th, were measured in the proximal tibial metaphysis of the mice.	At 5 weeks post-exposure, IR affected BV/TV and Tb.N in an identical manner. High doses of 56Fe radiation (0.5 and 2 Gy) resulted in a 16% and 31% decrease, respectively, in both parameters compared to non-irradiated controls, while 2 Gy of protons similarly caused a 22% reduction in both. 0.5 Gy of protons caused non-significant decreases in BV/TV and Tb.N (11 and 13%, respectively). 2 Gy of proton irradiation also resulted in an increase in Tb.Sp, but it did not affect Tb.Th. Low doses (0.05 and 0.1 Gy) did not have an effect on bone loss after exposure to either protons or 56Fe heavy ions. Ct.BV and Ct.Th were not significantly affected in the femur midshaft.

Lloyd et al., 2012	In vivo. 16-week-old, adult, female, C57BL/6 mice were exposed to whole body irradiation with 1 Gy of low LET protons at a rate of ~0.6 Gy/min. Microarchitectural parameters, including BV/TV, Conn. D, Tb.N, Tb.Sp, Ct.BV, Ct.Po, and pMOI were measured in the proximal tibia and distal femur of the mice. Three-point bending tests on the left femur were performed to assess mechanical parameters.	Compared to non-irradiated controls, BV/TV, Conn. D, and Tb.N in the proximal tibiae of the mice decreased significantly by 16%, 28%, and 7.7%, respectively, while Tb.Sp increased significantly by 9%. Microarchitectural parameters of the distal femur were not as affected, with BV/TV and Conn. D decreasing significantly by 22% and 37%, respectively, while Tb.N and Tb.Sp were unchanged. Ct.BV, Ct.TV, Ct.Po, and pMOI were not significantly affected by radiotherapy in the femur or tibiae. Mechanical strength was not significantly changed by radiation.
Chandra et al., 2017	In vivo. The distal metaphyseal region of right femurs of 8- to 10-week-old male mice were irradiated with 8 Gy of focal SARRP (small animal radiation research platform) X-ray radiation at a rate of 1.65 Gy/min. vBMD, BV/TV, Tb.N, and Tb.Sp were measured from the femurs of the mice. Linear elastic analysis was performed to assess stiffness.	Compared to non-irradiated controls, irradiated mice experienced a 30% decrease in vBMD, a 31% decrease in BV/TV, a 13% decrease in Tb.N, and a 19% increase in Tb.Sp. Trabecular bone stiffness decreased 56%.
Chandra et al., 2014	In vivo. Three-month-old female Sprague-Dawley rats were irradiated at the proximal metaphyseal region of the right tibiae with 16 Gy of SARRP X-rays, fractionated into two 8 Gy doses at a rate of 1.65 Gy/min. Stiffness, BMD, BV/TV, Tb.N, and Tb.Sp were measured from the tibiae of the rats.	Compared to non-irradiated controls, IR exposure resulted in a 14.3% decrease in BMD, a 17.7% decrease in BV/TV, a 17.7% decrease Tb.N, and a ~25% increase in Tb.Sp at 28 days post-exposure. Trabecular stiffness was decreased 51%.
Hui et al., 2014	In vivo. 16-week-old adult female BALB/c mice were exposed to a single 16 Gy dose of 250 kVp X-rays. The BV/TV and Ct.Th of the distal femurs of irradiated mice were measured.	Compared to non-irradiated controls, irradiation resulted in the mice experiencing a ~55% decrease in trabecular BV/TV at 30 days post-exposure. Ct.Th increased significantly by ~12% at day 8 post-exposure.
Wright et al., 2015	In vivo. The hindlimbs of 20-week-old adult male mice were irradiated with 2 Gy of 320 kV X-rays at a rate of 1.6 Gy/min to the right hindlimb. 7 days post-irradiation, microarchitectural measurements, including BV/TV, Conn. D, Tb.N, Tb.Th, and Tb.Sp, were measured in the tibia and femur of the affected hindlimb.	Compared to baseline levels, 2 Gy of IR resulted in a 22% and 14% (significant only against controls) decrease in BV/TV, a 50% and 45% (significant only against baseline) decrease in Conn. D, a 16% (significant only against baseline) and 13% decrease in Tb.N, and a 20% (significant only against baseline) and 16% increase in Tb.Sp in the proximal tibia and distal femur, respectively.
Oest et al., 2018	In vivo. An experiment was done on 6-week-old female BALB/cj mice exposed to 5 Gy X-ray radiation (225 kV beam at 17 mA) to the femur. Changes in BV/TV, Conn.D, Tb.Th, Tb.N, Ct.BA and Ct.Th were measured up to 26 weeks after exposure. Three-point bending tests were used to assess the mechanical properties of the whole bone and of cortical bone at the mid-diaphysis of the femur.	In metaphyseal trabecular bone at 12 weeks, BV/TV was decreased by 69%, Tb.N by 79%, and Conn.D by 93% compared to the sham group. Tb.Th was increased compared to controls until 8 weeks. In the epiphyseal compartment, similar trends were seen. BV/TV decreased by 21%, Tb.N decreased by 30%, connectivity density decreased by 51%, and Tb.Th increased by 12%. Ct.Th decreased 8.1% and Ct.BA decreased 8.3% in the mid-diaphysis after 12 weeks compared to controls. In the metaphyseal region, cortical parameters increased. By 12 weeks, bending strength was reduced by 14.1% and bending stiffness was reduced by 13.3%. For cortical bone at 12 weeks, flexural strength decreased 5.7% and the flexural modulus decreased 4.9%.
Zou et al., 2016	In vivo. Male Sprague-Dawley rats were exposed to 20 Gy radiation (0.8 Gy/min) using 137Cs gamma ray irradiation chamber for tibia and distal femur. Non-irradiation body parts were shielded, and contralateral sides of the femur and tibia were also harvested. BMD, BV/TV, Ct.Po, Tb.Th, and Tb.N of the irradiated femur were determined 12 weeks after exposure. Three-point bending tests were performed on the femur to assess mechanical parameters.	Trabecular BMD of the irradiated femur was reduced by 21.2% in comparison with the control group. Trabecular BV/TV was reduced by 30.8% at the irradiated femur. Compared to the control group, BS/BV was increased by 32.9% at the irradiated femur. Both Tb.Th and Tb.N decreased after irradiation 17.5% and 18.1%, respectively. Tb.Sp increased after irradiation by 39% in the irradiated femur. Ct.Po was increased by 13.8% and 17.9%. Regarding tibia, BMD decreased 8.5%, and trabecular bone volume did not change significantly at 2 weeks post irradiation but decreased significantly in both irradiated and contralateral tibia at 12 weeks. The maximum loading of the femur was decreased 32.6% after 12 weeks.
Zhang et al., 2019	In vivo. An experiment was done on 4-week-old male C57BL/6 mice exposed to 2 Gy X-ray radiation at the mid-shaft of the left femur. Changes in BMD, BV/TV, Tb.Th, Tb.N were measured 7 and 28 days after exposure.	7 days after irradiation, substantial degeneration of trabecular microarchitecture, with losses of 19% for BMD, 17% for BV/TV, 16% for Tb.Th, and an increase of 31% for Tb.Sp. Irradiated femurs showed further degeneration after 28 days. BMD decreased 15%, BV/TV decreased 42%, Tb.Th decreased 17%, Tb.N decreased 30%, and Tb.Sp increased 62%.
Blaber et al., 2013	In vivo. 16-week-old female mice were subjected to 15-days of spaceflight. Changes in BV/TV and Tb.Th were analyzed with micro-computed tomography (μ CT).	Spaceflight resulted in a 6.23% decrease in BV/TV and a 11.91% decrease Tb.Th in the pelvis compared to the ground control.
Jia et al., 2011	In vivo. 10 to 12-weeks-old male mice were exposed to 0, 5, 10, 15 and 20 Gy of X-ray. BMD was determined at day 7 to 14 after irradiation and using the standard DEXA technique.	Decreases in BMD in the femur, tibia and lumbar vertebrae were approximately 2-fold with each increasing dose (5, 10, 15, 20 Gy) from 0 Gy.
Macias et al., 2016	In vivo, four-month-old female BALB/cByJ were exposed to a fractionated dose of 0.5 Gy (3X 0.17), single dose of 0.17 or 0.5 Gy high-LET 28Si ions. Bone volume was assessed using microcomputed tomography (micro-CT)	Mice exposed to 0.5 Gy in an acute or fractionated dose produced a -14 and -18% bone volume reductions, respectively, when compared to sham controls.
Pendleton et al., 2021	In vivo. 17-week-old male mice were exposed to 0, 1, 5 Gy of 137Cs gamma rays at 0.76 Gy/min. BV/TV, were measured 11 days and 12 weeks post radiation using micro-computed tomography.	BV/TV decreased for 0 Gy by 11.5% after 12 weeks compared to the control at 11 days. For 5 Gy, BV/TV decreased by 23% after 11 days and by 21.6% after 12 weeks compared to the control group. Results for 1 Gy were not significant.

Time-scale**Time Concordance**

Reference	Experiment Description	Result
Holm et al., 1996	In vivo. Rectal carcinoma patients received preoperative radiotherapy with photons at 25 Gy (500 irradiated, 527 control). The source of photons was either 60Co or a 6-21 MV linear accelerator. The incidence of hospitalizations for femoral neck or pelvic fracture was determined at a 5-year follow-up.	By 5 years post-radiotherapy, 5.3% of irradiated patients were admitted for a fracture, while 2.4% of non-irradiated patients were admitted for a fracture.
Nishiyama et al., 1992	In vivo. Patients with uterine cervix carcinoma from 1989 to 1990 with or without 4 MV photon irradiation to lumbar vertebrae had bone mineral content (measured in mg CaCO ₃ eq/cm ³) determined. Radiation was given in 1.8 Gy fractions over 5 weeks for a total dose of either 22.5 or 45 Gy to the vertebrae.	The control group did not show a change in bone mineral content over time. Bone mineral content was 140 mg in the pre-treatment for the irradiated group. Bone mineral content was 95 mg after irradiation (5 weeks), 84 mg after 3 months, 74 mg after 6 months, and 71 mg after 12 months.
Hui et al., 2014	In vivo. 16-week-old adult female BALB/c mice were exposed to a single 16 Gy dose of 250 kVp X-ray radiation. The BV/TV of the distal femurs of irradiated mice were measured.	Trabecular BV/TV initially increased relative to the non-irradiated control on day 3, but gradually declined to day 8 until it was ~55% lower relative to controls on day 30. Ct.Th increased significantly by ~12% at day 8 post-exposure.

Zou et al., 2016	In vivo. Male Sprague-Dawley rats were exposed to 20 Gy radiation (0.8 Gy/min) using 137Cs gamma ray irradiation chamber for tibia and distal femur. Non-irradiation body parts were shielded, and contralateral sides of the femur and tibia were also harvested. BMD, BV/TV, Ct.Po, Tb.Th, and Tb.N of the irradiated femur were determined 12 weeks after exposure. Three-point bending tests were performed on the femur to assess mechanical parameters.	Trabecular BMD of the irradiated femur was reduced by 21.2% after 12 weeks. Trabecular BV/TV was reduced by 30.8% after 12 weeks. Compared to the control group, BS/BV was increased by 32.9% after 12 weeks. Both Tb.Th and Tb.N decreased after 12 weeks 17.5% and 18.1%, respectively. Tb.Sp increased after 12 weeks by 39% in the irradiated femur. Ct.Po was increased by 13.8% and 17.9% after 12 weeks. Regarding tibia, BMD decreased 8.5% after 12 weeks, and trabecular bone volume did not change significantly at 2 weeks post irradiation but decreased significantly in both irradiated and contralateral tibia at 12 weeks. The maximum loading of the femur was decreased 32.6% after 12 weeks.
Oest et al., 2018	In vivo. An experiment was done on 6-weeks old female BALB/Cj mice exposed to 5 Gy X-ray radiation to the femur. Changes in BV/TV, Conn.D, Tb.Th, Tb.N, Ct.BA and Ct.Th were measured up to 26 weeks after exposure. Three-point bending tests were used to assess the mechanical properties of the whole bone and of cortical bone at the mid-diaphysis of the femur.	In metaphyseal trabecular bone BV/TV, Tb.N, and Conn.D increased slightly during the radiation period but declined almost linearly between 1 and 26 weeks, reaching 69%, 79%, and 93% below the initial values, respectively, by 12 weeks. Tb.Th was increased. In the epiphyseal compartment, similar trends can be seen. By 12 weeks, BV/TV, Tb.N, and Conn.D declined linearly after exposure reaching 21%, 30%, and 51% below the control group, respectively. Tb.Th was increased. All mechanical parameters increased over time up to 26 weeks, but the parameters of irradiated mice were lower than those for control mice. Both cortical parameters were decreased about 8% in the mid-diaphysis by 12 weeks. By 12 weeks, bending strength was reduced by 14.1% and bending stiffness was reduced by 13.3%. For cortical bone at 12 weeks, flexural strength decreased 5.7% and the flexural modulus decreased 4.9%.
Alwood et al., 2017	In vivo. 16-week-old, male, C57BL6/J mice were subjected to low LET protons or high-LET 56Fe ions using either low (5 or 10 cGy) or high (50 or 200 cGy) doses. Trabecular microarchitectural parameters such as BV/TV, and Tb.N were measured in the proximal tibial metaphysis.	In the proximal tibia, 50 and 200 cGy 56Fe induced a reduction in BV/TV (16 percent and 31%, respectively) and Tb.N (16 percent, and 31%, respectively) at 5 weeks after irradiation, compared to the control group. For protons, 200 cGy resulted in a 22% reduction in BV/TV and Tb.N, while 50 cGy resulted in a trend toward lower BV/TV and Tb.N. After 1 year, no changes in any endpoints were observed other than a 25% decrease in both BV/TV and Tb.N at 200 cGy (non-significant).
Zhang et al., 2019	In vivo. An experiment was done on 4-week-old male C57BL/6 mice exposed to 2 Gy X-ray radiation at the mid-shaft of the left femur. Changes in BMD, BV/TV, Tb.Th, Tb.N were measured 7 and 28 days after exposure.	7 days after irradiation, substantial degeneration of trabecular microarchitecture occurred, with losses of 19% for BMD, 17% for BV/TV, 16% for Tb.Th, and an increase of 31% for Tb.Sp. Irradiated femurs showed further degeneration after 28 days. BMD decreased 15%, BV/TV decreased 42%, Tb.Th decreased 17%, Tb.N decreased 30%, and Tb.Sp increased 62%.
Green et al., 2012	In vivo. Eight-week-old and 16-week-old mice were irradiated with 5 Gy of 137Cs gamma rays. BV/TV, Conn.D, Tb.Sp, and Tb.N were measured 2 days, 10 days, and 8 weeks post radiation in the proximal tibia.	None of the microarchitecture parameters indicated significant bone loss at 2 days post-irradiation. BV/TV, Tb.N, Tb.Sp, and Conn.D all demonstrated significant bone loss at 10 days and 8 weeks post-irradiation. By 8 weeks, mice showed decreases of 45% and 51% for BV/TV, 34% and 21% for Tb.N, and 81% and 85% for Conn. D, as well as a 56% and 28% increase in Tb.Sp, in young and mature mice, respectively.
Green et al., 2013	In vivo. eight-week old male C57BL/6 mice were irradiated with gamma irradiation at a total dose of 5 Gy. Mineral composition was assessed using Fourier transform infrared imaging (FTIR). Trabecular bone volume was measured using micro-computed tomography (micro-CT)	10 days post-irradiation, significant decline was observed in the mineral/matrix ratio when compared to control groups. 10 days post-irradiation, a significant $-41 \pm 12\%$ and $-33 \pm 4\%$ decrease was also shown in bone volume fraction, with no improvement by 8 weeks post-irradiation.
Pendleton et al., 2021	In vivo. 17-week-old male mice were exposed to 0, 1, 5 Gy of 137Cs gamma rays at 0.76 Gy/min. BV/TV, were measured 11 days and 12 weeks post radiation using micro-computed tomography.	BV/TV decreased for 0 Gy by 11.5% after 12 weeks compared to the control at 11 days. For 5 Gy, BV/TV decreased by 23% after 11 days and by 21.6% after 12 weeks compared to the control group. Results for 1 Gy were not significant.
Mandair et al., 2020	In vivo. 12-week-old female BALB/cj mice aged 12-weeks were exposed to 5 Gy radiation doses for four consecutive days, for a final dose of 20 Gy. Cortical mineral matrix ratio was evaluated by Raman spectroscopy.	Cortical mineral matrix ratio showed significant decrease by -16.9% in the endosteal bone and -7.5% in the mid cortical bone 2 weeks post-irradiation when compared to controls. Mineral matrix ratio progressively decreased continually 4- and 8-weeks post radiation.
Wernle et al. 2010	In vivo, female mice aged 12-14 weeks were exposed to 5 Gy or 20 Gy of X-ray irradiation. Trabecular bone volume and trabecular spacing were measured via micro-computed tomography up to 26 weeks post-irradiation.	A significant decrease in BV/TV was shown in irradiated mice with both 5 Gy and 20 Gy at 6-, 12- and 26-weeks post irradiation. A significant increase in Trabecular spacing (Tb sp) was also shown in the 20 Gy irradiated mice when compared with control groups up to 13 weeks post-irradiation.

Known modulating factors

Modulating Factor	MF details	Effects on the KER	References
Drug	Risedronate	Led to restored BV/TV and Conn. D levels after radiation.	Willey et al., 2010
Genotype	Loss of function mutations (like in sclerosteosis and van Buchem disease) in the SOST gene for sclerostin (sclerostin is a Wnt receptor antagonist that inhibits osteoclastogenesis).	Radiation did not affect BMD and BV/TV in sclerostin knockout mice.	Chandra et al., 2017
Drug	1-34 amino-terminal fragment of parathyroid hormone (osteoporosis treatment that attenuates osteoblast apoptosis).	Treatment with 60 $\mu\text{g}/\text{kg}/\text{day}$ for 27 days led to increased BV/TV and BMD after radiation-induced decreases.	Chandra et al., 2014
Age	Old age	Lower estrogen at old age is thought to contribute to the detrimental effects of radiotherapy on bone loss in elderly patients.	Pacheco and Stock, 2013

Known Feedforward/Feedback loops influencing this KER

Not Identified

References

Alwood, J. S. et al. (2017), "Dose-and Ion-Dependent Effects in the Oxidative Stress Response to Space-Like Radiation Exposure in the Skeletal System", International Journal of Molecular Sciences, Vol. 18/10, MDPI, Basel, <https://doi.org/10.3390/ijms18102117>.

Alwood, J. S. et al. (2010), "Heavy ion irradiation and unloading effects on mouse lumbar vertebral microarchitecture, mechanical properties and tissue stresses", Bone, Vol. 47/2, Elsevier B.V., <https://doi.org/10.1016/j.bone.2010.05.004>.

Bandstra, E. R. et al. (2009), "Musculoskeletal changes in mice from 2050 cGy of simulated galactic cosmic rays", Radiation Research, Vol. 172/1, <https://doi.org/10.1667/RR1509.1>.

Bandstra, E. R. et al. (2008), "Long-term dose response of trabecular bone in mice to proton radiation", Radiation Research, Vol. 169/6, <https://doi.org/10.1667/RR1310.1>.

Baxter N. N. et al. (2005), "Risk of Pelvic Fractures in Older Women Following Pelvic Irradiation", JAMA, Vol. 294, <https://doi.org/10.1001/jama.294.20.2587>

Blaber, E.A. et al. (2013), "Microgravity induces pelvic bone loss through osteoclastic activity, osteocytic osteolysis, and osteoblastic cell cycle inhibition by CDKN1a/p21", PloS one, Vol. 8/4, e61372. <https://doi.org/10.1371/journal.pone.0061372>

Bokhari, R. S. et al. (2019), "Positive impact of low-dose, high-energy radiation on bone in partial- and/or full-weightbearing mice", NPJ Microgravity, Vol. 5/13.

Chandra, A. et al. (2017), "Suppression of Sclerostin Alleviates Radiation-Induced Bone Loss by Protecting Bone-Forming Cells and Their Progenitors Through Distinct Mechanisms", *Journal of Bone and Mineral Research*, Vol. 32/2, <https://doi.org/10.1002/jbmr.2996>.

Chandra, A. et al. (2014), "PTH1-34 Alleviates Radiotherapy-induced Local Bone Loss by Improving Osteoblast and Osteocyte Survival", *Bone*, Vol. 67/1, Elsevier, Amsterdam, <https://doi.org/10.1016/j.bone.2014.06.030>

Costa, S., & Reagan, M. R. (2019), "Therapeutic Irradiation: Consequences for Bone and Bone Marrow Adipose Tissue" *Frontiers in endocrinology*, Vol. 10, *Frontiers in Endocrinology*, <https://doi.org/10.3389/fendo.2019.00587>

Cummings, S. R., D. Bates, and D. M. Black (2002), "Clinical Use of Bone Densitometry: Scientific Review", *Journal of the American Medical Association*, Vol. 288/15, <https://doi.org/10.1001/jama.288.15.1889>.

Dickie, C. I. et al. (2009), "Bone Fractures Following External Beam Radiotherapy and Limb-Preservation Surgery for Lower Extremity Soft Tissue Sarcoma: Relationship to Irradiated Bone Length, Volume, Tumor Location and Dose", *International Journal of Radiation Oncology*Biology*Physics*, Vol. 75/4, Elsevier, Amsterdam, <https://doi.org/10.1016/j.ijrobp.2008.12.006>

Donaubauer, A. J. et al. (2020), "The influence of radiation on bone and bone cells—differential effects on osteoclasts and osteoblasts", *International Journal of Molecular Sciences*, Vol. 21/17, <https://doi.org/10.3390/ijms21176377>.

Farris, M. K., et al. (2020), "Bench to Bedside: Animal Models of Radiation Induced Musculoskeletal Toxicity", *Cancers*, Vol. 12/2, MDPI, Basel, <https://doi.org/10.3390/cancers12020427>

Fonseca, H. et al. (2014). "Bone Quality: The Determinants of Bone Strength and Fragility", *Sports Medicine*, Vol. 44/1, Springer Nature, <https://doi.org/10.1007/s40279-013-0100-7>

Ghosh, P. et al. (2016), "Effects of High-LET Radiation Exposure and Hindlimb Unloading on Skeletal Muscle Resistance Artery Vasomotor Properties and Cancellous Bone Microarchitecture in Mice", *Radiation Research*, Vol. 185/3, <https://doi.org/10.1667/RR4308.1>.

Gong, B., Oest, M. E., Mann, K. A., Damron, T. A., & Morris, M. D. (2013). Raman spectroscopy demonstrates prolonged alteration of bone chemical composition following extremity localized irradiation. *Bone*, 57(1), 252–258. <https://doi.org/10.1016/j.bone.2013.08.014>

Green, D. E. et al. (2012), "Devastation of Adult Stem Cell Pools by Irradiation Precedes Collapse of Trabecular Bone Quality and Quantity", *Journal of Bone and Mineral Research*, Vol. 27, American Society for Bone and Mineral Research, Washington, <https://doi.org/10.1002/JBMR.1505>.

Green, D. E. et al. (2013). Altered composition of bone as triggered by irradiation facilitates the rapid erosion of the matrix by both cellular and physicochemical processes. *PLoS one*, 8(5), e64952. <https://doi.org/10.1371/journal.pone.0064952>

Green, D. E., & Rubin, C. T. (2014), "Consequences of irradiation on bone and marrow phenotypes, and its relation to disruption of hematopoietic precursors", *Bone*, Vol. 63, <https://doi.org/10.1016/j.bone.2014.02.018>

Hamilton, S. A. et al. (2006), "A murine model for bone loss from therapeutic and space-relevant sources of radiation", *Journal of Applied Physiology*, Vol. 101/3, <https://doi.org/10.1152/japplphysiol.01078.2005>.

Holm, T. et al. (1996), "Adjuvant preoperative radiotherapy in patients with rectal carcinoma: Adverse effects during long term follow-up of two randomized trials", *Cancer*, Vol. 78/5, Wiley, [https://doi.org/10.1002/\(SICI\)1097-0142\(19960901\)78:5<968::AID-CNCR5>3.0.CO;2-8](https://doi.org/10.1002/(SICI)1097-0142(19960901)78:5<968::AID-CNCR5>3.0.CO;2-8)

Hui, S. K. et al. (2014), "The Influence of Therapeutic Radiation on the Patterns of Bone Remodeling in Ovary-Intact and Ovariectomized Mice", *Calcified Tissue International*, Vol. 23/1, Nature, <https://doi.org/10.1007/s00223-012-9688-0>

ICRP. (2007), "The 2007 Recommendations of the International Commission on Radiological Protection, Publication 103", *Annals of the ICRP*, Vol.37

Jia, D. et al. (2011), "Rapid loss of bone mass and strength in mice after abdominal irradiation", *Radiation research*, Vol. 176/5, 624–635. <https://doi.org/10.1667/rr2505.1>

Karim, L. and Judex, S. (2014), "Low level irradiation in mice can lead to enhanced trabecular bone morphology", *Journal of bone and mineral metabolism*, Vol. 32/5, 476–483. <https://doi.org/10.1007/s00774-013-0518-x>

Lloyd, S. A. et al. (2012), "Effect of proton irradiation followed by hindlimb unloading on bone in mature mice: A model of long-duration spaceflight", *Bone*, Vol. 51/4, Elsevier, Amsterdam, <https://doi.org/10.1016/j.bone.2012.07.001>.

Macias, B. R. et al. (2016). Simulating the Lunar Environment: Partial Weightbearing and High-LET Radiation-Induce Bone Loss and Increase Sclerostin-Positive Osteocytes. *Radiation research*, 186(3), 254–263. <https://doi.org/10.1667/RR13579.1>

Mandair, G. S., Oest, M. E., Mann, K. A., Morris, M. D., Damron, T. A., & Kohn, D. H. (2020). Radiation-induced changes to bone composition extend beyond periosteal bone. *Bone reports*, 12, 100262. <https://doi.org/10.1016/j.bonr.2020.100262>

Nishiyama, K. et al. (1992), "Radiation osteoporosis - an assessment using single energy quantitative computed tomography", *European Radiology*, Vol. 2, Nature, <https://doi.org/10.1007/BF00175435>

Oest, M. E. et al. (2016), "Parathyroid hormone attenuates radiation-induced increases in collagen crosslink ratio at periosteal surfaces of mouse tibia", *Bone*, Vol. 86, 91–97. <https://doi.org/10.1016/j.bone.2016.03.003>

Oest, M. E., et al. (2018), "Longitudinal Effects of Single Hindlimb Radiation Therapy on Bone Strength and Morphology at Local and Contralateral Sites" *Journal of bone and mineral research*, Vol. 33/1, <https://doi.org/10.1002/jbmr.3289>

Orwoll, Eric S et al. (2013), "Skeletal health in long-duration astronauts: nature, assessment, and management recommendations from the NASA Bone Summit." *Journal of bone and mineral research : the official journal of the American Society for Bone and Mineral Research*, Vol. 28/6, <https://doi.org/10.1002/jbmr.1948>

Overgaard, M. (1988), "Spontaneous Radiation-Induced Rib Fractures in Breast Cancer Patients Treated with Postmastectomy Irradiation—A Clinical Radiobiological Analysis of the Influence of Fraction Size and Dose-Response Relationships on Late Bone Damage", *Acta Oncologica*, Vol. 27/2, Informa, London, <https://doi.org/10.3109/02841868809090331>

Pacheco, R. and H. Stock (2013), "Effects of radiation on bone", *Current osteoporosis reports*, Vol. 11/4, Nature <https://doi.org/10.1007/s11914-013-0174-z>

Pendleton, M. M. et al. (2021), "Relations Between Bone Quantity, Microarchitecture, and Collagen Cross-links on Mechanics Following In Vivo Irradiation in Mice", *JBMR plus*, Vol. 5/11, e10545. <https://doi.org/10.1002/jbm4.10545>

Slyfield, C. R., et al. (2012), "Three-dimensional dynamic bone histomorphometry", *Journal of bone and mineral research*, Vol. 27/2, Wiley, <https://doi.org/10.1002/jbmr.553>.

Stavnichuk, M., et al. (2020), "A systematic review and meta-analysis of bone loss in space travelers", *NPJ microgravity*, Vol. 6, Nature, <https://doi.org/10.1038/s41526-020-0103-2>

Steczina, S. et al. (2020), "Dietary countermeasure mitigates simulated spaceflight-induced osteopenia in mice", *Scientific reports*, Vol. 10/1, 6484. <https://doi.org/10.1038/s41598-020-63404-x>

Tian, Y. et al. (2017), "The Impact of Oxidative Stress on the Bone System in Response to the Space Special Environment", *International Journal of Molecular Sciences*, Vol. 18/10, MDPI, Basel, <https://doi.org/10.3390/ijms18102132>.

Turner, C. H. (2002). "Biomechanics of Bone: Determinants of Skeletal Fragility and Bone Quality", *Osteoporosis International*, Vol. 13/2, Springer Nature, <https://doi.org/10.1007/s001980200000>

Wernle, J. D., Damron, T. A., Allen, M. J., & Mann, K. A. (2010). Local irradiation alters bone morphology and increases bone fragility in a mouse model. *Journal of biomechanics*, 43(14), 2738–2746. <https://doi.org/10.1016/j.jbiomech.2010.06.017>

Willey, J. S. et al. (2011), "Ionizing Radiation and Bone Loss: Space Exploration and Clinical Therapy Applications", *Clinical Reviews in Bone and Mineral Metabolism*, Vol. 9, Nature, <https://doi.org/10.1007/s12018-011-9092-8>.

Willey, J. S., (2010), "Risedronate prevents early radiation-induced osteoporosis in mice at multiple skeletal locations", *Bone*, Vol. 46/1, <https://doi.org/10.1016/j.bone.2009.09.002>

Willey, J. S. et al. (2013), "Radiation Therapy-Induced Osteoporosis", *Primer on the Metabolic Bone Diseases and Disorders of Mineral Metabolism*, Eighth Ed., John Wiley & Sons

Wright, L. E. et al. (2015), "Single-Limb Irradiation Induces Local and Systemic Bone Loss in a Murine Model", *Journal of Bone and Mineral Research*, American Society for Bone and Mineral Research, Washington, <https://doi.org/10.1002/jbmr.2458>

Wright, L. E. (2018), "Radiotherapy-Induced Osteoporosis", *Primer on the Metabolic Bone Diseases and Disorders of Mineral Metabolism*, Ninth ed, John Wiley & Sons

Yang, J., et al. (2018), "Effects of Iron Overload and Oxidative Damage on the Musculoskeletal System in the Space Environment: Data from Spaceflights and Ground-Based Simulation Models", *International journal of molecular sciences*, Vol. 19/9, MDPI, Basel, <https://doi.org/10.3390/ijms19092608>

Yumoto, K., et al. (2010), "Short-term effects of whole-body exposure to 56Fe ions in combination with musculoskeletal disuse on bone cells", *Radiation Research*, Vol. 173/4, BioOne, <https://doi.org/10.1667/RR1754.1>

Zhang, J., et al. (2019), "Lowering iron level protects against bone loss in focally irradiated and contralateral femurs through distinct mechanisms", *Bone*, Vol. 120, Elsevier, <https://doi.org/10.1016/j.bone.2018.10.005>

Zou, Q., et al. (2016), "Bone marrow stem cell dysfunction in radiation-induced abscopal bone loss", *Journal of orthopaedic surgery and research*, Vol. 11, *Nature* <https://doi.org/10.1186/s13018-015-0339-9>